UNITED STATES AIR FORCE

SUMMER RESEARCH PROGRAM -- 1998

HIGH SCHOOL APPRENTICESHIP PROGRAM FINAL REPORTS

VOLUME 15C

WRIGHT LABORATORY

RESEARCH & DEVELOPMENT LABORATORIES

5800 Uplander Way

Culver City, CA 90230-6608

Program Director, RDL
Gary Moore

Program Manager, AFOSR
Colonel Jan Cerveny

Program Manager, RDL
Scott Licoscos

Program Administrator, RDL
Johnetta Thompson

Program Administrator, RDL
Rebecca Kelly-Clemmons

Submitted to:

AIR FORCE OFFICE OF SCIENTIFIC RESEARCH

Bolling Air Force Base

Washington, D.C.

December 1998

PREFACE

Reports in this volume are numbered consecutively beginning with number 1. Each report is paginated with the report number followed by consecutive page numbers, e.g., 1-1, 1-2, 1-3; 2-1, 2-2, 2-3.

Due to its length, Volume 15 is bound in three parts, 5A, 5B and 5C. Volume 5A contains #1-18. Volume 5B contains reports #19-36, and Volume 5B contains reports #37-59. The Table of Contents for Volume 5 is included in all parts.

This document is one of a set of 15 volumes describing the 1998 AFOSR Summer Research Program. The following volumes comprise the set:

VOLUME	TITLE
1	Program Management Report
	Summer Faculty Research Program (SFRP) Reports
2	Armstrong Laboratory
3	Phillips Laboratory
4	Rome Laboratory
5A & 5B	Wright Laboratory
6	Arnold Engineering Development Center, United States Air Force Academy and Air Logistics Centers
	Graduate Student Research Program (GSRP) Reports
7	Armstrong Laboratory
8	Phillips Laboratory
9	Rome Laboratory
10	Wright Laboratory
11	Arnold Engineering Development Center and Wilford Hall Medical Center
	High School Apprenticeship Program (HSAP) Reports
12	Armstrong Laboratory
13	Phillips Laboratory
14	Rome Laboratory
15A, 15B & 15C	Wright Laboratory

REPORT DOCUMENTATION PAGE

AFRL-SR-BL-TR-00-

0793

1. AGENCY USE ONLY *(Leave blank)*	2. REPORT DATE	3. REPORT TYPE AND DATES
	December, 1998	

4. TITLE AND SUBTITLE
1998 Summer Research Program (SRP), High School Apprenticeship Program (HSAP), Final Reports, Volume 15C, Wright Laboratory

5. FUNDING NUMBERS
F49620-93-C-0063

6. AUTHOR(S)
Gary Moore

7. PERFORMING ORGANIZATION NAME(S) AND ADDRESS(ES)
Research & Development Laboratories (RDL)
5800 Uplander Way
Culver City, CA 90230-6608

8. PERFORMING ORGANIZATION REPORT NUMBER

9. SPONSORING/MONITORING AGENCY NAME(S) AND ADDRESS(ES)
Air Force Office of Scientific Research (AFOSR)
801 N. Randolph St.
Arlington, VA 22203-1977

10. SPONSORING/MONITORING AGENCY REPORT NUMBER

11. SUPPLEMENTARY NOTES

12a. DISTRIBUTION AVAILABILITY STATEMENT
Approved for Public Release

12b. DISTRIBUTION CODE

13. ABSTRACT *(Maximum 200 words)*

The United States Air Force Summer Research Program (USAF-SRP) is designed to introduce university, college, and technical institute faculty members, graduate students, and high school students to Air Force research. This is accomplished by the faculty members (Summer Faculty Research Program, (SFRP)), graduate students (Graduate Student Research Program (GSRP)), and high school students (High School Apprenticeship Program (HSAP)) being selected on a nationally advertised competitive basis during the summer intersession period to perform research at Air Force Research Laboratory (AFRL) Technical Directorates, Air Force Air Logistics Centers (ALC), and other AF Laboratories. This volume consists of a program overview, program management statistics, and the final technical reports from the HSAP participants at the Wright Laboratory.

14. SUBJECT TERMS
Air Force Research, Air Force, Engineering, Laboratories, Reports, Summer, Universities, Faculty, Graduate Student, High School Student

15. NUMBER OF PAGES

16. PRICE CODE

17. SECURITY CLASSIFICATION OF REPORT	18. SECURITY CLASSIFICATION OF THIS PAGE	19. SECURITY CLASSIFICATION OF ABSTRACT	20. LIMITATION OF ABSTRACT
Unclassified	Unclassified	Unclassified	UL

GENERAL INSTRUCTIONS FOR COMPLETING SF 298

The Report Documentation Page (RDP) is used in announcing and cataloging reports. It is important that this information be consistent with the rest of the report, particularly the cover and title page. Instructions for filling in each block of the form follow. It is important to ***stay within the lines*** to meet ***optical scanning requirements.***

Block 1. Agency Use Only *(Leave blank)*.

Block 2. Report Date. Full publication date including day, month, and year, if available (e.g. 1 Jan 88). Must cite at least the year.

Block 3. Type of Report and Dates Covered. State whether report is interim, final, etc. If applicable, enter inclusive report dates (e.g. 10 Jun 87 - 30 Jun 88).

Block 4. Title and Subtitle. A title is taken from the part of the report that provides the most meaningful and complete information. When a report is prepared in more than one volume, repeat the primary title, add volume number, and include subtitle for the specific volume. On classified documents enter the title classification in parentheses.

Block 5. Funding Numbers. To include contract and grant numbers; may include program element number(s), project number(s), task number(s), and work unit number(s). Use the following labels:

C - Contract	**PR** - Project
G - Grant	**TA** - Task
PE - Program Element	**WU** - Work Unit Accession No.

Block 6. Author(s). Name(s) of person(s) responsible for writing the report, performing the research, or credited with the content of the report. If editor or compiler, this should follow the name(s).

Block 7. Performing Organization Name(s) and Address(es). Self-explanatory.

Block 8. Performing Organization Report Number. Enter the unique alphanumeric report number(s) assigned by the organization performing the report.

Block 9. Sponsoring/Monitoring Agency Name(s) and Address(es). Self-explanatory.

Block 10. Sponsoring/Monitoring Agency Report Number. *(If known)*

Block 11. Supplementary Notes. Enter information not included elsewhere such as: Prepared in cooperation with....; Trans. of....; To be published in.... When a report is revised, include a statement whether the new report supersedes or supplements the older report.

Block 12a. Distribution/Availability Statement. Denotes public availability or limitations. Cite any availability to the public. Enter additional limitations or special markings in all capitals (e.g. NOFORN, REL, ITAR).

DOD - See DoDD 5230.24, "Distribution Statements on Technical Documents."
DOE - See authorities.
NASA - See Handbook NHB 2200.2.
NTIS - Leave blank.

Block 12b. Distribution Code.

DOD - Leave blank.
DOE - Enter DOE distribution categories from the Standard Distribution for Unclassified Scientific and Technical Reports.
Leave blank.
NASA - Leave blank.
NTIS -

Block 13. Abstract. Include a brief *(Maximum 200 words)* factual summary of the most significant information contained in the report.

Block 14. Subject Terms. Keywords or phrases identifying major subjects in the report.

Block 15. Number of Pages. Enter the total number of pages.

Block 16. Price Code. Enter appropriate price code *(NTIS only)*.

Blocks 17. - 19. Security Classifications. Self- explanatory. Enter U.S. Security Classification in accordance with U.S. Security Regulations (i.e., UNCLASSIFIED). If form contains classified information, stamp classification on the top and bottom of the page.

Block 20. Limitation of Abstract. This block must be completed to assign a limitation to the abstract. Enter either UL (unlimited) or SAR (same as report). An entry in this block is necessary if the abstract is to be limited. If blank, the abstract is assumed to be unlimited.

HSAP FINAL REPORT TABLE OF CONTENTS i-ix

1. INTRODUCTION 1

2. PARTICIPATION IN THE SUMMER RESEARCH PROGRAM 2

3. RECRUITING AND SELECTION 3

4. SITE VISITS 4

5. HBCU/MI PARTICIPATION 4

6. SRP FUNDING SOURCES 5

7. COMPENSATION FOR PARTICIPATIONS 5

8. CONTENTS OF THE 1995 REPORT 6

APPENDICIES:

A. PROGRAM STATISTICAL SUMMARY A-1

B. SRP EVALUATION RESPONSES B-1

HSAP FINAL REPORTS

SRP Final Report Table of Contents

Author	University/Institution Report Title	Armstrong Laboratory Directorate	Vol-Page
MR Michael G Anderson	Judson High School , Converse , TX Study of Induced Transmittance In Laser Eye Protection At Ultrashort Pulses	AFRL/HED	12- 1
MR Jacob S Blumberg	Tom C. Clark High School , San Antonio , TX	AFRL/HEJ	12- 2
MR John T Hereford	East Central High School , San Antonio , TX Realistically Duplicating The Appearance and Interface of Actual UAV Dempc Equipment on a Desktop PC	AFRL/HEJ	12- 3
MS Kathleen S Kao	Keystone School , San Antonio , TX A Study in the Selective Heating of The Rat Anatomy	AFRL/HED	12- 4
MS Lauren M Lamm	Keystone School , San Antonio , TX Rpt on Publication of Rsrch Papers on Internet Using Hot Dog Professional 5 & Microsoft Front Pg 98	AFRL/HED	12- 5
MS Christina R Maimone	Chaminade-Julienne High School , Dayton , OH Analysis of Error Frequencies of an On-Line Pen-Input Handwriting Recognition Sys	AFRL/HES	12- 6
MR Edwin E McKenzie	MacArthur High School , San Antonio , TX Software Analysis of EEG Waveforms & Real-Time Measurement of Subject Consciousness	AFRL/HEP	12- 7
MR Charles H Mims	Tom C. Clark High School , San Antonio , TX Study of Induced Transmittance in Laser Eye Protection at Ultrashort Pulses	AFRL/HED	12- 8
Kavitha K Reddy	Miami Valley School , Dayton , OH The Configuration of Anatomical & Seat Coordinate Axis Systems	AFRL/HES	12- 9
MR William J Squicciarini	Floresville High School , Floresville , TX Hypertext Markup Language: An Instructional Guide for WEB Page Design	AFRL/HEJ	12- 10

SRP Final Report Table of Contents

Author	University/Institution Report Title	Phillips Laboratory Directorate	Vol-Page
MS Lauren A Ferguson	Moriarity High School , Moriarity , NM Characterization of the Co2 Laser	AFRL/DEB	13- 1
MR Kevin L Grimes	Albuquerque High School , Albuquerque , NM Satellite Orbit Determination From Optical sighting	AFRL/VSS	13- 2
MS Andrea C Hunt	Phillips Academy , Andover , MA MSX-Observed Objects with Unusual Infared Emission	AFRL/VS	13- 3
MS Mary H Ly	Billerica Mem High School , Billerica , MA The Charging and Discharging of Spacecraft: An Introduction	AFRL/VSB	13- 4
MR Camden B Mullen	Del Norte High School , Albuquerque , NM Radiometric and Radiation Characterization of Rockwell Science Center Detectors	AFRL/VSS	13- 5
MS Kimberly A Robinson	Sandia Prep School , Albuquerque , NM Development of Visualization Modules For Icepic	AFRL/DEA	13- 6
MR Timothy M Swierzbin	Chelmsford High School , North Chelmsford , MA Investigating Interference Patterns in Celestial Images	AFRL/VSB	13- 7
MR Arun K Wahi	Albuquerque Academy , Albuquerque , NM Commercial Power Interface For The Isacc Alarm System	AFRL/VSS	13- 8
MR Jeremy G Wertheimer	Buckingham Browne Nichols School , Cambridge , MA Modtran Validation	AFRL/VSB	13- 9
MR Jeremy L White	Sandia Prep School , Albuquerque , NM Summer Work Projects	AFRL/VSS	13- 10

SRP Final Report Table of Contents

Author	University/Institution Report Title	Rome Laboratory Directorate	Vol-Page
MS Kari A Berg		AFRL/IFT	14- 1
	Holland Patent High School , Holland Patent , NY		
	Computer Animation of Global Search algorithms		
MR Todd S Burnop		AFRL/IFSE	14- 2
	Oriskiany High School , Oriskany , NY		
	Visualizing Multipath w/POV-Ray		
MR Stefan M Enjem		AFRL/IFSB	14- 3
	Whitesboro High School , Whitesboro , NY		
	A Study of Programming and IView 2000		
MR Michael J Favata		AFRL/IFT	14- 4
	Poland Central Schoo , Poland , NY		
	The Development of Web Pages for the Air Force ressearch Laboratory Information Technology Directora		
MR Michael P Galime		AFRL/IFE	14- 5
	Thomas R. Proctor High School , Utica , NY		
	The Study of U.S. Cellular Technology		
MR Colin M Kinsella		AFRL/IFT	14- 6
	Oneida Senior High School , Oneida , NY		
	Campaign Assessment		
MR Peter M LaMonica		AFRL/IFT	14- 7
	Rome Free Academy , Rome , NY		
	Research Investigations of Hypertext Markup Language (HTML) for Web Pages & The Start Natural Langua		
MR Christopher A Lipe		AFRL/IFT	14- 8
	Holland Patent High School , Holland Patent , NY		
	New Metrics for measuring Semantic Relatedness Using Roget's Thesaurus		
MR James M Scherzi		AFRL/IFO	14- 9
	Oneida Senior High School , Oneida , NY		
	Web Management at a Government Site		

SRP Final Report Table of Contents

Author	University/Institution Report Title	Wright Laboratory Directorate	Vol-Page
MS Jessica A Baltes	Carroll High School , Dayton , OH Subjective Assessment of Digital Infared Images	AFRL/SNA	15- 1
MR Brett R Beckett	Waynesville Local High School , Waybesville , OH Gallium Diffusion on The Surface of Gallium Arsenide	AFRL/MLP	15- 2
MR Jeffrey S Becknell	Beavercreek High School , Dayton , OH My Summer Tour at the Air Force Research Laboratory	AFRL/VAC	15- 3
MS Beth A Behr	Niceville Senior High School , Niceville , FL Trace Metals Analysis of Soil & Water at Munitions Test Sites	AFRL/MN	15- 4
MS Crystal W Bhagat	Dayton Christian High School , Dayton , OH	AFRL/MLP	15- 5
MR Chris Broscious	A. Crawford Mosely High School , Lynn Haven , FL Scanning and Organization of Reports	AFRL/ML	15- 6
MS Theresa D Carr	West Carrollton High School , West Carrollton , OH Prelimanary Design of An electrically Conducting Nitrogen-Benzene Ring Starburst Dendrimer	AFRL/ML	15- 7
MS Sarah J Childers	Centerville High School , Centerville , OH Comparison of Objective and Sbjective Assessment of Digital Infrared Image Sequences	AFRL/SNA	15- 8
MR Daniel A Cleyrat	Bellbrook High School , Bellbrook , OH Image Analysis of Polymer Dispersed Liquid Crystals	AFRL/MLP	15- 9
MS Amanda J Colleary	Miamisburg High School , Miamisburg , OH Tensile Properties of Aligned Chopped-Fiber Carbon Fiber Reinforced polymeric Composites	AFRL/ML	15- 10
MR Frank J Fasano	Centerville High School , Centerville , OH A Study of Acoustic adn Sonic Fatigue	AFRL/VAS	15- 11

SRP Final Report Table of Contents

Author	University/Institution Report Title	Wright Laboratory Directorate	Vol-Page
MS Tracey E Fitzgerald	PSJ High School , Port Saint Joe , FL Computer Software Experimentation and Modificartion	AFRL/ML	15- 12
MR Jeffrey L Friedman	Niceville Senior High School , Niceville , FL Two-Dimensional Multiple-Frame Image Analysis	AFRL/MN	15- 13
MS Adria D Gaitros	A. Crawford Mosely High School , Lynn Haven , FL Follower of Dan The "Lan" Man	AFRL/ML	15- 14
MR David L Greenwald	Oakwood High School , Dayton , OH Summary of Summer Work on A Searchable Database Thalt contains The PRSL'S Tech Report Library	AFRL/PRS	15- 15
MR Maneesh K Gupta	Beavercreek High School , Dayton , OH The Synthesis of Monomer for Use in Water-Soluble Rigid-Rod Polymer Systems	AFRL/ML	15- 16
MR Trenton Hamilton	Rocky Bayou Christian School , Niceville , FL High Density Poly-Ethylene "Waffle" Liner Study	AFRL/MN	15- 17
MR Neil Harrison	Ft Walton Beach High SC , Ft Walton BEACH , FL Development of DVAT: A Dimensionally Varying Analytical Tool	AFRL/MN	15- 18
MR William B Haynal	Spring Valley Academy , Centerville , OH JavaScript Applied to Intranet Documents	AFRL/ML	15- 19
MS Jessica L Hill	PSJ High School , Port Saint Joe , FL Optimizing Formulation of AFFF-EMB Using mixture Designs and Response Surface Methods	AFRL/ML	15- 20
MR Taylor L Hughes	Niceville Senior High School , Niceville , FL Development of a Guidance Law Using Optimal Control Theory	AFRL/MN	15- 21
MR Joshua B Jamison	Dixie High School , New Lebannon , OH A Study of Wind Tunnel Test Procedures	AFRL/VAA	15- 22

SRP Final Report Table of Contents

Author	University/Institution Report Title	Wright Laboratory Directorate	Vol-Page
MR Ryan A Jones	Crestview High School , Crestview , FL A WEB Page for MNAL	AFRL/MN	15- 23
MR Kevin S Katerberg	Dayton Christian High School , Dayton , OH Multiple studies at Wright Patterson Air Force Base	AFRL/PRT	15- 24
MR Joseph M Kesler	Carroll High School , Dayton , OH The Development of a Search Engine for an Intranet	AFRL/ML	15- 25
MR Josh M Knopp	Carroll High School , Dayton , OH An Interface for the Automated Control of heat TReatment Furnaces	AFRL/ML	15- 26
MR John P Lightle	Tippecanoe High School , Tipp City , OH A Study of The Prediction of Pilot-Induced Oscillation	AFRL/VAC	15- 27
MR Alexander R Lippert	Choctawhatchee High School , Ft Walton BEACH , FL Infrared Characterization of Photovoltaic Semiconductive Junction Devices	AFRL/MN	15- 28
MS Lisa A Mattingley	A. Crawford Mosely High School , Lynn Haven , FL Reductive Dehalogenation of TCE,Carbon Tetrachloride,& EDB by Humic-Metal Complex	AFRL/ML	15- 29
MR Daniel B McMurtry	Northmont High School , Clayton , OH A Study of Ppilot-Induced Oscillation Tendencies	AFRL/VAO	15- 30
MR Joseph R Moate	Rutherford High School , PANAMA CITY , FL	AFRL/ML	15- 31
MR John D Murchison	Ft Walton Beach High SC , Ft Walton BEACH , FL BRL-CAD Modeling of a Hardened Facility	AFRL/MN	15- 32
MS Nina Natarajan	Beavercreek High School , Dayton , OH A Study in Computational Chemistry	AFRL/MLP	15- 33

SRP Final Report Table of Contents

Author	University/Institution Report Title	Wright Laboratory Directorate	Vol-Page
MR Joshua B Nelson	Home Educated , , FL Biomimetics: Emulating the Human Visual Sys for Military Applications	AFRL/MN	15- 34
MR Eric C Nielsen	Xenia High School , Xenia , OH Building a Building Database	AFRL/SNO	15- 35
MR Bruce W Nolte Jr.	A. Crawford Mosely High School , Lynn Haven , FL Updating the Inventory and Creating Heterogeneous System	AFRL/ML	15- 36
MR Brendan V O'Sullivan	A. Crawford Mosely High School , Lynn Haven , FL A Study of DNAPL'S In a Hetrogeneuos system	AFRL/ML	15- 37
MR Jeremy D Olson	Centerville High School , Centerville , OH Protecting Aircraft Surfaces: A Strudy of Ablative Materials and Their Physical Limitations	AFRL/VAV	15- 38
MS Disha J Patel	Fairmont High School , Kettering , OH A Study of Hyperspectral Imaging (HSI)	AFRL/SNA	15- 39
MS Kathleen A Pirog	Niceville Senior High School , Niceville , FL The Effects of Target Motion on Critical Mobile Target Algorithm Performance	AFRL/MN	15- 40
MR Nathan A Power	Heritage Christian School , Xenia , OH Web Page Designing and Assistant in other Fields	AFRL/SNA	15- 41
MR David S Revill	Choctawhatchee High School , Ft Walton BEACH , FL Development of a Database for Multi-Sensor Imagery	AFRL/MN	15- 42
MR Christopher A Rice	Southeastern High School , South Charleston , OH Finite Element Analysis of Large a Frame Used in Support Structure	AFRL/VAS	15- 43
MS Monica Roy	Beavercreek High School , Dayton , OH The Basic Study & Seat Structure Assembly of the Reclined Ejection Seat	AFRL/HES	15- 44

SRP Final Report Table of Contents

Author	University/Institution Report Title	Wright Laboratory Directorate	Vol-Page
MS Anita Roy	Beavercreek High School , Dayton , OH A Study of the Necessity,Effectiveness & Correlation of Anthropomorphic Manikins to Humans	AFRL/HES	15- 45
Sanjida S Saklayen	Centerville High School , Centerville , OH A Review of the Development of Efficient Helicopter Escape Systems	AFRL/HES	15- 46
MS Jill M Seger	Alter High School , Kettering , OH Gallium Arsenide Surfaces	AFRL/MLP	15- 47
MR Jonah L Shaver	Waynesville Local High School , Waybesville , OH Infrared Small Crack detection System	AFRL/ML	15- 48
MR Douglas E Smith	Tippecanoe High School , Tipp City , OH An In-Depth Study of Synthetic Aperature Rader (SAR) Imagery	AFRL/SNA	15- 49
MR Andrew T Snow	Fairborn High School , Fairborn , OH Study of the Potential for the Growth of Potassium Carbon Thin Films	AFRL/ML	15- 50
MR Matthew J Spriggs	Alter High School , Kettering , OH High School Apprentice Summer Research Studies	AFRL/PRP	15- 51
MS Jane M Stegall	Walton High School , DeFuniak SPRINGS , FL Construction of the MNAC Webpage & Software Verification of Moments'96	AFRL/MN	15- 52
MS Lydia R Strickland	A. Crawford Mosely High School , Lynn Haven , FL What I Did on My Summer Vacation	AFRL/ML	15- 53
MS Rachel J Strickland	A. Crawford Mosely High School , Lynn Haven , FL Study of Paint Waste Decomposition	AFRL/ML	15- 54
MR Robert L Todd	Carroll High School , Dayton , OH The Study of the Change In Strength of Unreinforced Aluminum 7093 alloy and Aluminum 15 Volumes SiCp	AFRL/ML	15- 55

SRP Final Report Table of Contents

Author	University/Institution Report Title	Wright Laboratory Directorate	Vol-Page
My Tran	Choctawhatchee High School , Ft Walton BEACH , FL Damage Studies on Inerts & Explosives Using Rod-On-Rod Impact & Split-Hopkinson Pressure BarTechniqu	AFRL/MN	15- 56
MS Danielle D Turner	Tehachapi High School , Tehachapi , CA The Process of Trappimg Carbon and Boron Atoms in an Argon Matrix	AFRL/PR	15- 57
MR Donald S Weaver	Centerville High School , Centerville , OH A Study fo the Influence of Ceramic Particles on the Aging Behavior of aluminum Alloys	AFRL/ML	15- 58
MS Ming L Xia	Fairmont High School , Kettering , OH Development of Environmental Chamber & Controls to Study the Effect of Environment of Interface Trib	AFRL/ML	15- 59

1. INTRODUCTION

The Summer Research Program (SRP), sponsored by the Air Force Office of Scientific Research (AFOSR), offers paid opportunities for university faculty, graduate students, and high school students to conduct research in U.S. Air Force research laboratories nationwide during the summer.

Introduced by AFOSR in 1978, this innovative program is based on the concept of teaming academic researchers with Air Force scientists in the same disciplines using laboratory facilities and equipment not often available at associates' institutions.

The Summer Faculty Research Program (SFRP) is open annually to approximately 150 faculty members with at least two years of teaching and/or research experience in accredited U.S. colleges, universities, or technical institutions. SFRP associates must be either U.S. citizens or permanent residents.

The Graduate Student Research Program (GSRP) is open annually to approximately 100 graduate students holding a bachelor's or a master's degree; GSRP associates must be U.S. citizens enrolled full time at an accredited institution.

The High School Apprentice Program (HSAP) annually selects about 125 high school students located within a twenty mile commuting distance of participating Air Force laboratories.

AFOSR also offers its research associates an opportunity, under the Summer Research Extension Program (SREP), to continue their AFOSR-sponsored research at their home institutions through the award of research grants. In 1994 the maximum amount of each grant was increased from $20,000 to $25,000, and the number of AFOSR-sponsored grants decreased from 75 to 60. A separate annual report is compiled on the SREP.

The numbers of projected summer research participants in each of the three categories and SREP "grants" are usually increased through direct sponsorship by participating laboratories.

AFOSR's SRP has well served its objectives of building critical links between Air Force research laboratories and the academic community, opening avenues of communications and forging new research relationships between Air Force and academic technical experts in areas of national interest, and strengthening the nation's efforts to sustain careers in science and engineering. The success of the SRP can be gauged from its growth from inception (see Table 1) and from the favorable responses the 1997 participants expressed in end-of-tour SRP evaluations (Appendix B).

AFOSR contracts for administration of the SRP by civilian contractors. The contract was first awarded to Research & Development Laboratories (RDL) in September 1990. After completion of the 1990 contract, RDL (in 1993) won the recompetition for the basic year and four 1-year options.

2. PARTICIPATION IN THE SUMMER RESEARCH PROGRAM

The SRP began with faculty associates in 1979; graduate students were added in 1982 and high school students in 1986. The following table shows the number of associates in the program each year.

YEAR	SRP Participation, by Year			TOTAL
	SFRP	GSRP	HSAP	
1979	70			70
1980	87			87
1981	87			87
1982	91	17		108
1983	101	53		154
1984	152	84		236
1985	154	92		246
1986	158	100	42	300
1987	159	101	73	333
1988	153	107	101	361
1989	168	102	103	373
1990	165	121	132	418
1991	170	142	132	444
1992	185	121	159	464
1993	187	117	136	440
1994	192	117	133	442
1995	190	115	137	442
1996	188	109	138	435
1997	148	98	140	427
1998	85	40	88	213

Beginning in 1993, due to budget cuts, some of the laboratories weren't able to afford to fund as many associates as in previous years. Since then, the number of funded positions has remained fairly constant at a slightly lower level.

3. RECRUITING AND SELECTION

The SRP is conducted on a nationally advertised and competitive-selection basis. The advertising for faculty and graduate students consisted primarily of the mailing of 8,000 52-page SRP brochures to chairpersons of departments relevant to AFOSR research and to administrators of grants in accredited universities, colleges, and technical institutions. Historically Black Colleges and Universities (HBCUs) and Minority Institutions (MIs) were included. Brochures also went to all participating USAF laboratories, the previous year's participants, and numerous individual requesters (over 1000 annually).

RDL placed advertisements in the following publications: *Black Issues in Higher Education, Winds of Change,* and *IEEE Spectrum.* Because no participants list either *Physics Today* or *Chemical & Engineering News* as being their source of learning about the program for the past several years, advertisements in these magazines were dropped, and the funds were used to cover increases in brochure printing costs.

High school applicants can participate only in laboratories located no more than 20 miles from their residence. Tailored brochures on the HSAP were sent to the head counselors of 180 high schools in the vicinity of participating laboratories, with instructions for publicizing the program in their schools. High school students selected to serve at Wright Laboratory's Armament Directorate (Eglin Air Force Base, Florida) serve eleven weeks as opposed to the eight weeks normally worked by high school students at all other participating laboratories.

Each SFRP or GSRP applicant is given a first, second, and third choice of laboratory. High school students who have more than one laboratory or directorate near their homes are also given first, second, and third choices.

Laboratories make their selections and prioritize their nominees. AFOSR then determines the number to be funded at each laboratory and approves laboratories' selections.

Subsequently, laboratories use their own funds to sponsor additional candidates. Some selectees do not accept the appointment, so alternate candidates are chosen. This multi-step selection procedure results in some candidates being notified of their acceptance after scheduled deadlines. The total applicants and participants for 1998 are shown in this table.

1998 Applicants and Participants			
PARTICIPANT CATEGORY	TOTAL APPLICANTS	SELECTEES	DECLINING SELECTEES
SFRP	382	85	13
(HBCU/MI)	(0)	(0)	(0)
GSRP	130	40	7
(HBCU/MI)	(0)	(0)	(0)
HSAP	328	88	22
TOTAL	840	213	42

4. SITE VISITS

During June and July of 1998, representatives of both AFOSR/NI and RDL visited each participating laboratory to provide briefings, answer questions, and resolve problems for both laboratory personnel and participants. The objective was to ensure that the SRP would be as constructive as possible for all participants. Both SRP participants and RDL representatives found these visits beneficial. At many of the laboratories, this was the only opportunity for all participants to meet at one time to share their experiences and exchange ideas.

5. HISTORICALLY BLACK COLLEGES AND UNIVERSITIES AND MINORITY INSTITUTIONS (HBCU/MIs)

Before 1993, an RDL program representative visited from seven to ten different HBCU/MIs annually to promote interest in the SRP among the faculty and graduate students. These efforts were marginally effective, yielding a doubling of HBCI/MI applicants. In an effort to achieve AFOSR's goal of 10% of all applicants and selectees being HBCU/MI qualified, the RDL team decided to try other avenues of approach to increase the number of qualified applicants. Through the combined efforts of the AFOSR Program Office at Bolling AFB and RDL, two very active minority groups were found, HACU (Hispanic American Colleges and Universities) and AISES (American Indian Science and Engineering Society). RDL is in communication with representatives of each of these organizations on a monthly basis to keep up with the their activities and special events. Both organizations have widely-distributed magazines/quarterlies in which RDL placed ads.

Since 1994 the number of both SFRP and GSRP HBCU/MI applicants and participants has increased ten-fold, from about two dozen SFRP applicants and a half dozen selectees to over 100 applicants and two dozen selectees, and a half-dozen GSRP applicants and two or three selectees to 18 applicants and 7 or 8 selectees. Since 1993, the SFRP had a two-fold applicant increase and a two-fold selectee increase. Since 1993, the GSRP had a three-fold applicant increase and a three to four-fold increase in selectees.

In addition to RDL's special recruiting efforts, AFOSR attempts each year to obtain additional funding or use leftover funding from cancellations the past year to fund HBCU/MI associates.

SRP HBCU/MI Participation, By Year				
YEAR	SFRP		GSRP	
	Applicants	Participants	Applicants	Participants
1985	76	23	15	11
1986	70	18	20	10
1987	82	32	32	10
1988	53	17	23	14
1989	39	15	13	4
1990	43	14	17	3
1991	42	13	8	5
1992	70	13	9	5
1993	60	13	6	2
1994	90	16	11	6
1995	90	21	20	8
1996	119	27	18	7

6. SRP FUNDING SOURCES

Funding sources for the 1998 SRP were the AFOSR-provided slots for the basic contract and laboratory funds. Funding sources by category for the 1998 SRP selected participants are shown here.

1998 SRP FUNDING CATEGORY	SFRP	GSRP	HSAP
AFOSR Basic Allocation Funds	67	38	75
USAF Laboratory Funds	17	2	13
Slots Added by AFOSR (Leftover Funds)	0	0	0
HBCU/MI By AFOSR (Using Procured Addn'l Funds)	0	0	N/A
TOTAL	84	40	88

7. COMPENSATION FOR PARTICIPANTS

Compensation for SRP participants, per five-day work week, is shown in this table.

1998 SRP Associate Compensation

PARTICIPANT CATEGORY	1991	1992	1993	1994	1995	1996	1997	1998
Faculty Members	$690	$718	$740	$740	$740	$770	$770	$793
Graduate Student (Master's Degree)	$425	$442	$455	$455	$455	$470	$470	$484
Graduate Student (Bachelor's Degree)	$365	$380	$391	$391	$391	$400	$400	$412
High School Student (First Year)	$200	$200	$200	$200	$200	$200	$200	$200
High School Student (Subsequent Years)	$240	$240	$240	$240	$240	$240	$240	$240

The program also offered associates whose homes were more than 50 miles from the laboratory an expense allowance (seven days per week) of $52/day for faculty and $41/day for graduate students. Transportation to the laboratory at the beginning of their tour and back to their home destinations at the end was also reimbursed for these participants. Of the combined SFRP and GSRP associates, 65 % claimed travel reimbursements at an average round-trip cost of $730.

Faculty members were encouraged to visit their laboratories before their summer tour began. All costs of these orientation visits were reimbursed. Forty-three percent (85 out of 188) of faculty associates took orientation trips at an average cost of $449. By contrast, in 1993, 58 % of SFRP associates elected to take an orientation visits at an average cost of $685; that was the highest percentage of associates opting to take an orientation trip since RDL has administered the SRP, and the highest average cost of an orientation trip.

Program participants submitted biweekly vouchers countersigned by their laboratory research focal point, and RDL issued paychecks so as to arrive in associates' hands two weeks later.

This is the third year of using direct deposit for the SFRP and GSRP associates. The process went much more smoothly with respect to obtaining required information from the associates, about 15% of the associates' information needed clarification in order for direct deposit to properly function as opposed to 7% from last year. The remaining associates received their stipend and expense payments via checks sent in the US mail.

HSAP program participants were considered actual RDL employees, and their respective state and federal income tax and Social Security were withheld from their paychecks. By the nature of their independent research, SFRP and GSRP program participants were considered to be consultants or independent contractors. As such, SFRP and GSRP associates were responsible for their own income taxes, Social Security, and insurance.

8. CONTENTS OF THE 1998 REPORT

The complete set of reports for the 1998 SRP includes this program management report (Volume 1) augmented by fifteen volumes of final research reports by the 1998 associates, as indicated below:

1998 SRP Final Report Volume Assignments

LABORATORY	SFRP	GSRP	HSAP
Armstrong	2	7	12
Phillips	3	8	13
Rome	4	9	14
Wright	5A, 5B	10	15
AEDC, ALCs, USAFA, WHMC	6	11	

APPENDIX A – PROGRAM STATISTICAL SUMMARY

A. Colleges/Universities Represented

Selected SFRP associates represented 169 different colleges, universities, and institutions, GSRP associates represented 95 different colleges, universities, and institutions.

B. States Represented

SFRP -Applicants came from 47 states plus Washington D.C. Selectees represent 44 states.

GSRP - Applicants came from 44 states. Selectees represent 32 states.

HSAP - Applicants came from thirteen states. Selectees represent nine states.

Total Number of Participants	
SFRP	85
GSRP	40
HSAP	88
TOTAL	213

Degrees Represented			
	SFRP	GSRP	TOTAL
Doctoral	83	0	83
Master's	1	3	4
Bachelor's	0	22	22
TOTAL	186	25	109

SFRP Academic Titles	
Assistant Professor	36
Associate Professor	34
Professor	15
Instructor	0
Chairman	0
Visiting Professor	0
Visiting Assoc. Prof.	0
Research Associate	0
TOTAL	85

Source of Learning About the SRP		
Category	Applicants	Selectees
Applied/participated in prior years	177	47
Colleague familiar with SRP	104	24
Brochure mailed to institution	101	21
Contact with Air Force laboratory	101	39
IEEE Spectrum	12	1
BIIHE	4	0
Other source	117	30
TOTAL	616	162

APPENDIX B -- SRP EVALUATION RESPONSES

1. OVERVIEW

Evaluations were completed and returned to RDL by four groups at the completion of the SRP. The number of respondents in each group is shown below.

Table B-1. Total SRP Evaluations Received

Evaluation Group	Responses
SFRP & GSRPs	100
HSAPs	75
USAF Laboratory Focal Points	84
USAF Laboratory HSAP Mentors	6

All groups indicate unanimous enthusiasm for the SRP experience.

The summarized recommendations for program improvement from both associates and laboratory personnel are listed below:

A. Better preparation on the labs' part prior to associates' arrival (i.e., office space, computer assets, clearly defined scope of work).

B. Faculty Associates suggest higher stipends for SFRP associates.

C. Both HSAP Air Force laboratory mentors and associates would like the summer tour extended from the current 8 weeks to either 10 or 11 weeks; the groups state it takes 4-6 weeks just to get high school students up-to-speed on what's going on at laboratory. (Note: this same argument was used to raise the faculty and graduate student participation time a few years ago.)

2. 1998 USAF LABORATORY FOCAL POINT (LFP) EVALUATION RESPONSES

The summarized results listed below are from the 84 LFP evaluations received.

1. LFP evaluations received and associate preferences:

Table B-2. Air Force LFP Evaluation Responses (By Type)

		How Many Associates Would You Prefer To Get ? (% Response)											
		SFRP				GSRP (w/Univ Professor)				GSRP (w/o Univ Professor)			
Lab	**Evals Recv'd**	**0**	**1**	**2**	**3+**	**0**	**1**	**2**	**3+**	**0**	**1**	**2**	**3+**
AEDC	0	-	-	-	-	-	-	-	-	-	-	-	-
WHMC	0	-	-	-	-	-	-	-	-	-	-	-	-
AL	7	28	28	28	14	54	14	28	0	86	0	14	0
USAFA	1	0	100	0	0	100	0	0	0	0	100	0	0
PL	25	40	40	16	4	88	12	0	0	84	12	4	0
RL	5	60	40	0	0	80	10	0	0	100	0	0	0
WL	46	30	43	20	6	78	17	4	0	93	4	2	0
Total	**84**	**32%**	**50%**	**13%**	**5%**	**80%**	**11%**	**6%**	**0%**	**73%**	**23%**	**4%**	**0%**

LFP Evaluation Summary. The summarized responses, by laboratory, are listed on the following page. LFPs were asked to rate the following questions on a scale from 1 (below average) to 5 (above average).

2. LFPs involved in SRP associate application evaluation process:
   a. Time available for evaluation of applications:
   b. Adequacy of applications for selection process:
3. Value of orientation trips:
4. Length of research tour:
5 a. Benefits of associate's work to laboratory:
   b. Benefits of associate's work to Air Force:
6. a. Enhancement of research qualifications for LFP and staff:
   b. Enhancement of research qualifications for SFRP associate:
   c. Enhancement of research qualifications for GSRP associate:
7. a. Enhancement of knowledge for LFP and staff:
   b. Enhancement of knowledge for SFRP associate:
   c. Enhancement of knowledge for GSRP associate:
8. Value of Air Force and university links:
9. Potential for future collaboration:
10. a. Your working relationship with SFRP:
    b. Your working relationship with GSRP:
11. Expenditure of your time worthwhile:

(Continued on next page)

12. Quality of program literature for associate:
13. a. Quality of RDL's communications with you:
b. Quality of RDL's communications with associates:
14. Overall assessment of SRP:

Table B-3. Laboratory Focal Point Reponses to above questions

	AEDC	*AL*	*USAFA*	*PL*	*RL*	*WHMC*	*WL*
# Evals Recv'd	0	7	1	14	5	0	46
Question #							
2	-	86 %	0 %	88 %	80 %	-	85 %
2a	-	4.3	n/a	3.8	4.0	-	3.6
2b	-	4.0	n/a	3.9	4.5	-	4.1
3	-	4.5	n/a	4.3	4.3	-	3.7
4	-	4.1	4.0	4.1	4.2	-	3.9
5a	-	4.3	5.0	4.3	4.6	-	4.4
5b	-	4.5	n/a	4.2	4.6	-	4.3
6a	-	4.5	5.0	4.0	4.4	-	4.3
6b	-	4.3	n/a	4.1	5.0	-	4.4
6c	-	3.7	5.0	3.5	5.0	-	4.3
7a	-	4.7	5.0	4.0	4.4	-	4.3
7b	-	4.3	n/a	4.2	5.0	-	4.4
7c	-	4.0	5.0	3.9	5.0	-	4.3
8	-	4.6	4.0	4.5	4.6	-	4.3
9	-	4.9	5.0	4.4	4.8	-	4.2
10a	-	5.0	n/a	4.6	4.6	-	4.6
10b	-	4.7	5.0	3.9	5.0	-	4.4
11	-	4.6	5.0	4.4	4.8	-	4.4
12	-	4.0	4.0	4.0	4.2	-	3.8
13a	-	3.2	4.0	3.5	3.8	-	3.4
13b	-	3.4	4.0	3.6	4.5	-	3.6
14	-	4.4	5.0	4.4	4.8	-	4.4

3. 1998 SFRP & GSRP EVALUATION RESPONSES

The summarized results listed below are from the 120 SFRP/GSRP evaluations received.

Associates were asked to rate the following questions on a scale from 1 (below average) to 5 (above average) - by Air Force base results and over-all results of the 1998 evaluations are listed after the questions.

1. The match between the laboratories research and your field:
2. Your working relationship with your LFP:
3. Enhancement of your academic qualifications:
4. Enhancement of your research qualifications:
5. Lab readiness for you: LFP, task, plan:
6. Lab readiness for you: equipment, supplies, facilities:
7. Lab resources:
8. Lab research and administrative support:
9. Adequacy of brochure and associate handbook:
10. RDL communications with you:
11. Overall payment procedures:
12. Overall assessment of the SRP:
13. a. Would you apply again?
    b. Will you continue this or related research?
14. Was length of your tour satisfactory?
15. Percentage of associates who experienced difficulties in finding housing:
16. Where did you stay during your SRP tour?
    a. At Home:
    b. With Friend:
    c. On Local Economy:
    d. Base Quarters:
17. Value of orientation visit:
    a. Essential:
    b. Convenient:
    c. Not Worth Cost:
    d. Not Used:

SFRP and GSRP associate's responses are listed in tabular format on the following page.

Table B-4. 1997 SFRP & GSRP Associate Responses to SRP Evaluation

	Arnold	Brooks	Edwards	Eglin	Griffis	Hanscom	Kelly	Kirtland	Lackland	Robins	Tyndall	WPAFB	average
# res	6	48	6	14	31	19	3	32	1	2	10	85	257
1	4.8	4.4	4.6	4.7	4.4	4.9	4.6	4.6	5.0	5.0	4.0	4.7	4.6
2	5.0	4.6	4.1	4.9	4.7	4.7	5.0	4.7	5.0	5.0	4.6	4.8	4.7
3	4.5	4.4	4.0	4.6	4.3	4.2	4.3	4.4	5.0	5.0	4.5	4.3	4.4
4	4.3	4.5	3.8	4.6	4.4	4.4	4.3	4.6	5.0	4.0	4.4	4.5	4.5
5	4.5	4.3	3.3	4.8	4.4	4.5	4.3	4.2	5.0	5.0	3.9	4.4	4.4
6	4.3	4.3	3.7	4.7	4.4	4.5	4.0	3.8	5.0	5.0	3.8	4.2	4.2
7	4.5	4.4	4.2	4.8	4.5	4.3	4.3	4.1	5.0	5.0	4.3	4.3	4.4
8	4.5	4.6	3.0	4.9	4.4	4.3	4.3	4.5	5.0	5.0	4.7	4.5	4.5
9	4.7	4.5	4.7	4.5	4.3	4.5	4.7	4.3	5.0	5.0	4.1	4.5	4.5
10	4.2	4.4	4.7	4.4	4.1	4.1	4.0	4.2	5.0	4.5	3.6	4.4	4.3
11	3.8	4.1	4.5	4.0	3.9	4.1	4.0	4.0	3.0	4.0	3.7	4.0	4.0
12	5.7	4.7	4.3	4.9	4.5	4.9	4.7	4.6	5.0	4.5	4.6	4.5	4.6
Numbers below are percentages													
13a	83	90	83	93	87	75	100	81	100	100	100	86	87
13b	100	89	83	100	94	98	100	94	100	100	100	94	93
14	83	96	100	90	87	80	100	92	100	100	70	84	88
15	17	6	0	33	20	76	33	25	0	100	20	8	39
16a	-	26	17	9	38	23	33	4	-	-	-	30	
16b	100	33	-	40	-	8	-	-	-	-	36	2	
16c	-	41	83	40	62	69	67	96	100	100	64	68	
16d	-	-	-	-	-	-	-	-	-	-	-	0	
17a	-	33	100	17	50	14	67	39	-	50	40	31	35
17b	-	21	-	17	10	14	-	24	-	50	20	16	16
17c	-	-	-	-	10	7	-	-	-	-	-	2	3
17d	100	46	-	66	30	69	33	37	100	-	40	51	46

4. 1998 USAF LABORATORY HSAP MENTOR EVALUATION RESPONSES

Not enough evaluations received (5 total) from Mentors to do useful summary.

5. 1998 HSAP EVALUATION RESPONSES

The summarized results listed below are from the 23 HSAP evaluations received.

HSAP apprentices were asked to rate the following questions on a scale from
1 (below average) to 5 (above average)

1. Your influence on selection of topic/type of work.
2. Working relationship with mentor, other lab scientists.
3. Enhancement of your academic qualifications.
4. Technically challenging work.
5. Lab readiness for you: mentor, task, work plan, equipment.
6. Influence on your career.
7. Increased interest in math/science.
8. Lab research & administrative support.
9. Adequacy of RDL's Apprentice Handbook and administrative materials.
10. Responsiveness of RDL communications.
11. Overall payment procedures.
12. Overall assessment of SRP value to you.
13. Would you apply again next year? Yes (92 %)
14. Will you pursue future studies related to this research? Yes (68 %)
15. Was Tour length satisfactory? Yes (82 %)

	Arnold	Brooks	Edwards	Eglin	Griffiss	Hanscom	Kirtland	Tyndall	WPAFB	Totals
# resp	5	19	7	15	13	2	7	5	40	113
1	2.8	3.3	3.4	3.5	3.4	4.0	3.2	3.6	3.6	3.4
2	4.4	4.6	4.5	4.8	4.6	4.0	4.4	4.0	4.6	4.6
3	4.0	4.2	4.1	4.3	4.5	5.0	4.3	4.6	4.4	4.4
4	3.6	3.9	4.0	4.5	4.2	5.0	4.6	3.8	4.3	4.2
5	4.4	4.1	3.7	4.5	4.1	3.0	3.9	3.6	3.9	4.0
6	3.2	3.6	3.6	4.1	3.8	5.0	3.3	3.8	3.6	3.7
7	2.8	4.1	4.0	3.9	3.9	5.0	3.6	4.0	4.0	3.9
8	3.8	4.1	4.0	4.3	4.0	4.0	4.3	3.8	4.3	4.2
9	4.4	3.6	4.1	4.1	3.5	4.0	3.9	4.0	3.7	3.8
10	4.0	3.8	4.1	3.7	4.1	4.0	3.9	2.4	3.8	3.8
11	4.2	4.2	3.7	3.9	3.8	3.0	3.7	2.6	3.7	3.8
12	4.0	4.5	4.9	4.6	4.6	5.0	4.6	4.2	4.3	4.5
Numbers below are percentages										
13	60%	95%	100%	100%	85%	100%	100%	100%	90%	92%
14	20%	80%	71%	80%	54%	100%	71%	80%	65%	68%
15	100%	70%	71%	100%	100%	50%	86%	60%	80%	82%

A STUDY OF DNAPL'S IN A HETEROGENEUOS SYSTEM

Brendan O'Sullivan

Mosley High School
501 Mosley Drive
Lynn Haven, FL 32444

Final Report for:
High School Apprentice Program
Armstrong Laboratory

Sponsored by:
Air Force Office of Scientific Research
Bolling Air Force Base, DC

And

Armstrong Laboratory

August 1997

A STUDY OF DNAPL'S IN A HETEROGENEUOS SYSTEM

Brendan O'Sullivan
Mosley High School

Abstract

The movement of a chlorinated solvent in a heterogeneous system is the object of our study. A sand tank, 2 m x 0.5 m 1.02 m, was filled with three types of sand in two patterns. The two patterns were alternated every other layer to provide a heterogeneous system for the experiment. Each layer is 10cm tall by 20cm wide and varied from 25cm deep to 50cm depending on the pattern. Sample ports were added as the layers were poured into the tank. When all ten layers have been poured into the tank, a chlorinated solvent will be injected into a particular area of the tank. Flooding the tank with a slight current going from left to right with de-ionized water begins the experiment. The tank will remain flooded for 6 to 18 months and the movement of the chlorinated solvent will be monitored. A mathematical model of the movement will be developed.

A STUDY OF DNAPL'S IN A HETEROGENEUOS SYSTEM

Chlorinated solvents are big problem because of their low water solubility. They are a long-term groundwater contaminate. The results from this experiment will be compared to the results gathered from the homogeneous system experiment done last year. With the results from both experiments Dr. Hayworth hopes to create a mathematical model that will allow for the radius of the solvents movement to be calculated.

Creating the heterogeneous system was a time consuming experience. Each layer took two people approximately eight hours to build. While filling the tank, sample ports were put in so that water samples can be extracted and tested for the chlorinated solvent. Once the tank has been drained, it will be excavated one centimeter at a time. As each centimeter is excavated, a picture will be taken from above with a digital camera. The pictures are then down loaded in to a computer and a three- dimensional model is created.

We had three different grain sizes of silica sand that were used in filling the tank. The sand is from a quarry in Pennsylvania but packaged by Sands of Time in Ottawa, IL. With the tank completely filled with the sand a distinct pattern is seen. With the tank filled, a DNAPL and other tracers will be injected into the sand. The DNAPL used for this experiment is Tetra Chloral Ethylene. This chlorinated solvent is an EPA Class A carcinogen.

Collecting and analyzing the water samples is a very important part in the experiment. Samples will be taken through a sample port with a hypodermic needle and tested for tetra chloral ethylene and other chemicals such as reaction products. That might have been injected to trace their movement through the sand and reaction with the chlorinated solvent. The need for needles is great because of the size of the tank. Once a needle is used it can not be used again because of the slight chance that after it is cleaned residue of the chlorinated solvent could still be present with its very low water solubility.

PROTECTING AIRCRAFT SURFACES: A STUDY OF ABLATIVE MATERIALS AND THEIR PHYSICAL LIMITATIONS

Jeremy Olson

Centerville High School
500 E. Franklin Street
Centerville, OH 45459

Final Report for:
High School Apprenticeship Program
AFRL/Wright Laboratory

Sponsored by:
Air Force Office of Scientific Research
Bolling Air Force Base, DC

And

Wright Laboratory

August 1998

PROTECTING AIRCRAFT SURFACES: A STUDY OF ABLATIVE MATERIALS AND THEIR PHYSICAL LIMITATIONS

Jeremy Olson

Centerville High School
500 E. Franklin Street
Centerville, OH 45459

Abstract

As part of a larger investigation into the possibilities of protecting aircraft from various high temperature conditions with ablative and intumescent materials, this study has sought to determine the physical limits of these substances. For these tests, several heat-resistant materials from assorted sources were used to coat aluminum, titanium, graphite epoxy and bismaleimide panels. One group of these panels were immersed in water and measured to determine the absorbtion and deformation of the coatings. Another set of panels were subjected to rapid temperature cycles and similar observations were taken. Initial data indicates that several of these materials will be unsuitable for use in high-performance aircraft, and suggests further investigation into the properties of several others. Most materials, however, showed little or no change during the test periods. This study will continue by investigating the effects of several aeronautical fluids and additional physical stresses on these materials.

PROTECTING AIRCRAFT SURFACES: A STUDY OF ABLATIVE MATERIALS AND THEIR PHYSICAL LIMITATIONS

Jeremy Olson

Background

Aircraft require materials which are highly resistant to melting and structural failure under high temperature conditions. Studies conducted by the Air Vehicles Directorate at Wright Patterson Air Force Base in Dayton, OH have indicated that aluminum aircraft skin will suffer complete structural failure after approximately 90-second of exposure to 3000-degree Fahrenheit temperatures produced by an open aircraft fuel (JP-8) fire. As fuel fires are a frequent element of aircraft crashes, studies were needed to determine ways to reduce the loss of critical aircraft parts and protect the crew and passengers. Various ablative and intumescent materials (referred to in this study as ablative materials) were considered as coatings for protecting sensitive aircraft parts. To determine which material provides the best thermal protection and will also survive standard aeronautical conditions, tests were devised to determine physical characteristics of the ablatives that would limit the feasibility of their use on high performance aircraft. The studies described in this paper involves immersing the materials in water and subjecting them to rapid, extreme temperature cycles. Further tests will confirm which coating or coatings are most appropriate for widespread usage.

Methods

The ablative materials were applied at a constant thickness of 1/8 inch to aluminum, titanium, graphite epoxy and bismaleimide panels measuring 3 inches by 8 inches and 4 inches by 4 inches. Four additional ablative materials were intended to be used without a substrate. One of each type of panel was assigned to each test. The control group chosen was the blank bismaleimide and graphite epoxy panels, as no blank titanium or aluminum panels were available. Under the conditions tested in this experiment, titanium and aluminum panels would have been expected to show no change in either thickness or mass, and thus, any change shown by the bismaleimide or graphite epoxy renders our statistical analysis more conservative.

The panels for the thermal cycling test were first photographed and then inserted into a sealed thermal cycling chamber. Each temperature cycle ranged from 160 degrees Fahrenheit to -40 degrees Fahrenheit and back to 160 degrees in a complete cycle of approximately 30 minutes. For the first 5 cycles, the coatings were visually monitored after each cycle and the panels that suffered structural failure were removed. At approximately 5, 10, 50, 100, and 500 cycles, the panels were removed and allowed to cool before measurements were taken. The panels were each massed on a single-beam balance (accuracy ±2 grams) and their thickness along one edge was determined with a pair of electronic calipers.

The immersion test involved placing each panel in a plastic-coated wire baskets for insertion into a tub of distilled water. The panels were first immersed for 1 second and then dried to determine initial values of weight and thickness. Then, the panels were immersed for total times of 5, 10, 30, 60 minutes, 2, 4, 28, and 76 hours. After removal, each panel was massed on an electric balance and thickness at the center of the panel was determined by calipers. During times when testing was not possible, the panels were sealed in airtight containers to prevent water loss.

Mass and thickness data were fit to a straight line versus thermal cycle number or immersion time as appropriate. The line of best fit was determined for each data set, together with the difference of this slope to that of the control group. Data sets were considered different if the difference between the control and experimental groups was larger than the 95% confidence interval of this difference.

Results

Some of the products failed physically during the testing. During the thermal cycling procedure, Flex 117 and Flex 118 underwent complete delamination from their respective substrates after 2 cycles. The ablative remained completely intact and was cleanly separated from the composite it was bonded to. Char IV products separated at around 50 thermal cycles. Complete delamination was never achieved, but clean separation occurred over ~90% of the ablative surface. KMS products warped significantly during the testing (~.100 inch radius) and deep cracks developed, spanning the upper surface. The Firex 2390 ablative, which was originally a yellow color, paled significantly to almost off-white and micro-bubbles began to form. Firex 2555 also changed color and texture, becoming very silvered and rough. Flexfram 605 products formed large >.25 inch bubbles which seemed to be releasing a stick resin by 132 cycles. Lastly, the Fire Research Labs product showed a complex network of cracks by 132 cycles, which steadily grew in size and depth until the end of the test. These cracks eventually began to undercut the ablative, releasing some of the smaller pieces of ablative.

In the water submersion test, the NoFire ablative showed dissolution and structural failure at 30 minutes of soak time. By 2 hours, the product had to be removed to avoid affecting the other products due to its extensive erosion. The Duraboard ablative, a soft standalone ablative, was completely without structure by 2 hours. The MI15 ablative showed a loosening of the top surface of the ablative at 10 minutes, and the rubbery top surface became progressively separated as the test progressed. All of the Dow-Corning products became highly pliable after 30 minutes, and thickness measurements were difficult to collect due to the softness of the material. Firex 2555 became erodable by fingernail after 28 hours. Lastly, the FRC Pyrotechnic ablative completely lost its yellow coloration and became pale and brown.

Table 1 shows the statistical results from this study. The control slopes were not statistically different from zero. However, the only test that resulted in statistically different slopes compared with the control group was the mass of the materials during the water immersion. The materials that experienced a statistically different change in weight compared to the control are highlighted in Table 1.

Table 1: **Mass of ablative materials over time during water immersion.**
Values shown are the best fit slope ±asymptotic standard error

Product Name	Estimated Slope of mass versus time (g/min)	Difference Between Experimental and Control Slopes (g/min)
Amercoat 3335-BMI	.0000586 ± .0004602	.0000471 ± .0005636
Amercoat 3335-GE	.0000293 ± .0004601	.0000178 ± .0005635
Blank-BMI	.0000184 ± .0004600	.0000070 ± .0005634
Blank-GE	.0000045 ± .0004600	-.0000070 ± .0005634
Ceraset-BMI	.0000432 ± .0004600	.0000318 ± .0005634
Ceraset-GE	.0000559 ± .0004600	.0000444 ± .0005634
Char IV-Titanium	.0004408 ± .0004630	.0004293 ± .0005630

Product Name	Estimated Slope of mass versus time (g/min)	Difference Between Experimental and Control Slopes (g/min)
Char IV-Aluminum	.0018419 ± .0015198	.0018304 ± .0018614
Char IV-GE	.0004689 ± .0004646	.0004575 ± .0005690
Char IV-BMI	.0004896 ± .0004636	.0004781 ± .0005678
Courtalds-BMI	.0000665 ± .0004601	.0000551 ± .0005635
Courtalds-GE	-.0000047 ± .0004629	-.0000162 ± .0005669
Dow-Corning 104-Titanium	.0000505 ± .0004600	.0000390 ± .0005634
Dow-Corning 6376-Alum.	.0000460 ± .0004626	.0000345 ± .0005666
Dow-Corning 6378-Titanium	.0000386 ± .0004600	.0000272 ± .0005634
Dow-Corning 36077-GE	.0000381 ± .0004600	.0000267 ± .0005634
Dow-Corning 33516-BMI	.0000114 ± .0004600	-.0000001 ± .0005634
Dow-Corning 33516-GE	.0000164 ± .0004600	.0000050 ± .0005634
Dow-Corning 93104-GE	.0000309 ± .0004600	.0000194 ± .0005634
Dow-Corning 93104-BMI	.0000306 ± .0004600	.0000192 ± .0005634
Dow-Corning 36077-BMI	.0000309 ± .0004600	.0000194 ± .0005634
Dow-Corning-Aluminum	.0000772 ± .0004600	.0000658 ± .0005634
Duraboard	.1156461 ± .0233027	.1156346 ± .0233056
Fire Research Labs-BMI	.0000833 ± .0004601	.0000719 ± .0005635
Fire Research Labs-GE	.0000767 ± .0004601	.0000653 ± .0005635
Firex 2390-BMI	.0001284 ± .0004610	.0001169 ± .0005646
Firex 2555-GE	.0003588 ± .0004615	.0003474 ± .0005652
Firex 2390-GE	.0001413 ± .0004606	.0001298 ± .0005641
Firex 2555-BMI	.0002929 ± .0004617	.0002815 ± .0005654
Flex 119-Aluminum	.0000434 ± .0004600	.0000319 ± .0005634
Flex 117-GE	.0000397 ± .0004600	.0000282 ± .0005634

Product Name	Estimated Slope of mass versus time (g/min)	Difference Between Experimental and Control Slopes (g/min)
Flex 118-Titanium	.0000470 ± .0004600	.0000355 ± .0005634
Flex 117-BMI	.0000415 ± .0004600	.0000300 ± .0005634
Flex 118-BMI	.0000641 ± .0004601	.0000526 ± .0005635
Flex 117-Aluminum	.0000373 ± .0004600	.0000258 ± .0005634
Flex 118-GE	.0000570 ± .0004601	.0000456 ± .0005635
Flex 118-Aluminum	.0000630 ± .0004601	.0000515 ± .0005635
Flex 117-Titanium	.0000356 ± .0004600	.0000242 ± .0005634
Flex 119-Titanium	.0000299 ± .0004601	.0000185 ± .0005635
Flexfram 605-BMI	.0000681 ± .0004601	.0000566 ± .0005635
Flexfram 605-GE	.0000631 ± .0004601	.0000516 ± .0005635
Flexfram 605-Aluminum	.0000508 ± .0004600	.0000393 ± .0005634
Flexfram605-Titanium	.0000477 ± .0004601	.0000363 ± .0005635
FM26-Aluminum	.0001356 ± .0004602	.0001242 ± .0005636
FM26-Titanium	.0001170 ± .0004601	.0001056 ± .0005635
FRC Pyrotechnics-GE	.0003359 ± .0004612	.0003244 ± .0005648
FRC Pyrotechnics-BMI	.0000931 ± .0004601	.0000816 ± .0005635
Haveg 41N	.0002858 ± .0004611	.0002743 ± .0005647
Kmass-BMI	.0001032 ± .0004602	.0000918 ± .0005637
Kmass-GE	.0000683 ± .0004601	.0000569 ± .0005635
KMS-C Hex-Aluminum	.0003804 ± .0004628	.0003689 ± .0005668
KMS-C Round-Titanium	.0003330 ± .0004616	.0003215 ± .0005653
KMS-C-Aluminum	.0002639 ± .0004606	.0002524 ± .0005642
KMS-C-Hex-Titanium	.0003919 ± .0004627	.0003804 ± .0005667
KMS-C-Round-Aluminum	.0003071 ± .0004611	.0002956 ± .0005647

Product Name	Estimated Slope of mass versus time (g/min)	Difference Between Experimental and Control Slopes (g/min)
KMS-C-Titanium	.0006431 ± .0006640	.0006317 ± .0008132
KMS-M Round-Titanium	.0002498 ± .0004604	.0002383 ± .0005639
KMS-M Round-Titanium	.0002465 ± .0004607	.0002350 ± .0005642
KMS-M-Aluminum	.0002391 ± .0004603	.0002277 ± .0005638
KMS-M-Hex-Titanium	.0002636 ± .0004610	.0002525 ± .0005646
KMS-M-Titanium	.0002479 ± .0004606	.0002365 ± .0005641
MA25-BMI	.0000488 ± .0004600	.0000373 ± .0005634
MA25-GE	.0003346 ± .0004643	.0003231 ± .0005686
MA25TC-Aluminum	.0010493 ± .0004756	.0010378 ± .0005825
MA25TC-Titanium	.0011276 ± .0004713	.0011161 ± .0005773
MI 15TC-Titanium	.0022804 ± .0004773	.0022689 ± .0005846
MI 15TC-Aluminum	.0019497 ± .0004633	.0019383 ± .0005675
MXBE 350	.0000783 ± .0004601	.0000668 ± .0005635
MXBE 360	.0001784 ± .0004606	.0001670 ± .0005642
NoFire-BMI	.0021060 ± .0014570	.0020945 ± .0015015
NoFire-GE	.0004968 ± .0015147	.0004854 ± .0015610
Nusil 9975-GE	.0000608 ± .0004600	.0000493 ± .0005634
Nusil 9702-Titanium	.0000851 ± .0004602	.0000737 ± .0005636
Nusil 9975-BMI	.0000447 ± .0004600	.0000333 ± .0005634
Nusil 9702-Aluminum	.00010000 ± .0004600	.0000886 ± .0005634
Pitchar-BMI	.0012411 ± .0004740	.0012296 ± .0005805
Pitchar-GE	.0013081 ± .0004617	.0012966 ± .0005900

Discussion

These results indicate that most products did not undergo any significant change as a result of the thermal cycle or water immersion tests. However, those products that have shown a significant change necessitate further testing. This test involved only one panel of each product and a limited number of physical characteristics. Further testing needs to be done to secure the significance of the changes that have been observed and to uncover any other physical limitations that these products may have.

Furthermore, a more accurate method of measuring the thickness of these panels needs to be developed. For many of these materials, repeteated thickness measurements varied by as much as .20 inches due to the extreme surface roughness. This inaccuracy may make otherwise significant coating growth negligible.

In conclusion, those products that have showed significant physical failure, either by erosion or separation after prolonged exposure to these physical conditions are not suitable for general aviation use. Further testing can establish what products are acceptable and offer the optimum protection for the pilot and aircraft over a wide range of possible conditions.

A STUDY OF HYPERSPECTRAL IMAGING (HSI)

Disha Jayantilal Patel

Kettering Fairmont High School
3301 Shroyer Road
Kettering, Ohio 45429

Final Report for:
High School Apprenticeship Program

Sponsoring Laboratory:
Wright Laboratory-AFRL/SNAS

Sponsored by:
Air Force Office of Scientific Research
Bolling Air Force Base, Washington DC

and

Wright Laboratory

and

Wright Patterson Air Force Base, OH

21 August 1998

A STUDY OF HYPERSPECTRAL IMAGING (HSI)

Disha Jayantilal Patel
Kettering Fairmont High School

Abstract

Research was done on hyperspectral imaging (HSI). HSI is a fairly recent, technological advancement in the research and development field. HSI uses hundreds of contiguous, discrete spectral bands at a resolution of 5 to 10 nanometers (nm) in order to identify and discriminate targets from their backgrounds. HSI is commonly used in agricultural and environmental monitoring as well as military target discrimination. The project that was researched dealt mainly with military target discrimination (whether a friend or foe, target typing, mine detection, etc.). The primary purpose of the research was to extract 2x2 pixels from six vehicle targets and from three backgrounds and compare their spectral responses to each other using MATLAB programming. However, before extraction of the pixels could occur, HSI and MATLAB concepts had to be understood. After these concepts were understood, extraction of the pixels and signature matching began. Experimental results indicated that even though everything was performed correctly, the signature matching process did not come out the way it was supposed to. The two remaining pixels from each graph did not match with their corresponding graph mean. For example, target A sample did not match with the target A mean. However, even though errors hindered the research, progress was made in the areas of learning MATLAB, learning how to use HSI imaging, and learning how to do signature matching. Overall, this research will continue to help in the improvement of HSI technique.

A STUDY OF HYPERSPECTRAL IMAGING (HSI)

Disha Jayantilal Patel

Introduction

Research was done on discriminating targets with the use of hyperspectral imaging (HSI). Hyperspectral imaging is a fairly recent, technological advancement in the research and development field. HSI started in the 1970's with the evolution and development of the Scanning Imaging Spectroradiometer (SIS). HSI technically developed from multispectral imaging, a technique used to identify images using small number of broad spectral bands. HSI uses hundreds of contiguous, discrete spectral bands at a resolution of 5 to 10 nm in order to identify and discriminate targets from their backgrounds. HSI uses discrete detectors to split image data into multiple spectral bands. These bands are important because they help detect the difference between one target and another. In addition, the more spectral bands, the more detail is seen.

Some of the instruments used in HSI are AVIRIS, TRWIS A, TRWIS B, TRWIS II, HYDICE, and TRWIS III. The primitive instruments used small numbers of spectral bands that measured wavelength from 100-200 nm. However, through continuous development, instruments like the TRWIS III, can measure hundreds of spectral bands from 400 to 2500 nm.

HSI is regularly used in agricultural productivity, environmental monitoring, natural resource management, geological surveying, urban planning, fishing, and military target discrimination. This project dealt mainly with military target discrimination. HSI helps in figuring out if the aircraft/vehicle is a friend or foe and it helps in target typing and mine detection.

HSI works on a 3-plane coordinate system-the x and y coordinates (the 2 spatial dimensions) and the wavelength coordinate (the spectral axis). It typically uses a 2-D matrix array and produces a 3-D data cube.

Overall, HSI is a beneficial technique to discriminate between objects and is a technique that continues to undergo improvements.

Purpose

There were numerous purposes for this research project. A principle purpose was to extract 2x2 pixels from six vehicle targets and from three backgrounds and compare their spectral responses to each other using MATLAB. Another purpose was to become computer literate with MATLAB. One other purpose was to strengthen my science and math skills.

Problem

The problem that needed to be solved was to learn how to use MATLAB in order to extract 2x2 pixels from three backgrounds and from the center of six targets. Furthermore, each pixel had 49 spectral bands. The other problem was to come up with an x-axis that corresponded the 49 spectral bands to wavelength (400-2500nm) measurements and compare the spectral response of each pixel of the nine images to each other.

Methodology

In order to solve the problems, several steps were taken and several materials were needed. The materials needed were a PC, the MATLAB program, the HSI image of the targets and backgrounds, and instructional books on HSI. The first step was to understand the concept of HSI, and followed by understanding MATLAB. In order to grasp these concepts, reading was done, notes were taken, and explanations by the mentor occurred. After grasping those concepts, the next step was to study the HSI image that contained the six targets and three backgrounds. Then, a 2x2 pixel block had to be extracted from each target and background. The centers of the targets were extracted and three background examples were extracted. After each target/background was extracted, they were saved. Then, after collecting nine samples, using MATLAB, each target/background's spectral response was graphed. Four pixels were extracted for each target/background, resulting in a total of 36 readings. These graphs were saved after the x-axis was changed into wavelength. After that, the problem of matching the targets had to be tackled. In order to do this, the two highest readings from each of the nine targets were taken. A mean was produced for each of the targets/backgrounds. For example, target A had a mean, target B had a mean, target C had a mean, and so on. Then the remaining two readings from each graph were saved and compared to the mean average of all the target samples. For example, from target A one of the remaining two readings would be compared to mean target A, B, C, D, E, F, background A, B, and C. Then the remaining reading from target A would be compared to all the means. This would be repeated for all the targets/backgrounds. The numbers were recorded. After getting all the numbers, for each of the remaining readings, the numbers were compared. The smallest number meant that the target/background was the closest to that respective target/background. So, each of the remaining two readings from each target/background were compared to each of the means from target A to background C, and the background/target which matched the background/target with the lowest number was classified to the respective class.

Data/Results

The following results are from all the work that was done:

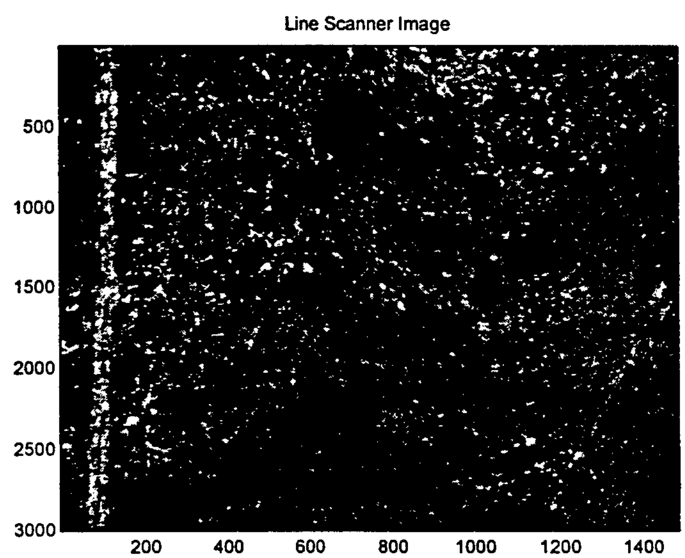

HSI Image

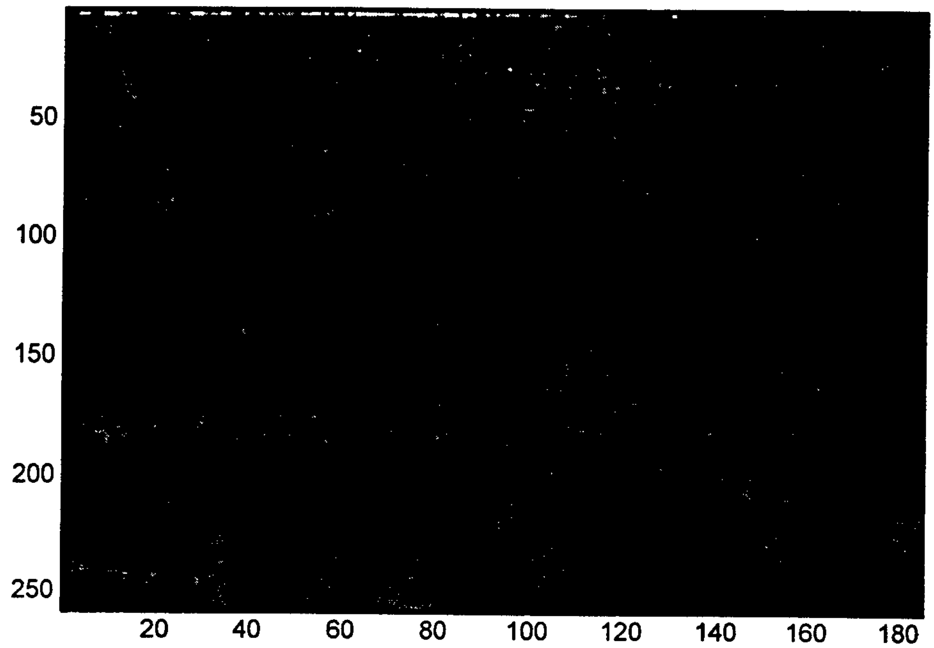

Target A Spectral Response

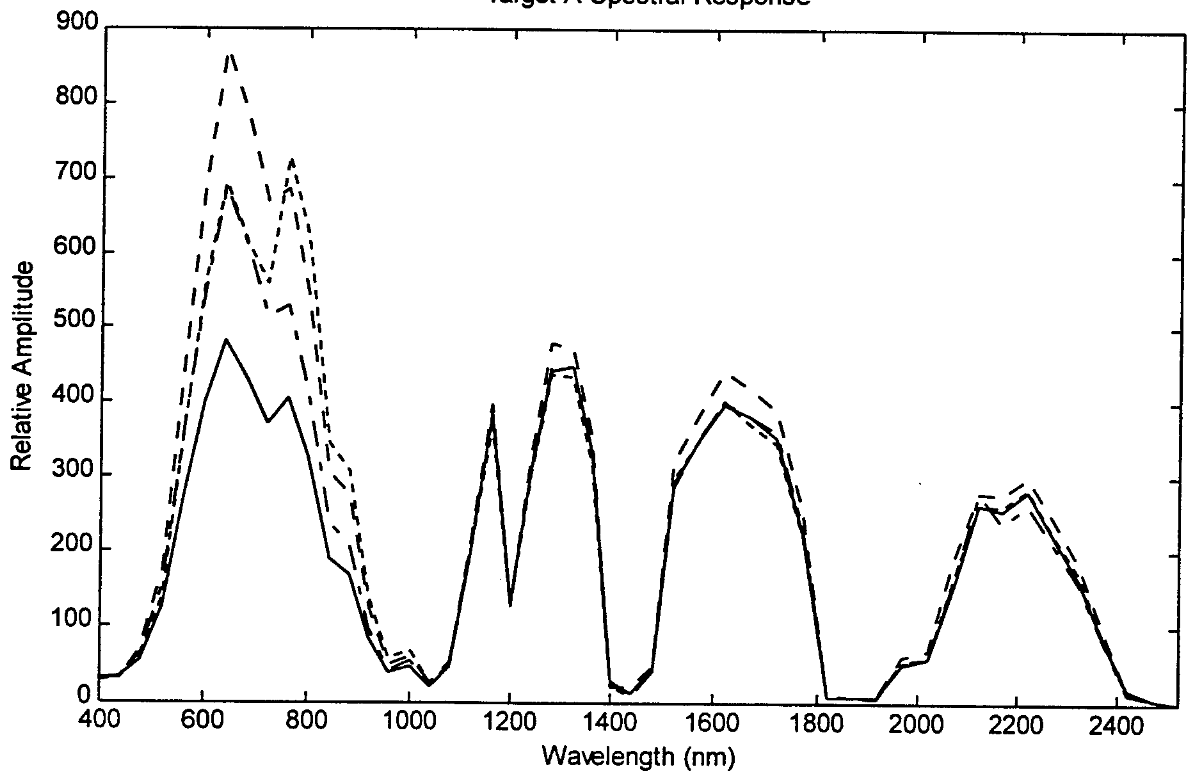

Target B Spectral Response

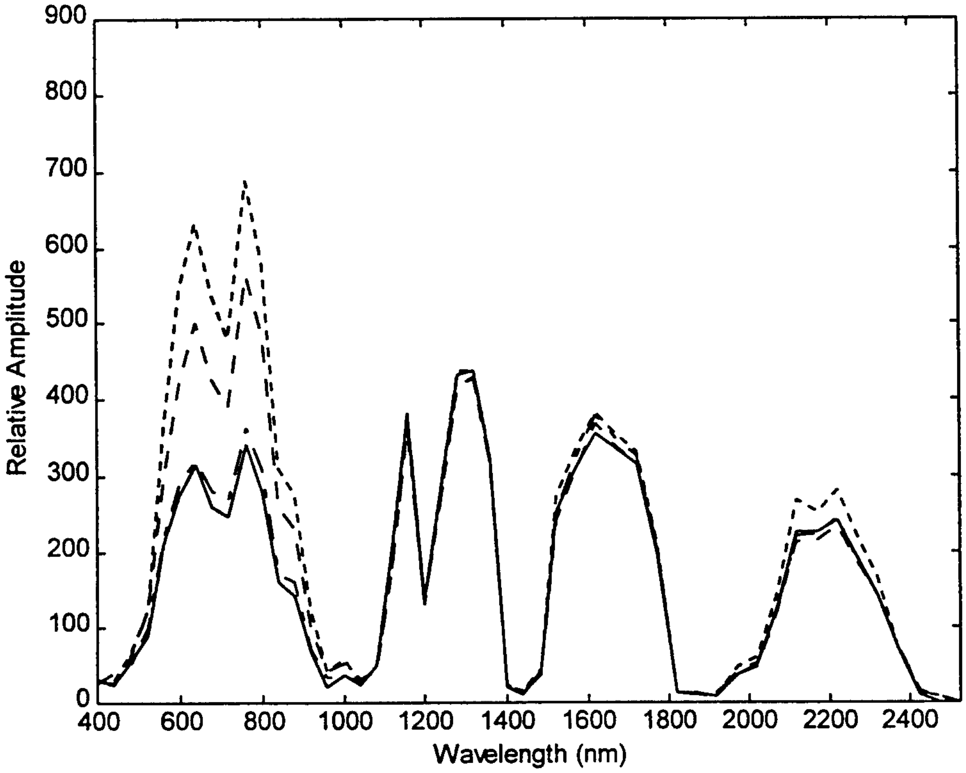

Target C Spectral Response

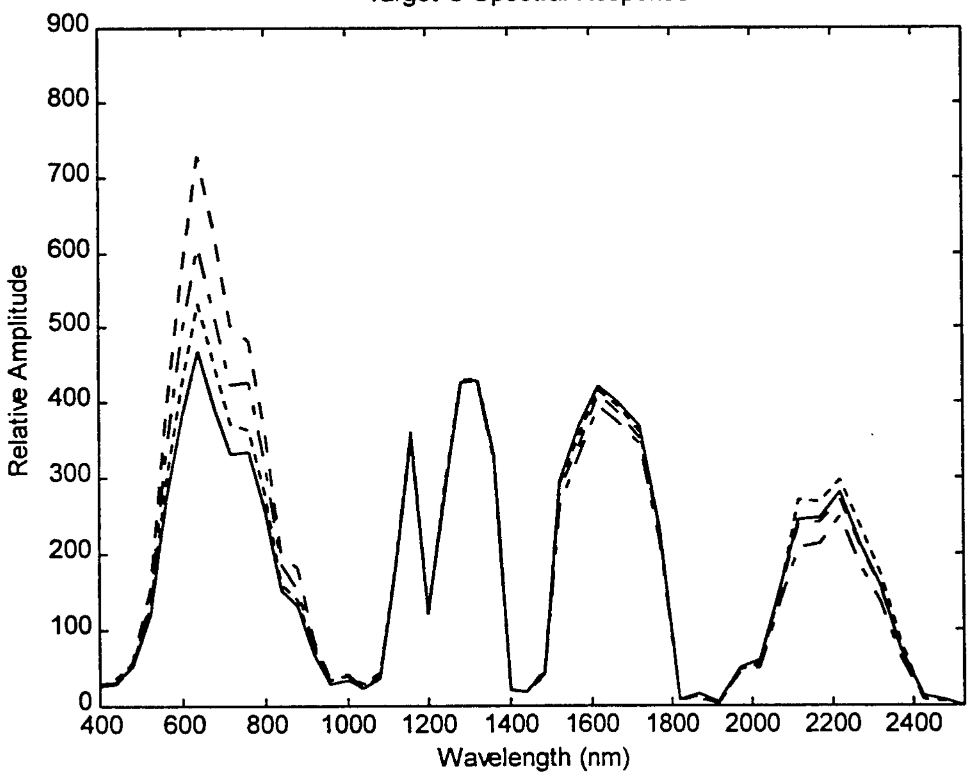

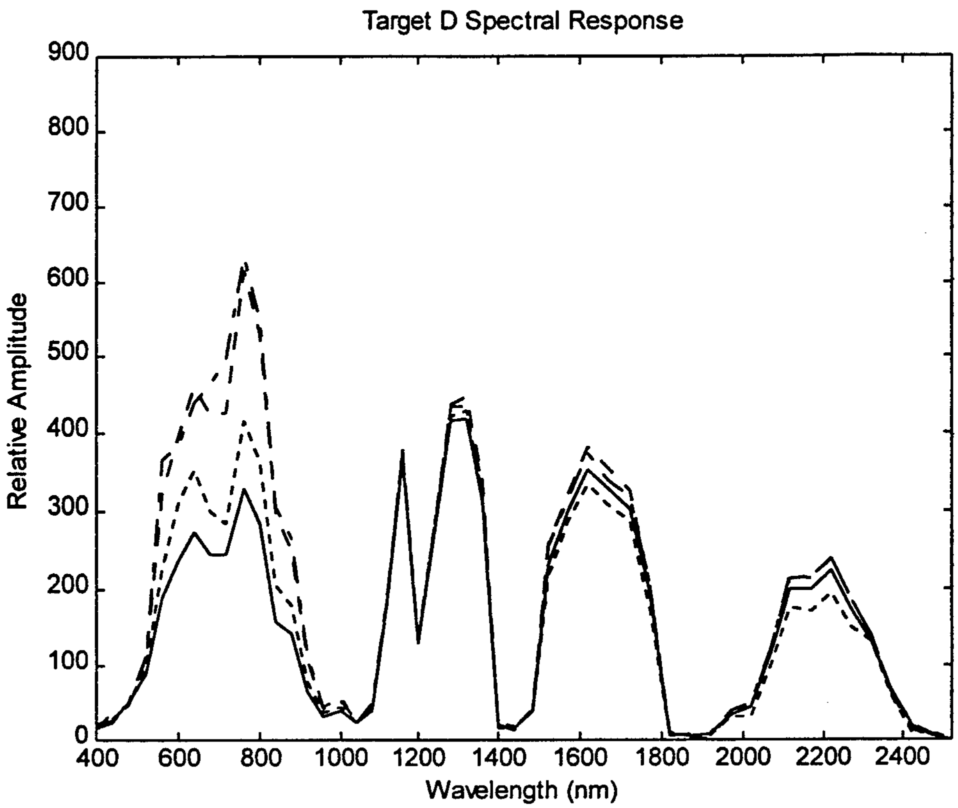
Target D Spectral Response
Relative Amplitude
Wavelength (nm)
0
100
200
300
400
500
600
700
800
900
400
600
800
1000
1200
1400
1600
1800
2000
2200
2400

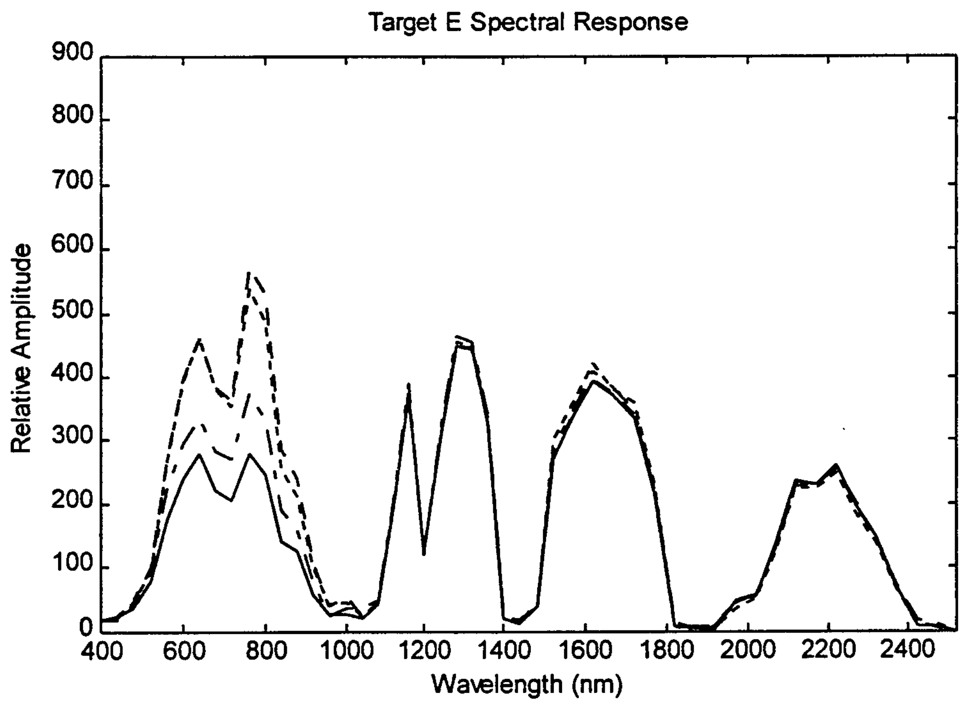
Target E Spectral Response
Relative Amplitude
Wavelength (nm)
0
100
200
300
400
500
600
700
800
900
400
600
800
1000
1200
1400
1600
1800
2000
2200
2400

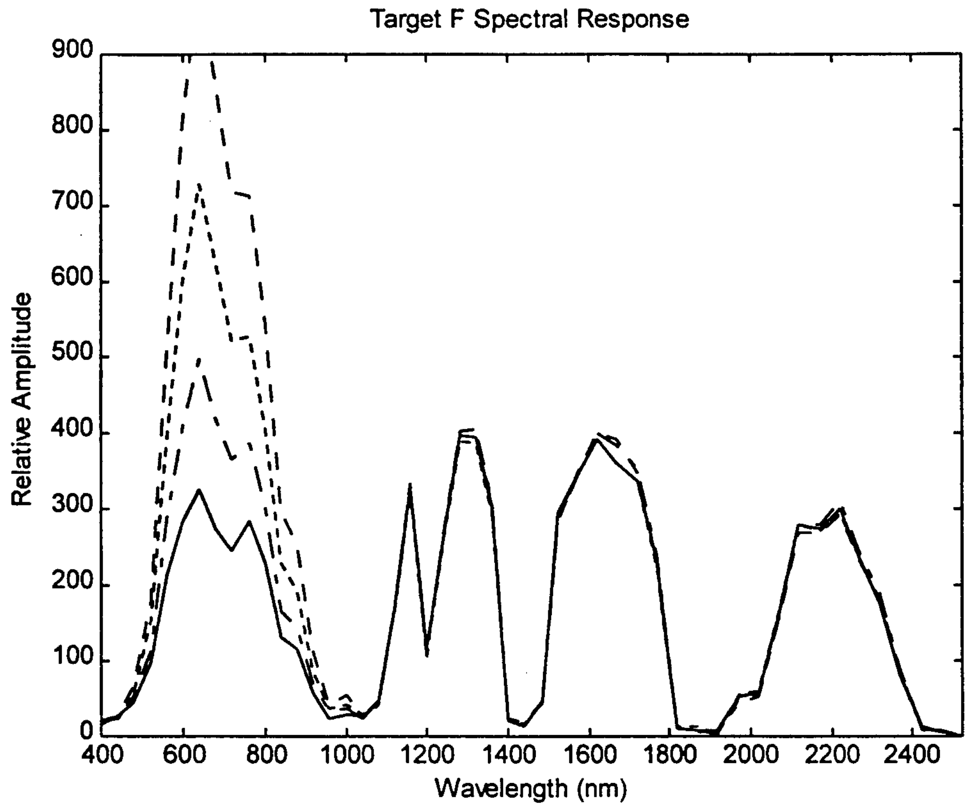
Target F Spectral Response
Relative Amplitude
Wavelength (nm)
0
100
200
300
400
500
600
700
800
900
400
600
800
1000
1200
1400
1600
1800
2000
2200
2400

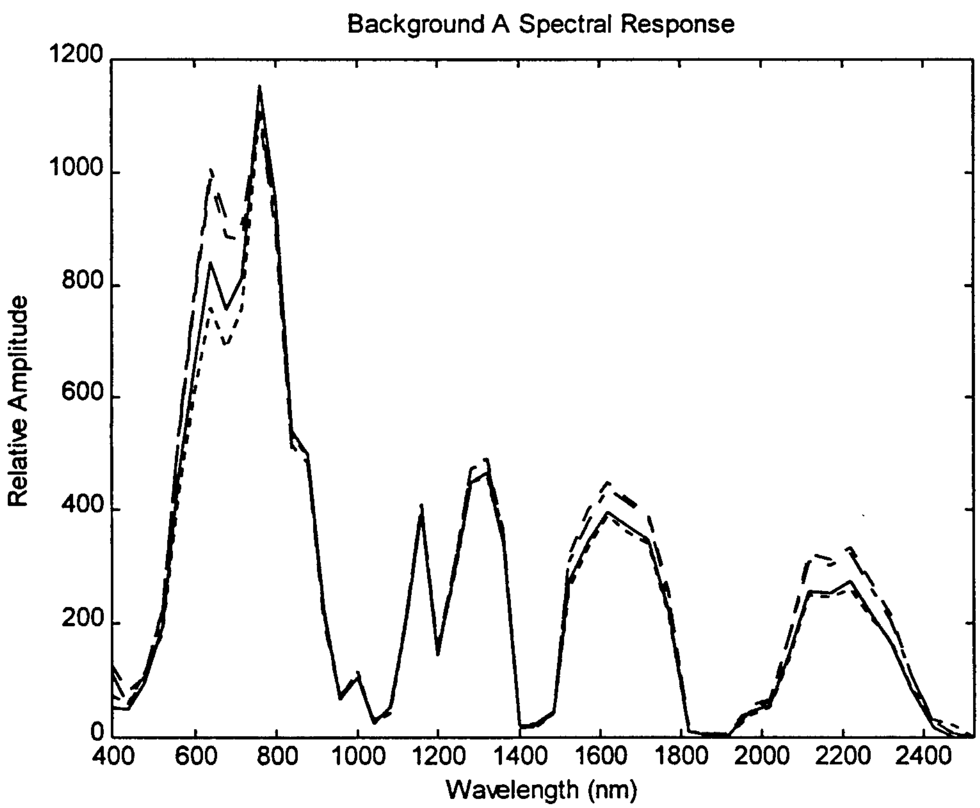
Background A Spectral Response
Relative Amplitude
Wavelength (nm)
0
200
400
600
800
1000
1200
400
600
800
1000
1200
1400
1600
1800
2000
2200
2400

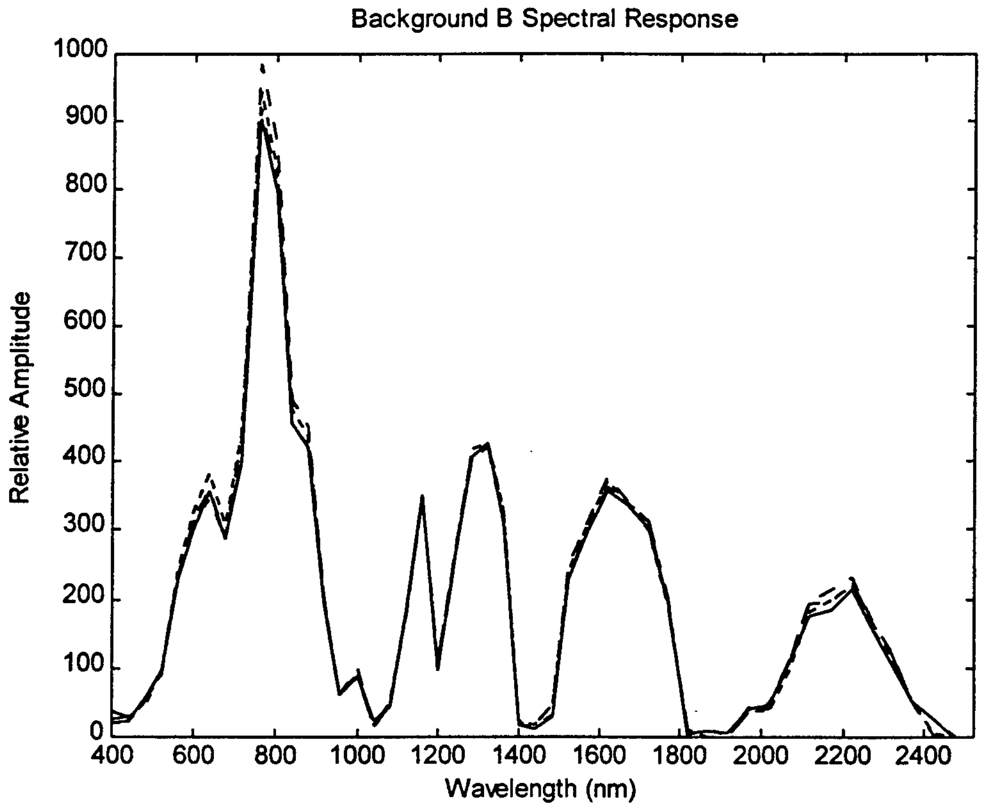
Background B Spectral Response
Relative Amplitude
Wavelength (nm)
1000
900
800
700
600
500
400
300
200
100
0
400
600
800
1000
1200
1400
1600
1800
2000
2200
2400

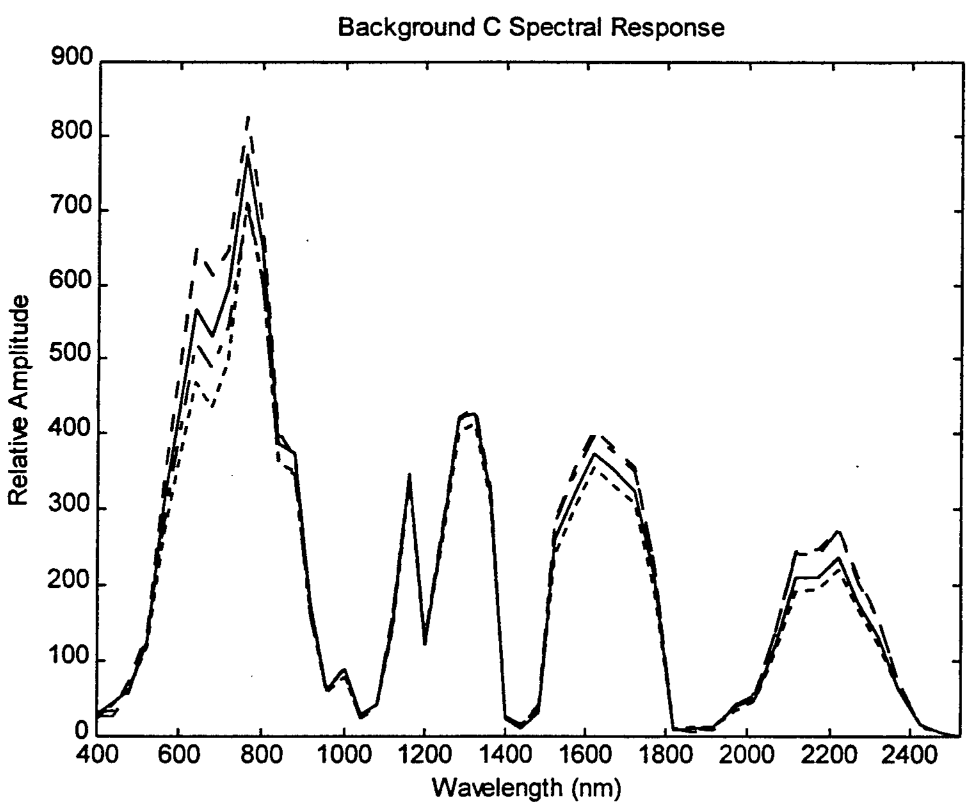
Background C Spectral Response
Relative Amplitude
Wavelength (nm)
900
800
700
600
500
400
300
200
100
0
400
600
800
1000
1200
1400
1600
1800
2000
2200
2400

Signature Matching

Target A Pixel (1,1) closely matched Target E

Target A Pixel (2,1) closely matched Target C

Target B Pixel (1,1) closely matched Target E

Target B Pixel (2,1) closely matched Target E

Target C Pixel (1,1) closely matched Target E

Target C Pixel (1,2) closely matched Target C

Target D Pixel (1,1) closely matched Target E

Target D Pixel (1,2) closely matched Target E

Target E Pixel (1,1) closely matched Target E

Target E Pixel (2,1) closely matched Target E

Target F Pixel (1,1) closely matched Target E

Target F Pixel (2,1) closely matched Target C

Background A Pixel (1,2) closely matched Background A

Background A Pixel (2,2) closely matched Background A

Background B Pixel (1,1) closely matched Background B

Background B Pixel (2,1) closely matched Background B

Background C Pixel (1,2) closely matched Target D

Background C Pixel (2,1) closely matched Background C

Conclusion

From the results of this research project, even though everything was done correctly, the matching process did not come out the way it was supposed to. Technically, the remaining two readings from each graph should have matched up with their corresponding target/background. For example, the readings from target A should have matched up with target A, but that did not happen. Possible reasons for the mismatches are that the signatures may need to be energy normalized, calibration needs to be improved, or more sophisticated matching techniques need to be employed. However, calibrating the graphs so that the detector response would read more easily would take extra time. However, overall, from this research a lot was learned and a lot of improvements were made in the HSI field.

References

1. Bryski, Daniel D. "Baseline Collection-System Operating Parameter Analysis." NVESD, 27 Mar 1998.

2. Folkman, Mark A., Raymond K. Delong, Charles T. Willoughby, Darrell Gleichauf, Sveinn Thordarson, Miguel Figueroa, and Wes Procino. TRWIS III: An Aircraft Based Hyperspectral Imager. Redondo Beach: TRW Space and Electronics Group, 14 Mar 1996.

3. Gat, Nahum, and Suresh Subramanian. "Spectral Imaging: Technology and Applications." OKSI, 1 Feb 1997.

4. Lewotsky, Kristin. "Hyperspectral Imaging: Evolution of Imaging Spectrometry." SPIE, Nov 1994.

5. MATLAB. Natick: The Math Works, Inc., Aug 1992.

6. My mentor, Steve Worrell, gave oral tutorials.

THE EFFECTS OF TARGET MOTION ON CRITICAL MOBILE TARGET ALGORITHM PERFORMANCE

Kathleen A. Pirog

Niceville High School
800 East John Sims Parkway
Niceville, FL 32578

Final Report for:
High School Apprenticeship Program
AFRL/Wright Laboratory

Sponsored by:
Air Force Office of Scientific Research
Bolling Air Force Base, DC

And

Wright Laboratory

August 1998

THE EFFECTS OF TARGET MOTION ON CRITICAL MOBILE TARGET ALGORITHM PERFORMANCE

Kathleen A. Pirog

Abstract

The purpose of the Critical Mobile Target (CMT) algorithm is to detect and identify targets in laser radar (LADAR) imagery. A study of the effects of target motion on CMT algorithm performance and accuracy was undertaken. Synthetically generated LADAR imagery containing images of nine targets moving at four speeds was run through the CMT algorithm on a UNIX-based workstation. The data was also hand-truthed for comparison purposes. The results of the CMT algorithm runs were evaluated using segmentation quality, probability of detection, probability of correct identification, and probability of correct identification given detection performance metrics calculated on an Excel spreadsheet. These results revealed that target motion had little effect on either the segmentation or detection portions of the CMT algorithm, but that during the classification stage of the algorithm, the probability of correct identification dropped off slightly when target motion increased. However, poor overall classification results indicate underlying problems, possibly stemming from poorly centered reference models. Secondary processing with new models was not completed, making validation of the results of this study impossible at this time.

THE EFFECTS OF TARGET MOTION ON CRITICAL MOBILE TARGET ALGORITHM PERFORMANCE

Kathleen A. Pirog

Introduction:

The purpose of the Critical Mobile Target (CMT) algorithm is to detect and identify targets in laser radar (LADAR) imagery. It consists of two program modules, the segmentation/detection (SegDet) module and the classification module. The SegDet module operates on raw LADAR data, grouping pixels together into regions and detecting potential target regions by comparing region pixel count and target measurements to a supplied list of minimums and maximums. Segmentation is the process of grouping pixels together based on pixel range and intensity data. Once the regions defined by the edges have been grouped together, detection can take place. Detection occurs when the properties of the region fit within the specified detection limits, which regulate potential target dimensions and pixel on target count. Detected targets are passed on as potential target regions to the classification module. In the classification module, the target's orientation, or pose angle, is determined based on a long-axis measurement. This stage also renders pixel projections of a list of reference models. The rendered models are then compared to the target region, and the model most closely matching the target is given as the target's identification.

As its name suggests, the Critical Mobile Target algorithm must be able to detect and identify *mobile* targets. While the performance of the CMT algorithm against stationary mobile targets has been evaluated, a study of CMT algorithm performance against moving mobile targets was needed. Synthetic LADAR imagery containing images of M-1, M-2, SA-6, SA-13, ZSU-23/4, BTR-70, MAZ-543, BMP-1, and BMP-2 target vehicles either at rest or moving at speeds of 10, 20, or 30 meters per second was generated for this study. The goal of this project was to determine if target motion affected the various aspects of CMT algorithm performance.

Procedure:

Each synthetically generated LADAR image consisted of nine target vehicles of the same type moving outward at the same speed. In order to process these images, it was necessary first to convert the imagery into a format compatible with the CMT algorithm. Then, each image had to be truthed to extract and measure each target. First, individual vehicles were pulled out of larger composite images, as seen Figure T-1. Their pose angles were measured. Also, length, width, and height measurements were taken and averaged for each vehicle type. These averages were used as a basis of comparison with the listed model measurements to ensure that the models and the targets they were being matched to were approximately the same size. The number of pixels on target was also recorded. Since the purpose of the SegDet algorithm is to isolate potential target regions, this first stage seemed extraneous. However, the truthing stage was necessary to provide a basis for comparison with the next stage, the segmentation/detection stage.

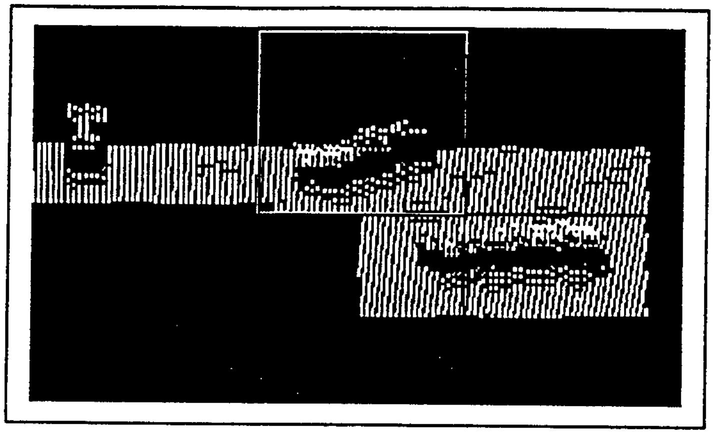

Figure T-1: SA-6 composite image

Using a command line script file, each image was passed through the SegDet portion of the CMT algorithm. After each run, the number of detected targets was recorded. If necessary, the minimum number of pixels on target detection limit was lowered until all of the targets had been successfully detected. At this point, the segmentation quality metric and the probability of detection metric were calculated. Segmentation quality is defined as:

$$SegQual = \frac{count(T \cap S)}{count(T \cup S)}$$

where T is the set of pixels counted in the truthing stage and S is the set of pixels counted by the SegDet program module. This metric gives an idea of how well the set of pixels grouped together by the algorithm compares with the set of pixels manually selected. Probability of detection is defined as the number of successfully detected targets divided by the total number of targets imaged. This metric evaluates the performance of the CMT algorithm by determining the likelihood of the SegDet portion of algorithm to accurately detect and report targets.

Using the measurements gathered in the truthing process, a list of reference models, one of which is seen in Figure M-1, was created. An input file was made with the names of all of the detected images, which was then run through the classification module of the CMT algorithm. The classifier matched rendered reference models with the detected target regions and output a list of identified targets. At this point, the probability of correct identification and probability of correct identification given detection metrics were calculated. The probability of correct identification is defined as the number of correctly identified targets divided by the total number of targets imaged. This gives an overall view of the performance of the CMT algorithm. The probability of correct identification given detection is defined as the number of correctly identified targets divided by the total number of targets detected. The probability of correct identification given detection gives a closer look at how the classification portion of the algorithm performs alone since it removes the number of targets not detected by the SegDet module that therefore cannot be properly identified.

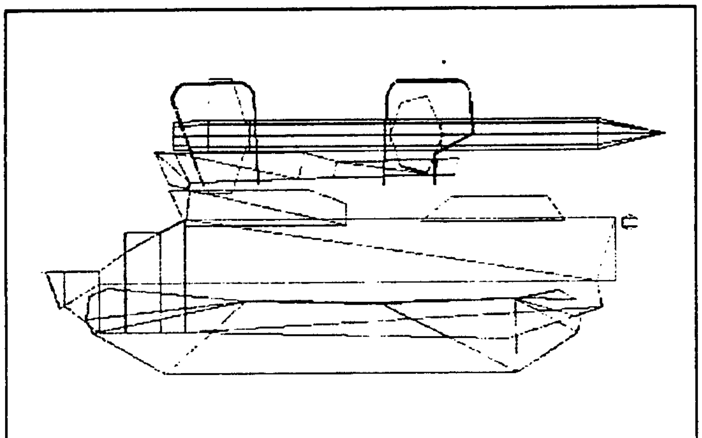

Figure M-1: SA-6 reference model

Results:

The SegDet portion of the algorithm successfully segmented all 648 targets. The overall mean segmentation quality was 0.85 with a minimum value of 0.28 and a maximum of 1.00. Complete overall segmentation quality results can be found in Table S-1, target by target results in Table S-2, and speed results in Table S-3. Bar graphs of target by target and speed segmentation quality results can be found in Figures S-2 and S-3, respectively.

Table S-1: Segmentation Quality Statistics

OVERALL	Value
Mean	0.85
Median	0.87
Standard Deviation	0.08
Minimum	0.28
Maximum	1.00
Data Points	648

Table S-2: Target by Target Segmentation Quality Statistics

Target	Mean SegQual
M-2	0.81
M-1	0.88
SA-6	0.85
SA-13	0.86
ZSU-234	0.84
BTR-70	0.86
MAZ-543	0.88
BMP-1	0.83
BMP-2	0.83

Table S-3: Speed Segmentation Quality Statistics:

Speed	Mean SegQual
0 m/s	0.85
10 m/s	0.84
20 m/s	0.85
30 m/s	0.85

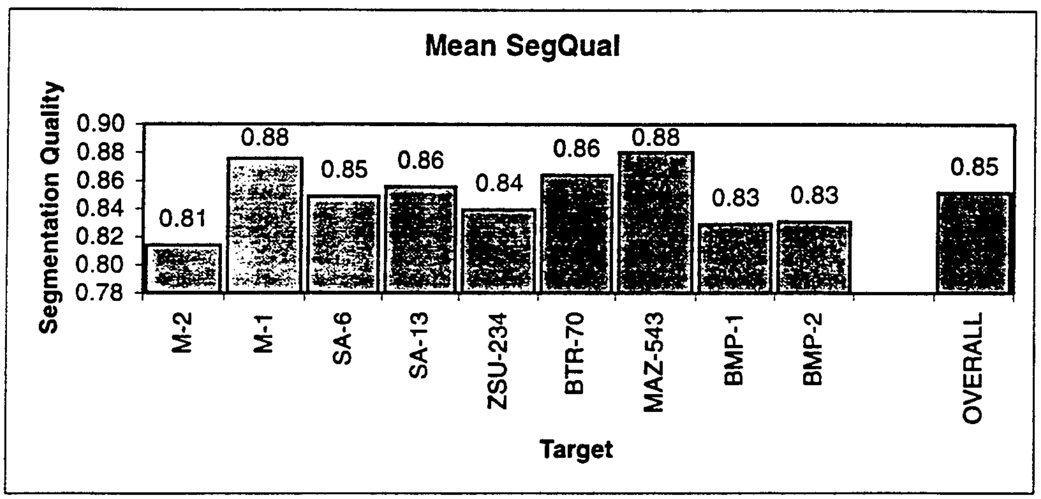

Figure S-1: Target by Target Segmentation Quality Results

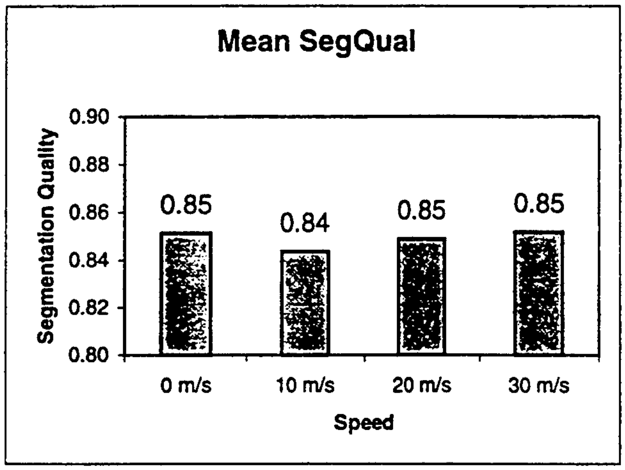

Figure S-2: Speed Segmentation Quality Results

As seen in Table S-3 and Figure S-2, target motion appears to have no readily determined effect on segmentation quality.

Target detection results were similar. With a minimum of 50 pixels on target, 589 of 648 targets were detected for a probability of detection of 0.91. Since the targets appearing in the imagery generated for this study were imaged at a distance greater than usual, the pixel on target count was lower than usual. When the minimum number of pixels on target was reduced to 25 pixels to compensate for this extra distance, only two of the 648 targets were not detected resulting in a probability of detection of 0.99. Target by target and speed probability of detection results are shown in tables D-1 and D-2, and bar graphs are available in Figures D-1 and D-2, respectively.

Table D-1: Target by Target Detection Results

Target	Min. 50	Min. 25
M-2	64	71
M-1	72	72
SA-6	66	72
SA-13	63	72
ZSU-234	69	71
BTR-70	61	72
MAZ-543	72	72
BMP-1	61	72
BMP-2	61	72
OVERALL	589	646

Table D-2: Speed Detection Results

Speed	Min. 50	p(D) at 50	Min. 25
0 m/s	148	0.91	162
10 m/s	146	0.90	161
20 m/s	148	0.91	162
30 m/s	146	0.90	161

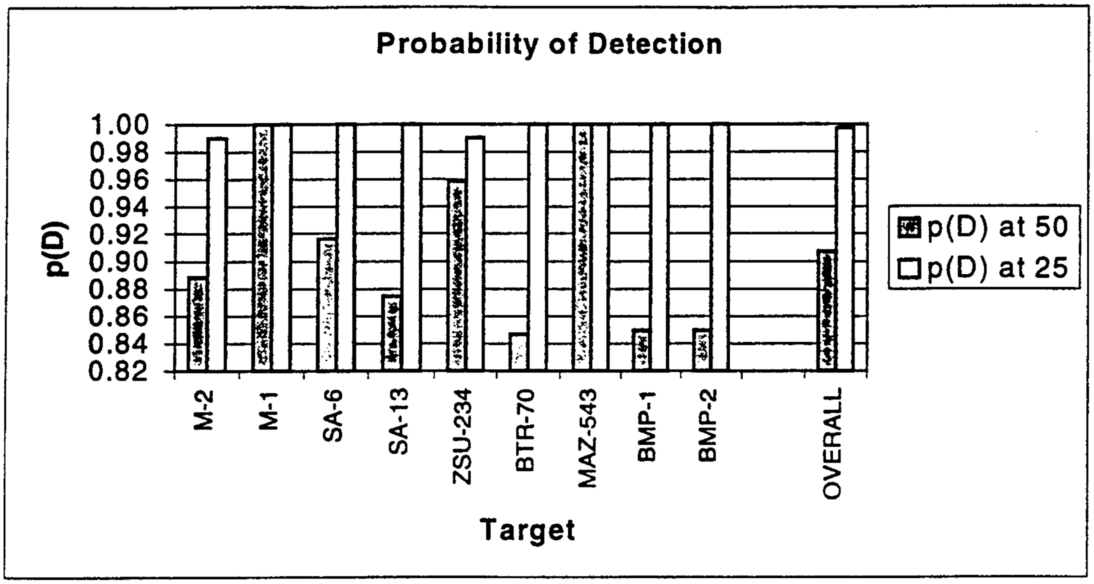

Figure D-1: Target by Target Probability of Detection Results

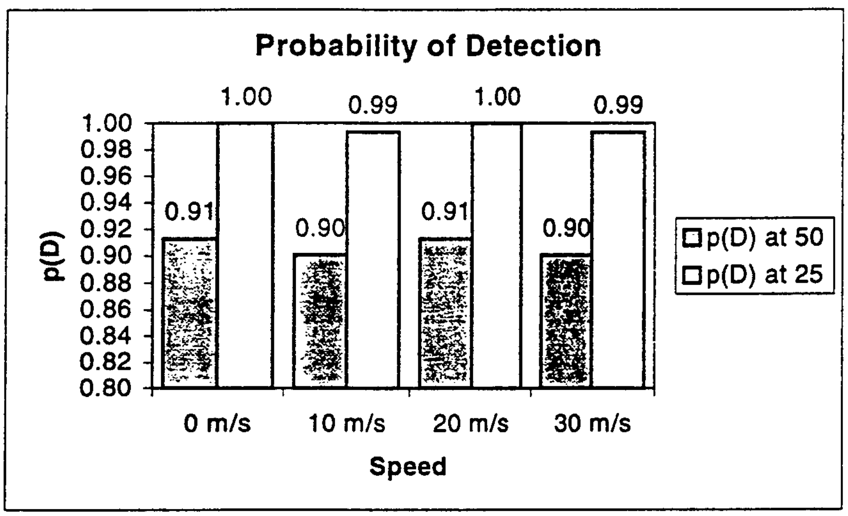

Figure D-2: Speed Probability of Detection Results

As seen in Table D-2 and Figure D-2, target motion also had no visible effect on the probability of detection. Both segmentation and detection metric values were comparable to values observed in previous studies.

The results of the classification stage were varied. Some targets had a very high probability of correct identification, while others had a very low probability of correct identification. The average probability of correct identification for all nine targets was 0.32. Only 210 of 648 targets were identified correctly. This metric is substantially lower than the probability of correct identification in other CMT algorithm performance studies. The possible implications and causes of this result will be discussed further in the conclusions. Target by target correct identification results can be found in Table C-1 and Figure C-1, and speed correct identification data can be found in Table C-2 and Figure C-2.

Table C-1: Target by Target Correct Identification Results

Target	Correct ID
M-2	24
M-1	7
SA-6	12
SA-13	42
ZSU-234	9
BTR-70	18
MAZ-543	70
BMP-1	17
BMP-2	11

Table C-2: Speed Correct Identification Results

Speed	Correct ID
0 m/s	57
10 m/s	54
20 m/s	50
30 m/s	49

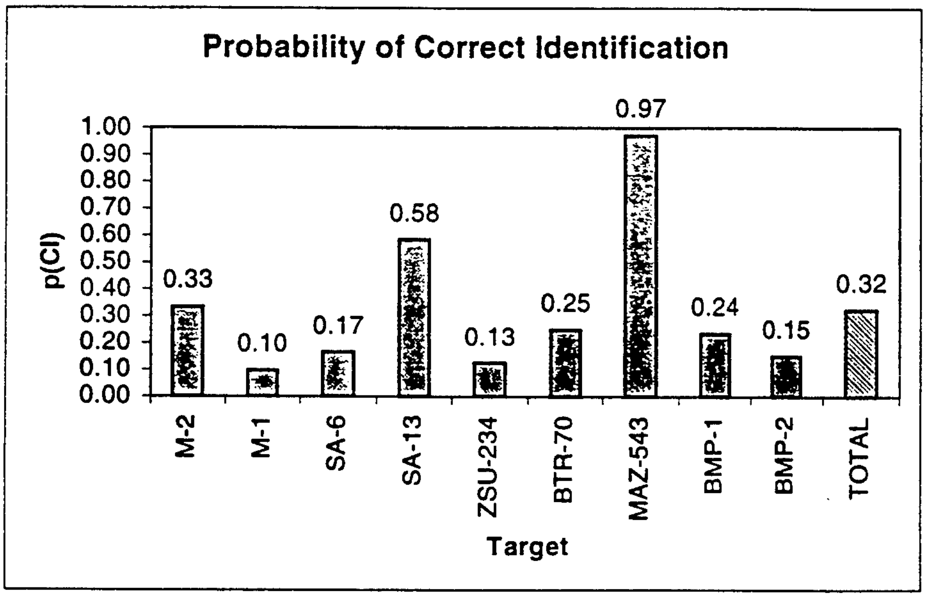

Figure C-1: Target by Target Probability of Correct Identification Results

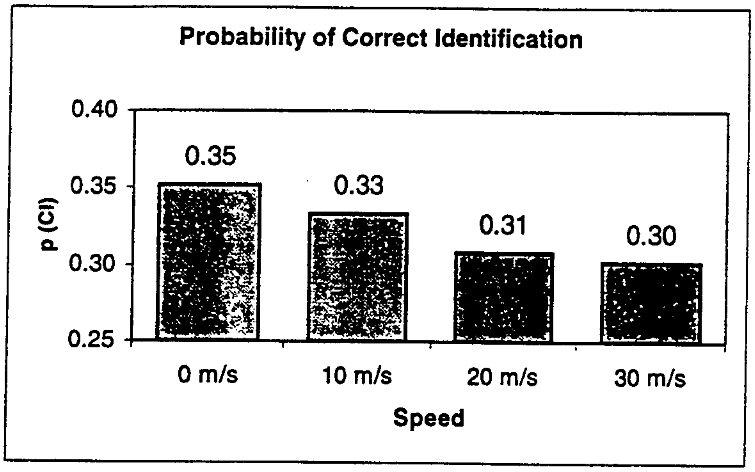

Figure C-2: Speed Probability of Correct Identification Results

Unlike the results of the SegDet module, the output of the classification module does seem to be influenced by target motion. Although the drop in probability of correct identification between a stationary target and one moving at 30 m/s is only 0.05, this is a larger variation than the other data has shown. A dropping-off trend in correct identification probability as speed increases can be clearly seen in Figure C-2.

Results were very similar for the probability of correct identification given detection metric. Since only two targets were missed at a pixel on target minimum of 25 pixels, both target by target and speed data show no change between probability of correct identification and probability of correct identification given detection. When probability of correct identification given detection was evaluated at 50 pixels, results improved slightly since the extraneous non-detected targets had been removed, but still followed similar trendlines. Tables and graphs comparing the probability of correct identification and the probabilities of correct identification given detection at 25 and 50 pixels can be found in Table CD-1 and Figure CD-1 for target by target data and Table CD-2 and Figure CD-2 for speed data.

Table CD-1: Target by Target Correct Identification Given Detection Results

Target	Correct ID	Correct at 50	Correct at 25
M-2	24	22	24
M-1	7	7	7
SA-6	12	12	12
SA-13	42	41	42
ZSU-234	9	9	9
BTR-70	18	15	18
MAZ-543	70	70	70
BMP-1	17	15	17
BMP-2	11	11	11

Table CD-2: Speed Correct Identification Given Detection Results

Speed	Correct ID	Correct at 50	Correct at 25
0 m/s	57	55	57
10 m/s	54	53	54
20 m/s	50	48	50
30 m/s	49	46	49

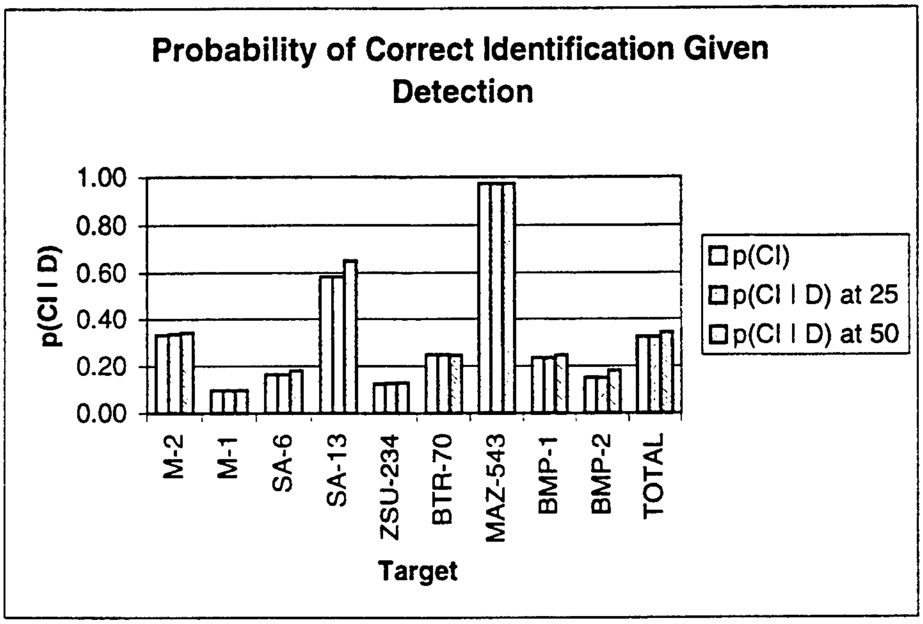

Figure CD-1: Target by Target Probability of Correct Identification Given Detection Results

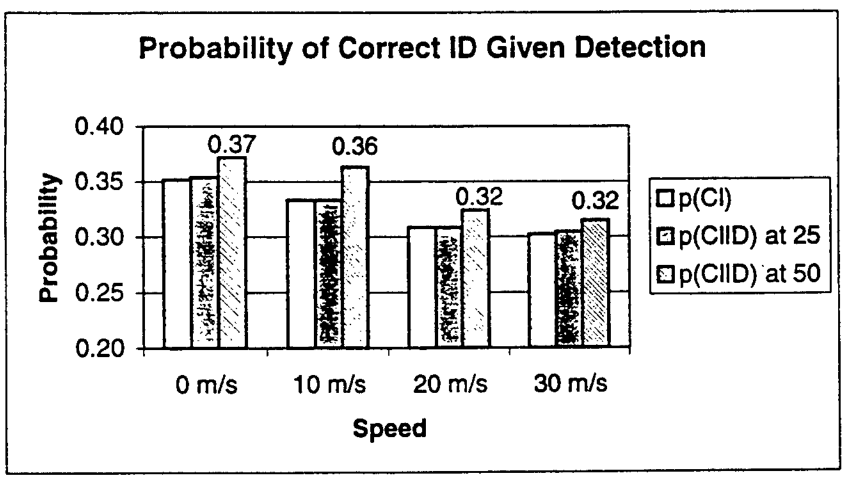

Figure CD-2: Speed Probability of Correct Identification Given Detection Results

Like probability of correct identification, probability of correct identification given detection drops off as target speed increases.

Conclusions:

Target motion appears to have no visible effect on CMT algorithm performance in the segmentation and detection stages. Changes in metric values were small and showed no specific pattern as speed increased. Overall segmentation quality and probability of detection numbers were also comparable to numbers generated in other CMT algorithm performance studies that had been deemed successful. This did not hold true for the classification program module, however. Speed did seem to affect the probability of correct identification as correct identification numbers dropped off when speed increased. Although the changes were still small, they were larger than the changes in the other metrics and did show a definite decreasing correct identification trend as speed increased. One possible explanation for this phenomenon is that during the time it took the LADAR sensor to scan the vehicle, the far end of a quickly-moving vehicle would have moved by the time the scan reached that edge, making the vehicle appear longer than its actual size. An elongated model might not match up with the properly sized but smaller reference model, leading to a higher rate of incorrect identification as speed, and therefore the degree of target elongation, increased.

The overall probability of correct identification for this CMT algorithm performance study was 0.32, which compared to previous studies, is quite low. Because of this, the data generated in the classification stage may be flawed or unreliable, and more studies should be undertaken to see if the decrease in identification accuracy as speed increases holds true for a set of data with a more acceptable probability of correct identification. Several possible reasons for the low overall classification accuracy were suggested. After the conclusion of the classification stages, it was discovered that several of the reference models had not been properly centered. When compared with the target regions, these non-centered models were not aligning properly with the target, and the overhanging and undercut pixel regions were frequently causing incorrect rejection of the correct reference model. A preliminary run with re-centered models showed limited improvement, but a complete study with the re-centered models could not be attempted due to time constraints. Another factor that might account for poor identification results could be the distance from which the targets were synthetically scanned. The imagery had been generated as if scanned from a greater distance than usual, causing the targets to have a lower pixel on target count than usual, making comparison and identification more difficult. Also, many of the targets used in this study were very similar. Targets like the BMP-1 and BMP-2 and the M-1 and M-2 are similar in shape and size, difficult to distinguish between even in a photograph. To be able to tell them apart with consistency on the basis of fifty pixels is very unlikely.

The aim of the project was to determine the effects of target motion on the performance of the Critical Mobile Target algorithm. This goal was partially accomplished, with preliminary findings indicating that target motion did not affect the segmentation and detection program module of the CMT algorithm but that it did affect the performance of the classification module. This stage's overall poor results, however, make these conclusions less reliable and demonstrate the need for further study.

On a more personal note, this summer has proved very fulfilling. I was able to complete the original project that I was assigned, and preliminary results indicate that this study was worthwhile. I have learned about LADAR imagery and also about how the CMT algorithm works to locate and identify potential targets. In addition, I have gained valuable experience working with both the UNIX operating system and Excel's spreadsheet functions. I have also benefited from being in a professional environment and from having the opportunity to work with other employees and apprentices. I have enjoyed my two summers here very much.

References:

- Geci, et al., "**Segmentation of Relocatable Targets in Low-Cost Ladar Seeker Imagery**", IRIS Active Systems Specialty Group, May 1996.
- Wellfare, et al., "**Identification of Vehicle Targets from Low-Cost Ladar Seeker Imagery**", SPIE AeroSense, Apr 1996.
- Wellfare, et al., "**Ladar Seeker Identification of Critical Mobile Targets**", NATO/IRIS Active Systems Specialty Group Conference, Monterey, CA, May 1995.

Acknowledgements:

- Karen Norris Zachery, for being a supportive and helpful mentor for the last two summers and for always taking time out to answer my questions
- Major Mark Hunter, for generating the LADAR imagery used in this study
- Mr. Harrison, Mr. Deiler, and Mrs. Williams, for coordinating and administrating the HSAP program
- The IPL people, for sharing knowledge and computers with me and for their patience when my program crashed the system
- My fellow apprentices, for helping with popcorn duty and generally making the summers enjoyable and entertaining

WEB PAGE DESIGNING AND ASSISTANT IN OTHER FIELDS

Nathan A. Power

Heritage Christian School
287 Cincinnati Ave.
Xenia, OH 45385

Final Report for:
High School Apprenticeship Program
AFRL/Wright Laboratory

Sponsored by:
Air Force Office of Scientific Research
Bolling Air Force Base, DC

And

Wright Laboratory

August 1998

WEB PAGE DESIGNING AND ASSISTANT IN OTHER FIELDS

Nathan A. Power

Sensors Directorate

Heritage Christian School

Abstract

I was assigned several different projects this summer. My assignments ranged from pricing specialized equipment on the Internet to using HTML (hyper text markup language) and other tools to design a web page. I was introduced to a variety of new computer programs that assisted me with my work during the summer. MATLAB, Excel, Word 7.0, and Power Point were some of the programs that I used to complete the projects assigned to me.

Introduction

This summer I worked for the Sensors Directorate at Wright Patterson Air Force Base. I was given series of projects to complete as the summer progressed. My first project involved locating and pricing computer components. My next project involved the evaluation of a specialized compiler for use with MATLAB, a matrix manipulation and mathematical imaging software tool. The project that took the most time to complete was the creation of a web page for the branch. I also helped develop a new equipment inventory database and I assisted an Ohio State University professor who was hired for the summer to investigate targeting sensitivities associated with sensor image registration.

Discussion of Problem

Throughout the summer I was assigned a series of projects, each with a different set of challenges. Some tasks were more difficult than others, but I had many opportunities to express my creativity in developing or helping to develop solutions for each problem. Some projects had well defined goals and others were open-ended. I had to learn some of the basic MATLAB functions before I could actually start working on the problem. MATLAB took some time to understand, and it wasn't always easy. I had books to work with and learned some of MATLAB's functions. When I was building the branch web site, the main problem was trying to get every ones information on time. I need information when I was ready for it, and needed to put it on the server when I was done with the web page. Once I got the information, I was ready from there.

Methodology

Assignment 1

My first assignment was to research computer component prices and availability to determine the feasibility of building or upgrading a computer system to complete future assignments. I began by using the search engine on Yahoo's Internet site to find computer component vendors on the web. I had to find at least web sites to compare prices. I compiled a list of compatible parts for building a computer. I found the parts and prices and compared them on the web at different web sites. I also compared prices on tape drives and other peripheral devices for my mentor. I did most of my searching at http://www.pricewatch.com. The Internet was one of the best sources to find the right parts at the lowest cost. Once the components were priced out we needed to decide if it was better to build a new computer; upgrade an older system; or to tie-up a portable Pentium laptop system for the summer. We could upgrade or build an Intel 333 MHz system with 128MB memory, a 4 GB SCSI hard drive (SCSI's are faster then IDE), CD-ROM, 3.5 floppy drive and a 64 bit SVGA graphics card for just under a thousand dollars. The estimated construction cost was reasonable, but after considering time and performance trade-offs it was decided that is would be more practical to dedicate a portable computer for my use over the summer. Still, A state-of-the-art computer would have been fun to build.

Assignment 2

I used MATLAB a little but wasn't assigned any specific tasks. The goal for this project was to experiment with the program and become familiar with the MATLAB environment so that I could help evaluate a software program that compiles MATLAB functions to make them run faster. I figured out some of the basic functions but didn't have time to go into detail. I was shown how to program some mathematical equations and how they could be applied to solving real problems, like homework assignments. Below (figure 1) is graphical representation of a function programmed in MATLAB.

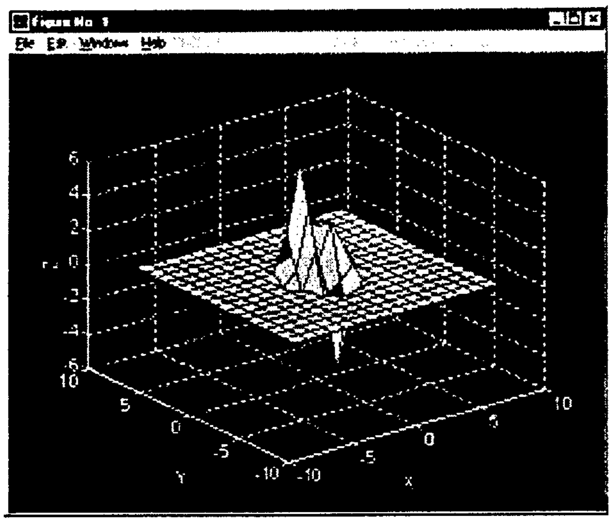

figure 1

Below are some basic command strings used in MATLAB.

» Y= reshape(x,4,5)= reshape x into a 4x5 array
» y'= transpose vector or matrix
» ; = next line, blank line
» .* = array multiply
» y(:,1) = column 1
» y(1,:) = row 1
» y(1,2:4) = row 1 of columns 2 thru 4
» y(2:3, 2:3)=rows 2 and 3 of columns 2 and 3
» a=[1:5] = a vector of the numbers 1 thru 5
» length (a(:)')= array length

» a=[0:5:100]= a vector of numbers from 0 to100 in increments of 5
» [5^0 5^1] = powers
» a= ones(1,7)= a 1 x7 array of 1's
» a*5=scalar multiplication by 5

Assignment 3

Another of my projects was to create a web page for our branch (SNAR) using HTML. One goal of this project was to make it easy for the user navigate around the web page. We wanted people to be able to view our page with most common web browsers. The web page design was constrained by local guidelines and the need to present information to a diverse audience. For example, we couldn't use frames (a split screen on a web page that brought up two web pages at once), Java Applet code, or Active-X controllers which are objects that load into the page and perform specialized functions. The Java applet and Active-X controllers would have given us a more dynamic-looking page. Using some Java Applets created by a former HSAP participant, we could have put a button pop up menu bar in the browser that would have made it easier for the user to navigate without having to change pages to frequently. That pop up menu bar was the highlight of the page till we couldn't use it any more. Example of pop up menu bar (figure 2).

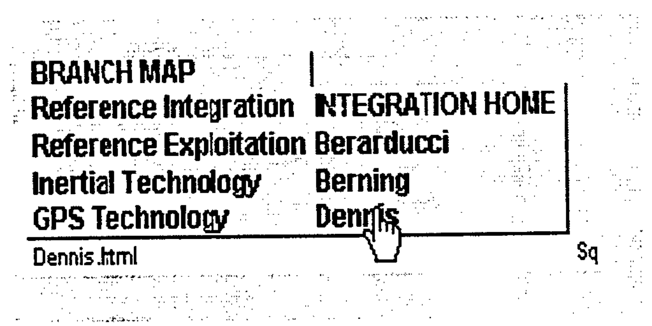

figure 2

With the frames, we also made it so that there was a list of options always on the side for the user to navigate. Unfortunately, the new constraints required us to remove that feature also. I believe that the organization I was working for felt that if the web page were too complex, some people would not be able to access it or would be hesitant to. Yet, we still had to create an interesting web page. You can see where we might have some dilemmas.

We solved the problem with limited resources and a lot of creative thinking. Knowing that we couldn't use frames, we made fake frames (a group of images) on the side bar using images. (The frames would have made it easier for someone to browse the site, but it wouldn't have met the design constraints, as stated earlier). Frames also would have made creating the pages easier by eliminating the need to place the images on every page so that the pages would look similar. Designing the page was a more difficult without frames, but the results were satisfying. The following images will show what I mean.

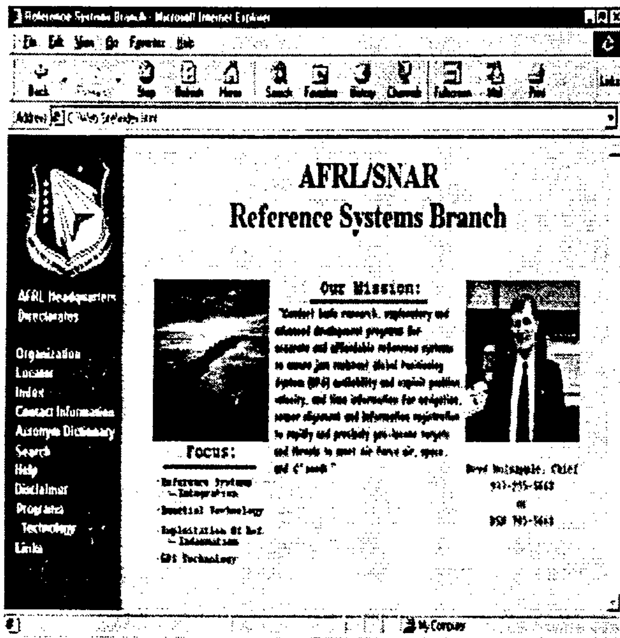

figure 3

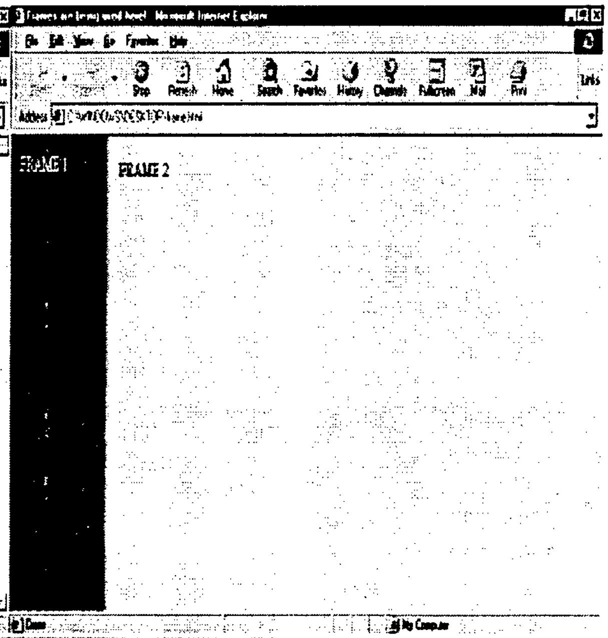

figure 4

As you can see, figure 3 above is a fake frame. It looks like it is in a frame, but it's actually overlapping images put in place by a table. The fake frame doesn't function like a frame would, but it gives the same basic effect by using tables. (A table is an object in which you can group multiply objects together on a web page. The purpose of the table is to position objects on the page in their groups). Figure 4 is a web page using frames. As you can see, there isn't much visual difference, and they almost look identical. The second image (figure 4) is actually made up of two different web pages, unlike the first image above. I used a lot of images in the making of the figure 3 web page. Most images for the fake frame (figure 3) were transparent gif's. A .gif is a type of image file supported by most image viewers. The gif played a powerful part in the development of the web page side bar.

The gif's made it possible to overlap images. The end results of using the gif's gave us a sharp looking side bar. I formatted all of the other images that weren't transparent to .jpg (another image file type). You cannot make .jpg's transparent, because they are different file types, but I preferred using them. Below I have two images in an Internet explorer browser. Figure 5 is a transparent .gif file type; this is how its looks. Figure 6 is a .jpg file type, this image is not transparent as you can see. You can see the advantage you have by using transparent .gif's.

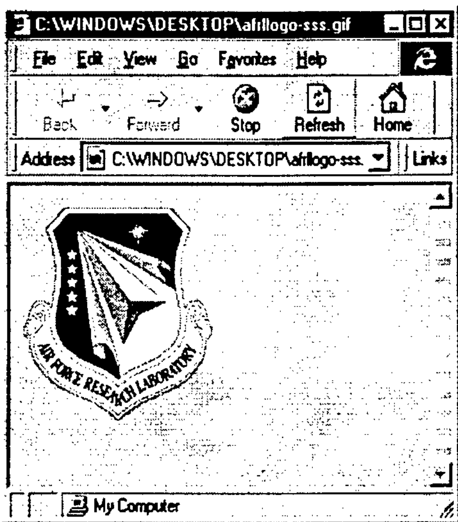

figure 5

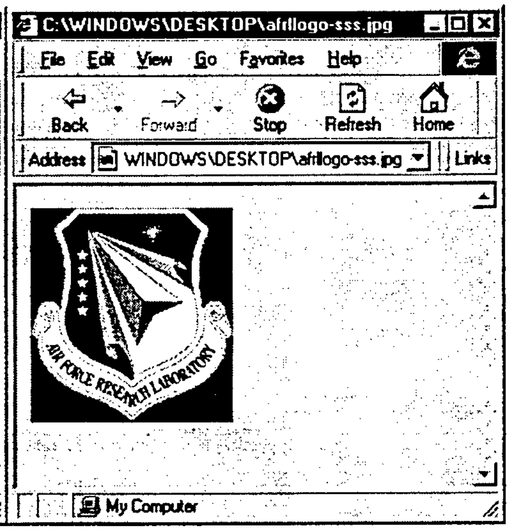

figure 6

I also image-mapped the images on the side bar. I used "Map Edit" to image map my images. Image mapping is using an image and selecting certain parts or areas of that image to become a link or creating multiple links on that image. So I could make an image in "Paint Shop Pro," for example, and create the whole image out of text. You could make each text word a link using "Map Edit." So, it's a very useful tool for making links on images.

Assignment 4

My next assignment was to update the branch computer equipment inventory and examine various sample databases to determine whether or not a Microsoft Access database could meet the branch needs better than the current spreadsheet based inventory system. A primary goal of this assignment was to compile a current list of computers, printers, and other computer-type equipment assigned to each employee in the branch that included the employee's name and the serial number of his/her equipment. After compiling this information, I entered it into the computer. This task was assigned a low priority, so investigation into the development of a new database prototype was discontinued when I was requested to assist a visiting professor with more import work.

Assignment 5

Another one of my projects was assisting Dr. Li in converting his notes onto the computer and in presentation form. The goal of this assignment was to aid Dr. Li's work with computer support. This involved converting equations on the computer on Microsoft Word 97, and making graphics. I used Microsoft Power Point to overlap images and to create effective graphics that could be presented and observed clearly.

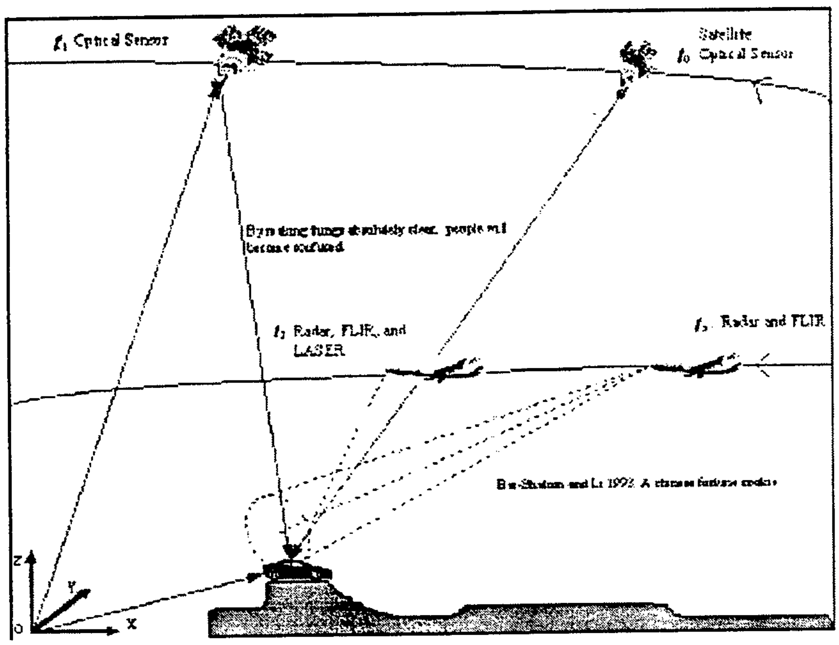

figure 7

Here in figure 7 is a graphical image made of several other images. These images are overlapping and defining one another. This figure was made in Microsoft Power Point. What this figure is showing is the two different planes targeting the same target (the car) at different angles. The plane's sensors that are targeting the target, combine target information with the satellite's information. By pooling information, the sensors are getting a better lock on the target and have a more likely chance of hitting the target. For demonstration purposes, we used non-military machines to show where the plane and target would be positioned because the presentation was presented to a non-military organization. The equations that I edited and put on the computer were done using Microsoft Word 7.0. Word 7.0 provides an equation making tool.

Where LOS are direction cosines of unit vector of the line of sight (LOS)

$$LOS_x = -\frac{(x - x_s)}{\sqrt{(x - x_s)^2 + (y - y_s)^2 + (z - z_s)^2}}$$

$$LOS_y = \frac{(y - y_s)}{\sqrt{}}$$

$$LOS_z = \frac{(z - z_s)}{\sqrt{}}$$

$$R_n = \sqrt{(x_n - x_s)^2 + (y_n - y_s)^2 + (z - z_s)^2} \quad - \textit{approximate range}$$

Linearised equation

$$R_m - R_n = (LOS_x, LOS_y, LOS_z, -LOS_x, -LOS_y, -LOS_z) \begin{pmatrix} d_x \\ d_y \\ d_z \\ d_{xs} \\ d_{ys} \\ d_{zs} \end{pmatrix} + (-v_{sc})$$

Note
- $R_m - R_n$ is small but usually not zero
- $d_x, d_y, d_z, d_{xs}, d_{ys}$, and d_{zs} are known to be estimated. They are signals, not noises (V_k)

figure 8

Above in figure 8 is a sample of the equation work that I did. I had to give this task a high priority it complete in time for a crucial video conferencing meeting.

Results

As a result of my work for the Sensor directorate, I finished the SNAR web page which is posted on the web. It is yet to be approved by Public Affairs, but is uploaded on the web. I also finished my work of graphing equations and images for Dr. Li. I never finished my task of completing the data base inventory program because I accepted Dr. Li's assignment. I did have all the information given to me for the data base. The little assignments like the MATLAB and the web search for the computer parts did go well and were finished.

Conclusions

It was a great privilege working in the Sensors Directorate for RDL this past summer. I was able to use the skills I had learned the previous summer for creating the branch web page. I also learned new skills. I learned the basics of MATLAB, and I learned how to use Power Point in a presentation format. I am grateful for this opportunity to expand my computer skills. I'm sure I'll be able to use this valuable knowledge in all of my future endeavors.

DEVELOPMENT OF A DATABASE FOR MULTI-SENSOR IMAGERY

David S. Revill

Choctawhatchee High School
110 Racetrack Road
Ft. Walton Beach, FL 32548-0000

Final Report for:
High School Apprenticeship Program
AFRL/Wright Laboratory

Sponsored by:
Air Force Office of Scientific Research
Bolling Air Force Base, DC

And

Wright Laboratory

August 1998

DEVELOPMENT OF A DATABASE FOR MULTI-SENSOR IMAGERY

David S. Revill
Choctawhatchee High School

Abstract

The task of the program was to create a database for multi-sensor imagery, specifically those used with the Irma signature modeling software. This database was created using Microsoft Access. The primary purpose for creating this database was to facilitate the accessibility of the Irma imagery. The database will eventually be pre-approved for public release so that the images in the database can be easily used for distribution to outside organizations and for presentations and reports. A secondary purpose was for the apprentice to gain familiarity with the properties related to multi-sensor imagery.

DEVELOPMENT OF A DATABASE FOR MULTI-SENSOR IMAGERY

David S. Revill

INTRODUCTION

Irma software, created for the Advanced Guidance Division, Munitions Directorate of the U.S. Air Force Research Laboratory, Eglin AFB, FL models various scenes as they would be seen using either a passive infrared sensor, passive millimeter wave sensor, active millimeter wave sensor, or a Laser Radar (LADAR) sensor. The ability to generate these images provides an inexpensive way for the testing of sensors used in state-of-the-art seeker systems. The demand for these images in technical reports and presentations is increasing. However, access to the imagery is difficult, especially when one also needs information about the imagery as well, such as the sensor band. Also, with the growing number of these images available, it is becoming increasingly troublesome to find a suitable image for one's purpose. It was for these reasons that an Irma image database was created.

METHODOLOGY

The first step in creating the Irma image database was to gather a few sample images and derive from these images the properties that should be included in the database. From close evaluation of fifteen sample images, several important properties were found. One of the most important items to include was the image filename which would allow the actual image to be found without difficulty. The second item placed in the database was a series of check boxes which allowed the user to specify whether the Irma image is from a Passive IR, Active Millimeter Wave, Passive Millimeter Wave, or LADAR image. Two important properties that were included in the database were the types of targets in the scene and the type of background in the scene. Knowing the specific target in the scene allows the user to determine exactly what they will be looking at when they find the image and significantly decrease the seek time to find a useful scene. The background of the target was also included and is considered quite important because it allows for the testing of seekers in many different environments. For example, a scene of a t72 tank in a dry desert can be viewed as well as a t72 tank amongst deciduous trees. The final property included upon the first draft of the database was the sensor waveband of the image. The appropriate waveband of the image is chosen in the database by using a group of radio buttons which allow the user to choose from the LWIR (Long Wave Infrared), MWIR (Medium Wave Infrared), SWIR (Short Wave Infrared), UV (Ultraviolet), Visible, Ka, and W bands of the electromagnetic spectrum.

After further development of the page, it was decided that there were other attributes to be included in this database. The first of the additions to the second draft of the database was the inclusion of the filenames of the targets and backgrounds. Previously, only the descriptions were included and did not provide enough information to the user. The appropriate weather information was also recorded in the database so as to know whether the image was taken in a rainstorm or a hot sunny day. The file type of the image was also given in the database. The image types specific to Irma imagery are Apparent Temperature, Doppler Images, Intensity Cross Section Images, Phase Images, Polarized Radiance Images, Range Images, Radar Images, Surface Images, Temperature Images, Texture Images, Truth Images, Unpolarized Radiance Images, and Visual Images. The name of the eyepoint file was also included in this second draft. The eyepoint file tells the software how to look at the target and where it is in the World Coordinate System. The last additions to the second draft of the database were text boxes giving the validation information and any further comments.

After this second draft, the database was converted from Microsoft Access 7.0 to Microsoft Access 97. This conversion allowed for greater portability throughout the lab in order that the database could be reviewed by various personnel. Along with the conversion to Microsoft Access 97 came two significant upgrades to the database. The idea was proposed to include a thumbnail of the Irma image alongside its myriad properties. In order to do this, an OLE object frame was placed into the database and a macro was created which allows for the insertion of a picture into the OLE object frame. In order to place the Irma images into the database, they first had to be converted into a usable format in which the file size was small enough so that the image did not increase the size of the database tenfold. JPEG was chosen because it is an extremely portable file type with a remarkably conservative file size. These files could then be placed into the Irma image database without significantly increasing the size of the database. The next significant addition to the Irma image database was the startup welcome screen. The welcome screen states the objective of the Irma image database and includes a command button which closes the welcome screen and automatically opens the primary database form. This welcome screen substantially increases the ease of use for the Irma image database. With the completion of the physical portions of the database, the database was evaluated by several individuals, who could possibly use this database in the future, to determine its usefulness.

In the final draft of the database. several of the information fields mentioned above were removed. The date and time fields were removed due to the fact that they appeared of little use and the best way to use these fields could not be determined. They could either be used to relate the date and time that the images occurred, the date and time that the image was generated (which seemed futile because the image could be regenerated at any time), or the date and time that the image information was entered in the database, which serves little purpose except to provide a reference of the cataloguing chronology. Also in the final draft, the fields for background facet files, weather, and eyepoint file were removed. Along with this removal, the field for target description was combined with the field for the target facet filename. All of these fields were replaced in this last revision with the insertion of a field for the filename of the master file. The master file gives all this same information relating to weather, the background data, the eyepoint, etc. in a small concise format. However, in order to view this data, one must first find the master file. Therefore a copy of the master files is to be kept in a folder along with the database.

DESIGN AND FUNCTIONALITY

The Irma Image Database was designed in a concise easy to read and easy to access manner. A minimal amount of information is given in the database in order to ease the process of publicly releasing the images. However, enough detail is given so that one can receive a good understanding of the image just by seeing the database, and so that all of the information could be found if one were to go search for this information.

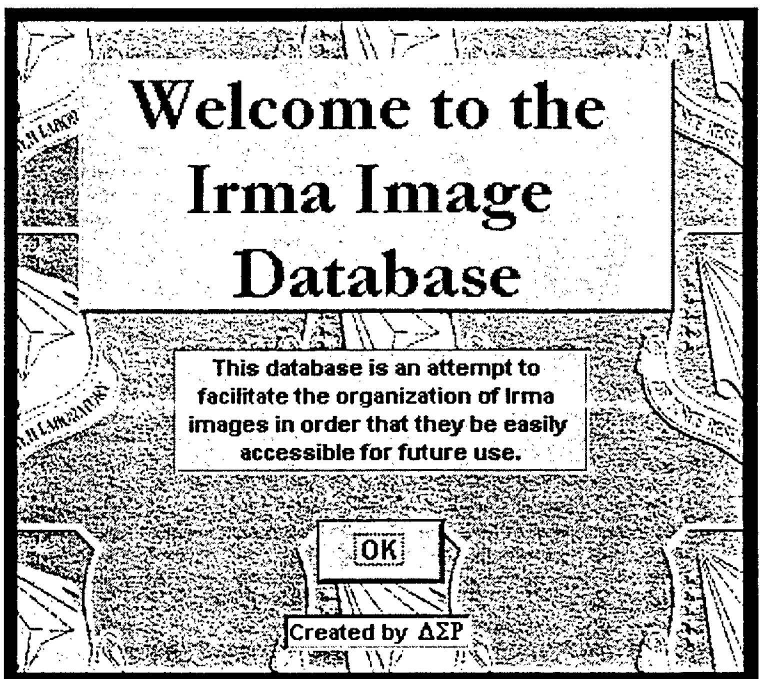

Figure 1: Welcome Form

Startup Form: The database opens with a welcome screen that was simply another form created in Microsoft Access. This welcome form is a pop-up modal form, meaning that it stays on top of other forms and cannot lose the focus. The form appears as you open the Irma Image

Database and states the title of the database and its purpose. The form appears on open by placing it in the startup menu. This was done by selecting it as the **Display Form** under the **Tools | Startup...** menu item. The welcome form contains a button control which closes the form and opens the main database form. This was done by creating a button which closes the form and then, editing the Visual Basic code that was automatically created by Access to close the form in order to allow it to also open the new form.

Header: Upon pressing the "OK" button of the startup form, the main database form opens automatically in read-only mode. The read-only mode was accomplished by using a macro, *Lock to Read Only*, to change each of the field properties to locked and the thumbnail frame properties to locked and disabled. The title of the main form is made from a label control. There are two buttons and two labels to the left of the title which control whether

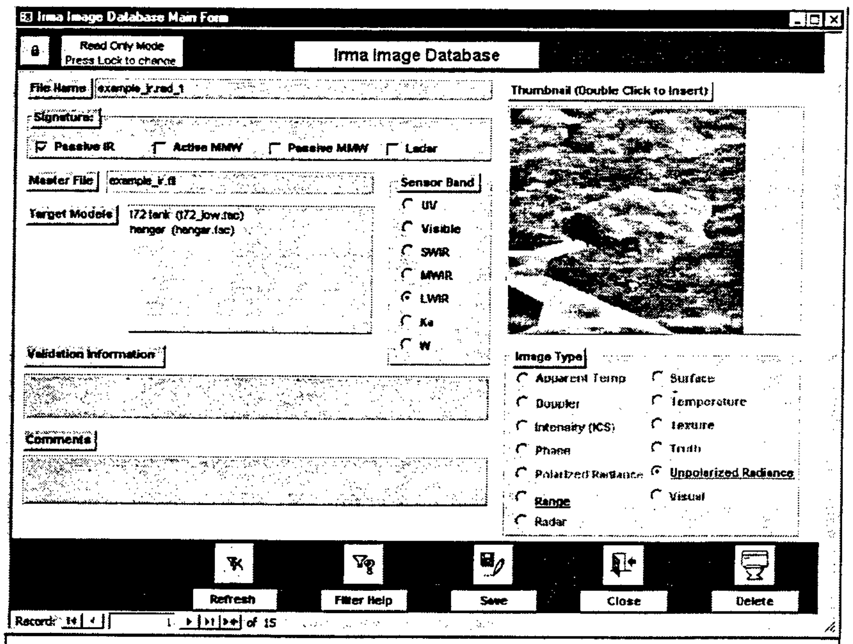

Figure 2: Main Database Form

Figure 3: Read-Only Mode Configuration

Figure 4: Edit Mode Configuration

the database is in read-only or edit mode (see figures 3 and 4). However, only 1 button and 1 label is visible at any one time. The visibility of these buttons and labels is controlled by macros, *makeitreadonly* and *makeitedit*, the same macros that control the locked state of all of the other controls on the form. The proper macro is initiated whenever the button in the left of the header is pressed. There are actually two macros that control this process: one, *makeitreadonly*, that locks the fields, makes the edit mode label invisible, makes the read-only mode label visible, makes the go to read-only mode button invisible, and makes the go to edit mode button visible, and one, *makeitedit*, that unlocks the fields, makes the edit mode label visible, makes the read-only mode label invisible, makes the go to read-only mode button visible, and makes the go to edit mode button invisible. The go to read-only mode button initiates the *makeitreadonly* macro that locks all of the controls, and the go to edit mode button initiates the *makeitedit* macro that unlocks all of the controls. Since you cannot make a control invisible while it holds the focus, the focus is shifted to the image filename field during the macro.

File Name, Signature, Masterfile File Name, and Target Models Fields: The first field in the body of the form is the image filename control. This field allows text entry up to one hundred characters (which can be extended to up to 255 characters). It is through this field that the Associated Image Types form is connected to the main database form.

This will be discussed at length later. The second field in the database is made up of actually four fields, allowing for the choice of either the passive infrared (IR) signature, the active millimeter wave signature, the passive millimeter wave signature, or the laser radar (LADAR) signature. Each of these fields is a check box control and is stored in the database table as a yes/no data type. The next field in the database is another one hundred character text field. This field holds the name of the master file that rendered the image. The master file filename field is the field which is used to filter the database according to associated image types. This advanced filtering will be discussed in greater detail in the section concerning the image type control. The next field is a text field which holds the target model description and filename. This field is a large text field which holds up to 255 characters. The information is recorded in this field with the syntax: "target model description (target model filename)".

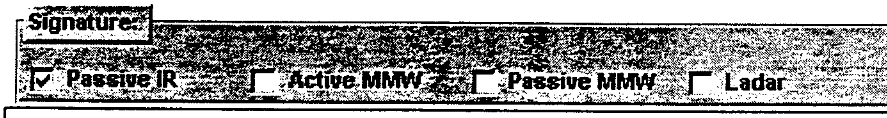

Figure 5: Check box Signature Controls

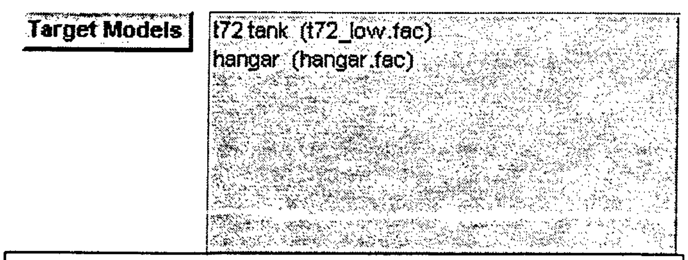

Figure 6: Target Model Text Field

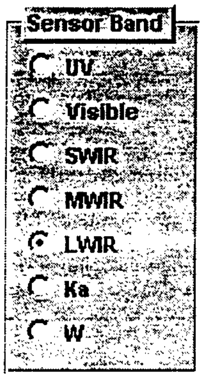

Figure 7: Sensor Band Control

Sensor Band: The next field in the database is a special type of field. This field appears to be made out of multiple controls, in this case seven, but in actuality, is only one control. This control is an option group made out of radio buttons and allows for the displaying of the sensor band information. This option group provides a radio button for each of seven bands: UV, Visible, SWIR, MWIR, LWIR, Ka, and W. This data is stored as an integer, numbered one through seven, in the database table.

Validation Information and Comments Fields: The next two fields in the database are simply large text fields. These controls each hold 255 characters of text for the validation information and additional comments. These controls allow for a scroll bar when the text becomes a greater length than the space allotted in the form.

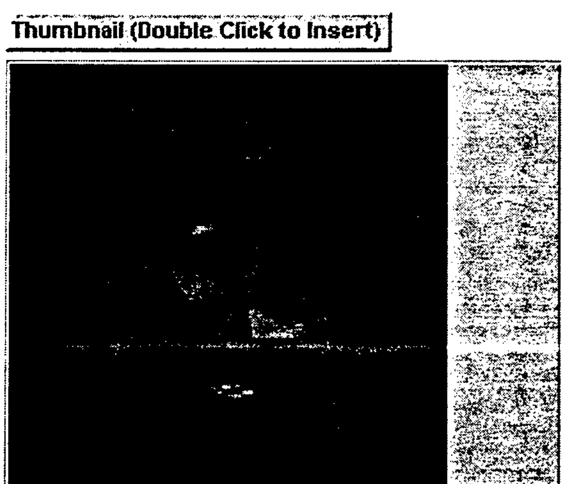

Figure 8: Thumbnail Control

Thumbnail: The next type of field in the form is made from a more complex control. This control is an OLE object frame. This frame allows for the insertion of many different kinds of objects; however, in this database, it is used to hold the thumbnail image of the Irma image.

When you double click on the field it runs a macro, named *insert_picture*, which tells Access to insert an object. One can then select the image filename from either the local or network drives connected to that computer. For the example images that were inserted into the database, the Irma image was converted into a TIFF image using the cvtimg utility which was packaged with the Irma software. The TIFF was then transferred via FTP to a PC, where it was converted to a JPEG with the Microsoft Photo Editor.

Image Type Field: The image type control is another group made of radio buttons. The group stores its information in the data table as an integer, one through thirteen. However, this group also contains some complex functions. The group functions as a normal option group of radio buttons when in the edit mode. While in the read-only mode, it serves as a link to associated images. This function is useful because when a job is rendered with Irma, the data is displayed in several different types of image output files. For example, when a ladar scene is generated, one almost always generates a range image and an intensity image. Therefore, it is useful, when looking at the range image, to go directly to the intensity image to compare this information. One can determine which images were

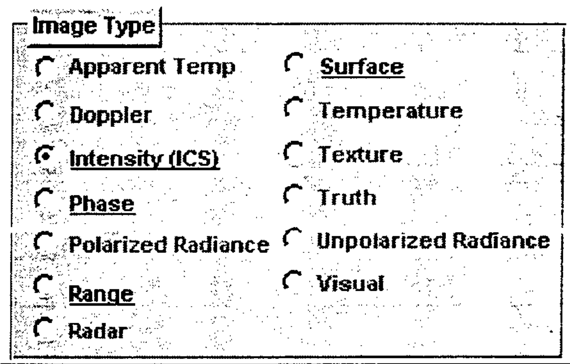

Figure 9: Image Type Control Group

generated in a particular job by viewing the master file. It denotes which output images are created in each run.

The way this process works from a user perspective, in read-only mode, is that in the image type option group, the radio button which is currently filled is the image that appears on the screen. The images that were created alongside that image with the same master file are in red text and underlined, making them look much like a hyperlink. When the user clicks on the red text, the database is automatically filtered to find the record of information for the associated image.

From a design standpoint, this option group is much more complicated. The first step in understanding how this group works is to understand how the different images are associated with each other. When in edit mode, there is a command button that becomes visible that allows you to select the associated image types. After pressing the **Select Associated Image Types** button, the Associated Image Types form opens.

There was a particular problem with the **Select Associated Image Types** button in that when in edit mode, you must also select the image type for the current image. Since this button sits on top of the image type option group, whenever the group had the focus, it would come to the front and the select associated images button would no longer be visible to the user. This problem was solved by making the background of the image type option group transparent so that it when the image type option group had the focus, it did not cover up the **Select Associated Image Types** button. To maintain the aesthetics of the option group, an etched rectangle box that was identical to the background of the option group, before making it transparent, was placed behind the option group and the button to make it appear as if the rectangle was actually part of the option group control. It is important to note that it is not part of the option group control. However, it does make it difficult to differentiate whether one is selecting the rectangle or the image type option group when in the design view because they sit right on top of each other.

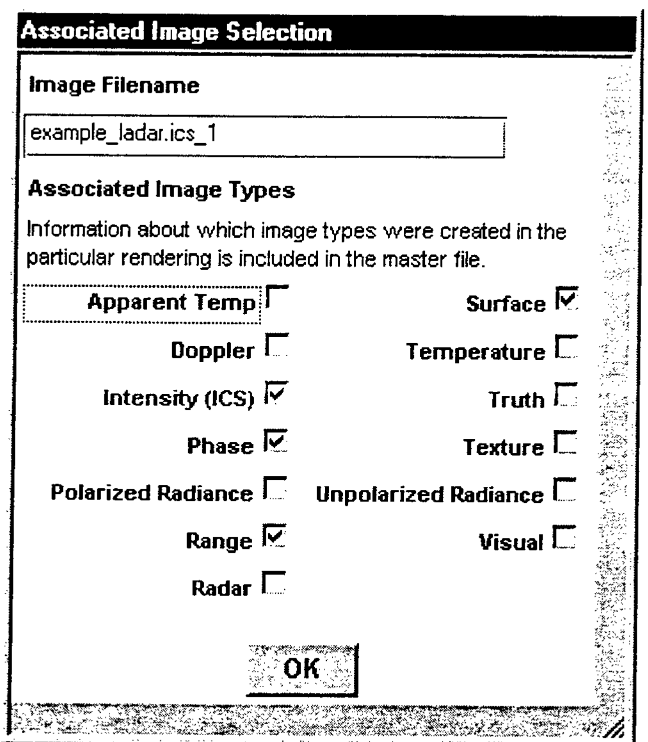

Figure 10: Select Associated Images Form

Associated Image Types Form: The associated image type form contains the image filename and thirteen check box controls which allow you to select which of the thirteen images are associated with that particular file. When the associated image type form is opened, it must be opened to the correct record in order to be useful. The easiest way to do this would be to make it as a subform in the main database. When a subform is created, Access asks for a particular field to use to link this form. In this case, it would be useful to link the form according to image filename. However, it would not be useful to have this subform visible from within the main form whenever in edit mode, mainly due to simple space limitations. Therefore, this form was created as a normal form, linked as a subform within the main form, and then the visible property of the subform control within the main form was set to "No." The information from the associated image type form is kept in the same table as all of the other information from the database.

Image Links: The second step in understand this group is to comprehend the linking process of the multiple images. The links to the other records work in a fairly simple manner. The links are actually all red text labels that run a macro, specific to each button (e.g. *Find Doppler*, *Find Phase*, etc.), whenever one is clicked. These text labels sit on top of the grey text labels that were created with the image type option group. So, it appears that the text changes color when a link is present, but actually, the visible property of the labels is just set to "Yes." Access determines which of the labels to show through a conditional macro, *Make Image Selection Buttons Visible*. This conditional macro is run whenever a new record is opened and every time that read-only mode is initiated. The *Make Image Selection Buttons Visible* macro tests the data table and determines which of the image types were selected from the check boxes of the associated image form. The conditional statements look like this (see figure 11):

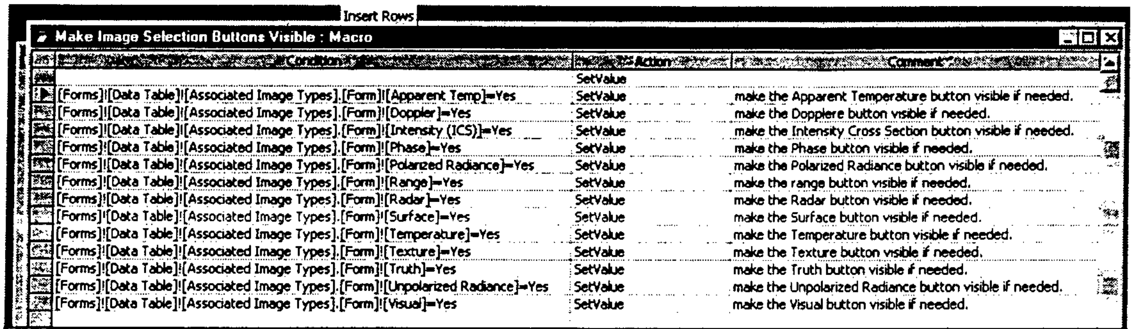

Figure 11: Macro with conditional statements

If this statement is true then that particular label is made visible by using the command "SetValue" from within the macro.

Advanced Filtering: The third step to understanding this processes adjoined to this group is to understand the filtering process. When the label, which appears as a hyperlink (see figure 9), is clicked in read-only mode it runs a different macro. This macro applies a filter to the database. This filter allows it to find the associated image that one desires. The filters for each of the labels were created and saved separately. The filter used was called an "Advanced Filter." This type of filter is created in the same fashion that queries are created and actually saved as queries. It allows for the database to be filtered on multiple criteria. In this case, the database is filtered first to find all of the images generated under the same master file, and then those images are filtered to find the particular image that corresponds with the label selected. Therefore the database is filtered by the master file control and then the image type option group.

Figure 12: Form Footer

Footer: The remaining controls are all located within the form's footer. These controls are all command button controls and were added to facilitate the ease of use of the database. The first of these command buttons is a button, entitled **Refresh**, that runs the macro *Refresh Database*. This macro performs the command "ShowAllRecords" which in essence simply removes the filters from the database. It is necessary to use this button after using the links to the associated image types due to the fact that they cause the database to be filtered down to a minute number (usually one) of records. The second command button, **Filter Help**, opens a form containing help on the different methods of filtering. This filter help form contains a command button which closes the form. The third command button, **Save**, on the footer of the main form saves the database. The next command button, **Close**, closes the main database form, and the last button, **Delete**, deletes the current record. With the exception of the **Refresh** button which uses a macro, all of the command buttons in the footer of the form perform actions that were built into Microsoft Access and run through Visual Basic code.

SKILLS DEVELOPED

The skills developed within the portion of the project include a proficiency at developing databases with Microsoft Access. Also, a great deal of knowledge was acquired concerning the properties of multi-sensor images, such as information about the frequency bands. A good deal of knowledge was also gained in the area of image file conversion when the Irma images had to be converted to the JPEG type.

CONCLUSIONS

The results of the database are that a coherent, effective, and easy-to-use database was created which greatly facilitates the organization of Irma images. The embedded thumbnail image which is included in the database is quite efficacious in that it allows the user to see exactly what the actual image will look like, thus greatly reducing the number of searches one might do in order to find the appropriate image. Future Upgrades to the database could be extensive. One important upgrade which could be added would be making the Startup form a switchboard, which allows the user to go to multiple places from the form instead of only allowing them to enter the main database form. One such form that could be created that would be of great benefit to the user would be a full query form. This form could allow the user to filter the entire database by any combination of fields and strings, using Boolean expressions such as and, or, and not freely. An upgrade that could be made to the main form would be for the Masterfile File Name label to become a button that would open the masterfile in a text editor such as Notepad. The masterfiles could reside in a folder in the same directory as the database itself. Another upgrade, akin to the previous one mentioned, would be to allow for the user to export a high quality TIFF image to Microsoft PowerPoint when the Thumbnail is selected. These TIFF images could also be kept in a folder in the same directory as the database.

REFERENCES:

Viescas, John L. *Running Microsoft Access for Windows 95.* Microsoft Press: Redmond, Washington, 1996.

"Irma 4.1 User's Guide." Nichols Research Corporation. May, 1998.

Lee, Warren M. "IR Course." Feb, 1996.

ACKNOWLEDGMENTS

First, I would like to thank my mentor, Capt. Vincent Underwood, for his assistance and guidance throughout the summer. I would like to thank Mr. Don Harrison and Mr. Mike Deiler for being the coordinators of the HSAP program, and Ms. Jeanette Williams for administrating the HSAP program. I would like to thank Ms. Karen Norris Zachery and Mr. Duane Geci for reviewing my database and giving their constructive criticism. A thanks goes to Mr. Mike Wellfare for helping me find imagery for the database. I would also like to thank Mr. Tom Potowski for his friendly smile and all of his help this summer. I would like to thank all of the apprentices for their support. An added thanks is given for the support of everyone in MNGG. An acknowledgment must go to the Air Force Research Laboratory, Munitions Directorate for sponsoring the High School

Apprentice Program. A final thanks is given to Research & Development Laboratories (RDL) and the Air Force Office of Scientific Research (AFOSR).

FINITE ELEMENT ANALYSIS OF LARGE A FRAME USED IN SUPPORT STRUCTURE

Christopher A. Rice

Southeastern High School
195 E. Jamestown St. PO Box Z
S. Charleston, OH 45368
(937) 462-8308

Final Report for:
High School Apprentice Program
Thermal Structures Laboratory
Wright Patterson Air Force Base, Dayton, OH

Sponsored by:
Air Force Office of Scientific Research
Bolling Air Force Base, DC

And

Thermal Structures Laboratory
Wright Patterson Air Force Base, Dayton, OH

August 1998

FINITE ELEMENT ANALYSIS OF LARGE A FRAME USED IN TEST PROGRAM RoCSS

Christopher A. Rice
Southeastern Local Schools
Wright Patterson Air Force Base, Dayton, OH
Thermal Structures Laboratory

Abstract

A finite element model was built of a support structure for the RoCSS (Robust Composite Sandwich Structure, pronounced "Rocks") test program to investigate the likelihood of failure and excessive motion of the structure. The model was constructed and loaded according to actual conditions specified by the initial concept design. The FE equations were solved for displacement and stress. The maximum allowable stress experienced by the structure at any test condition was chosen to be two-thirds of the yield stress. Resulting displacements and stresses were found to be above the acceptable limits, thus the model was altered accordingly and a new finite element analysis done. Stresses in the second model were acceptable, however deflections were still large. Therefore, an alternate configuration was recommended based upon the understanding of the structure gained during this study.

FINITE ELEMENT ANALYSIS OF LARGE A FRAME USED IN TEST PROGRAM RoCSS

Christopher A. Rice

Introduction

The primary reason for generating a finite element model of the support structure used in this test is to ensure that yield stress is not reached such that the support structure can be used for later tests. The support structure that was initially designed for RoCSS was comprised of large pre-fabricated A-frames, one of which is shown in figure 1. Figure 2 shows the entire support system for RoCSS including the large A-frames, hydraulics, support beams and 18" MC channels bolted to the edge of the 15" C. Two different configurations were studied in for this program. The first, applied loads directly to the A-frame. The second included the 18" MC channel attached to the vertical member of the A-frame to stiffen the structure. (Figure 2) A third configuration (Figure 3) may be studied in the future if necessity dictates. This

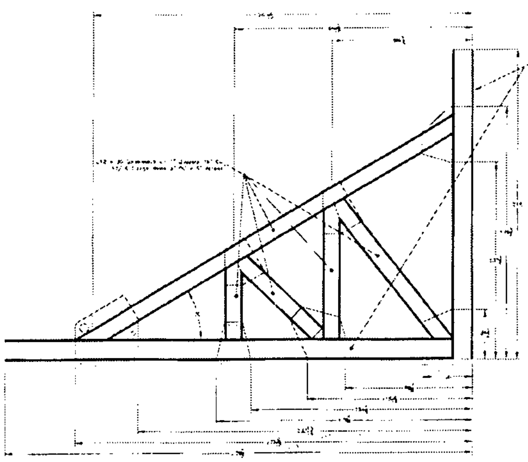

Figure 1. A-frame

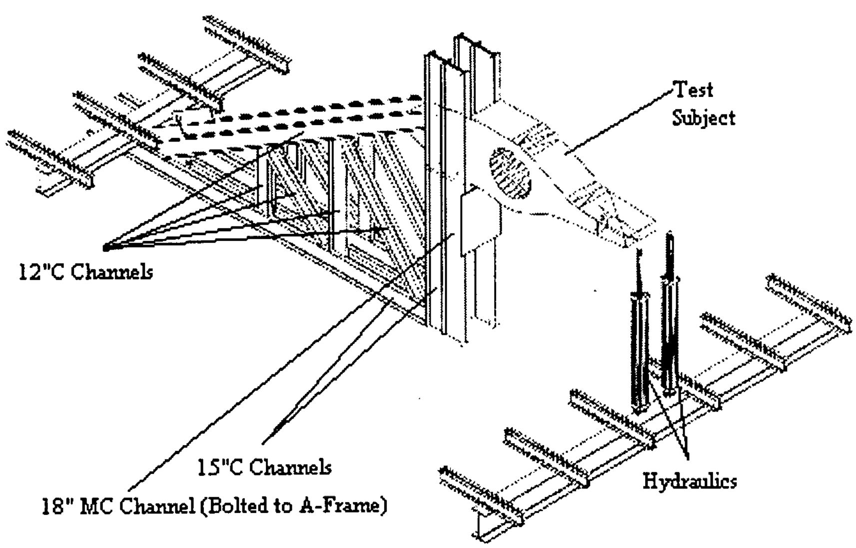

Figure 2. Support Structure

configuration places the test article over the A-frame, as opposed to hanging it from the end, making the test more self-contained and saving floor space.

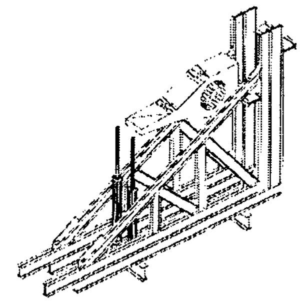

Figure 3.

About RoCSS

RoCSS, or Robust Composite Sandwich Structure, is a program that is studying the life span of a new type of fixed structure. Instead of being riveted or bolted like most aircraft strucures, RoCSS uses joints that are bonded together. The advantage of bonded joints is a better distribution of stress throughout the structure therefore resulting in a longer useful life and a lower weight. A cross section of an airframe will be manufctured with bonded joints and, as shown in Figure 2 and 3, is the test subject for the RoCSS experiment. Loads applied to the test subject will be transfered to the A-frames.

Model Specifictions

The large A-frame is ~27' long x 18' high, made by C channels 15" high with 3.716" flanges, a web thickness of .716 and flange thickness of .65". These make up the bottom and vertical side of the A-frame. All other beams are C channels 12" high with 3.17" flanges, a web thickness of .51" and a flange thickness of .5". All beams are doubleback on 1" gussets 36". The material used to construct the A-frames is a mild steel with a yield strength of 36ksi and an ultimate strength of 55ksi. The endurance limit of the material is estimated to be around two-thirds of yield strength, or ~21.6ksi.

Finite Element Analysis

Finite element analysis takes a large complex object and breaks it down into smaller pieces (finite elements). The element equations are assembled into a global matrix, which is inverted to solve for model displacements. From these displacements, stresses and reaction forces are calculated. When building a finite element model it is important to determine where the model in question is most likely to experience high stress so that these areas can be made with higher mesh density and thus a more accurate solution can be obtained. After the initial solution further mesh refinements can take place if necessary to address other high stress areas.

Methodology

All specifications of the large A-frame were found; size, material properties, and how the joints in the A-frame were put together. In order to model the A-frame properly it was important to understand if the joints in the structure acted as separate pieces or as one piece. It was decided that the model would be put together as if all joints were one piece for the sake of simplicity of design. Also, this was sensible since the compression forces from the rivets on the steel joints would make the joints act as one piece. This removed the need for gap elements in the model which significantly reduced the building time for the model as well as the time that was needed to solve the model. Also for simplicity the model was made without the holes in the flange thickness. Without these holes in the model, the stiffness of the model was much higher than in the physical frame and the resulting displacements were lower. In order to calculate more accurate values for stress, smaller test models were made. One test model had a C channel with flange holes while another test model used a C channel without flange holes. In the results it was found that a C channel with holes had 60% higher stress than a C channel without holes. As a result any stresses modeled in the A-frame needed to be multiplied by a factor of 1.6 to account for lack of detail in the model. Displacement in the two models differed by 10% and thus reported deflections were increased by this amount.

The Model

The first goal of the project was to build a finite element model of a large A-frame. It was decided that the best way to build the model was to keep it simple and use all opportunities to reduce the model size and its mesh density. Taking into account that the RoCSS test article will load both A-frames symmetrically, only one A-frame needed to be modelled. (Test subject is attached only to A-frames, not to any other part of the support structure.) Similarily, because each A-frame and its loads are symmetric, symmetry could be used along the centerline of the gussets reducing the finite element model to a single A-frame shown in Figure 4. In this figure the gussets

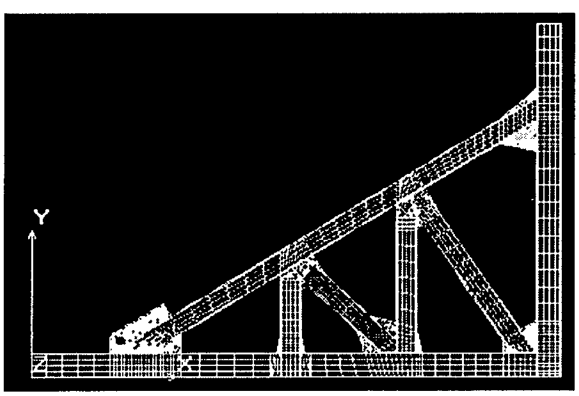

Figure 4. FEM of A-frame

are modeled .5" thick and the C channels are not doubleback on the gussets. Also in figure 3 the mesh is more dense where gussets and joints are located and less dense in areas where high stress gradients are not likely to be present.

The First Results

Once the first model of the A-frame was finished, it was analyzed with loads as close to actual loads as possible, however, the way the loads were introduced differed greatly from how they would be introduced in the final test model because of a lack of information at the time the first model was built. This run-through test was successful in removing any defects in the main section of the model and addressing mesh density issues. At this point the model had been verified and could be loaded in any fashion and added to in any way.

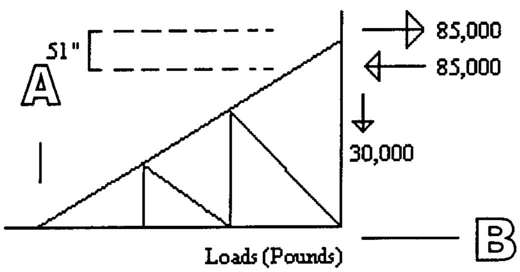

Figure 5 Load Conditions

The Loads

The test article will load a single A-frame with a couple of 170,000 LB @ 51" apart via loading pads. (The centers of the holes on loading pads were 51" apart, 51" 170,000 LB each loading pad = 722,500 ft LB) In addition there will be a 60,000 LB force down. Taking into account that the A-frame was modeled in symmetry all values were divided by ½ so 170,000 LB ea. pad / 2 sides of A-frame = 85,000 LB and 60,000 LB / 2 loading pads / 2 sides = 15,000 LB down. See Fig 5. The frame was constrained in Y along a row of nodes at point A and in XYZ at point B.

MC Channel Studied

From the results of the preliminary test it was agreed that two more models should be made and analyzed before deciding which would be better, one model with no MC channel and another with an MC channel. Both models would include new loading pads. (Figure 6 w/o MC channel, Figure 7 includes MC.) The

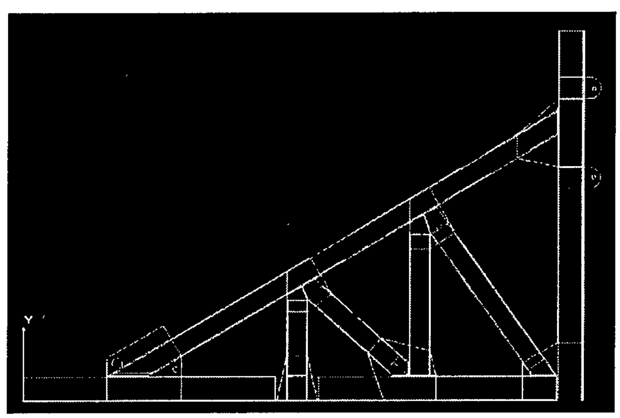

Figure 6 Without MC Channel

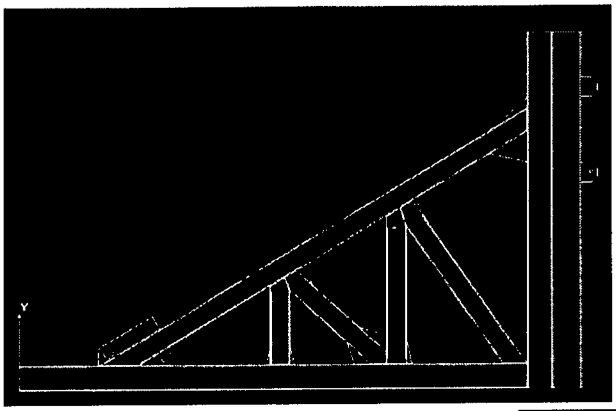

Figure 7 With MC Channel

reason for this was because in the preliminary model the vertical C channel deflected too much locally where the force was applied and it was agreed that loading pads were needed to distribute the load into the C channel. In the results, shown in Figures 8 and 9, one can see that without the MC channel the stresses are significantly higher than with the MC channel. From these results it was decided to use the extra MC channel to keep the A-frame from reaching a stress that could cause permanent damage to the A-frame. Note that the high stresses found in the loading pads are not accurate because the loads in actuality are applied to a larger loading pad. Fig 8 and 9 are also more easily seen in color. Color copies can be obtained from Southeastern High School.

From Table 1, one can see how the MC channel significantly reduces stress and displacement, and with a factor of 1.6 (Factor mentioned at the top of page 5.) the stresses, even with the MC channel, are high.

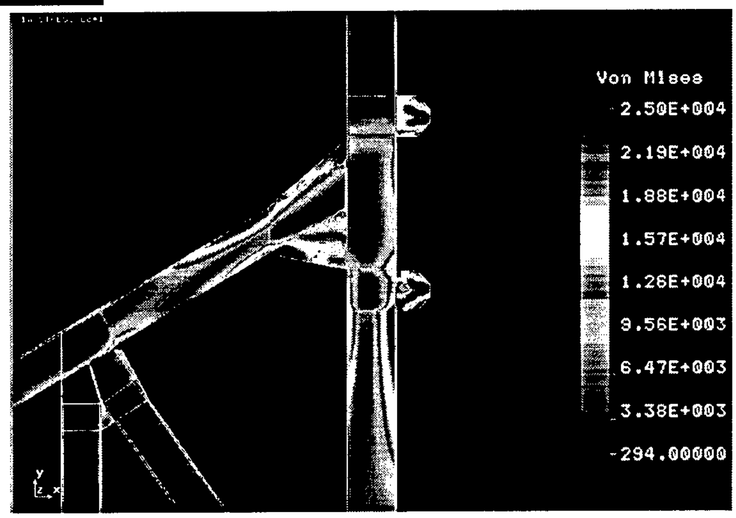

Figure 8, Results of A-frame w/o MC

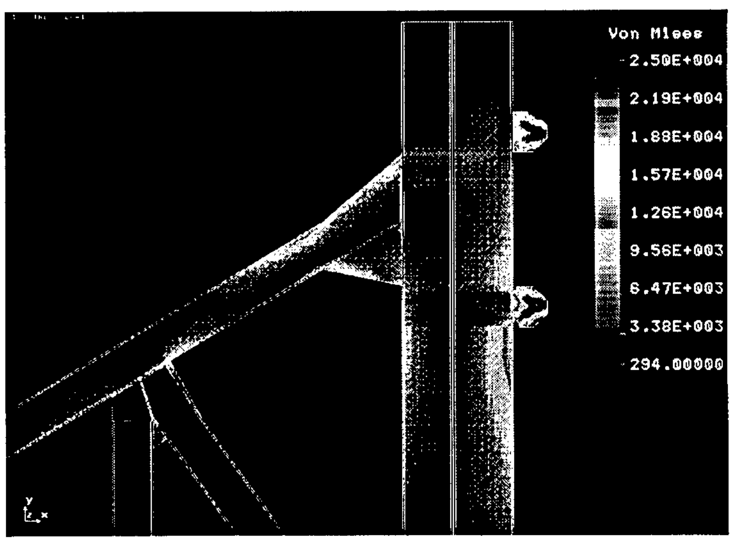

Figure 9, Results of A-frame w/ MC

Table 1 - Results

	Without MC Channel	With MC Channel
Max Stress	25ksi	14ksi
Max Disp.	.32"	.12"
Stress Concentration	40ksi	22.4ksi
Displacement Correction	.352"	.132"

Conclusions and Recommendations

It was concluded that if the stresses were to stay under acceptable limits in the support structure an MC channel would need to be bolted to the edge of the C channel. With the MC channel bolted to the end of the C channel the resulting stresses, even with the stress correction for the holes, were under acceptable limits and it was decided to use MC channels in the support structure. From the analysis results, recomendations were made on how to reduce areas of high stress by reenforcing these areas with extra doubleback 12" C channels or by changing the assembly to induce loads along the opposite leg, thus taking better advantage of the A-Frame design. Depending on which recommendation is preferred, the finite element model should be modified and solved to see if the resulting stresses are reduced to acceptable limits in the areas of concern.

THE BASIC STUDY AND SEAT STRUCTRUE ASSEMBLY OF THE RECLINED EJECTION SEAT

Monica Roy

Beavercreek High School
2660 Dayton-Xenia Road
Beavercreek, OH 45434

Final Report for:
High School Apprenticeship Program
AFRL/Wright Laboratory

Sponsored by:
Air Force Office of Scientific Research
Bolling Air Force Base, DC

And

Wright Laboratory

August 1998

THE BASIC STUDY AND SEAT STRUCTURE ASSEMBLY OF THE RECLINED EJECTION SEAT

Monica Roy

Abstract

The Reclined Ejection Seat System is designed to fit into Low Profile Cockpits and to provide safe escape during emergencies occurring at airspeeds from 0 to 687 knots at altitudes form sea level to 50,000 feet. In order to comprehend the importance and amazement of the reclined ejection seat system, it is of first priority to learn the seat structure assembly. This necessary equipment is composed of two major subassemblies: a seat bucket structure and a headrest assembly.

THE BASIC STUDY AND SEAT STRUCTURE ASSEMBLY
OF THE
RECLINED SEAT EJECTION

Monica Roy

Introduction

The Air Force Research Laboratory of Escape and Impact Protection Branch of the Biodynamics and Biocommunications Division conducts experimental research and analyses of the human response to transient biodynamic stresses caused by impact acceleration, aerodynamic forces, and thermal energy. One of their main missions is to formulate principles and techniques to protect personnel and demonstrate developmental protection concepts. Also to develop concept evaluation methods for emergency escape systems, experimentally verify, apply models, and establish aeromedical criteria for biodynamic response, apply to this branch.

Their research is conducted on male and female anthro-pomety to comprehend the characteristics of the neck and lower spine, to develop protection methods, to define acceptable impact tolerance, and to effectively evaluate biochemical injury. In order to aid them in the process of testing, they use Advanced Dynamic Anthropomorphic Manikins (ADAM). The purpose of ADAM is to aid in developing databases to be used in design, analytical modeling, and evaluation *Figure 1*. The Acceleration Effects and Escape Branch (HESA) has the facilities and expertise to test human volunteers and manikins over a full range of impact acceleration levels, durations, and body axes. One of their main equipments is the reclined ejection seat. The Reclined Ejection Seat System is designed to fit into Low Profile Cockpits and to provide safe escape during emergencies occurring at airspeeds from 0 to 687 knots at altitudes form sea level to 50,000 feet. *Figure 2*

Studies for advanced fighter aircraft configuration have indicated potential benefits to be obtained from the incorporation of a low profile cockpit (LPC). These benefits are the reduction of aircraft size, weight, cost, and drag leading to improved aircraft performance. Results have also shown that an increase in pilot effectiveness under high acceleration results from placing the pilot in a near supine position. The cockpit geometry, which is the primary feature of the LPC, is developed around a pilot seated in a semi-

THE BASIC STUDY AND SEAT STRUCTURE ASSEMBLY
OF THE
RECLINED SEAT EJECTION

Monica Roy

supine position with the seat back fixed at a high recline angle. Due to the fact that a conventional ejection seat cannot be used in this situation, these benefits can be realized only through the development of an effective escape system which can be integrated with the LPC.

Methodology

One of the jobs completed by the High School Apprentices at this branch was filing the information brought to Ohio in the Holloman Archives. These files included information on the many topics such as the Project Lifeline, tractor Rocket, Drop Test Vehicle, and High Speed Ejection Seats. Within the category of the High Speed Ejection Seats, a rather striking subject delt with the reclined ejection seat. The amazing technique of this equipment grasped the attention of the apprentices. Thus allowing to file, read, and learn more about this topic. By doing this job, one can easily learn a large amount of information about the experiments and their results that take place and the Acceleration Effects and Escape Branch and the Escape and Impact Protection Branch.

The method of development of the reclined ejection seat is very complex. Therefore, a closer look at the seat structure assembly is required. The seat structure assembly is composed of two major subassemblies: a seat bucket structure and a headrest assembly.

The first is made of two milled aluminum side panels joined laterally at the front by a milled aluminum front panel, at the mid point by a forged aluminum lower lateral beam and at the top by a forged upper lateral beam. This structure is closed up by an aluminum sheet. What is so special about this seat is that unlike present seats, this one provides vertical support for the rider's feet and legs after positioning and restraint for ejection had been accomplished. Also this seat has integral, deployable knee/leg braces which provide lateral support for and against which the legs are restrained during ejection. The braces deal with the side arm ejection controls and they are basically attached together in such a way that actuation of one control unlock both. The seat bucket structure is designed to accept the structual loadings and the loads provided by a 687 knot ejection without failure. The seat panel, which is made of aluminum and honeycomb sandwich material, is supported by a steel seat/man release shaft and along its forward edge by the front panel. It is separable to allow for removal of the survival kit.

The headrest assembly is the second major structural subassembly. It has two vertical supports which are attached at their lower end to the upper lateral beam of the seat bucket. Now, the uppermost holds the aerodynamic stabilizer loads and the second, immediately below the first, carries seat loads into cockpit structure. *Figure 3 & Figure 4.*

Results

After much research, the reclined ejection seat is proven to be in effect. It is incorporating a repositioning catapult and ejection rocket with thrust vector control is a feasible concept for escape throughout the flight envelope of a high performance aircraft. Greater aerodynamics stabilization was provided by the fin devices as tested in the wind tunnel. Under all escape conditions, good tail clearance was achieved due to the high positive life of the seat in the 90 degree reclined attitude. In order to maintain aerodynamic loads within tolerance, a delay of drogue chute deployment is required. The reason why aerodynamics deceleration is critical is because the crewmember's spine is aligned with the deceleration force with the seat in the reclined attitude. In conclusion, the seat structure of the reclined ejection seat enables it to be thus far an effective equipment.

THE BASIC STUDY AND SEAT STRUCTURE ASSEMBLY OF THE RECLINED SEAT EJECTION

Monica Roy

References:

1. Bull, J. O., Ther, D. T., and Yurczyk, R. .F., "Advanced Ejection Seat for High Dynamic Prerssure Escape-Wind Tunnel Test Report", AFWAL-TR-80-3084, August 1980.

2. Brister, J. G. and Yurczyk, R. F., " Reclined Ejection Seat Development-Wind Tunnel Test Report", Boeing Document D180-26609-1 May 1981.

3. Tanby, W.C., et al, "Investigation of Minimum Sized Low-Profile cockpits (MSLPC) and Crew Escape System Integration", AFFDL-TR-793104, September 1979.

4. Ther, D. T., and Yurczyk, R. F., " Reclined Ejection Seat Development-Intrim Report", Boeing Document D180-26171-1, November 1980.

5. West, C. L., Ummel, B.R., and yurczyk, R. F., "Analysis of Ejection Seat Stability Using EASY Program, Volume I", Boeing Document D180-26310-1, February 1981

6. "Investigation of Minimum Speed Low-Profile Cockpits (MSLPC) and Crew Escape System Integration," AFFDL-TR-3104, Air Force Flight Dynamics Lab, WPAFB, Ohio, September 1979.

THREE TYPES OF DUMMIES PROVIDE DIFFERENT LEVELS OF SIMULATION

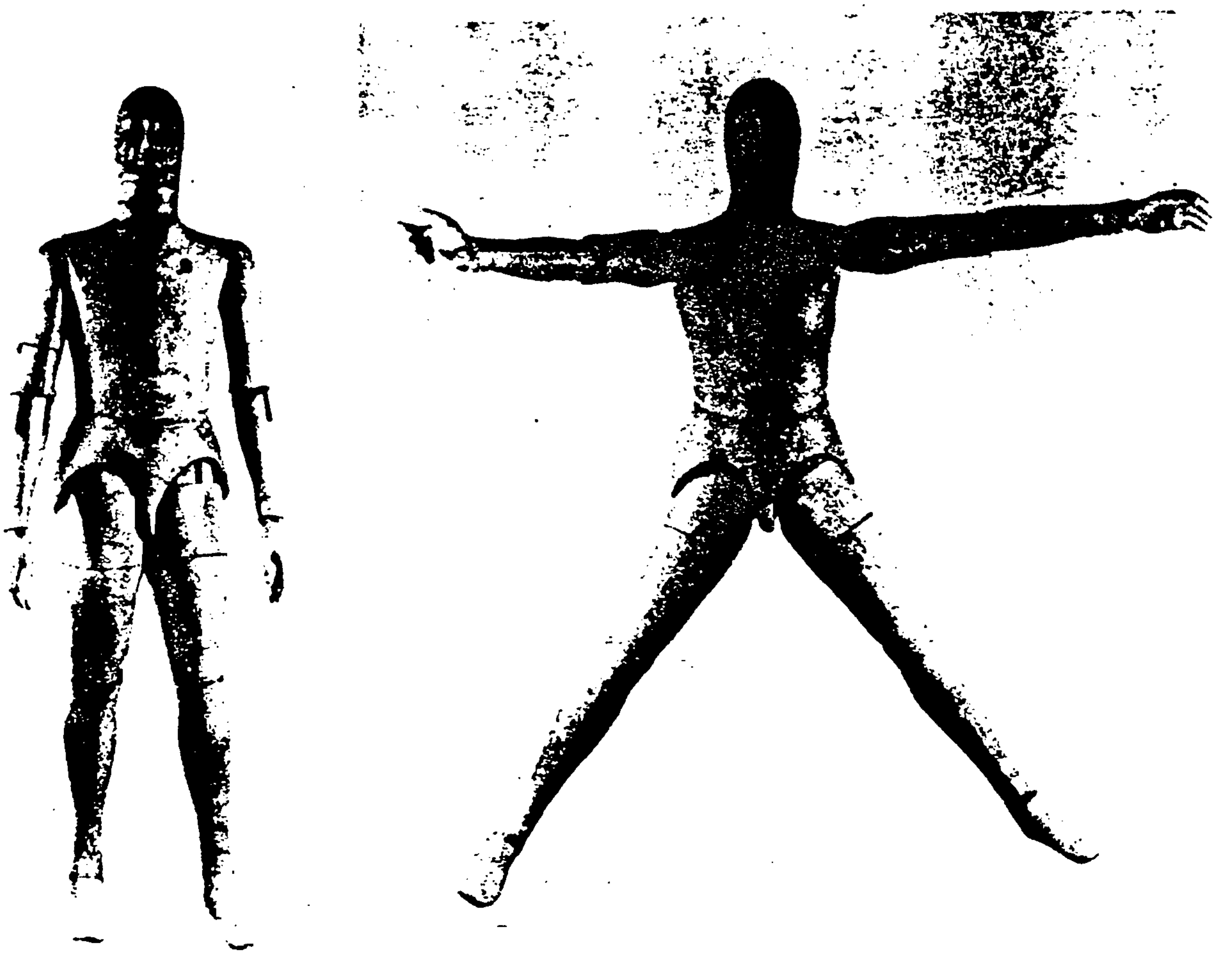

Figure 1 Model F-95 Anthropomorphic Test Dummy

THE MODULAR SERIES

The various models in this series are the most accurate of all human simulations in this field. A typical model is shown in Fig. 5. They are used where contours of the human body and the action of flesh over the skeleton must be duplicated closely, and where full ranges of the major human motions are needed. Their most usual applications include flight-testing of escape systems, crash research, blast-effects studies, and tests of personal equipment.

Figure 1

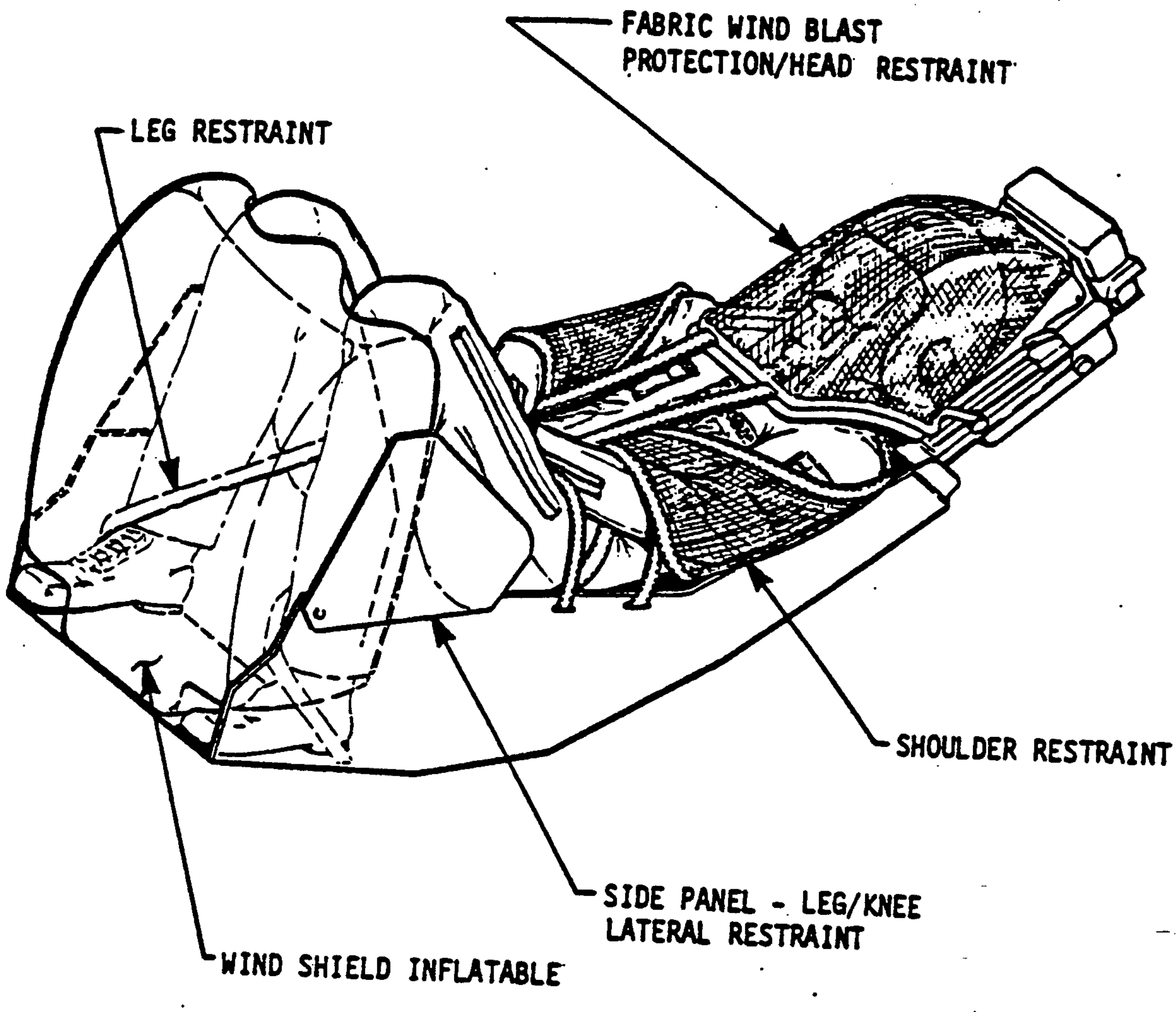

FIGURE 2. RECLINED EJECTION SEAT RESTRAINT/PROTECTION SUBSYSTEM

[illegible] about C. G. = $\frac{[illegible]}{23.4'' - 4.8''} = 1.97''$

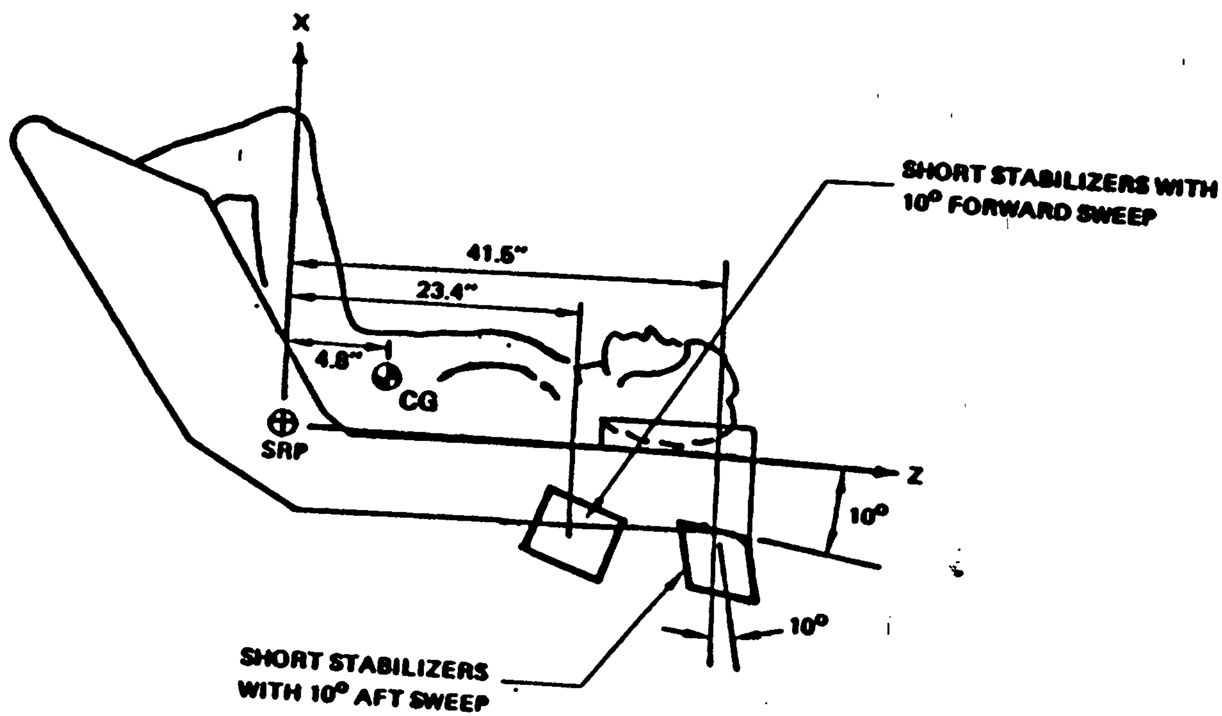

Figure 3 Moment Arm Increase from Moving Stabilizers to Headrest

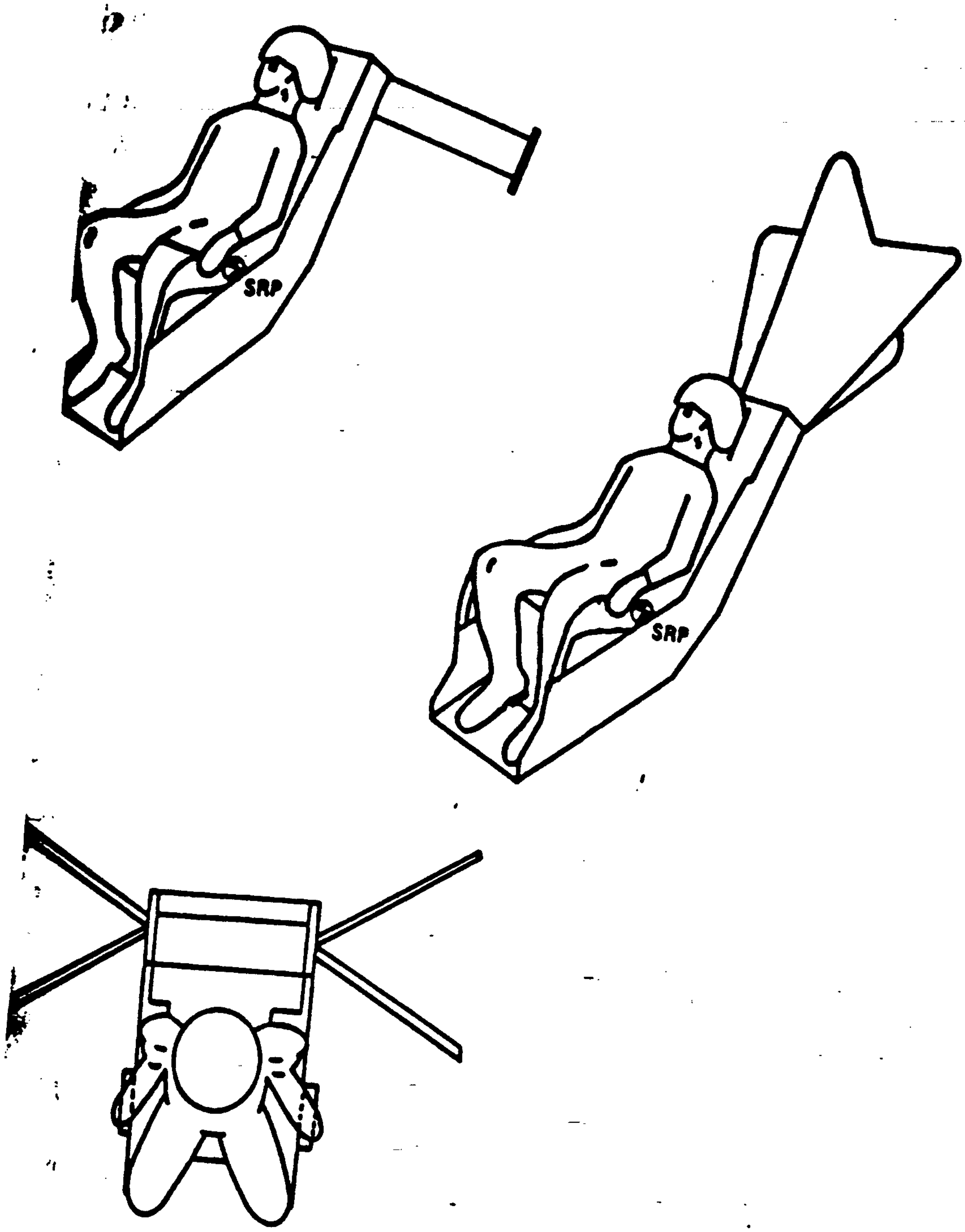

Figure 4 Proposed Stabilization Devices

A STUDY OF THE NECESSITY, EFFECTIVENESS AND CORRELATION ANTHROPOMORPHIC MANIKINS TO HUMANS

Anita Roy

Beavercreek High School
2660 Dayton-Xenia Road
Beavercreek, OH 45434

Final Report for:
High School Apprenticeship Program
AFRL/Wright Laboratory

Sponsored by:
Air Force Office of Scientific Research
Bolling Air Force Base, DC

And

Wright Laboratory

August 1998

A STUDY OF THE NECESSITY, EFFECTIVENESS, AND CORRELATION OF ANTHROPOMORPHIC MANIKINS TO HUMANS

Anita Roy
Beavercreek High School

Abstract

Anthropomorphic manikins served as human substitutes to better understand the limits of the human body during the ejection process. Their effectiveness could only be measured through their design and correlation to humans. This essential relationship first called on human misfortunes: accidents, injuries, and deaths. In turn, these substitutes, designed to simulate human limits, provided information not feasible for normal human subjects; this gave insight to the betterment of human testing, advancement, and changes required in the ejection seat development.

A STUDY OF THE NECESSITY, EFFECTIVENESS, AND CORRELATION OF ANTHROPOMORPHIC MANIKINS TO HUMANS

Anita Roy

Introduction:

The Escape and Impact Protection Branch of the Armstrong Laboratory at Wright Patterson Air Force Base (AFRL/HEPA) conducts testing on humans and manikins for restraint systems, specializing in the assessment of emergency escape systems. A Vertical Deceleration Tower, Horizontal Impact Accelerator, and a prototype ejection "black box" performance recorder provide information to evaluate ejection acceleration hazards. The complexity of data collection and management requires interactive access to this acquired information and calls for a biodynamics data bank which will expand in the future to a local area network and engineers' workstation. This biodynamics work environment (BWE) will eventually be used by researchers to perform virtual experiments. The biodynamics data bank filing was the project given to the apprentice. Through this and the observation of testing on the various equipment, the interest in anthropomorphic manikins emerged.

First, the filing arose interest in the dangers involved in the ejection seat process, and later reached into the development of testing to alleviate the problems. The question of testing dummies lead to more research and finally to the vital query of the interrelationship between humans and manikins. This key concept was rather intriguing and lead to the investigation of the design of anthropomorphic manikins, especially the ones used at this lab. Therefore, this thesis develops an understanding of the work performed at this lab, the ejection seat process and its hazards, and the evaluation of manikins.

A STUDY OF THE NECESSITY, EFFECTIVENESS, AND CORRELATION OF ANTHROPOMORPHIC MANIKINS TO HUMANS

Anita Roy

Methodology:

The Escape and Impact Protection Branch analyzes the experiments conducted to define human response to transient biodynamic stresses caused by impact acceleration, aerodynamic forces, and thermal energy. Through the obtained data, protection techniques of personnel and evaluation of emergency escape systems were created to establish aeromedical criteria for biodynamic response to mechanical force and to estimate injury potential. As technology advances and aircraft fly faster and higher, hazards for emergency escape develop. Spinal injuries are of critical importance and dummies are essential to the understanding of the lower neck and spine regions to define acceptable impact tolerance. Crew Escape Technologies (CREST) developed three-dimensional thrust vectoring that improves acceleration tolerance with a spinal preloading system and position the body that align the spinal column with restraint devices for maximum tolerance to ejection acceleration forces. To better understand the dangers in question, the ejection process needs to be studied closer.

Military operations require manned aircraft and performance capabilities continue to increase and will probably do so in the future. Aircrews need successful training with critical selection criteria and the underlying escape problems surfaced. Some of the problems faced

A STUDY OF THE NECESSITY, EFFECTIVENESS, AND CORRELATION OF ANTHROPOMORPHIC MANIKINS TO HUMANS

Anita Roy

include: clearing the aircraft, the airman's own kinetic energy, surviving in the ambient atmosphere and safe contact with the earth's surface. This thesis is most concerned with the first two but must consider all aspects to create the most effective manikin and results. Clearing the aircraft faces three distinct problems: 1) the most obvious hazard is the compactness of the aircraft and the limited internal clearance of the crew work-space which could block body passage, 2) free passage might not be accessible due to projections from the fuselage, and finally 3) there needs to be a safe miss distance when making a high exit velocity from such fast aircraft. These problems eventually led to the development to the ejection seats. Other escape mechanisms including the escape chutes and escape capsules were also invented. However, high airspeeds eliminate the first from consideration and weight considerations create difficulties for the latter. Also, no advantages are detected for either over the ejection seat.

The second problem of the airman's own kinetic energy results form the transition from the rapidly forward-moving projectile to free-falling object with a new motion equilibrium in an ambient atmosphere. Drag causes rapid deceleration of the seat and the man. For every 15% increase in speed above 500K the ejected man is faced with a 50% increase in G's. Tumbling and windblast are other perils. These cause overstressing of body parts. Ways to solve such dilemmas include: increasing the mass of the ejected load, streamlining the ejected mass, repositioning the seat, stabilization of the seat, and shielding the body. As with any proposition each of these would create new problems and cannot be discussed without further research. This finally leads to the study of anthropomorphic manikins.

Sierra Engineering Company has engaged in design and construction of anthropometric dummies since 1949. Aircraft companies needed an expendable dummy for high-speed ejection tests. "Sierra Sam" as the dummy is called was used in rocket sleds and even test automobiles. Later Grumann-Alderson Research Dummy (GARD) came instilled with instruments which accurately simulated anatomical characteristics of his human counterpart. Finally, the Advanced Dynamic Anthropomorphic Manikins (ADAMs) became the leading dummy used at this base research center. The ADAM manikins contain an improved spinal system, joint systems, more sensors and channels, an internal data storage system, and an external data transmission link. Tests conducted reached definitive yet not conclusive results.

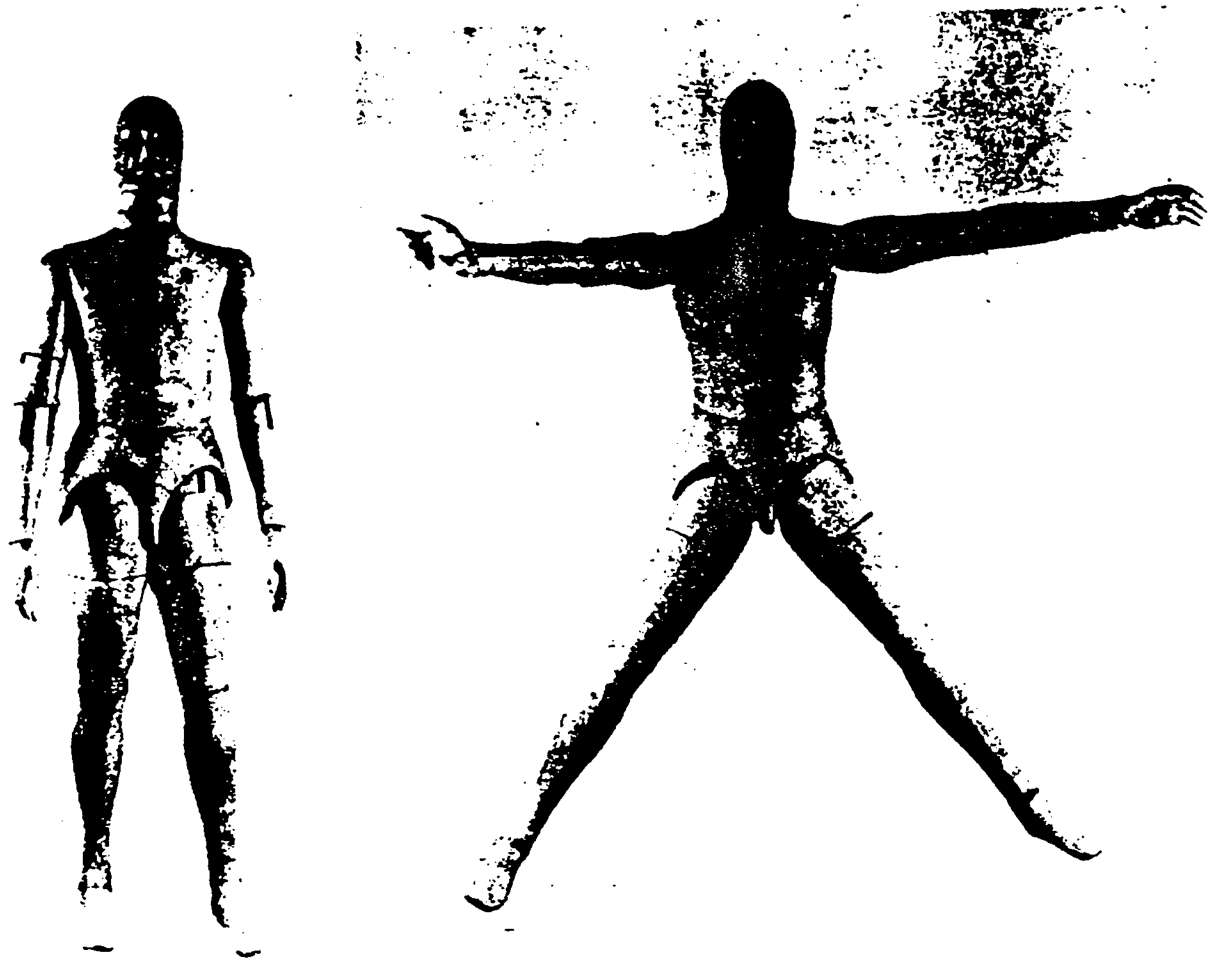

Figure 5 Model F-95 Anthropomorphic Test Dummy

THE MODULAR SERIES

The various models in this series are the most accurate of all human simulations in this field. A typical model is shown in Fig. 5. They are used where contours of the human body and the action of flesh over the skeleton must be duplicated closely, and where full ranges of the major human motions are needed. Their most usual applications include flight-testing of escape systems, crash research, blast-effects studies, and tests of personal equipment.

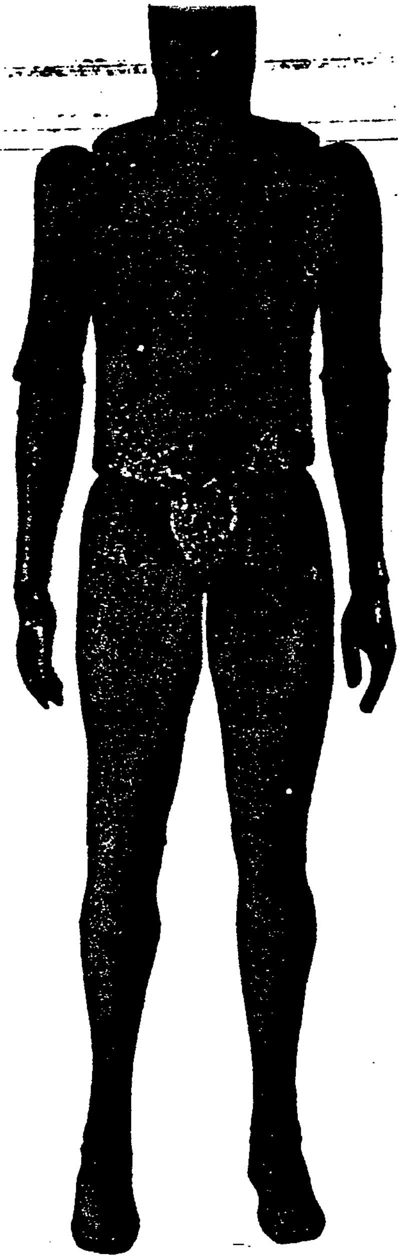

Figure 6 Model C-95 Anthropomorphic Test Dummy

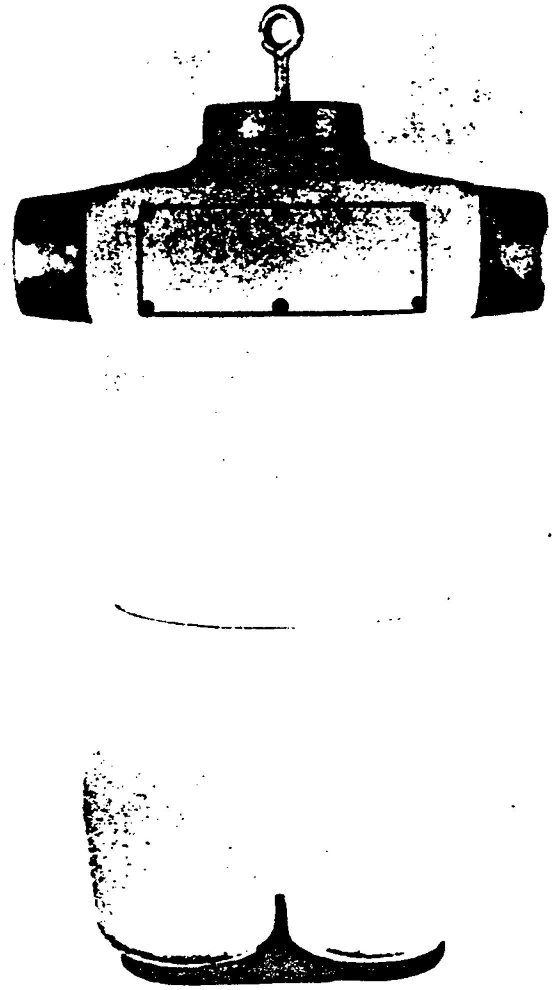

Figure 7 Model T Parachute Dummy

THE ROCKET-SLED SERIES

The models of this series are simplified in contour (Note Fig. 6) and motion capabilities, gaining extreme ruggedness and additional space for bulky instrumentation systems. They give adequate simulation, at low cost, for rocket-sled tests, where the subject is restrained against torso motion, and for other applications where a rigid torso is permissible.

THE PARACHUTE SERIES

These are the simplest and most durable of all anthropomorphic test dummies. For most parachute tests, they are used in the torso form shown in Fig. 7. They can be articulated, to extend the range of parachute test procedures, by adding adaptors and appendages.

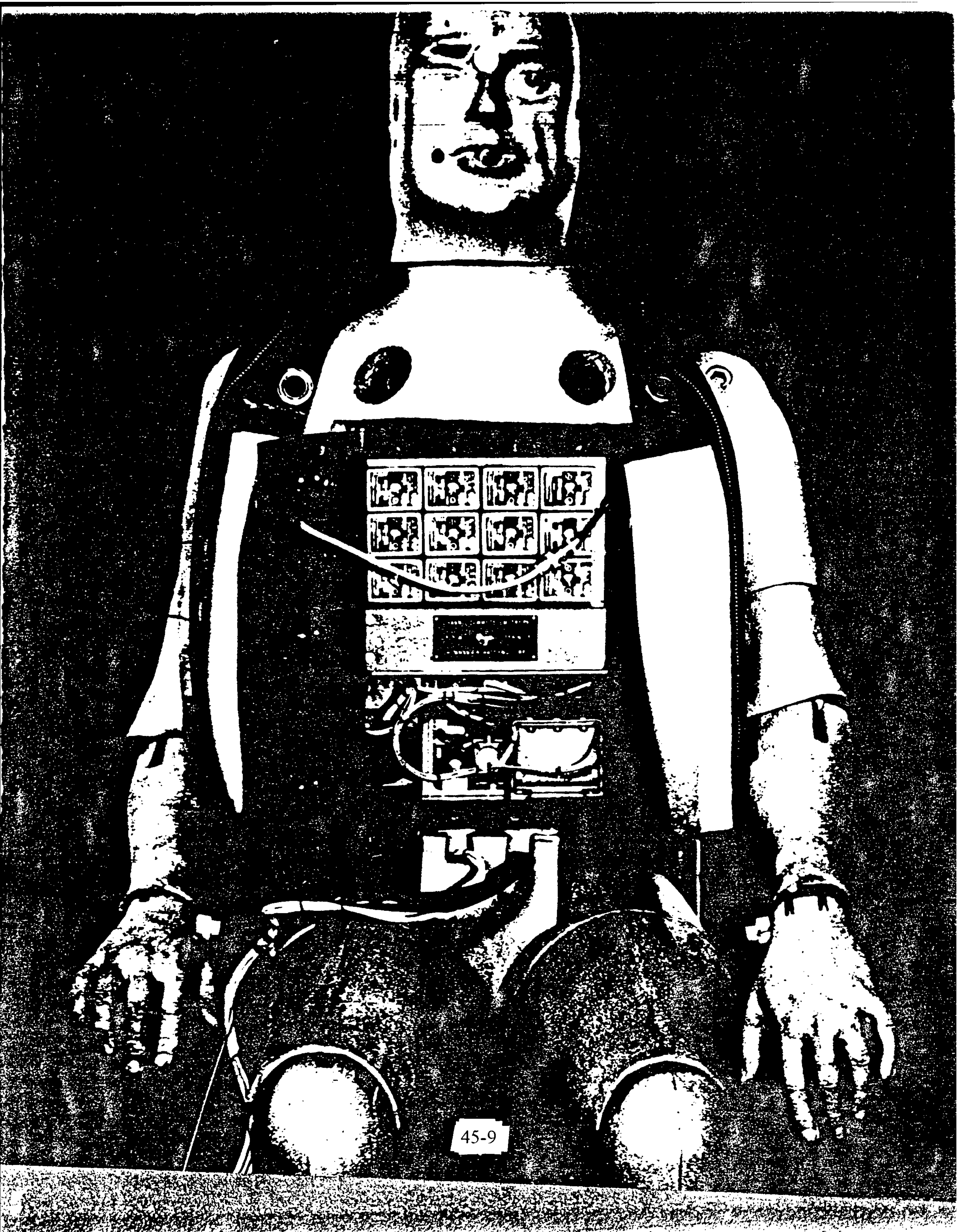
45-9

A STUDY OF THE NECESSITY, EFFECTIVENESS, AND CORRELATION OF ANTHROPOMORPHIC MANIKINS TO HUMANS

Anita Roy

Results:

Tests were conducted to determine the correlation between humans and anthropomorphic manikins via the Aerospace Crew Equipment Department Vertical Drop Tower. Both humans and dummies were restrained in identical seated platforms and high-speed motion picture cameras analyzed body displacements at various pre-selected points (as seen in Figure 1). Both the dummy and human reached their peak displacement at .040sec. At high G's, the results were practically identical and at lower G's, no difference greater than 3/8" were detected. The thigh and knee points of both provided similar data and can be concluded that dummies and humans are alike while positioned in the normal ejection seat configuration. However, the dummy responds quicker to the input pulse due to the more rigid configuration and material of the manikins. The dynamics of the human body as it affects the performance of pilot ejection systems is considered to be very significant and as yet, undetermined. It is obvious that there is an important need for a dummy with the same stiffness and dampening characteristics as a live human being, in order to evaluate ejection seat systems properly for what they were intended.

This also includes evaluation of all the necessary support and restraint system components on the seat (Schwartz).

Another test conducted with a small ADAM and humans resulted in no significant difference in any of the peak measurements. This was true in both numbers of mean acceleration response data within two standard deviations interval of the mean of the corresponding human data. The small ADAM seat force peak magnitudes were also consistently very close to the predicted human mean values as demonstrated by linear regression analysis. Results consistent with the human data were also obtained in the transfer function analysis computations of the resonant frequencies and damping ratios (Buhrman).

Conclusion:

An important criteria in determining the effectiveness of anthropomorphic manikins as human substitutes is the dummies' ability to simulate human dynamic responses. Once this correlation is proven, then the data obtained from manikin testing can help guide better advancements for humans. Thus far, test results have shown that a strong relationship exists; however, more testing needs to be conducted for full awareness. Whether regarding the ejection seat dangers or not, manikins have proven their necessity, effectiveness, and correlation to humans.

A STUDY OF THE NECESSITY, EFFECTIVENESS, AND CORRELATION OF ANTHROPOMORPHIC MANIKINS TO HUMANS

Anita Roy

References:

1. Alderson Research Laboratories. Anthropoporphic Test Dummies. NP.

2. Burhman, John. Vertical Impact of Humans and Anthropomorphic Manikins._1991.

3. Grumann-Anderson Research Laboratories. GARD Grumann-Anderson Research Dummy. NP.

4. Schwartz, Marcus. Comparative Study of Body Displacements in Both Humans and Anthropomorphic Dummies When Simultaneously Subjected to Controlled Vertical Impact Type Decelerations. 1968.

5. Sierra Engineering Company. Anthropomorphic-Anthropometric Family of Test Dummies. NP.

6. Sierra Engineering Co. Sierra Sam and Family. 1995.

* These are just the works I used directly in my paper; through the biodynamics filing I have gained much knowledge for this project. Also, I would like to thank Mr. Jeff Callaway Mr. Chris Perry, Mr. John Burhman, and Dr. Ted Knox for their help in this research and a sincere appreciation to Building 824 at Wright Patterson Air Force Base for allowing me to experience the first hand experiments to gain insight into my report. Finally to the AFOSR, I extend my greatest gratitude for allowing me to be a part of this honorable program. I have learned a lot this summer and wish to thank everyone who has made it possible. Thank you.

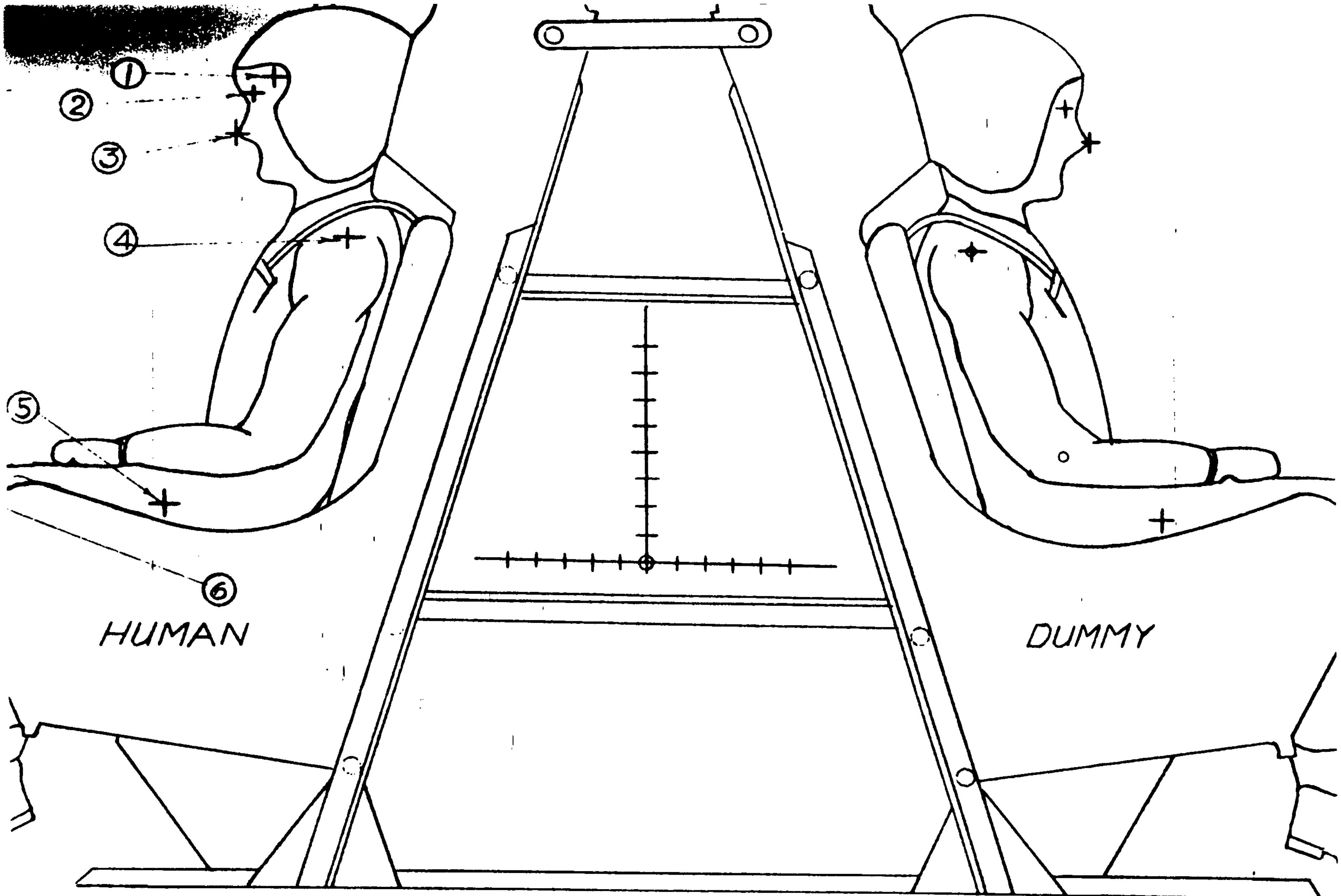

FIG NO 1 SET-UP FOR HUMAN-DUMMY TESTS

A REVIEW OF THE DEVELOPMENT OF EFFICIENT HELICOPTER ESCAPE SYSTEMS

Sanjida S. Saklayen

Centerville High School
500 E. Franklin St.
Centerville, OH 45458

Final Report for:
High School Apprenticeship Program
AFRL/Wright Laboratory

Sponsored by:
Air Force Office of Scientific Research
Bolling Air Force Base, DC

And

Wright Laboratory

August 1998

A REVIEW OF THE DEVELOPMENT OF EFFICIENT HELICOPTER ESCAPE SYSTEMS

Sanjida S. Saklayen
Centerville High School

Abstract

The development of efficient helicopter escape systems was reviewed. Through a general study of several technical reports, it was learned that rotary wing aircraft escape systems had not been developed until just two or three decades ago, as opposed to fixed wing aircraft escape systems, which were developed much earlier. It was also learned that a main problem considered in the development of helicopter escape systems was the presence of the rotor blades and its potential as an inhibitor to a successful escape. Numerous techniques have been studied, including but not limited to: manual bailout, ejection via ejection seat, extraction, and collective systems, such as total aircraft and capsule systems. In studying these techniques, feasibility, cost effectiveness, repeat success rate, human psychological factors, and other issues were considered. The Russian Ka-50 "Hokum" military helicopter, recently developed, is also reviewed, as it is the only operational military helicopter in the world to employ a fully-functional blade severance ejection system. This paper discusses positive and negative aspects of each type of helicopter escape system studied. The conclusion addresses the future of escape technology as well as a mention of the author's experience in the high school apprenticeship program in which she was involved.

A REVIEW OF THE DEVELOPMENT OF EFFICIENT HELICOPTER ESCAPE SYSTEMS

Sanjida S. Saklayen

Introduction

As a first-time applicant to the Air Force Summer Research Program, I was not at all sure what to expect. My first day of my first "real job," as an apprentice for the Acceleration Effects and Escape Branch at Wright Patterson Air Force Base, was a reality check of sorts. Within 8 hours, I was equipped with a place to "sit", i.e. my own desk and office equipment, my first "colleagues," a laboratory environment, an invitation to the Chief's retirement ceremony, a healthy relationship with fellow "interns" my age, and incredibly nice supportive mentors. Within a week, the other four "interns" and I were all settled into our "intern office" overlooking the bay, and had grown to be friends. I considered myself adjusted to the environment and was prepared to begin some real "scientific research," to be followed by a "serious scientific report." Not too much later, I was finally told the truth: my purpose for this summer was not to run the sled test equipment, nor to study the level of toxic toleration of rats (which was the experience of a friend of mine a year ago), nor even to invent a machine to ease the daily lives of the working class. I was to begin Biodata Systems Filing. In other words, I was going to file until I could file no more. For eight weeks, I would record all kinds of historical data, reports, and photos, recently shipped to Wright Patt from Holloman Air Force Base, into the computer database, the "Historical Data Archive," using the program Microsoft Access. I began my work, inwardly happy that I was aiding in the actual creation of a library search system. Once I adapted to the computer program and the organization of the files, the work became somewhat simple, even monotonous. However, I kept at it, and as I worked on my files, I grew rather interested in one of the subjects: helicopter escape. From merely reading and summarizing abstracts, as well as sifting through some of the more intriguing reports, I eventually learned a great deal. Thus begins my "serious scientific" final report

Years ago when military aircraft were first developed, a need was recognized for safety measures for pilots in distress. This need was further fueled by several records of fatal aircraft accidents. It was determined by one source, that over half of the fatal accidents during a certain time period could have been prevented by some reliable means of escape for the pilot and crew. Naturally, this was quite a while ago. Since then, Emergency Escape Systems have been thoroughly studied, developed, put into production, and employed by fixed-wing aircraft around the world. Unfortunately, as late as the early 1970's, development of such reliable, cost-efficient, and successfully repeatable means of escape had yet to be developed for rotary-wing aircraft--combat helicopters in particular. A main problem was that helicopter rotor blades inhibited proper upward ejection, a common form of escape in fixed wing aircraft. As a result, several methods of escape were considered. These include manual bailout (the most common method of escape from helicopters prior to the research), ejection, extraction, total aircraft and capsule systems. One of the most efficient means of escape, upward ejection following blade severance, was determined. Yet, as of today, 1998, only one modern military helicopter, the Russian Ka-50 employs an operational blade severance ejection system. This paper reviews the course of the development of helicopter escape systems from the 1970's through present day, and makes an effort to examine positive and negative aspects of some escape methods studied. It also presents a conclusion in which the future of escape technology is addressed.

Methodology

When the issue of the urgency for conceivable methods of helicopter escape was first introduced to scientists, feasibility was immediately discussed. Although widely in practice at the time, manual bailout from a helicopter in crisis had its weaknesses in terms of crashworthiness. Mainly, it was not very effective for low-altitude escape. The case was similar, if not worse, for downward ejection at low altitudes. For a more efficient helicopter escape system, new methods were needed. With those two methods rejected, the possibilities for upward ejection were investigated. The presence of helicopter rotor blades was an obstacle, however. Three possibilities for ejection were discussed: upward ejection maneuvering the trajectory around the rotor blade, upward ejection through a slowed or stopped strategically positioned rotor blade, or upward ejection following blade severance. Maneuvering around the blades posed the potential problem of impact or entanglement, due to the closeness of the rotating blades to the fuselage of the helicopter. According to one study, upward ejection through slowed or stopped blades posed hazards because: "Even if the rotor could be slowed without structural failure, the torque needed to accomplish this in the very short times required would be substantial, even for a small helicopter. Dissipation of the high energy of the rotor in a very short time would require very heavy and complex equipment." As a result, such an escape method was out of the question. Upward ejection following blade severance appeared to be quite feasible. First of all, removal of the rotor would easily clear the canopy and overhead area for normal upward ejection, as in a fixed-wing aircraft. Secondly, through the use of mild explosives to remove the blades, the procedure could easily be carried through within a very short period of time. The next consideration was the method of blade severance. Two such methods were introduced and discussed. The first method involved severing the individual blades; the second involved severing the actual rotor shaft with the blades still attached. Due to the continued action of the tail rotor, though, severing the main rotor shaft would lead to a very unstable fuselage and complicate ejection. On the other hand, severing all individual blades simultaneously would bring the danger of individual blades colliding after separation. Further, separating the individual blades in sequence brought the risk of fuselage instability. Later studies showed, however, that it was possible to separate the blades individually, in sequence, by having two blasts. The first would separate three blades (of the typical five) at specific azimuthal degrees (11°, 155°, and 227°). Thus, two blades would remain for a moment and maintain stability. A fifth of a rotation later, the second blast would remove the remaining two blades in relatively opposite directions, thus leaving the fuselage stable enough for proper upward ejection. After appropriate testing, it was found that this method of upward escape following blade severance was quite feasible, given the proper actions involved occurred within the relatively short time envelope.

Results

After ten years of development, in 1992, the Soviet Union unveiled the first helicopter equipped with a fully operational pilot ejection system that used the blade severance method, the Ka-50 Hokum. Currently, the Ka-50 is the only operational helicopter to possess such a system. Ka-50 Hokum offers some unique qualities. To begin, it allows for a single pilot to operate it during both daylight and darkness. In terms of speed, climb, and maneuvering, it exceeds the performance of any helicopter currently in operation, or even development, for that matter. It incorporates several survivability features, most significantly, the only operational blade severance pilot ejection system in the world. In order to aid successful ejection, and increase aircraft crashworthiness, it also has a coaxial (dual) rotor blade system. The Ka-50 Hokum's particular dual rotor blade "tends to have [so much] greater solidity" than single rotor blades, that it basically eliminates the need for a tail rotor. This is significant for two reasons. First, the absence of a tail rotor indicates that damage to the tail end of the helicopter does little in terms of altering stability or even combat capability of the entire aircraft. Second, the presence of only a coaxial rotor blade simplifies upward ejection, since there is less concern about instability after severing the shaft of the coaxial blade. Robert L. McDaniel's article in *Vertiflite* magazine describes the Ka-50 ejection sequence:

> First, rotor blades are severed "using explosive bolts at the blade root ends. Once severed, the blades are ejected from the rotor hub at high velocity, propelled by the centrifugal forces of rotation. This unique system does not save aircraft but saves pilots and, further, will tend to embolden pilots with more daring action in battle."

A major consideration though, is the possibility that the cause for ejection stemmed from damage to the rotor blades. However, since the actual rotor blades are not severed in the Ka-50, but the rotor shaft instead, the probability for successful separation is fairly high. As a result, the Ka-50's blade severance ejection system, in conjunction with the absence of its tail rotor, satisfies conditions for a very efficient helicopter escape system. Not only that, but it is the most advanced military combat helicopter in the world to date. That practically speaks for itself.

Conclusion

In sum, the development of an efficient helicopter escape system may have taken time, but the end product was "worth the wait." This concept is, perhaps, the most important thing I have learned this summer. True scientific discoveries do not happen overnight. They involve time, patience, hard work, tests, successes and failures, and constant questioning. To create something worthwhile, to invent something for another's benefit, involves close attention and a great deal of creative problem-solving. Hopefully, such great thinking, questioning, and development will progress well into the future of escape technology. After all, although the Ka-50 Hokum has been—and will most likely continue to be—" all that was projected—and perhaps more," there are still issues to address that could improve the aircraft and its escape system yet further. For example, is there any way to eject the pilot out of the aircraft, and save the aircraft as well? Is there a less expensive way to save crew members of space shuttles in distress? Can an automated escape initiation system—one that senses the need for emergency escape on its own—ever be developed? What about the issue of human psychological factors during escape and its effect on timing of the escape sequence? These topics have been discussed but, to my knowledge, not too many feasible ideas have been entertained. With further research, as with the development of the blade severance ejection system and the Ka-50 Hokum, we may see promising results even within the next few years.

As a last word, I would like to say I have had an incredibly interesting, educational, and fun summer working in Building 824, Acceleration Effects and Escape Branch. During my tour I observed several sled run tests, of two types: a G_y study involving human subjects, and the testing of a data recording device for ejection seats. From my office window, I observed manikin ejection seat tests on the vertical drop tower, which focuses on G_z as well as human subject tests on the six-degree-of-freedom vibration table, which simulates the stresses of a vehicle crash on the human body. During a tour of facilities with my mentor, I observed several tests on the Dynamic Environment Simulator (human centrifuge), and even had the opportunity to speak with the test subject and to climb into the cab. I have had so many unique experiences and have met so many wonderful new people here, I am already having a difficult time facing the fact that the tour is nearly over. This has been quite an experience.

References

Advisory Group for Aerospace Research and Development. "Escape Measures for Combat Helicopter Crews." No. 62.

Beggs, Bob. "Crew Stations and Human Factors Engineering." Vertiflite. May/June 1994. 34-35.

Bement, Laurence J. "Helicopter Emergency Escape." SAFE Journal. Fall Qtr. 1979. 28-36.

Bolukbasi, Akif. "Crashworthiness Subcomittee." Vertiflite. May/June 1994. 34.

Flickinger, Don and Albert W. Hetherington. "An Interpretation of the Problem." Haber. 1-6.

Haber, Heinz. A Symposium on Escape from High Performance Aircraft. Los Angeles: UCLA, 7 Oct. 1955.

Lenorovitz, Jeffrey M. and Boris Rybak. "Naval Design Experience Applied to Ka-50 Hokum." Aviation Week and Space Technology. 24 August 1992. 40-43

Mayo, A.M. "Selection of the Escape System." Haber. 91-95.

McDaniel, Robert L. "Hokum Confirmed: All That Was Projected—And Perhaps More." Vertiflite. March/April 1993. 22-27.

Wood, Derek. "Kamov Ka-50 'Hokum'." World Aircraft Recognition Handbook. UK: Butler and Tanner, 1979.

Zeller, Andrew F. "Psychological Factors in Escape." Haber. 43-46.

Figure 1

Army/NASA sponsored RSRA (Rotor Systems Research Aircraft) designed to serve as a research test vehicle to promote the study and evaluation of advanced helicopter rotor systems and helicopter escape.

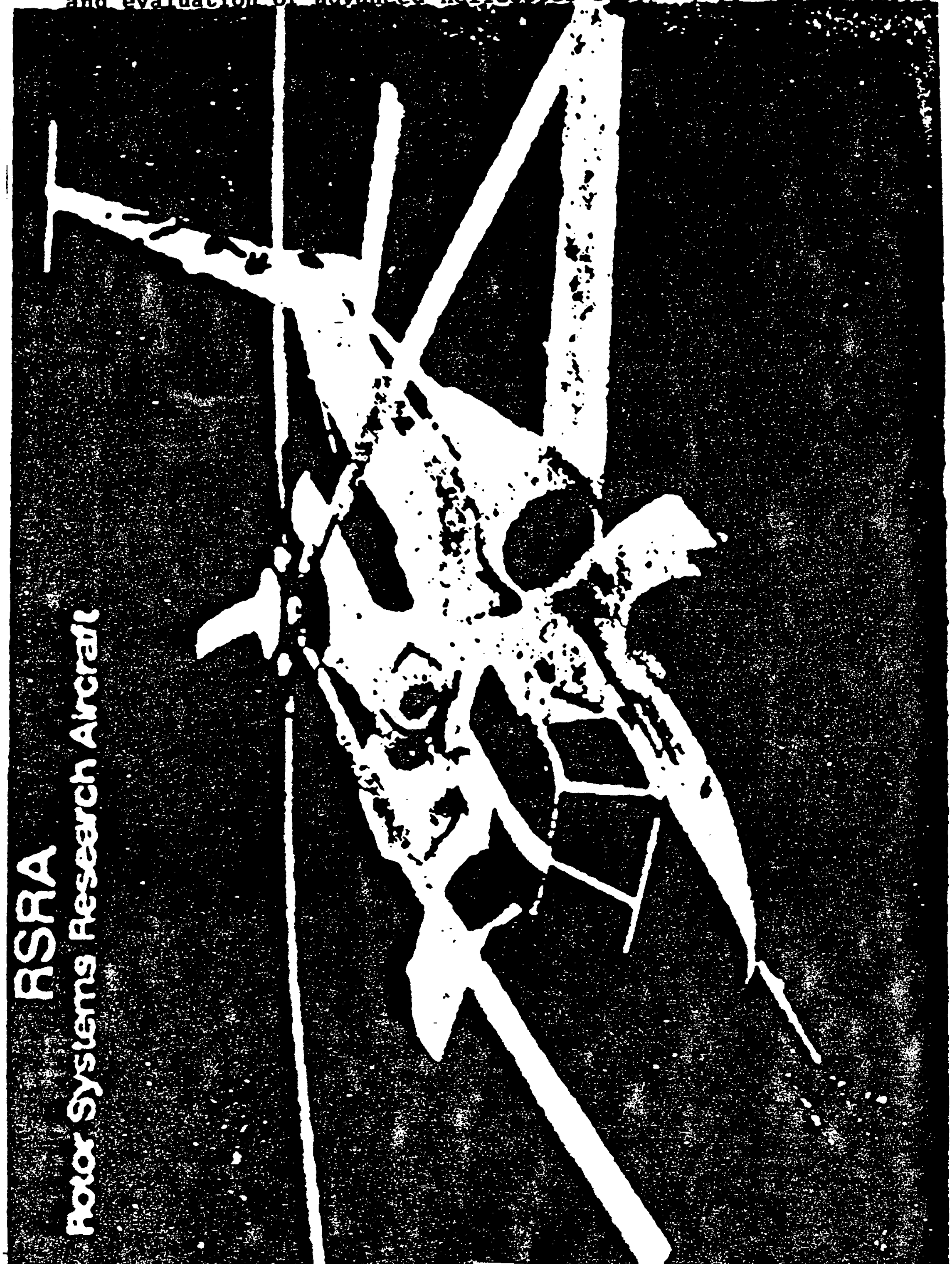

Figure 2

Exterior view of Russian military helicopter, "Hokum" KA-50.

Figure 3

Interior View of Russian military helicopter, "Hokum" KA-50.

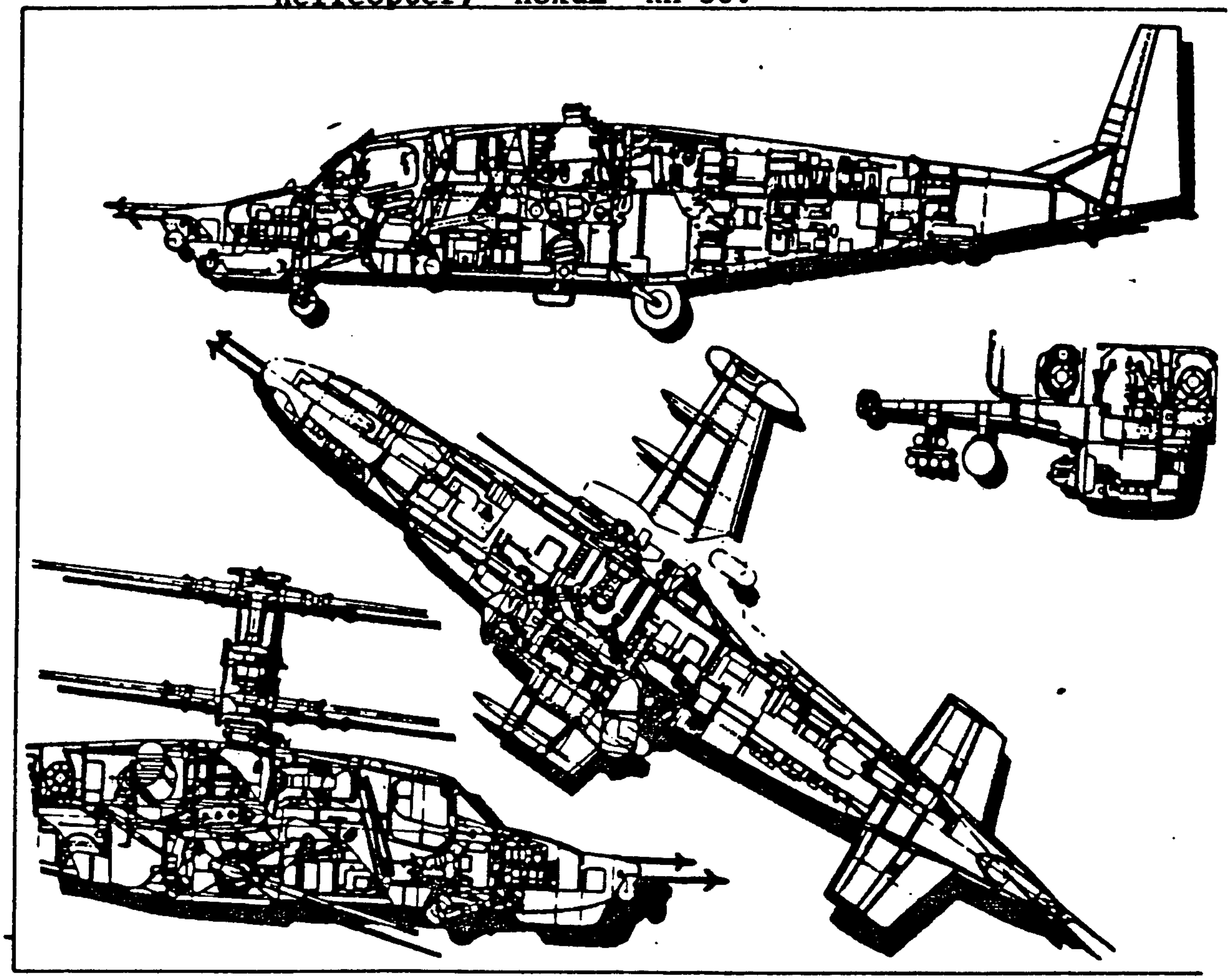

Figure 4

Rocket-assisted ejection seat installed
in Russian KA-50. The helicopter's dual rotor
(coaxial) blades are blown off prior to ejection.

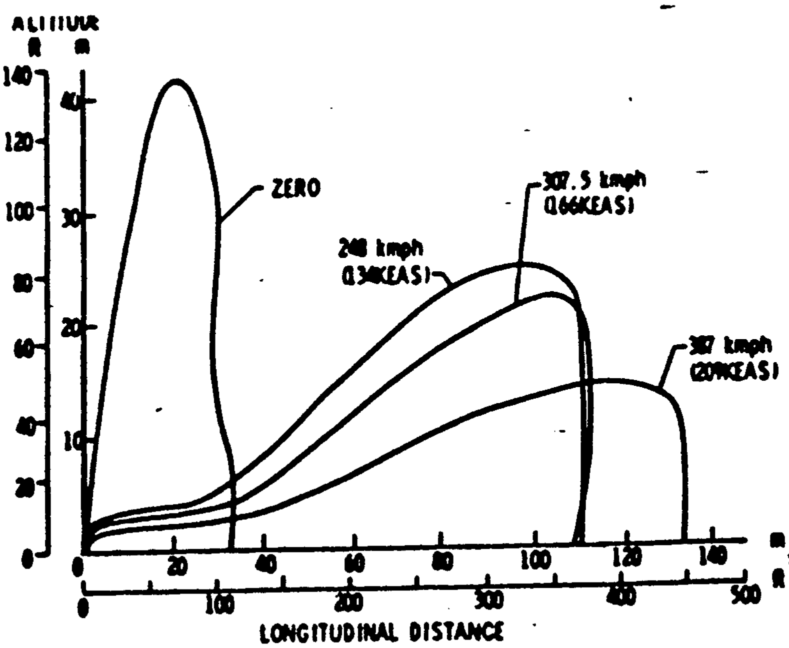

Figure 5

Pilot's Center of Gravity trajectories during sled test ejections in terms of his relation to the vehicle and initial velocity.

Figure 6

Visual Comparison of the AH-1 Cobra Huey helicopter (single rotor) and the KA-50 Hokum helicopter (double rotor). The KA-50 employs an operational blade severance ejection system, flies faster, is built lighter, and yet, appears more complex.

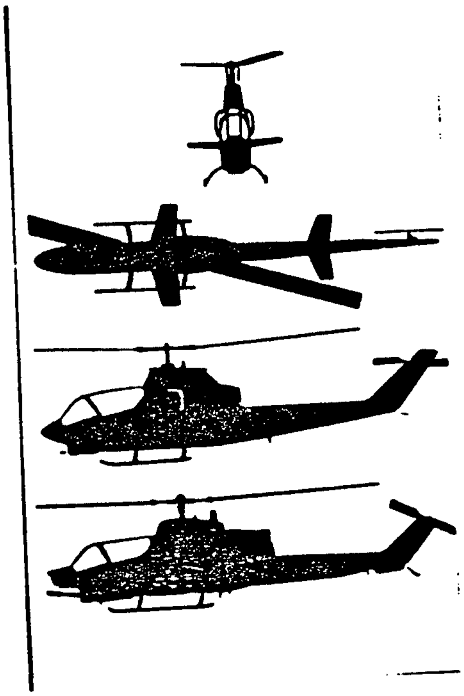

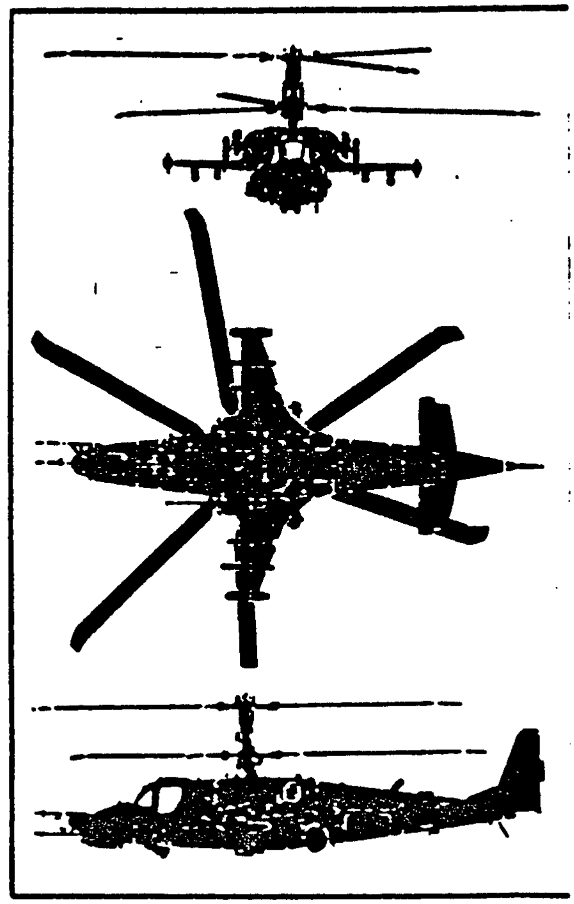

Sights around the Acceleration
and Human Effectiveness lab at
Wright Patterson Air Force Base

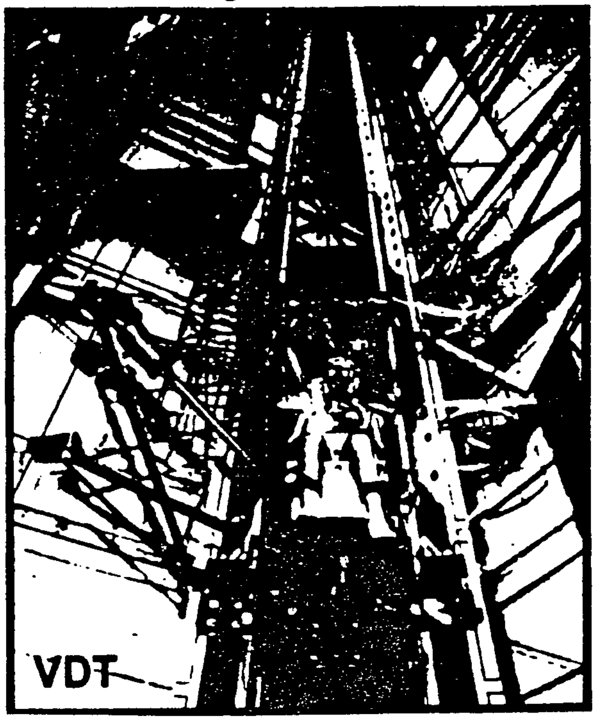

Vertical Drop Tower
"The Tower"

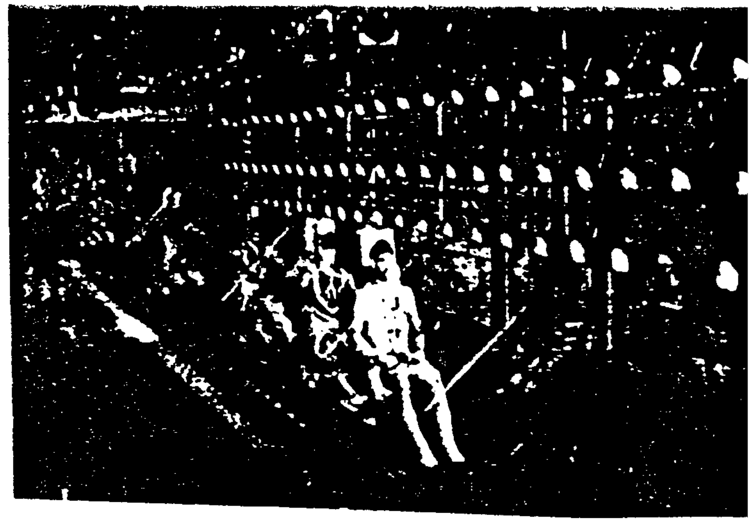

Horizontal Impulse Accelerator
"The Sled"

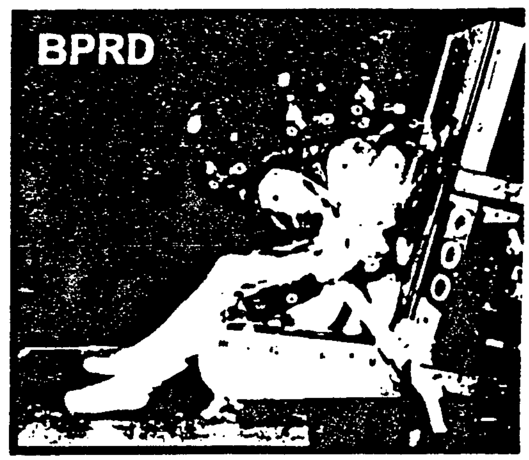

Body Positioning
and Restraint Device

The Manikins used
for testing purposes.
Often found in dark corners of the lab afterhours
resembling real-life people a little too closely
for comfort.

MAN-RATED IMPACT FACILITY CAPABILITIES

Facility	Maximum Payload (kg)	Maximum Accel. (G)	Pulse Duration (msec)	Maximum Velocity (m/s)	Power Stroke (m)	Track Length (m)	Onset Rate (G/s)	Mounting Surface Area
HIA	900	150	10-300	53	2.6	76		1.2 x 1.8 m
HD	900	100	20-300	38	23	76		1.2 x 1.8 m
VDT	225	80	40-180	17	1.4	15	150-5000	1.2 x 1.8 m
VID	2000	1000	1.6-30	9		5		0.9 x 0.9 m

DES, Dynamic Environment Simulator
"The Human Centrifuge"
My mentor took the other interns and me on a tour of facilities and we observed several tests, as well as climbed inside the cab.

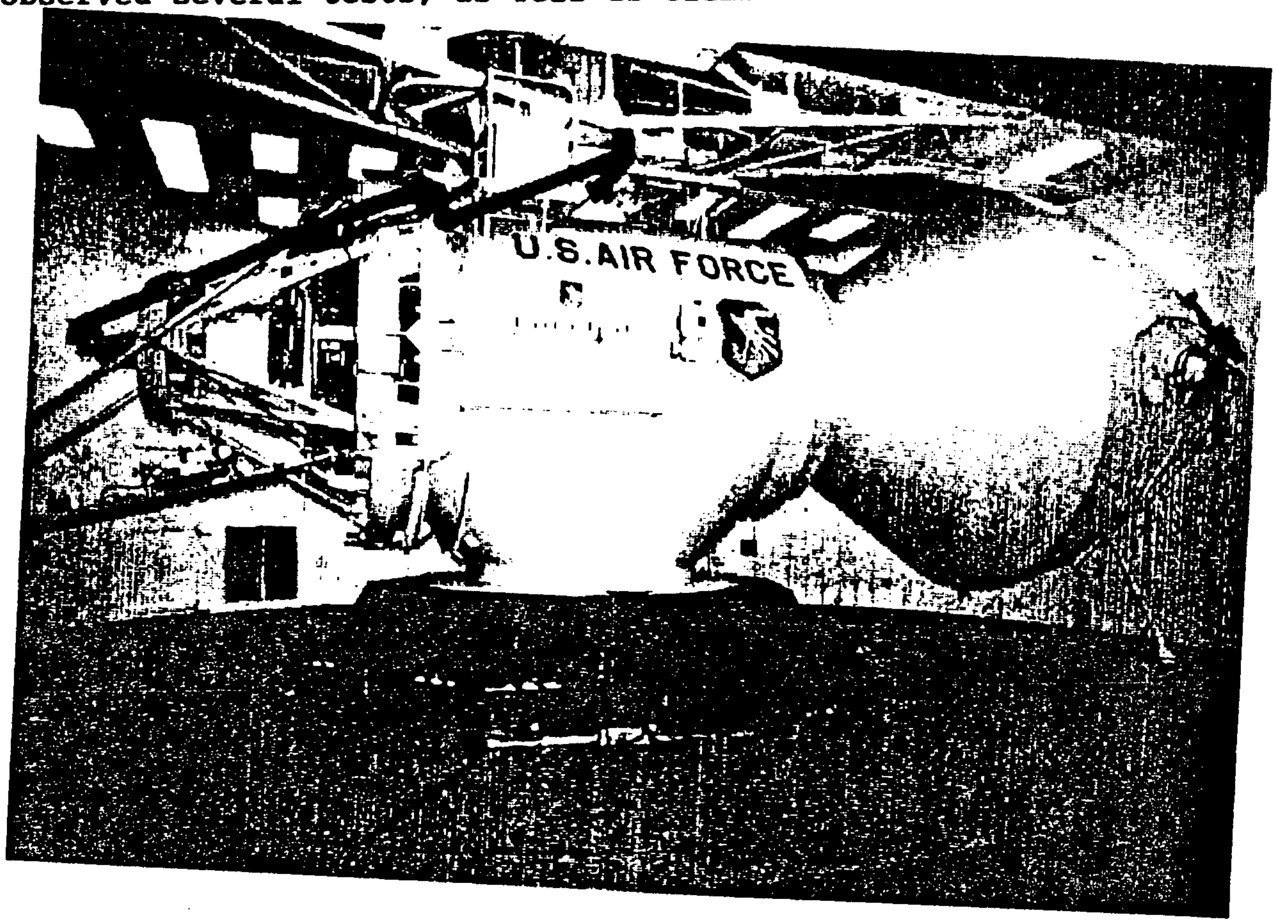

GALLIUM ARSENIDE SURFACES

Jill M. Seger

Archbishop Alter High School
940 E. David Road
Kettering, OH 45429

Final Report for:
High School Apprenticeship Program
AFRL/Wright Laboratory

Sponsored by:
Air Force Office of Scientific Research
Bolling Air Force Base, DC

And

Wright Laboratory

August 1998

GALLIUM ARSENIDE SURFACES

Jill M. Seger
Archbishop Alter High School

Abstract

Growth of the semi-conductor GaAs was studied. In particular, the surface structure of the substance was examined. Possible structures, including the beta 2x4 and the beta2 2x4, were animated using molecular dynamics. Pashley's electron counting rule was used to determine if a given structure was possible.

<u>Table of Contents</u>

Title Page	19-1
Abstract	19-2
Table of Contents	19-3
Introduction	19-4
Molecular Dynamics	19-4
Molecular Beam Epitaxy	19-4
Electron Counting Rule	19-5
Source Code	19-6

Introduction

Gallium Arsenide has a multitude of uses, including collecting solar energy and use in space applications. A band gap of 1.43 eV makes it ideal for solar cells, along with it's relative insensitivity to heat. In order to collect sunlight, only a few microns of GaAs are needed, compared to 100 microns of silicon. The growth and structure of GaAs, therefore, is important to study.

Molecular Dynamics

Molecular dynamics refers to the process in which a system of specific atoms is examined to determine how the system will act in a given situation. For example, how ten aluminum atoms will move when placed into a 20x20 angstrom box at 300 degrees Celsius. MD programs must take into account many forces. First of all, each atom has it's own initial velocity and acceleration. Second, the forces between other atoms in the given "box" must be calculated. The program must know whether these forces are attractive, repulsive, or whether no force is present. This must be calculated in the x, y, and z direction. The program must then calculate the force of atoms outside the "box." Then, the program must find the total force and direction. Next, the atoms are moved and the process starts over again. In order for accurate results to occur, atoms must not be too close, or an extremely large repulsive force will occur, causing the program to produce inaccurate results. The time step also must be small enough so that great changes in location don't occur between calculations of forces.

Molecular dynamics is important in determining how atoms and compounds will react to each other in a given environment, such as high temperature. This process can be useful in determining the steps in a surface formation of any substance, including GaAs. Molecular dynamics programs are available with many software packages, including MSI's Cerius2.

Molecular Beam Epitaxy

Molecular Beam Epitaxy is the method currently used to grow GaAs. First, a wafer must be made to grow the crystals on. To do this, high purity (99.999999%) Ga metal and high purity As metal are melted together to form molten GaAs. A seed crystal of appropriate crystallographic orientation is then touched to the surface and slowly raised, creating a solid crystal of GaAs. The neck and tail of the substance is then cut off to obtain a cylinder with a constant diameter. The outer edge of the cylinder is then ground smooth, and a wire saw used to cut wafers less than .5 mm thick. The individual wafers are then polished, and the wafers are then ready to be placed in the MBE machine. Pure gallium and pure arsenic are then placed in closed containers and released using shutters to assure exact quantities. The gallium and arsenic then settle on the wafer within the ultra-high vacuum. This process is used not only to grow GaAs, but also other semi-conductors. Use of MBE ensures high purity substances, and also allows for specific amounts of semi-conductor material to be grown (the growth rate is one atomic layer per second).

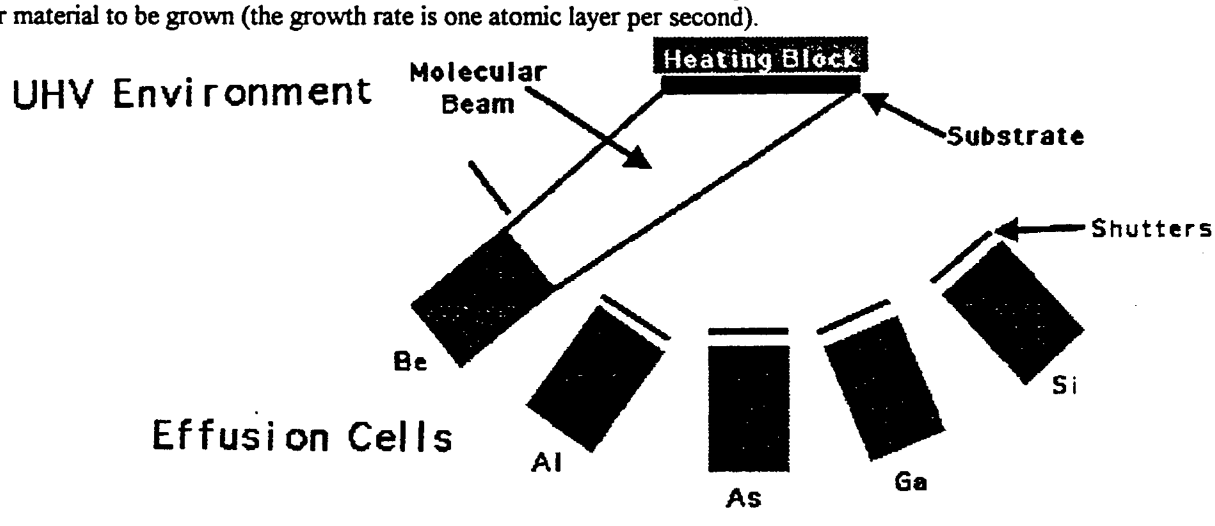

Electron Counting Rule

The electron counting rule is a simple, systematic way to find if the number of electrons present in a structure is sufficient considering the number of bonds. It is especially useful to determine whether surfaces are or are not possible.

The electron counting rule is used on GaAs surfaces to find possible configurations and to eliminate incorrect ones.

To apply the electron counting rule, first count the total number of electrons--5 for each As and 3 for each Ga. Then find the total number of bonds, including dangling bonds. Once you know the total number of electrons and bonds, assign two electrons to every bond, including As dangling bonds, but none to Ga dangling bonds.

For example, consider the following surface of GaAs, the beta 2x4.

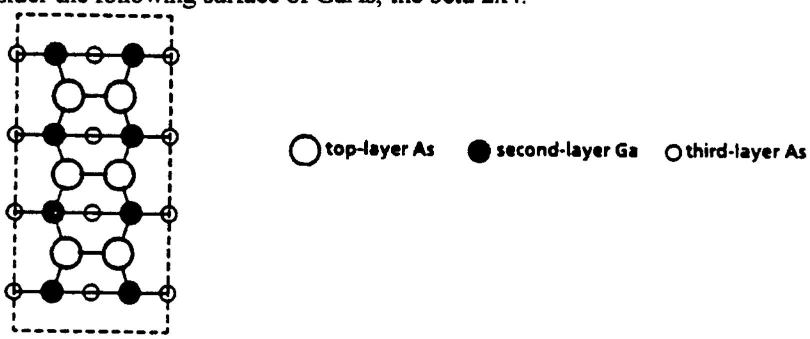

(a) β(2x4)

This structure contains the surface and one layer of bulk. On the surface, there are 14 As and 8 Ga. The total number of electrons equals:

$$(22 * 5) + (20 * 3) = 170$$

Then count the total number of bonds, including bonds outside the unit cell, as well as dangling bonds.

71 bonds +
14 As dangling bonds +
12 Ga dangling bonds

---

99 bonds total

Assign two atoms to each of the non-dangling bonds, using 142 electrons. Then assign two atoms to each As dangling bond, using 28 more electrons, and zero electrons to the Ga dangling bonds. This uses a total of 170 electrons, which is the number available. Therefore, the electron counting rule is obeyed, and the structure is stable.

ELECTRON COUNTING RULE: FORTRAN90 PROGRAM

By: Jill Seger & Brett Beckett

```
MODULE work

IMPLICIT NONE
REAL*8, ALLOCATABLE, SAVE :: x(:)            !position in x direction
REAL*8, ALLOCATABLE, SAVE :: y(:)            !position in y direction
REAL*8, ALLOCATABLE, SAVE :: z(:)            !position in z direction
REAL*8, ALLOCATABLE, SAVE :: vx(:)           !velocity in x direction
REAL*8, ALLOCATABLE, SAVE :: vy(:)           !velocity in y direction
REAL*8, ALLOCATABLE, SAVE :: vz(:)           !velocity in z direction
REAL*8, ALLOCATABLE, SAVE :: ax(:)           !acceleration in x direction
REAL*8, ALLOCATABLE, SAVE :: ay(:)           !acceleration in y direction
REAL*8, ALLOCATABLE, SAVE :: az(:)           !acceleration in z direction
REAL*8, ALLOCATABLE, SAVE :: fx(:)           !force in x direction
REAL*8, ALLOCATABLE, SAVE :: fy(:)           !force in y direction
REAL*8, ALLOCATABLE, SAVE :: fz(:)           !force in z direction
INTEGER, ALLOCATABLE, SAVE :: bonds(:)       !# of atoms bonded to an atom
INTEGER, SAVE :: bond_num                    !total number of bonds
CHARACTER*2, ALLOCATABLE :: species(:)       !atomic symbol
TYPE I5
  INTEGER :: vector(5)
END TYPE I5
TYPE (I5), ALLOCATABLE :: conn(:)            !connectivity of atoms; which
                                             !atoms each is connected to
INTEGER :: N                                 !number of atoms
REAL*8 :: Sx, Sy, Sz                         !Lattice constants
INTEGER :: electron_num                      !total # of electrons in system

END MODULE work


PROGRAM pashley                              !begin main program
USE work
IMPLICIT NONE

CALL start
CALL electrons
CALL find_bond_num
CALL calculate
CALL output

STOP
END PROGRAM pashley


SUBROUTINE start                             !read in positions
USE work
IMPLICIT NONE
INTEGER :: i                                 !loop counter
INTEGER :: error                             !allocate term checking
```

```
INTEGER :: ioerror                                   !end of file checking
REAL*8 :: Dummy2                                     !variable for irrelevant info
READ(10,*) N                                         !read number of atoms
REWIND 10                                            !reset file
ALLOCATE(x(N), STAT = error)                         !allocate arrays
IF (error /= 0) THEN
 PRINT *, 'Program could not allocate space for x.'
 STOP
ENDIF
ALLOCATE(y(N), STAT = error)
IF (error /=0) THEN
 PRINT *, 'Program could not allocate space for y.'
 STOP
ENDIF
ALLOCATE(z(N), STAT = error)
IF (error /=0) THEN
 PRINT *, 'Program could not allocate space for z.'
STOP
ENDIF
ALLOCATE(species(N), STAT = error)
IF (error /= 0) THEN
 PRINT *, 'Program could not allocate space for species.'
 STOP
ENDIF
READ(10,*,IOSTAT=ioerror) N                          !read in # of atoms
IF (ioerror /= 0) THEN
 PRINT *, 'Error reading file'
ENDIF
DO i=1,N                                             !read type & position
 READ(10,*) species(i), x(i), y(i), z(i), dummy2     !of atoms
ENDDO
READ (11,*) Sx, Sy, Sz                               !read size of unit cell

END SUBROUTINE start


SUBROUTINE electrons                                 !count # of total electrons
USE work
IMPLICIT NONE
INTEGER :: gallium_atoms                             !total # of Ga atoms
INTEGER :: arsenic_atoms                             !total # of As atoms
INTEGER :: i                                         !loop counter

gallium_atoms = 0
arsenic_atoms = 0
DO i=1,N                                             !decide if atom is As or Ga
 IF (species(i)=='Ga') THEN
  gallium_atoms = gallium_atoms + 1
 ENDIF
```

```
 IF (species(i)=='As') THEN
  arsenic_atoms = arsenic_atoms + 1
 ENDIF
ENDDO
electron_num = arsenic_atoms * 5 + gallium_atoms * 3          !calculate # electrons

END SUBROUTINE electrons
SUBROUTINE find_bond_num                           !find number of bonds
USE work
IMPLICIT NONE
REAL*8 :: r                                        !distance between atoms
REAL*8 :: r_equi                                   !equilibrium distance
REAL*8 :: xtemp, ytemp, ztemp                      !temporary variables for directions
INTEGER :: i, j                                    !loop counters
INTEGER :: error                                   !Allocate variable

ALLOCATE (conn(N), STAT=error)                     !allocate arrays
IF (error /= 0) THEN
 PRINT *, 'Program could not allocate space for conn'
 STOP
ENDIF
ALLOCATE (bonds(N), STAT=error)
IF (error /= 0) THEN
 PRINT *, 'Program could not allocate space for bonds'
 STOP
ENDIF
DO i = 1, N                                        !initialize bonds array
 bonds(i) = 0
ENDDO
DO i = 1, N                                        !initialize conn array
 DO j = 1, 5
  conn(i)%vector(j)=0
 ENDDO
ENDDO
r_equi = 5.6 * sqrt(3.0/16.0)                      !calculate equilibrium length
DO i = 1, N-1                                      !avoiding double counting, loop
 DO j = i+1, N                                     !over atoms and determine if a
                                                   !bond exists
  r = sqrt( (x(i)-x(j))**2 + (y(i)-y(j))**2 + (z(i)-z(j))**2 )      !calculate
                                                   !distance between atoms
  IF (r <= 1.2*r_equi) THEN                        !check if bond exists
   bond_num = bond_num + 1                         !increase total bond number
   bonds(i) = bonds(i) + 1                         !increase number of bonds on
   bonds(j) = bonds(j) + 1                         !each atom involved
   conn(i)%vector(bonds(i)) = j                    !write # of atom bonded with
   conn(j)%vector(bonds(j)) = i                    !for each atom involved
  ENDIF
 ENDDO
ENDDO
DO i = 1, N                                        !determine if bond is formed with
                                                   !atoms outside the unit cell
```

```
DO j = 1, N                                     !in the x direction
  xtemp = x(j) + Sx
  r = sqrt( (x(i)-xtemp)**2 + (y(i)-y(j))**2 + (z(i)-z(j))**2 )
  IF (r <= 1.2*r_equi) THEN
   bond_num = bond_num + 1
   bonds(i) = bonds(i) + 1
   bonds(j) = bonds(j) + 1
   conn(i)%vector(bonds(i)) = -j                !negative means bond outside
   conn(j)%vector(bonds(j)) = -i                !of unit cell
  ENDIF
 ENDDO
 DO j = 1, N                                    !in the y direction
  ytemp = y(j) + Sy
  r = sqrt( (x(i)-x(j))**2 + (y(i)-ytemp)**2 + (z(i)-z(j))**2 )
  IF (r <= 1.2*r_equi) THEN
   bond_num = bond_num + 1
   bonds(i) = bonds(i) + 1
   bonds(j) = bonds(j) + 1
   conn(i)%vector(bonds(i)) = -j
   conn(j)%vector(bonds(j)) = -i
  ENDIF
 ENDDO
DO j = 1, N                                     !in the z direction
  ztemp = z(j) + Sz
  r = sqrt( (x(i)-x(j))**2 + (y(i)-y(j))**2 + (z(i)-ztemp)**2 )
  IF (r <= 1.2*r_equi) THEN
   bond_num = bond_num + 1
   bonds(i) = bonds(i) + 1
   bonds(j) = bonds(j) + 1
   conn(i)%vector(bonds(i)) = -j
   conn(j)%vector(bonds(j)) = -i
  ENDIF
 ENDDO
ENDDO
DO i = 1, N                                     !account for dangling bonds
 IF (species(i)=='As') THEN
  SELECT CASE (bonds(i))
  CASE (1)
   bond_num = bond_num + 3
  CASE (2)
   bond_num = bond_num + 2
  CASE (3)
   bond_num = bond_num + 1
  END SELECT
 ENDIF
ENDDO

END SUBROUTINE find_bond_num
```

```
SUBROUTINE calculate                              !find bond lengths and angles
USE work
IMPLICIT NONE
REAL,ALLOCATABLE :: bond_length(:,:)              !length of bond
REAL,ALLOCATABLE :: bond_angle(:,:,:)             !length of bond angle
INTEGER :: error                                  !allocate variable
REAL*8 :: r                                       !Distance between atoms
REAL*8 :: r_equi                                  !bond equilibrium
INTEGER :: i, a, b, j, k                          !loop counters
REAL :: jx, jy, jz, kx, ky, kz                    !temporary positions
REAL :: bond_angle_degrees                        !bond angle in degrees

ALLOCATE (bond_length(N,N), STAT=error)           !allocate arrays
IF (error/=0) THEN
 PRINT *, 'Could not allocate space for bond lengths.'
 STOP
ENDIF
ALLOCATE (bond_angle(N,N,N), STAT=error)
IF (error/=0) THEN
 PRINT *, 'Could not allocate space for bond lengths.'
 STOP
ENDIF
OPEN (UNIT=20, FILE="lengths")                    !open files
OPEN (UNIT=21, FILE="angles")
r_equi = 5.6 * sqrt(3.0/16.0)
DO i = 1, N                                       !initialize arrays
 DO j = 1, N
  bond_length(i,j) = 0
  DO k = 1, N
   bond_angle(i,j,k) = 0
  ENDDO
 ENDDO
ENDDO
DO i = 1, N-1                                     !avoid double counting
 DO j = i+1, N                                    !write bond length to file
  r = sqrt( (x(i)-x(j))**2 + (y(i)-y(j))**2 + (z(i)-z(j))**2 )
  IF (r<=1.2*r_equi) THEN
   bond_length(i,j) = r
   bond_length(j,i) = r
   WRITE(20, FMT='(2I4,1f10.4)') i, j, bond_length(i,j)      !writes to file
  ENDIF                                                      !lengths
 ENDDO
ENDDO
WRITE (21,*) '  Angle     Radians    Degrees'
DO i = 1, N                                       !find bond angles
 DO a = 1, 4
  DO b = a+1, 5
   j = conn(i)%vector(a)                          !read 2 atom numbers in angle
   k = conn(i)%vector(b)
   IF (k<=0) THEN                                 !if atom outside unit cell: exit
    EXIT
   ENDIF
```

```
    jx = x(j) - x(i)                                        !moves configuration to origin
    jy = y(j) - y(i)
    jz = z(j) - z(i)
    kx = x(k) - x(i)
    ky = y(k) - y(i)
    kz = z(k) - z(i)
    bond_angle(j,i,k) = acos((jx*kx+jy*ky+jz*kz)/(bond_length(j,i)*bond_length
(i,k)))                                                     !calculate bond angle
    bond_angle_degrees = (bond_angle(j,i,k) * (180/3.141592654))
    WRITE(21, FMT='(3I4,F10.4,4X,F10.4)') j, i, k, bond_angle(j,i,k), bond_angle_degrees
                                                                        !write to file angles
   ENDDO
  ENDDO
 ENDDO

END SUBROUTINE calculate
SUBROUTINE output                                           !screen output
USE work
IMPLICIT NONE
INTEGER :: i
REAL*8 :: electrons_real, bonds_real                        !real values for electron_num
                                                            !& bond_num
INTEGER :: violators                                        !number of incorrect electrons
REAL*8 ::  energy                                           !total extra/missing energy

electrons_real = real(electron_num)                         !convert integer value to real
bonds_real = real(bond_num)
PRINT *, 'Number of bonds containing electrons is: ', bond_num
PRINT *, 'Number of electrons: ', electron_num
violators = abs(electron_num-(2*bond_num))                  !find # of violators
IF (electrons_real/bonds_real==2) THEN
 PRINT *, 'The electron counting rule has been obeyed'
ELSEIF (electrons_real/bonds_real>2) THEN
 PRINT *, 'There are', violators, ' extra electrons, the electron counting rule
 has been violated.'
ELSE
 PRINT *, 'There are', violators,' missing electrons, the electron counting rule has been violated.'
ENDIF
energy = 0.4 * violators
PRINT *, 'Additional energy is equivalent to ', energy,' eV'

END SUBROUTINE output
```

INFRARED SMALL CRACK DETECTION SYSTEM

Jonah Shaver

Waynesville High School
Dayton Rd.
Waynesville, OH 45068

Final Report for:
High School Apprentice Program
Wright Patterson Laboratory

Sponsored by:
Air Force Office of Scientific Research
Bolling Air Force Base, DC

and

Wright Patterson Laboratory

August 1998

INFRARED SMALL CRACK DETECTION SYSTEM

Jonah Shaver
Waynesville High School

Abstract

The purpose of this project was to develop an infrared system that had the ability to take images at given intervals for detection of small crack initiation sites in test specimens. A Raytheon Amber Radiance 1 infrared camera and Dipix XPG-1000 Power Grabber ISA card were set up and tested for this project. Though the camera had the ability of internal calibration, an external calibration source was made out of copper plate and tubing. It was determined that the software packaged with the camera did not fully meet our needs. George Hartman helped with the development of software that would better suit our purposes. In the time allotted for development, the system was set up and software was written to take single images. Further work is required to get the software to take multiple images at different intervals.

INFRARED SMALL CRACK DETECTION SYSTEM

Jonah Shaver

In the stress testing of different metal alloys it is useful to know at exactly how many cycles a sample starts to crack. The use of infrared technology has been used in non-destructive evaluation to determine if samples were damaged or corroded. In this project we applied infrared technology to the detection of small crack initiation sites. This crack detection system needed to be able to take images at different times during the fatigue cycle of a sample.

To accomplish this task, I had to first gather some specialized and general knowledge. Some of the specialized knowledge needed was the use of a scanning electron microscope, a confocal laser microscope, and learning Visual C++. The general skills included learning various sample shape names, material properties, how to use laboratory equipment, and further my knowledge of computers.

The scanning electron microscope was a tool that will be utilized in this project. John Porter and Andy Rosenburger helped me with to understand the workings of the SEM. It will be used to analyze the crack initiation sites in more detail. Andy Rosenburger also instructed me in the use of the confocal laser microscope. The confocal laser microscope will be used to take topography scans of initiation sites. The information from the microscope will then be translated using a program I co-authored with George Hartman, TOPS. The converted file will the be displayed using Stanford Graphics' 3-D graphing ability. TOPS was written in Visual C++ Studio, it converts topography files to a matrix format that can be imported to Stanford Graphics{see page 20-6 for user interface}. I had to find the addresses of the x, y, and z axes scale in microns of the binary format topography file, and then incorporate them into my program.

I learned how to identify the type of test done on a sample by its shape. This was necessary for telling what was being done to different samples. Knowledge of material properties is required for this project as well, I learned many metallurgical properties that help in identifying materials. The use of voltage meters, oscilloscopes, power supplies, and load frames was also required. Many people showed me how to use these pieces of equipment to help my project. I also performed upgrades and equipment exchanges on laboratory computers.

The Raytheon Amber Radiance 1 infrared camera was used in this project. This camera has a 256x256 indium-antimonide focal plane array that can detect differences in temperature as small as 0.025°C. A Dipix XPG-1000 Image Grabber was used to interface the camera to a computer.

The setup of the camera was very straight forward. A television and the on board controls were used to control the camera before software was written to control it from a computer. During this time an external calibration source was constructed. Though the camera's internal calibration flag has the ability to give an accurate source for calibration, it is limited to 10°C bellow ambient temperature and 40°C maximum. The calibration target was made from an six by six inch, eighth inch thick oxygen free copper plate and eighth inch copper tubing{see page 20-7 for a schematic}. The tubing was coiled into a repeating "S" pattern. The plate was then placed on a hot plate so it could be evenly heated. Lead free solder was used to fuse the tubing to the back of the plate. The plate was spray painted flat black to minimize reflections from other radiation sources present in the room. Two thermocouple wires were spot welded to the center of the plate between coils on the back, the wires were then covered with five minute epoxy resin to hold them in place. A piece of foam insulation was used on the back of the plate to keep the temperature more constant. Water was used to heat and cool the plate to given temperatures.

The XPG-1000 was a bit more difficult, the correct drivers were not provided by Dipix, and a fairly involved investigation was required to find the correct ones. The correct drivers were found at the Dipix ftp site. After setup of the XPG-1000, the camera had to be connected to it by use of a specialized cable. At first there were problems with the settings of the board and camera conflicting, resulting in no communication between the two. The problem was fixed by running diagnostic routines written by George Hartman and myself. We utilized Visual C++ and calls provided by Dipix to interface with the XPG-1000, which in turn interfaced with the camera.

After communication was established, we began to write routines that took images from the camera and displayed them on the computer. Again we used calls provided by Dipix. Progress was made to the point where pictures could be taken, but only when a command was given. The ideal goal was to have software that would automatically take images during a test cycle at any interval specified by the user, due to time constraints. Further work is required on the project to accomplish this goal.

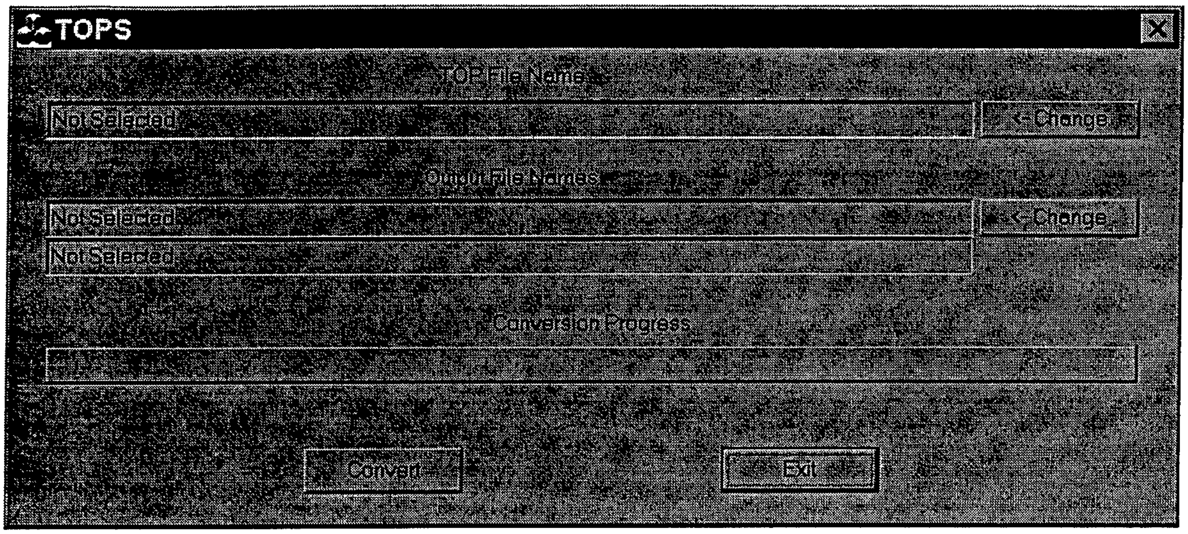
TOPS
TOP File Name
Not Selected
<- Change
Output File Names
Not Selected
<- Change
Not Selected
Conversion Progress
Convert
Exit

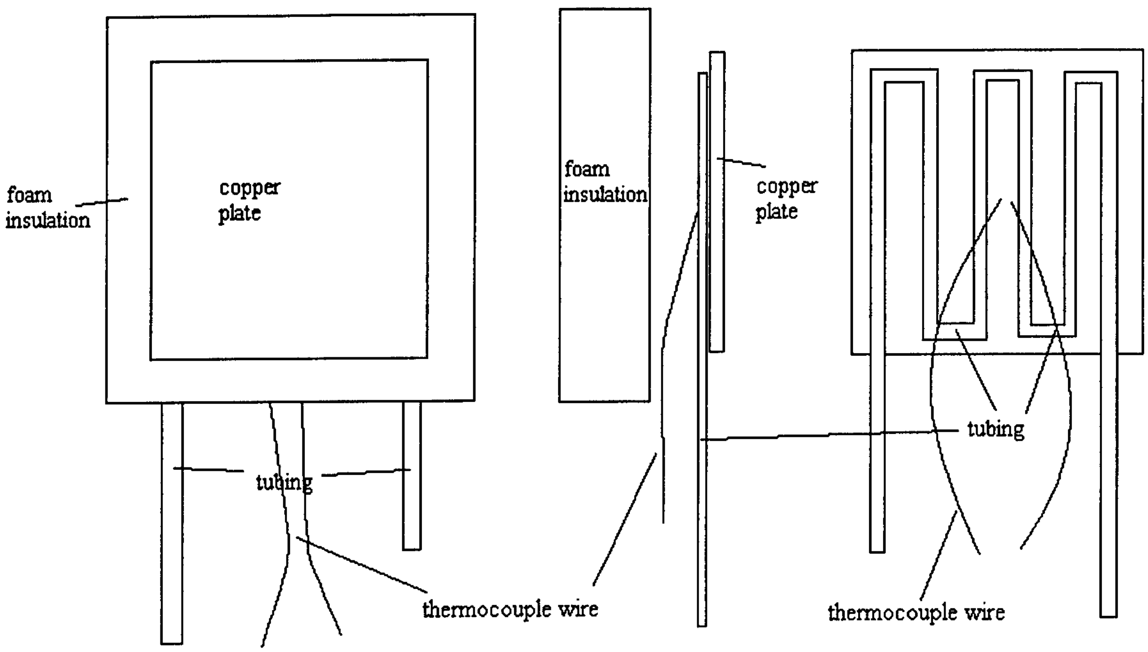

foam insulation
copper plate
tubing
thermocouple wire
foam insulation
copper plate
tubing
thermocouple wire

AN IN-DEPTH STUDY OF
SYNTHETIC APERATURE RADER (SAR) IMAGERY

Douglas E. Smith II

Tippecanoe High School
475 N. Hyatt Street
Tipp City, OH 45371

Final Report for:
High School Apprentice Program
Air Force Research Lab Site

Sponsored by:
Air Force Office of Scientific Research
Wright Pat Air Force Base, OH

and

Air Force Research Lab Site

July-August 1998

AN IN-DEPTH STUDY OF
SYNTHETIC APERTURE RADAR (SAR) IMAGERY

Douglas E. Smith II
Tippecanoe High School

Abstract

Research was done on Synthetic Aperature Radar (SAR) imagery. The images were produced by the Moving & Stationary Targer Acquisition and Recognition (MSTAR) project from Defense Advance Research Projects Agency (DARPA). A couple of weeks were spend on getting familar with the UNIX operating system and gaining background information on SAR and MSTAR. Then several weeks were needed to write and develop computer programs to view and manipulate the SAR imagery. The SAR images consist of a target, followed by its shadow, and the background is called clutter. Our main focus was on the target and the shadow. We wrote our programs to perform the function of cutting out the polygonal regions of the target and shadow in the images. These cutouts are used to find a more accurate target to clutter ratio and also as data for furthur analysis by the Model Based Vision researchers and developers at Wright Patterson Air Force Base.

AN IN-DEPTH STUDY OF SYNTHETIC APERTURE RADAR (SAR) IMAGERY

Douglas E. Smith II

Introduction

Recently, the study of sensors has become a main ingredient in the detection of objects. Tanks, planes, aircraft, buildings, etc. all reflect radio waves which is the flow of electromagnetic energy. So by using a receiver tuned into the objects frequency, the object is always susceptible to detection in the night, daytime, and even through clouds and fog. This is why radar is so important for military purposes. Objects can be detected by radar from far distances and in any type of weather conditon.

Synthetic Aperture Radar (SAR) follows these basic concepts. SAR detects the microwaves emitted by an object and interprets them into an image. A common term associated with SAR imagery is target-to-clutter ratio. The target is the main object that the radar is focusing on. The parameter of target imagery is changable through the intensity of the target. Clutter is a collecton of echoes from unwanted objects that surround the target such as terrain, grass, rain, etc. It randomly corrupts the target echo creating target detection problems. The goal is to get a high target-to-clutter ratio. A low target-to-clutter ratio hides the target creating artifically high false alarms.

SAR has three different polarities. SAR sensors hold three different responses (HH, VV, HV). Responses hold information on the polarity of transmitted and received signals. HH sends horizontally polarized impulses measuring the horizontal polarity response. The three different polarization responses create three different SAR images. HH is the most primative and simplest of the SAR imagery. The state of the art type of imagery is called polarimetrically whitened imagery (PW). It compiles data from various polarizations to cancel out some of the unwanted speckle noise in SAR imagery and increases the discrimination ability of the ATR system creating smoother imagery.

One of SAR's characteristics is that a particular form of noise is present in all SAR imagery. This is caused by a phase cancelation during the SAR imaging process. This type of noise is called speckle and is random and different in each SAR image. Hence, no SAR image of the same target will be identical since SAR speckle is completly random. Thankfully, noise reduction is associated with the PW imagery process, but is not with HH imaging. So PW SAR imagery contains less speckle creating a smoother image.

Moving & Stationary Target Acquistion and Recognition (MSTAR) studies SAR imagery. Their goal is to design, construct, and demonstrate in a laboratory an accurate and clear automatic target recognition (ATR) system, which is capable of recognizing and also locating time-critical targets in two-dimentional SAR imagery. The program uses an applied-system engineering approach and integrates ATR algorithm modules to achieve accurate performances in unconstrained ground image analysis scenes. The main focus is on targets hidden and obscured by such things as layover, partial maskings, covers, camouflage, and deception. So, the MSTAR algorithm design strategy is to display a model based approach so targets backgrounds and their uncertainty are measured and modeled mainly for obscurity.

Problem

In the past, most researchers finding the target-to-clutter ratio in a SAR image used a rectangular method. That is they would create a program that would allow them to put a rectangular parameter around the target. The program also contained some equations that would calculate the target-to-clutter ratio and display it on the screen once the rectangular cut-out was made. Then the person would run the program, make the rectangular cut-out of the target, and the computer would return the target-to-clutter ratio. There is one major problem with this procedure. That is the target is not a rectangular shape. It is polygonal with many different sides. So when you make a rectangular cut-out of the target, also included in the cut-out is unwanted clutter. This clutter distorts the target-to-clutter ratio and makes it more difficult to detect the target in Automatic Target Recognition (ATR). We needed to come up with a new method.

Methodology

Before we started our endeavor, we needed to get a program to display the SAR images. Now the images we were using came from a MSTAR compact disk. We transferred the images to a SUN microsystems computer for further study. The radar images were of T-72 tanks, BMP-2 tanks, and BTR-70 transports. They were taken at 17 degrees and rotated 360 degrees. We were only interested in the images every five degree, so we viewed the images ranging from 0 - 360 degrees at five degree intervals. The images not in the five degree intervals were deleted. There were three sets of images and each set contained the actual SAR radar imagery and computer-constructed SAR imagery.

To get the SAR imagery to appear on your computer you need to download a file from the

MSTAR web site. The file is named MSTAR tools and is formatted as a .tar file. MSTAR tools contain programs that let you view MSTAR imagery. What a .tar file means is that the file was compressed to not take up so much space on the hard drive. So, obviously, the file needs to be extracted so the programs under the .tar can be uncompressed. Since we are using a Unix operating system, we need to use the command: tar xf (filename), in my case the filename is mstartools.tar . So once that was completed I viewed all the extracted files and read the .readme files as well. I found that the program view-chip was of interest to me. When you run view-chip the program has you input the image's filename and it will bring up that image. This is what we wanted. The MSTAR images could now be viewed.

We used the program view-chip as a model for our future programs. View-chip made the images viewable but that was not enough. So we added on codes to view-chip, added in some equations, and manipulated some of view-chip's codes. View-chip is run in MATLAB, the language of technical computing, which is a mathematical language allowing computations and visualizations. MATLAB stands for matrix laboratory, and since our images are basically quality matrices, MATLAB fits in perfectly.

Our first goal was to create a program that would calculate the target-to-clutter ratio of a SAR image using a rectangular method. We wanted to create a box around the target to find its ratio. To put the rectangular box around the target we used the command: GINPUT. This command allows the user to interact with the image by placing coordinates on the upper left of the target and then the lower right to put a rectangular box around the target. Then we added in some mathematical equations to calculate the coordinates points to find the target-to-clutter ratio and added in a code to display the ratio on the screen.

Then we came up with an idea to solve our problem. We needed to make a program that would allow us to cut out the targets polygonal shape of the target. After conversations with my mentor, we found out that MATLAB has a command called ROIPOLY. This command allows you to place poygonal parameters around a object and that is exactly what we were looking for. So we added in some codes to our program using the ROIPOLY commmand. This was a success. It allowed the user to cut out the polygonal shape of the target. We also used the eval command which saved the cut-out as the filename with a T, for target, added to the end of it. In addition to the cut-out of the target, we also added in code to cut and save the shadow and the the target and shadow as a whole. Now it was possible to find the target-to-clutter ratio using the new polygonal method.

Fatigue and human error play a factor when cutting out the objects. So a program had to be written to evaluate the cut-outs. We called this quality control. The program had some equations in it which compared the area's of the joint target and shadow, that is it connected the target and shadow cut-outs, and measured it against the whole cutout and gave a percentage error. The program also calculated the gaps and overlaps inbetween the targets and shadows and gave pixel differentials between the joint target and shadow area over the whole target and shadow area.

The final two weeks of my apprenticeship was spent on what I called work shop. Work shop consisted of 3 people, including myself, that strictly dealt with creating data for later analysis. The data we created was of polygonal cut-outs of the targets and shadows of SAR imagery. Two people spent their time cutting out the targets and shadows of SAR images. Then they would cut out the whole area between the two. The third person dealt with quality control. Once a set was done, the quality control person would evaluate our cut-outs of the targets and shadows and write down the percentage errors between those cut-outs and the whole cut-out. Gaps and overlaps were evaluated too. Limits were placed on the percentage errors between the joint and whole cut-outs as well as the number of gaps and overlaps in the polygonal cut-outs. If the cut-outs surpassed these limits, then new target and shadow cut-outs needed to be done of that particular SAR image. In the end, work shop created accurate and pertinent data that would be used for later analysis.

Results

The polygonal cut-outs were a success. Much needed data was created by using this polygonal method. Since the cut-outs are polygonal, the data is more accurate and useful. A more accurate target-to-clutter ratio can now be found using the polygonal method. These polygonal cut-outs of the targets and shadows of SAR images are being used for futhur analysis and projects by the MBV researchers and developers. One researcher is incorporating these cut-outs into a computer program for segmentation purposes. This data is read by the program and is being used to try to show the computer what and how to find the boundaries of the targets and shadows. Hence, a computer program is in the making that will try to cut-out the targets and shadows. Another project deals with quality metrics. The data is being used to help find target intensities of SAR imagery.

Conclusion

Overall I feel my scientific research apprenticeship was a success. It was definetly a learning experience. The first couple of weeks were spent on getting familar with the UNIX operating system and gaining background information on SAR imagery. Just learning UNIX I think was a great acomplishment, but we endeavored deeper into scientific research.

The following four weeks were spent on creating computer programs to manipulate the SAR imagery. At times the coding placed me in consternation but as time went on things got more serene. Each day brought on new problems and at times it was frustrating and confusing. But the next day looked more lucid and we moved on. At first, we created a program to calculate the target-to-clutter ratio of a SAR iamge using rectangular methods. We added on to that program by adding some equations to calculate the shadow-to-clutter ratio as well as the target-to-clutter ratio. Those programs did not solve our problem but gave us a great starting point. After talking with my mentor we came up with the prestigious polygonal cutting program. We called it chipcut. The program uses the Matlab command: ROIPOLY , which allows the user to cut out regions of an image. It was a very exciting discovery and we used it to create our program to cut out the polygonal regions of the target and shadow. Hence, we created a program which allows us to have polygonal cut-outs of the target and clutter which can be used as data for furthur analysis or to find a more accurate target-to-clutter ratio.

The final two weeks were spent on creating the target and shadow data as well as writing my report. We started up a work shop. The work shop consisted of three people. Two other apprentices helped me. We had two people cutting out the targets and clutters of the sets of SAR images and a third person being the quality control person. That person monitered our cut-outs of the targets and shadows and made sure they were acceptible. When the work shop was done, we had SAR target and shadow data that the MBV researchers and developers could analyize as well as have the ability to find the target-to-clutter ratio using the more accurate polygonal method.

References

Carrarra, Walter G., and Ron S. Goodman. Spotlight Synthetic Aperture Radar Signal Processing Algorithms. Ed. Fawwaz T. Ulaby, et al. Norwoood, MA: Artech House, 1995.

Hahn, Harley. The Unix Companion. Ed. Lunaea Hougland, et al. Berkeley, CA: McGraw-Hill, 1995.

Hovanessian, S.A. Introduction to Synethetic Array and Imaging Radars. Dedham, MA: Artech House, 1980.

The Math Works. MATLAB The Language of Technical Computing. Natick, MA: The Math Works, Inc., 1996.

STUDY OF THE POTENTIAL FOR THE GROWTH OF POTASSIUM CARBON THIN FILMS

Andrew T. Snow

Kettering Fairmont High School
3301 Shroyer Road
Kettering, OH 45429

Final Report for:
High School Apprentice Program
Wright Laboratory

Sponsored by:
Air Force Office of Scientific Research
Bolling Air Force Base, DC

And

Wright Laboratory

August 1998

STUDY OF THE POTENTIAL FOR THE GROWTH OF POTASSIUM CARBON THIN FILMS

Andrew T. Snow
Kettering Fairmont High School

Abstract

The potential for the growth of potassium and carbon thin films was studied. To grow these films, a high-powered excimer laser was used to create a plume of excited potassium and carbon atoms that coated a silicon substrate. To determine the bonding in the film created, an XPS (x-ray photoelectron spectroscopy analysis) was run on the films. The ability of the two elements to bond was very low. Initial results of the analysis indicate that these films are too unstable for practical use. The initial film oxidized when exposed to air. Further testing revealed that the film was very soft. The film was also very inconsistent, consisting of patches of diamond-like carbon, potassium, and some film of an unknown type.

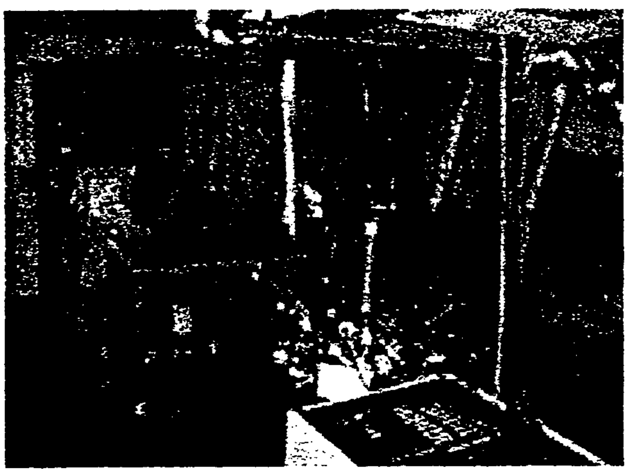

STUDY OF THE POTENTIAL FOR THE GROWTH OF POTASSIUM CARBON THIN FILMS

Andrew T. Snow

Introduction

The study of thin films and coatings has recently become of great interest to people in aerospace and other types of industry. Thin films are seen as a way to prolong the life of costly components that otherwise would have to be replaced. Uses of thin films and coatings range from heat shields for space ships to extending the life and ability of our nation's aging war planes. These applications need to have the best and most cost-effective materials that can be produced. This is a continuing challenge for researchers of thin films and coatings. It has led to many innovations and breakthroughs in thin film process and design. It has also led to new and occasionally unexpected materials.

Discussion of Problem

The problem being tested was the ability of potassium and carbon to bond and make a thin film. This is a new area of research for thin films. A thin film that includes potassium has previously seemed like an unproductive waste of resources. This is because potassium is a very volatile chemical and is hard to use for the purpose of thin film growth. The main reasons for this are its reactivity with everything, including skin, and the low amount of energy needed to excite its atoms. The high reactivity of potassium caused problems in the loading and unloading of the target material. It reacted with the air and required the laser to be fired on low power to clean off the reacted material from the potassium. The low amount of energy needed to excite potassium also caused problems because carbon needed a relatively high amount of energy to excite its atoms and create a plume. To solve this the potassium had to be moved back out of the focus of the laser beam. Without doing this, the potassium would get too excited and splatter all over the chamber. This happened during creation of the first film and caused a slight delay in our creation of the next thin film. The potassium also ignited once as it was being brought back up to air. These are the main reasons that potassium has been low on the list of thin film components.

Methodology

To determine if potassium and carbon will make a thin film they were placed in a vacuum chamber then ablated by the laser. The vacuum was at approximately 5.0 x 10^{-8} torr. This was required for a pure film. The laser was a high-powered excimer laser with beam length of 248 nm. This laser was at approximately half power for creation of the potassium carbon thin film. To coat the entire silicon substrate a set of mirrors was used to create a raster pattern on the potassium and carbon targets. The raster pattern allowed for an even coating of the substrate by the plume and for good combining of the potassium and carbon atoms. This method of growth resulted in the growth of a film that was mostly two separate chemicals. The film was determined not to be a compound of potassium and carbon by an XPS test. The film was also run through a hardness tester, a Raman spectroscopy, and a Daktak thickness measurer. The hardness tester

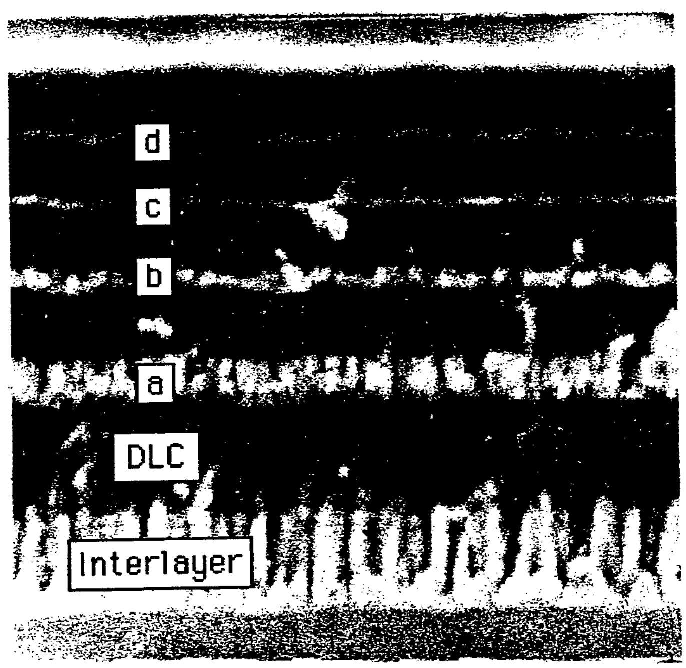

showed the film to be very soft. The Raman spectroscopy indicated that there was a lot of DLC and potassium, but very little, if any, potassium carbon thin film. The Daktak was used to see how thick the film was. It measured approximately 1000 angstroms.

Results

Tentative results from the testing of potassium carbon thin film growth indicate that potassium must be put with at least one other chemical besides carbon to form a stable compound. This is due to the fact that carbon is a covalent bond maker and potassium is an ionic bond maker. The results of early testing done on the initial thin films show a film of diamond-like carbon and some potassium splotches. This would indicate that the potassium and carbon did not bond on the silicon substrate. This caused the film to apparently continue to grow after it had been removed from the vacuum. This was actually the potassium splotches continuing to react with the air. The film was also very soft due to the limited amount of bonding by the chemicals. The hardness measured was approximately 85 on the Knoop hardness scale. This was partly because of the instability of the compound and partly because the potassium and carbon did not really combine. The film was also very bumpy due to the excess potassium on it. This was determined to have been caused by too much energy being directed at the potassium target. The potassium was moved out the focus of the laser and away from the carbon target to reduce the chances of explosion by the potassium target.

Conclusions

From very early results, it can be concluded that a thin film of potassium and carbon might not work out very well. It will be soft and very unstable. Without a stabilizing chemical, the film will most likely break down and form other compounds. These compounds are likely to be soft and possibly dangerous. To make sure that the film does not break down, a controlled combination of the film with other chemicals would have to be done. In this way a very hard and stable compound can be achieved. In the future this could lead to new and possibly harder thin films and coatings. To determine what chemicals need to be used in combination with the carbon and potassium, more research would have to be done. One way to do this is to use a creativity machine {1} to help find chemicals that could bond with both potassium and carbon to form a hard, stable compound.

References

1. Dr. Stephen Thaler, "The End of Science by Humans";
2. Binary Phase Diagrams of the Metal Systems vol. 1, 725-6;

HIGH SCHOOL APPRENTICE SUMMER RESEARCH STUDIES

Matthew J. Spriggs

Archbishop Alter High School

940 E. David Rd.

Dayton, OH 45429

Final Report for:

High School Apprentice Program

Wright Patterson AFRL/PRPS

Sponsored by:

Air Force Office of Scientific Research

Bolling Air Force Base, DC

August 1998

HIGH SCHOOL APPRENTICE SUMMER RESEARCH STUDIES

Matthew J. Spriggs

Archbishop Alter High School

Abstract

Over the summer I worked in the Wright Patterson Power Systems Branch Research lab. I was assigned three main tasks during the course of my tour: data reduction, C-coding for instrumentation, and computer upgrading. This report will explain the tasks and their value to the Research lab.

HIGH SCHOOL APPRENTICE SUMMER RESEARCH STUDIES

Matthew J. Spriggs

Introduction

The Power Systems Branch of Wright Patterson Air Force Base is a part of the Power Division, which is a part of the Propulsion Directorate. The Power Systems Branch develops materials, components and power systems for use in high power electrical systems for the Air Force. I was hired to work for Dr. Daniel Schweickart and John Horwath during my six week tour. I was assigned three main tasks throughout the course of my stay: data reduction, C-coding for instrumentation, and computer upgrading. Each task used different instruments and software exposing me to a wide variety of high tech systems and instruments.

Results

My mentor was conducting tests on electrical insulators over the summer, eroding an insulator with ions of a gas discharge. A sensor recorded the pattern of the ion generation and sent the data to a nearby computer. The computer would then run a program to take the data and put it in to a spreadsheet file. My task was to take the data from the spreadsheet and open it as a graph. Then I had to mathematically edit the spread sheet in order to make the graph readable and then make all the graphs of a particular test conform. Figure 1.1 is an example of three graphs that originally were not easily compared, one was in mA, the other in nA and still another in uA. I opened the spreadsheets and multiplied by a factor in order to make all three conform. Later, these graphs would be used by my mentor in presentations to explain the results of his tests. What you see here is the results of 3 days worth of data being read from the test. As you can see the ion current begins with an amplitude that jumps and spikes often, but as the test goes on and charges begin to "cake" along the bottom of the insulator, this space charge causes a reduction in current.

A digital Oscilloscope is used to read waveforms from a voltage source. The waveforms are read through a probe attached to the scope and then displayed on a screen. The graph displayed can show valuable information relating to a particular experiment. I was given the task of learning C-coding through the visual C for instrumentation program LabWindows/CVI. Through C, I was to write a program that would save waves from the oscilloscope to the hard disk of the laptop computer. The program then displayed the wave from the Oscilloscope on the computer screen. With this program one could open the wave in a spreadsheet form and make graphs for presentations etc. An example of a waveform that was sent from the Oscilloscope to the laptop, saved in an .xls file

Day 1 to Day 3 DC Currents Figure 1.1

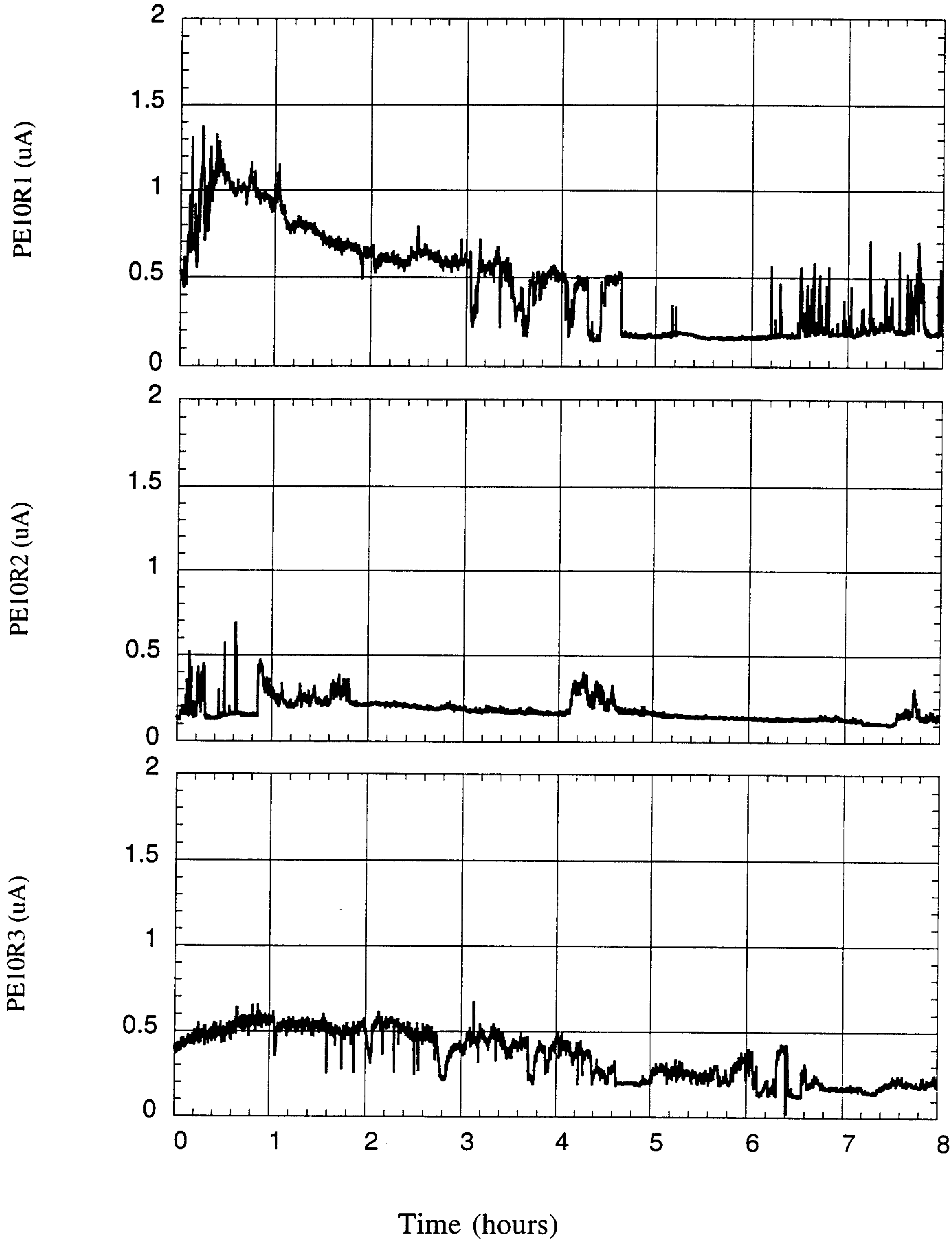

Figure 1.2

Oscilloscope program with wave graph

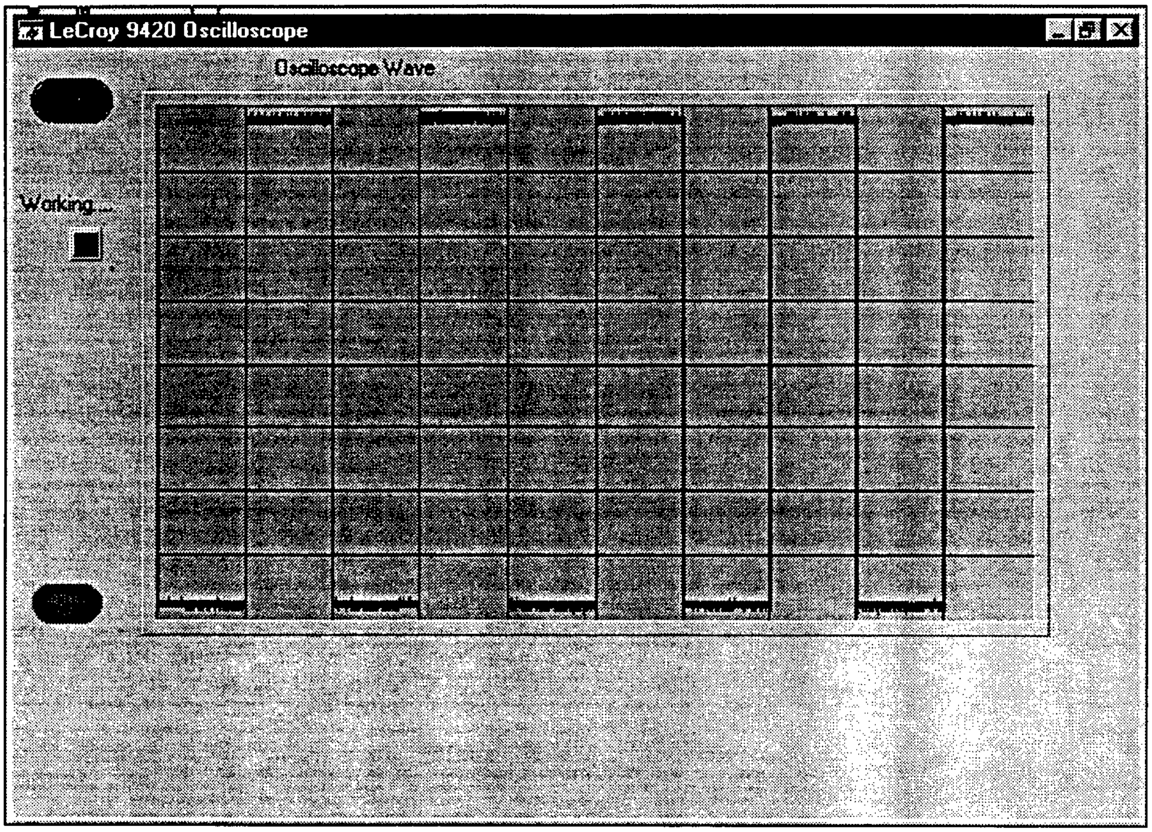

and then printed out in a graph form can be seen in item Figure 1.2. Through the course of this project not only did I get a small glimpse of the value of the C programming language, but I also learned the basics of an Oscilloscope and a Multimeter. The actual coding for the program used to talk to the Oscilloscope can be found in appendix A.

My final task for the summer was working on upgrading computers. Multiple times throughout my tour I was assigned the task of removing or re-installing a CD drive, a floppy disk drive of some other hardware device. I helped install a new CD writer, and later swapped hard drives and RAM cards. I also spent time reformatting a Macintosh computer and then loading a new Operating System on it. Through the constant interaction with computers I have become more knowledgeable about them then I ever had expected to. I now have a basic understanding of the inner hardware of a computer and feel confident upgrading and removing hardware devices.

Conclusion

Through the Summer Research Program I have gotten the opportunity to experience a high tech career in today's world. The influence of this program on my future career choice has been drastic. I now have a good idea of what I hope to pursue in the future and can be confident about my choice. I enjoyed the chance to have a summer job that makes me feel like I am accomplishing something and is educationally rewarding as well. The Summer Research Program at Wright Patterson Air Force Base was a tremendous success for me as both a summer job and as an educational experience, I hope to have the opportunity to do it again next year.

Appendix A

```
#include <userint.h>

#include <ansi_c.h>

#include <formatio.h>

#include <gpib.h>

#include <utility.h>

#include "LCWavGph.h"


int pnl_handle, device;

char path[500];


main()

{

        device = ibfind ("dso") /*dso is board name for scope*/

        pnl_handle = LoadPanel(0, "LCWavGph.uir", PNL); /*opens the .uir file*/

        DisplayPanel(pnl_handle);

        RunUserInterface ();

}


int CVICALLBACK BEGINCB(int panel, int control, int event, void *callbackData, int eventData1, int
eventData2)

{

        static int filesize, testfile;

        static double arraystuff[900000];


        if(event == EVENT_COMMIT)

        {

                PromptPopup("Save Wave", "Input save path", path, 100);

                SetCtrlVal(pnl_handle, PNL_LIGHT, 1);

                ibwrt(device, "C1:INSPECT? 'DUAL'", strlen("C1:INSPECT? 'DUAL'"));

                ibrdf(device, path);
```

```
            testfile = OpenFile(path, VAL_READ_ONLY, VAL_OPEN_AS_IS, VAL_ASCII);
            GetFileSize(path, &filesize);
            FileToArray(path, arraystuff, VAL_DOULBE, 50000, 1, VAL_GROUPS_TOGETHER,
                    VAL_GROUPS_AS_COLUMNS, val ascii);
            PlotWaveform(pnl_handle, PNL_CHART, arraystuff, filesize, VAL_DOUBLE, 1.0, 0.0, 0.0, 1.0,
                    VAL_THIN_LINE, VAL_NO_POINT, VAL_SOLID, 1, VAL_RED);
            Beep ();
            SetCtrlVal(pnl_handle, PNL_LIGHT, 0);
            CloseFile (testfile);
        }
        return(0);
}

int CVICALLBACK QUITCB(int panel, int control, int event void *callbackData, int eventData1, int eventData2)
{
        if (event ==EVENT_COMMIT)
        {
                QuitUserInterface (0);
        }
        return(0);
}
```

CONSTRUCTION OF THE MNAC WEBPAGE AND SOFTWARE VERIFICATION OF MOMENTS '96

Meredith Stegall

Walton High School
Route 8, Box 560
Defuniak Springs, FL 32433-0000

Final Report for:
High School Apprenticeship Program
AFRL/Wright Laboratory

Sponsored by:
Air Force Office of Scientific Research
Bolling Air Force Base, DC

And

Wright Laboratory

August 1998

Creation of the MNAC Webpage and Software Verification of *Moments* '96

Meredith Stegall
Walton High School

Abstract

My first project for the summer was to create a webpage for the Computational Mechanics Branch of the US Air Force Research Laboratory Munitions Directorate (AFRL/MNAC). This project was accomplished through utilization of several web-building programs including *Netscape Composer* and *AOL Press*. Microsoft's *Word Pad* was also used for more advanced HTML markups. The purpose of the webpage is to give the general public a knowledge of what the MNAC and of research opportunities and also to give the Department of Defense easy access to web based information.

Additionally, I was to cooperatively create a webpage for the High School Apprenticeship Program (HSAP). This page will serve as an informant to the public about the HSAP program. It will also be a point where former apprentices can look up old friends and newer apprentices. Interested parties and schools can download a job application from this website.

My primary project for my two-year apprenticeship is to verify and improve the *Moments* '96 code. *Moments* was originally written in FORTRAN in the 1980's. The current version of *Moments* is written in Visual Basic. *Moments* calculates the weight, center of gravity locations, and polar and transverse moment of inertia for axisymetric projectiles.

Introduction

Project 1- Webpage for AFRL/MNAC

The first project of the summer was to design create and execute a web page for the Computational Mechanics Branch of the US Air Force Research Laboratory Munitions Directorate (AFRL/MNAC). The first step in the process was to become familiarized with Department of Defense standard look and feel policy and other requirements regarding protection of government information. The AFRL Common Look and Feel Standards is a set of standards that applies to all external webpages developed throughout AFRL. The purpose is to maintain uniformity throughout all AFRL external sites.

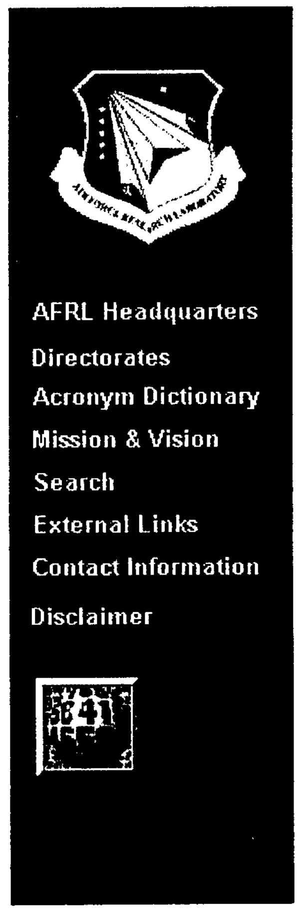

A sidebar for navigation throughout the AFRL web is required for the left side of each page and the right side is given flexibility regarding style and content. All sidebars are to use the standard background image, font size, font type, font colors, item positioning, and logos. The side bar to be dark with light colored text. The background used is to be uniform in a directorate. The required items on the side bar include Dictionary, Directorates, Search, Help, Disclaimer, and Contact Information. Additional information may be added to the side bar by the individual directorates of the AFRL. The bar is mandatory for all pages to the second level in the webpage tree. It is not required that the bar be printable.

Installing the sidebar was very challenging because it required the actual manipulation of HyperText Markup Language, or HTML. The side bar is actually a table that occupies approximately 25% of the browser window. To manipulate the HTML the Microsoft program *Word Pad* was utilized. It is difficult to maintain an idea of what the whole bar looks like when a visual aid is unavailable. *Word Pad* is normally only used for more complex HTML because webpage builders such as *Netscape Composer* provide a point and click method of web editing and building.

The second step of the project was actual creation of the pages. Creating a webpage can be compared to constructing a family tree. I began with a main page and branched out with each group and project division. I began by mapping out the tree I planned to use for the webpages.

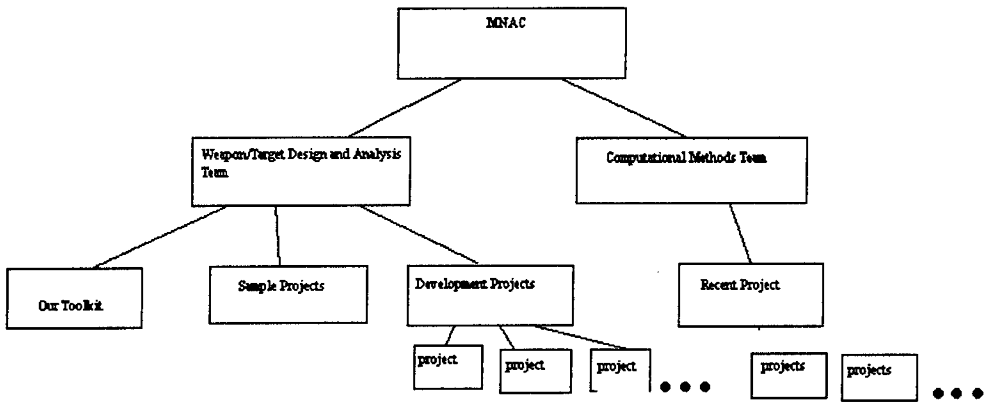

The first page was to represent the entire branch. Within the MNAC page were links to the two teams within the branch, which are the Weapon/Target Design and Analysis Team and the Computational Methods Team. On the Weapon /Target Design and Analysis Team page are links to Our Toolkit, Sample Projects and Development Projects. In Our Toolkit is a listing and brief description of different analysis tools used by the team and links to the commercial and government sites that are responsible for the tools. Sample Projects is a page that gives a pictorial overview and description of what the team does. Development projects gives brief view into what the projects that a currently underway. On the Computational Methods Team page are links to current projects. Each project page is a brief summary of the project and pictorial overview. One feature not on the chart is a link on the MNAC page link that contains Job and Research Opportunities in MNAC. Each page following the MNAC page contains links back to the MNAC page, the opposite team and to the original team. Each page contains an e-mail link to the team leaders and branch chief for further information on the page contents. The page is now facing the public affairs approval process. After the webpage is approved, it will be put on the Air Force Research Laboratory's server under the Munitions Directorate at http://www.afrl.af.mil .

Project 2 – Webpage for the High School Apprenticeship Program

The intent of the High School Apprenticeship Program (HSAP) page was to provide an easily accessible source of information about the program to schools and individuals. The main page provides links to information pages, to past and present apprentice pages, to a download sight for an application, and to an acknowledgement page. The past and present apprentice page is of particular value to the public because it provides the e-mail address of apprentices so the interested public may e-mail them for first hand information about the program. The page will be valuable to past apprentices also because they can look up old friends they worked with from as far back as 1984. Links to the individual high schools represented by the program are also available. The informative page provides basic information and general requirements of the program. It also provides the public with a view of what apprentices do and how it contributes to the Air Force. The application download is also a very nice feature. Often there are students who have never heard about the program and have never asked his or her guidance counselor about an application. Thus, if a student finds out about the program while surfing the web, he or she can easily download an application, fill it out, and mail it in. Also, if guidance counselors and accidentally lose an application, they can simply download a new application to make copies for the students who may be inquiring. It simply makes the program process less error- prone and more people friendly. The HSAP webpage is not yet complete but will be completed during the next school year. Because of HSAP's nature, the rules and standards for design are not as strict and rigorous.

Project 3- Software Verification and Improvement of Moments version 96

In the early 1980's, a FORTRAN program was developed for quickly determining the weight, center of gravity location, and the polar and transverse mass moments of inertia for axisymetric projectiles. The program was called MOMENT and would quickly load the projectiles information, stored as text in a separate file, and would output the calculations and a line drawing of the specified projectile. Many users complained of the programs difficult design process and asked for an updated version of the program. In 1994, Josh Weaver, an HSAP apprentice began to redesign the program in a Visual Basic, a Windows based environment. *Moments,* as the new Graphical User Interface (GUI) was referred to, combined the text-based data into the same screen as the graphical output and resulting calculations. This made the finetuning and modification a much easier process. The program was also rewritten to incorporate a memory management scheme optimized for low memory computers.

Between '95 and '96 *Moments* was again updated and translated into the newer version of Visual Basic. However, noticeable problems occurred in that certain features of the older version of Visual Basic were not compatible with the newer version. The algorithm and GUI of the program had to be completely redeveloped. After the program was rewritten, it was sent out for verification. At this time, major problems were noticed. In the conversion, the GUI became much harder to use, it frequently miscalculated the total transverse moment of inertia, total polar moment of inertia, and total projectile weight, lacked the capability to save the information in any form, and finally, it lacked the help files the GUI gave the impression of being available. Notice the similarities between Figure 1 and Figure 2. The GUI's look similar, but in fact, they function differently. *Moments* 96 is much more tedious to use. Also notice the difference in the numbers, excluding center of gravity locations, all of the numerics on Figure 2 are incorrect.

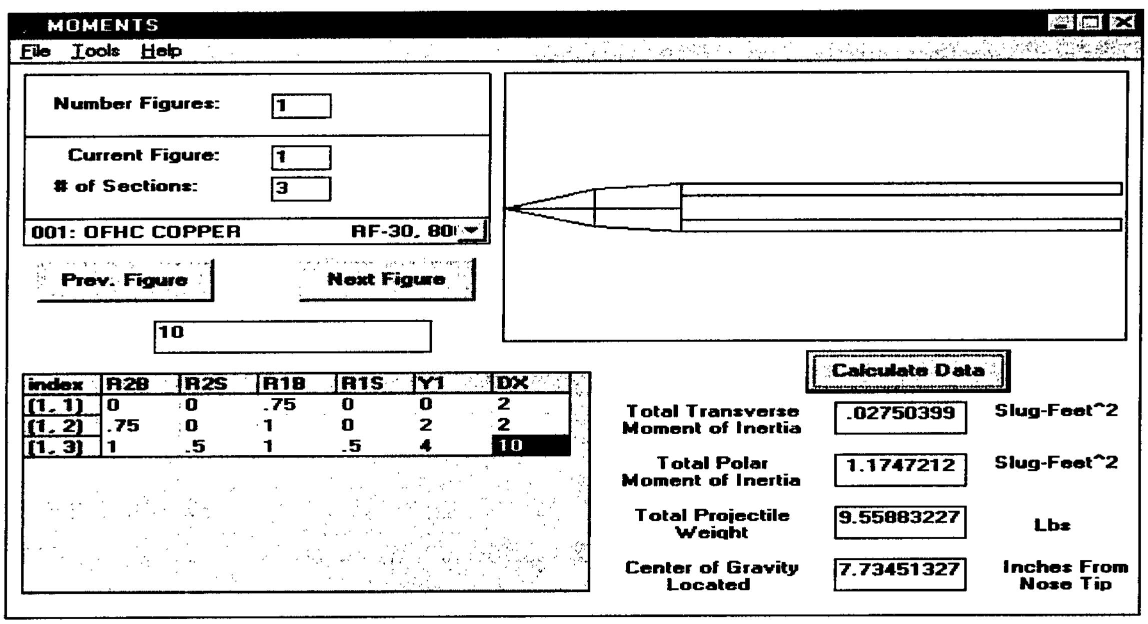

Figure 1. Main window of *Moments* 94 Graphical User Interface which reflects the text-based input, projectile simulation, and result calculation.

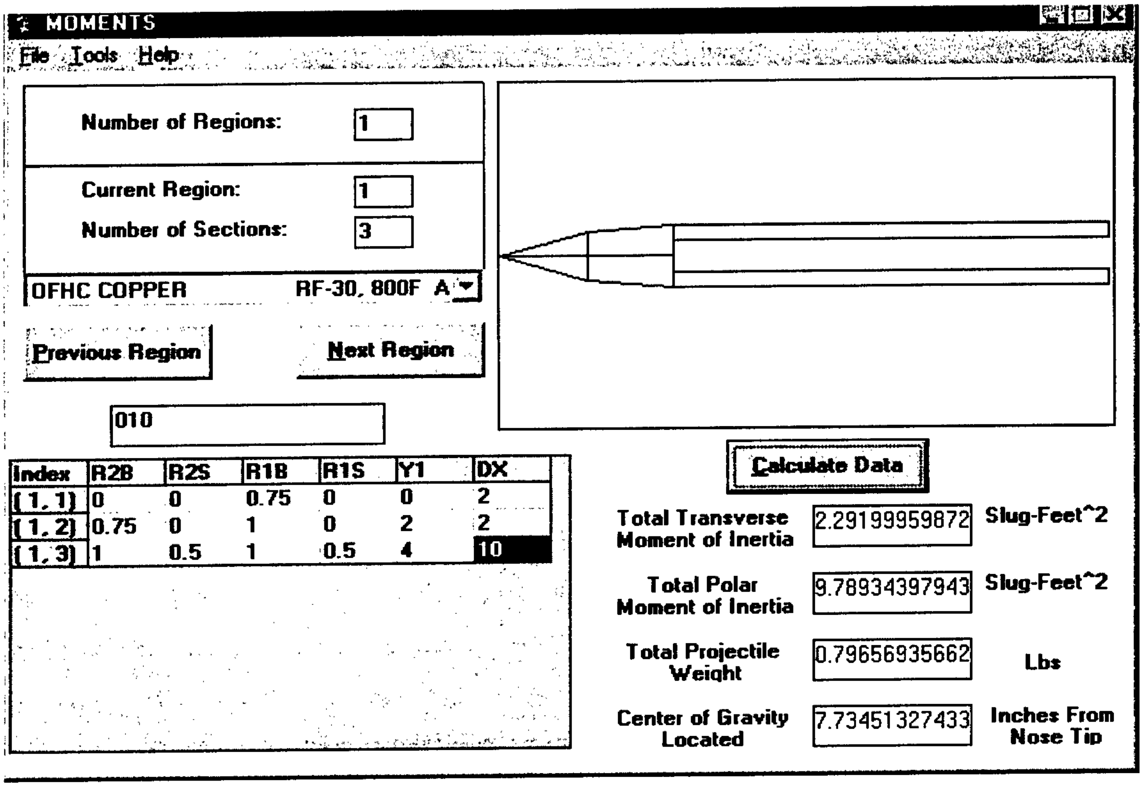

Figure 2. Illustration of the Graphical User Interface of *Moments* 96

Through experimentation and review of the source code for the program, I theorize that the problem with the miscalculation is based in the algorithm that had to be altered between the old version of Visual Basic and Visual Basic 4.0. The quite obvious reason for this is that the '94 version of the code calculated the total transverse moment of inertia, total polar moment of inertia, and total projectile weight correctly; however, this version left off the scientific notation needed for complete representation of the numerical values. Also, small variations in the algorithm can be noticed where a variable could have easily been mistyped or a constant incorrectly defined.

In continuation of this project, next year I plan to rework the algorithm, make any changes necessary for a properly working and defining program, convert the program to the metric system, improve the user interface, and finally, create the help and save capabilities the GUI gives the impression of existing. Hopefully, many other improvements and additions will also be made to the program for increased program capability and usage.

From these three projects I greatly increased my knowledge of HTML and Visual Basic. The projects also greatly improved my analytical skills. With my new knowledge of HTML and Visual Basic I am now greatly prepared for the technological world.

WHAT I DID ON MY SUMMER VACATION

Lydia R. Strickland

Mosley High school
501 Mosley Drive
Lynn Haven, FL 32444

Final Report for:
High School Apprenticeship Program
AFRL/Wright Laboratory

Sponsored by:
Air Force Office of Scientific Research
Bolling Air Force Base, DC

And

Wright Laboratory

August 1998

WHAT I DID ON MY SUMMER VACATION

Lydia Ruth Strickland
Mosley High School

Abstract

As a High School Apprentice student my summer project consisted of many small projects, instead of one main one. I was assigned the task to help publicize the projects done at our laboratories. This included updating and duplicating our reports, as well as making a web page to help people get to our software and reports. I also helped get many needed reference documents for our scientists, sort mail, and shelve books for the Technical Information Center. I created a trouble desk for the network users and kept in running. In addition I updated receiving files for the lab, database files of reports, and the Technical Summary Sheets. Perhaps the most challenging project was to make a "cheat sheet" for all users of the program database. What made the task so difficult was that I had never seen the database before. I was given access to the database familiarized myself with it well enough to make a sheet for all project managers to use as a quick reference guide.

What I Did On My Summer Vacation

This summer at Tyndall Air Force Base proved to be a memorable and interesting learning experience. I was assigned several task over a course of eight weeks. No large project was assigned to me but instead several small ones. While here over the summer I learned several new computer programs that had not been introduced to me before. It was very helpful and informative and will be quite useful to me in the future.

One of my tasks was to help publicize information about the scientific projects done at Air Force Research Labs. Since documents and letters are vital for publicizing the events and activities done here my task was to help duplicate many of these important documents for distribution at technical briefings and command sponsored meetings. Part of this project also included making a web page. This was new for me because I had never worked with Microsoft Front Page and was excited to learn the program. The web page that I developed allows people who are at our web site to read our Technical Summary Sheets (TSS) and decide if they want to download the software or documents that our scientists have developed. Not only did I have to make links from the web site to the TSSs but I had to update and edit them This was new to me because I had to just figure out how to use Image Composer to update them so that they would be compatible with the web page.

Another task was to work in the Technical Information Center (TIC) helping to research, file and distribute information. I spent my time researching for the scientists in the lab and giving them the needed information for their studies. I also organized reading material, shelved books and technical reports, and opened and sorted mail for all the workers in the TIC. This kept the workers from being so overwhelmed with their other important work.

I was also given the task to update some of the records for the office. One of the jobs was to update a receiving orders for the laboratory so that the records would be accurate. I had to do this in Microsoft Access, which was another computer program that had merely been introduced to me, but I had not used it much. Along with my task to update came the opportunity to scan technical reports into the computer to add to a database that was being produced so that the hard copies of the reports could be disposed of because they were in bad shape. This taught me how to use a scanner. I was also assigned to update a address book for all the people and bases that our research information is sent to which meant entering approximately two hundred names. This was a time consuming and tedious task.

One of my mentors had to leave for a two week training session and it was my job to create a trouble desk for all the network user to call in their complaints. Another one of the high school students and I produced a form to fill out for each project as well as putting a program called ESP on our computer which is specifically designed for a help desk. We kept a record of all the trouble calls so that my mentor could fix them in order when he returned. We also tried to fix as many of the problems that we could. We called our help desk the LAN Trouble Desk, with LAN standing for Local Area Network.

The final project assigned to me to create a cheat sheet for a database that the project managers updated. I was given a program that I had never seen before and told to familiarize myself with it in order to teach a class to all the project managers so that they could go through the program easier. Part of this also included making a "cheat sheet" so that all the project managers have to do is look on the sheet and know what to press to get the where they wanted to go. This was complicated because of the variety of ways that you can look at the projects. The five main ways were looking at the Financial, Manpower, Milestones, Contract and point of contact. The cheat sheet is shown in Figure One on page five and six.

It was an honor working with the HSAP this summer. I learned many new and useful computer programs that I have never been introduced to before. I found this summer to be a great learning experience.

Figure One

Getting in the Data Base

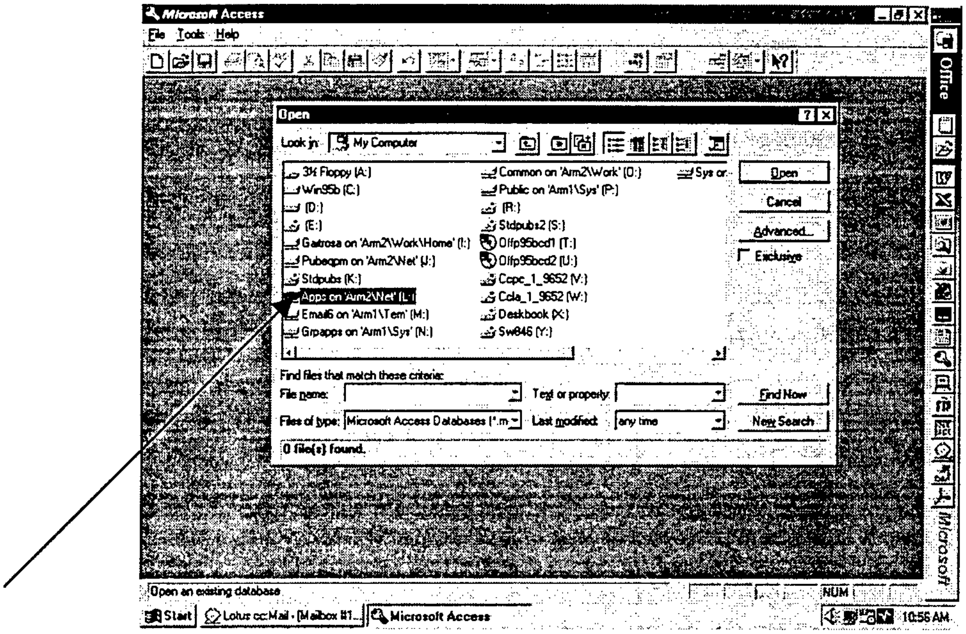

1. To get into the database look in the "L" drive and double click on it.
2. Click on Access folder.
3. Click on **Eqinfo-7.mdb**.
4. Click on the arrow beside the Subtrust
5. Choose a highlighted Subtrust
6. Do the same for the Focused Technology Area and Program.
7. This allows you to categorize the projects in order to make them easier to find.
8. To see all projects regardless of Direction choose the Show All icon.

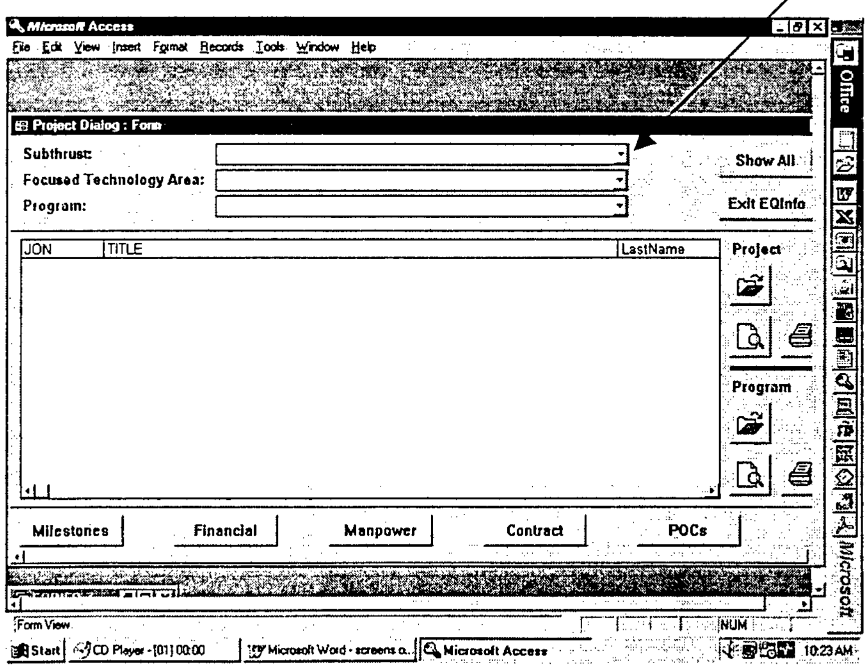

- The icon with the open folder opens a project summary where you will update the seven areas of the summary.
- The icon with the magnifying glass and paper allows you to view the complete project without editing it.
- The printer icon prints the summary of the highlighted project.
- The following fields are part of the project summary screen and are the responsibility of the FTA/Direction Manager for accuracy.
    1. Milestones
    2. Financial
    3. Manpower
    4. Contract
    5. POCs

Milestones: The button will display planned versus actual milestones and must be updated as milestones occur.

Financial: Project funding information in presented in two views. On the top of the screen you can enter your estimates of the total cost of all technical efforts associated with the specified project. By clicking the drop down arrow in the Projects Requirements box it will display specific budget categories used to show how the funding will be distributed and expended against this project (e.g., primary contracts, travel, etc.) Project Allotments, on the other hand, represent actual MLQ authorization and can only be entered by MLQP personnel. This is a read only format and can not be edited. The total requirement should equal the total allotment. If it does not, then you are identifying an unfunded requirement.

Manpower: By selecting this button you can forecast how you will use both government and contractor acquisition support personnel to monitor the performance of this project. The drop down boxes are provided for the quick entry of the names of government personnel and contract positions. Positions for laboratory support (DSG) are entered separately and are reflected in the project requirements. This area is only available for update by FTA Direction Managers during the annual TIR planning phase.

Contract: Contract summary information is entered by the EQPM contraction section after the project manager decides on a contracting vehicle.

POC: The point of contact identifies your focal point at base or MAJCOM level for a particular project. A drop down arrow is provided so you can choose the appropriate person. MLQP can add new POCs as required.

STUDY OF PAINT WASTE DECOMPOSITION

Rachel J.. Strickland

Mosley High school
501 Mosley Drive
Lynn Haven, FL 32444

Final Report for:
High School Apprenticeship Program
AFRL/Wright Laboratory

Sponsored by:
Air Force Office of Scientific Research
Bolling Air Force Base, DC

And

Wright Laboratory

August 1998

STUDY OF PAINT WASTE
DECOMPOSTION

Rachel J. Strickland
Mosley High School

Abstract

Analytical and microbiological research was done on a paint waste sample from Tinker Air Force Base. Five chemicals were established to be present in the paint waste sample. Each chemical was individually mixed with different amounts of pure water to establish three different concentrations of each chemical. SPME and gas chromatograph techniques were used to run tests on each separate chemical. These same instruments were used to test a combined solution that made up the same concentrations as the paint waste sample. The paint waste was then cultured to grow bacteria, this being the microbiological portion of the experiment. The results proved that there were several types of bacteria present in the paint waste. It was theorized that the paint waste contained bacteria that could decompose the chemicals present in the paint waste.

STUDY OF PAINT WASTE DECOMPOSITION

Rachel J. Strickland

Introduction

Many different elements of science and math come together in the experimental and analytical use of a laboratory. The tools used in the experiments are complicated and technologically advanced. Yet, with explanation of the uses and operation of the machines, high school students can operate them. This helps the students further their exposure and experience of working in a laboratory and the "real world" in general. Some of the machines include the gas chromatograph and solid phase microextraction.

A gas chromatograph is a machine that tests the concentrations and types of chemicals that are in a sample injected into the machine. The end result is a graph made with separate peaks for each individual chemical present in the sample. The pressure of the helium gas is high enough to vaporize the chemicals in an injection. The vaporized chemicals from the sample are pushed through the column. The temperature in the gas chromatograph helps to make the molecules from the sample move faster through the column. Depending on the type column in the gas chromatograph, the temperature can rise to several hundred degrees. The sample is injected through the injection port; it then travels through the column to the flame ionization detector. Refer to Figure 1. [1] This detector converts the information of electrical signals from the machine, and this information that is read at a computer. The information is shown as peaks on the computer. The peak area is shown in the time that it appeared in the run, and the peak area determines the amount of a particular molecule present in the sample. Each peak represents an individual chemical present in the sample being tested.[2]

The sample used through the project is referred to a paint stripping waste. This sample was sent from Tinker Air Force Base to be analyzed and tested. The paint waste is a combination of two chemicals, and is sprayed onto airplanes to remove the paint. The waste from this chemical mixture is what was used in the testing of the project. From research done previously at the lab, five major chemicals were found to be formed in the waste: benzaldehyde; 2-methyl pyrrlidinone; benzyl alcohol; 2-ethyl-2, 4-petanediol; and phenol. The paint stripping waste is the wastewater obtained when two chemicals are combined and sprayed onto airplanes to remove their paint. New paint can then applied to the plane.

A solid phase microextraction, or SPME, is a small device that extracts a sample by absorbing molecules onto silica fused fiber coated with polymeric compound.[3] Refer to Figure 2. It extracts a sample by locking the plunger retaining screw down into place and exposing the fiber to the sample. This process is usually done in a vial with a screw on septum lid. After a timed extraction, unlock the retaining screw and withdraw the fiber. After the timed extraction is finished, put the needle of the SPME into the injection port of the gas chromatograph and repeat the extraction process. The SPME has adjustable barrel gage the enable the user to adjust how long the needle is. The SPME technique is one where the sample is sorbed onto the fiber and the needle to protect the sample.

The experiment's purpose was to improve accuracy and expand on experiments done on the paint waste previously. From these previous experiments done in the lab, it was discovered that there were different types of bacteria present in the paint. It was hypothesized that in high concentrations the bacteria stayed dormant, but if diluted, the bacteria could grow and feed off of the waste components. This experiment was performed to determine if that hypothesis was correct.

Procedure

The experiment involved two different types of laboratory work, analytical and microbiological. The analytical procedure was performed on the chemicals within the paint waste solution. The microbiological procedure involved the growing of the bacteria. The analytical procedure involved mixing three different concentrations of each individual chemical within the paint waste. The chemicals were mixed in one hundred-milliliter volumetric flask. Different amounts of the chemical were pipetted into the flask. The flask was then filled to the line with purified water. The amounts of each chemical are shown in Table 1.

Ten milliliters of each solution was pipetted into a vial with a silicon septum screw on lid. A small magnetic stirrer was placed in the bottom of the vial and put on an automatic stirrer that was set on eight. An internal standard was made to attempt to cause the results of the experiments to become more precise and consistent. The internal standard was mixed in a ten-milliliter volumetric flask; ten microliters of

d_{10}ethyl benzene was pipetted into the flask and it was then filled to the line with methanol. The SPME punctured the septum and was extracted for ten minutes. After the time was expired, the plunger retaining screw was unlocked to protect the molecules on the fiber. The SPME was immediately injected into the gas chromatograph, the fiber was exposed and the gas chromatograph was started. The gas chromatograph was on a seventeen and one half minute run; the temperature rose from forty to two hundred and fifty degrees Celsius. A DB WAX column was used in the experiment and is equipped to withstand such high temperature. Three runs were made of each solution made, and linear lines were calculated from these results.

The same process of the use of an internal standard, the timing, the stirrer, and the vial was used for the paint waste and a combine standard solution. This combine standard solution was run because previous results suggested the possibility that some of the components reacted with each other. A sample of the paint waste was extracted with the SPME from the sample and then injected into the gas chromatograph. This was run five times, and from these results the concentrations of the paint waste was determined. A combine standard solution consisted of one thousand microliters of 2-methyl-2, 4-pentaediol; two hundred microliters of benzyl alcohol; two hundred microliters of 1-methyl-2-pyrrlidinone; ten microliters of benzaldehyde; and fifteen microliters of phenol. These chemicals were pipetted into a ten-milliliter volumetric flask and it was filled to the line with purified water. Ten milliliters was pipetted into a vial and the internal standard was immediately injected into the combined solution. Each of the five runs made was mixed individually, for it was found that after a certain amount of time the internal standard would begin to bond with the other chemical mixed together. Although the mixing of each individual sample solution causes more room for error, this was the only possible way to accomplish reliable results. Figure 3 shows the results of the combined solution.

The concentrations were determined to be the ones used in the combined standard solution. A linear line was made for the individual chemicals run. An example can be seen in Figure 4 on the linear response to phenol.

The microbiological procedure began by making eight samples; four undiluted, four diluted 10^{-1} One hundred microliters of the undiluted paint waste sample was transferred onto a Luria media in a petry dish. A sterilized hockey stick was used to spread the solution evenly over the media. The same procedure was used on the diluted solution. These samples were left at room temperature until there was growth on

media. Two of the diluted plates had several different types of bacteria growing on them. Each colony of bacteria was lifted off the plate with small-sterilized sticks and streaked onto nutrient media plates. There were thirteen different samples taken. These samples were incubated for an additional two days. The bacteria was streaked in the same fashion was before onto a new media, in order to attempt to isolate the different types of bacteria.

After the bacteria had grown on seven of the streaked plates, a gram stain test was performed. A drop of Milli-Q-Water was dropped onto clean seven microscope slides. With a loop wand, the bacteria is scraped from the media and mixed with the water on the slide. The wand is heated between transfers to sterilize it. A drop of the following was placed onto each slide, then rinsed; gram crystal for thirty seconds, iodine for thirty seconds, gram decolorizer for ten seconds, and gram safranin for twenty seconds. Each slide was left to air dry. After the slides were dry, they were examined under the microscope. The color of the bacteria showed whether the bacteria were gram positive or gram negative. If the bacteria appeared pink it was gram negative; if purple then is was gram positive. Only two of the samples tested were gram positive; the other five were gram negative.

A second set of samples on the plates was made in the same manner as the first; eight samples were made with the paint stripping waste diluted 10^{-1}, and eight undiluted. The bacteria was grown for seven days and then streaked onto new media. Although nothing was done with these samples, they did have a large assortment of colors.

The first set of samples made in the microbiological procedures only had seven plates with growth on them after the second streaking. Most of the plates with growth were from the diluted samples.

It was theorized that the reason for this outcome came about because the bacteria present in the paint waste sample was dormant in the higher concentrations, but when diluted it grew and found nutrients from the paint waste. The results of the two sets of plates are shown in Tables 2 and 3.

Discussion

If the bacteria does decompose the chemical in the paint waste, the results could be beneficial for environmental uses. The waste could be decomposed, instead of just being disposed of. Once the bacteria is identified and sample, if could be further researched to possibly even decompose other harmful chemicals as well.

The analytical procedures developed for the paint waste can be used to study various treatment scenes. In addition to the microbiological experiments, there is a parallel effort in process to study the destruction of the paint stripping waste in a hydrothermal oxidation reactor. Samples of the waste will be treated and the effluent water will be analyzed to detect any conversion of the waste components by the reactor.

Figure 1

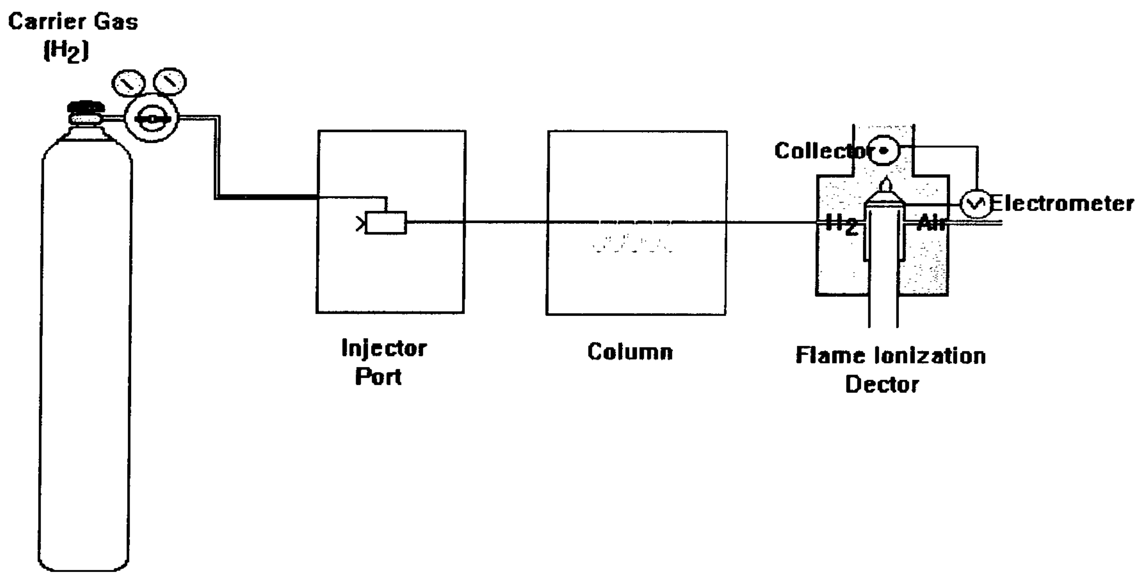

Figure 2

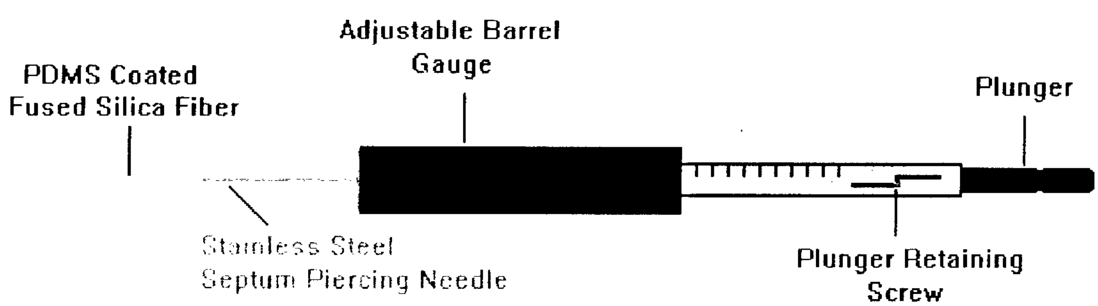

Table 1

CHEMICAL	SOLUTION 1	SOLUTION 2	SOLUTION 3
1-methyl-2-pyrrolidionone	2 mL	1 mL	0.5 mL
2-methyl-2,4 petanediol	10.8 mL	5.4 mL	2.2 mL
Benzyl Alcohol	2 mL	1 mL	0.5 mL
Benzaldehyde	100 uL	65 uL	25 uL
Phenol	150 uL	65 uL	25 uL

Figure 3

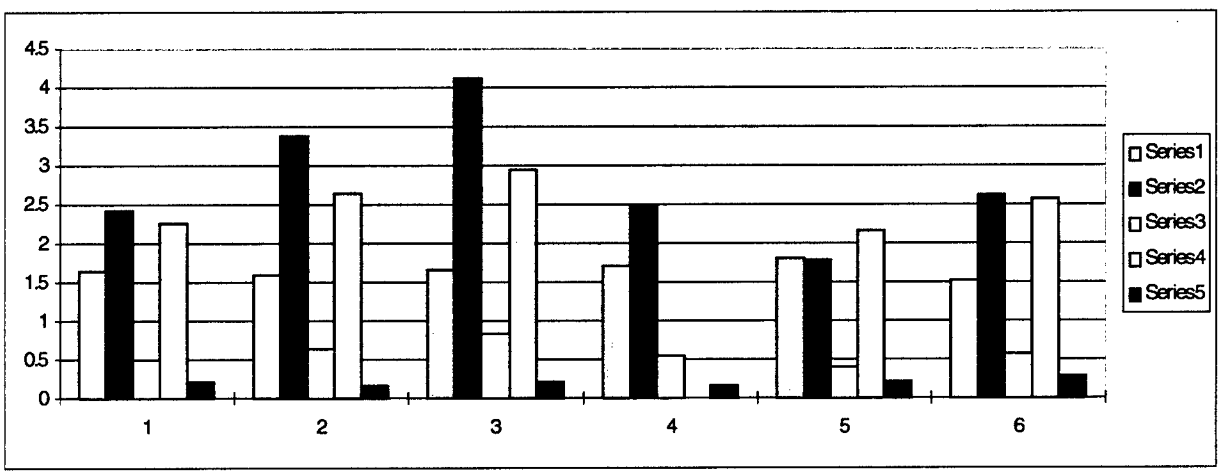

Series 1	Benzaldehyde
Series 2	2-methyl-2,4 petanediol
Series 3	1-methyl-2-pyrrolidionone
Series 4	Benzyl alcohol
Series 5	Phenol

Figure 4

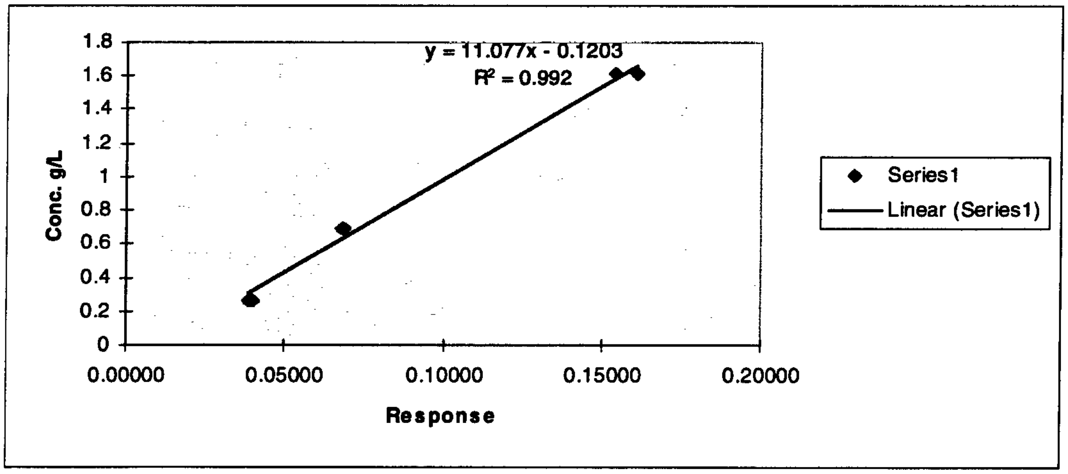

Table 2 (1st Set)

Name	Color	Form	Elevation	Margin	Surface
R1	Yellow-orange	Punctiform	Flat	Undulate	Rugose
R3	White-clear	Circular	Flat	Entire	Contoured
R5	Yellow-orange	Punctiform	Raised	Undulate	Rugose
R7	White	Irregular	Umbonate	Curled	Contoured
R8	White	Circular	Flat	Entire	Rugose
R9	White	Irregular	Umbonate	Curled	Contoured
R11	White	Circular	flat	Entire	Rugose

Table 3 (2nd Set)

Name	Color	Form	Elevation	Margin	Surface
M1	Orange	Circular	Convex	Entire	Concentric
M2	Clear	Punctiform	Raised	Entire	Smooth
M3	Orange	Circular	Convex	Entire	Concentric
M4	Orange	Circular	Convex	Entire	Smooth
M6	Yellow	Circular	Pulvinate	Entire	Smooth
M7	Pink	Punctiform	Raised	Entire	Smooth
M8	White	Circular	Convex	Entire	Smooth

References

[1] McNair, H.M., and E.J. Bonnelli, Basic Gas Chromatography, Consolidated Printers, Berkeley, California,
1968, p.169

[2] Willard, Hobart H., Instrumental Methods of Analysis, D. Van Nostrand Company, New York, 1979, p. 523

[3] Arthur, Catherine L., *Analytical Chemistry*, "Solids Phase Microextraction with Thermal Desorption Using Fused Silica Optical Fibers.", American Chemical Society, Ontario, Canada, 1990, p. 2145

THE STUDY OF THE CHANGE IN STRENGTH OF UNREINFORCED ALUMINUM 7093 ALLOY AND ALUMINUM 15 VOLUME% SICP/7093 DRA

Robert L. Todd

Carroll High School
4524 Linden Avenue
Dayton, OH 45432

Final Report for:
High School Apprenticeship Program
AFRL/Wright Laboratory

Sponsored by:
Air Force Office of Scientific Research
Bolling Air Force Base, DC

And

Wright Laboratory

August 1998

THE STUDY OF THE CHANGE IN STRENGTH OF UNREINFORCED ALUMINUM 7093 ALLOY AND ALUMINUM 15 VOLUME% SiCp/7093 DRA

Robert L. Todd
Carroll High School

Abstract

The effect of heat treatment on unreinforced aluminum 7093 alloy and aluminum 15 volume% SiCp/7093 DRA was studied. In order to study this effect, the unreinforced and DRA alloys were precipitation strengthened by solutionizing, water quenching, and aging. After being heated, the alloys were cut and polished. The alloys were examined with a scanning electron microscope (SEM). With the SEM excess amounts of carbon was found and the size of the precipitates increased as aging did. Using a macro-hardness testing machine, the hardness of the alloys were found to be weaker as the aging increased. This data indicates that the excess amounts of carbon played a major role in the strengthening of the alloys.

THE STUDY OF THE CHANGE IN STRENGTH OF UNREINFORCED ALUMINUM 7093 ALLOY AND AlUMINUM 15 VOLUME% SiCp/7093 DRA

Robert L. Todd

Introduction

Precipitation strengthening is a process of creating a dense and a fine distribution of precipitated particles in the matrix of a heat-treated alloy. The precipitate particles act as obstacles to slow movement and therefore strengthens the alloy. In order to precipitate strengthen an alloy, the alloy must be a terminal solid solution which has a decreasing solid solubility as the temperature decreases. The first of three steps in precipitation strengthening is to solutionize the alloy. Solutionizing is done by heating the alloy until precipitates begin to form. The second step is to quench the alloy in a cooling medium. Aging is the third step to this process. During aging the alloy will be strengthened.

Discussion of the Problem

The purpose of this experiment is to perform heat-treatment studies on unreinforced aluminum 7093 alloy and aluminum 15 volume% SiCp/7093 DRA.

Methodology

Ten samples of the unreinforced alloy and ten samples of the DRA, each being semicircle in shape, were solutionized-treated in a muffler oven at 490oC for four hours. Then they were removed and water quenched. All twenty samples were then placed in a freezer a 0oC. Next, nine samples of each aluminum were heated again but at different times. The samples were heat-treated at 120oC at these time intervals: 1500 seconds, 10000 seconds, 20000 seconds, 40000 seconds, 55000 seconds, 70000 seconds, 86400 seconds, 100000 seconds, and 1000000 seconds. One samples of each aluminum alloy was heated at each time interval. When the samples were finished being treated, they were water quenched and returned to the freezer to prevent further strengthening. Each sample at each time interval was labeled with a number for reference. The samples were then ready for the initial step of polishing. Each sample was polished using a manual operated wheel. All of the samples were polished using a verity of diamond based polishing compound. The size of the diamonds in the compound were: 400 grit, 600 grit, 15 micron, 9 micron, 3 micron, and 1 micron. All of the samples, were placed in a beaker filled with isopropanol alcohol. The beaker was placed in an ultrasonic cleaner to prepare the samples for the SEM. They were removed from the ultrasonic cleaner and placed in a vacuum oven for one hour and then returned to the freezer. The samples of each alloy that were heat-treated for 0 seconds, 86400 seconds, and 1000000 seconds were examined in the SEM in secondary electron imaging (SEI) and backscatter electron imaging (BEI) at 50x, 500x, and 5000x. The samples were also examined with an electron dispersion spectrum (EDS), for a spectrum analysis. This analysis is used to get an idea of the chemical make-up of the surface, and a little below the surface of the samples. All samples including those not examined in the SEM were tested in a macro-hardness testing machine.

Results

When the samples were examined in the SEM, excess amounts of carbon was in all of the samples. This was found by looking at each sample in backscatter electron imaging (BEI). The carbon appeared to be dark black in color and in large quantities throughout the entire sample. Through the spectrum analysis these large black particles were identified as carbon. Using the macro-hardness testing machine, the samples' hardness decreased as the time intervals increased. This is shown by the data table labeled "Macro-hardness Testing" and by the graph "Hardness Data".

Conclusion

In conclusion, the strengthening of each alloy decreased as the aging time increased. This variation was unexpected. The strengthening of each alloy should have increased as the aging increased, until a peek-age was acquired. After the

Macro-hardness Testing

Temp (C)	Time (sec)	Type	Test 1	Test 2	Test 3	Avg
0	0	Al 7093	84	85	85	84.667
0	0	Al 7093 w/ SiC	79	77	75	77
120	1,500	Al 7093 w/ SiC	74	73	73	73.333
120	10,000	Al 7093 w/ SiC	65	52	57	58
120	20,000	Al 7093 w/ SiC	60	62	52	58
120	40,000	Al 7093 w/ SiC	58	57	57	57.333
120	55,000	Al 7093 w/ SiC	49	39	50	46
120	70,000	Al 7093 w/ SiC	46	45	47	46
120	86,400	Al 7093 w/ SiC	42	44	43	43
120	100,000	Al 7093 w/ SiC	49	47	47	47.667
120	1,000,000	Al 7093 w/ SiC	27	24	25	25.333
120	1,500	Al 7093	73	73	76	74
120	10,000	Al 7093	62	50	63	58.333
120	20,000	Al 7093	43	45	37	41.667
120	40,000	Al 7093	64	52	54	56.667
120	55,000	Al 7093	59	58	53	56.667
120	70,000	Al 7093	30	27	27	28
120	86,400	Al 7093	24	25	26	25
120	100,000	Al 7093	34	32	28	31.333
120	1,000,000	Al 7093	24	24	27	25

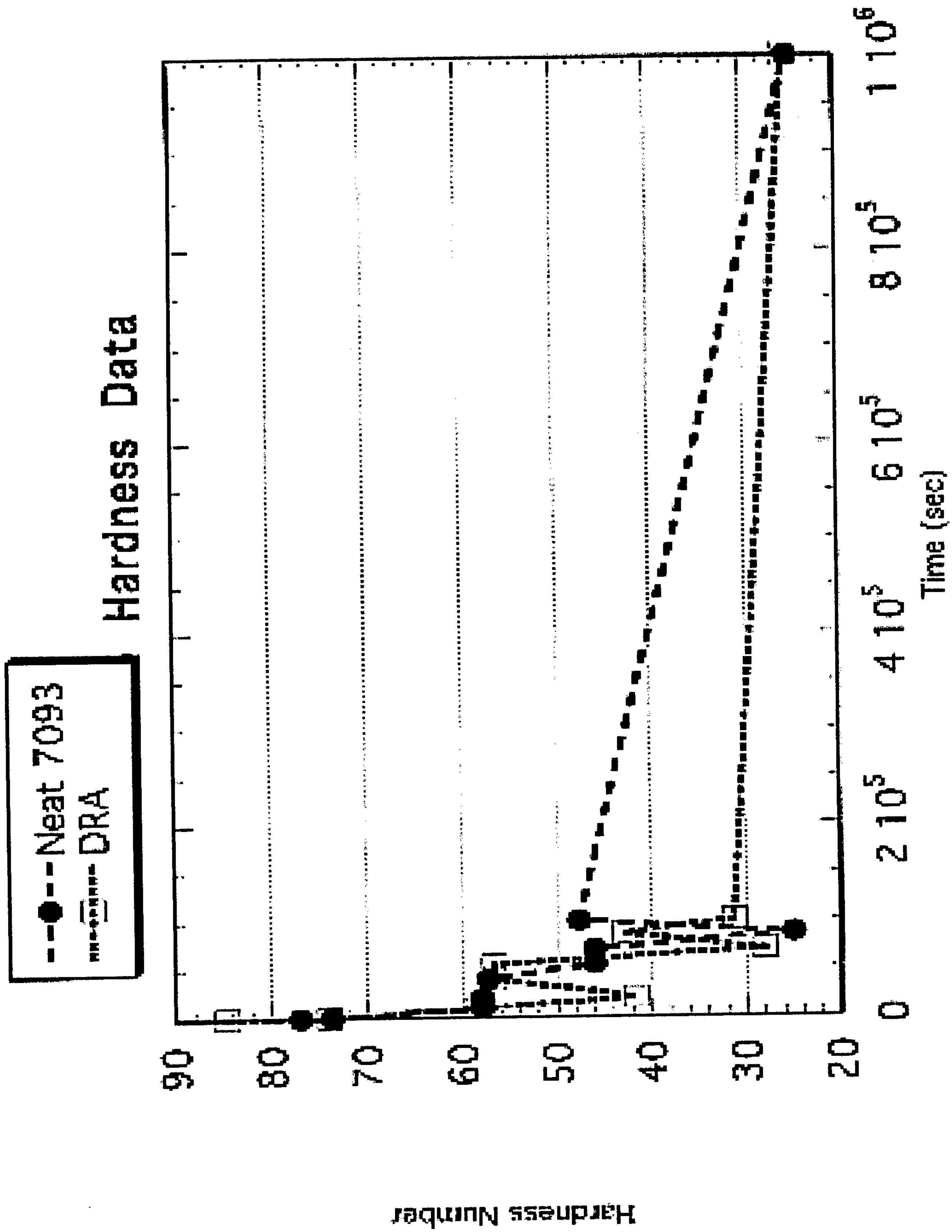

Hardness Data
Neat 7093
DRA
Hardness Number
Time (sec)
90
80
70
60
50
40
30
20
0
2 10^5
4 10^5
6 10^5
8 10^5
1 10^6

peek-age, the strengthening would then decrease.

The alloys decreased in strength instead of increasing because the excess amounts of carbon weakened the matrix of the alloys and the precipitates in the alloys.

References

1) Encarta 96 Encyclopedia, published by Funk & Wagnalls Corporation, 1993-1995.

2) "Influence of fibre reinforcement on the aging behavior of an AlSi12CuMgNi alloy", by J. Bar, H.-J. Gudladt, J. Illy, J. Lendvai, published by Materials Science & Engineering A, pg. 181-186, 1998.

DAMAGE STUDIES ON INERTS AND EXPLOSIVES USING ROD-ON-ROD IMPACT AND SPLIT-HOPKINSON PRESSURE BAR TECHNIQUES

My V. Tran

Choctawhatchee High School
110 Racetrack Road
Fort Walton Beach, FL 32548

Final Report for:
High School Apprenticeship Program
AFRL/Wright Laboratory

Sponsored by:
Air Force Office of Scientific Research
Bolling Air Force Base, DC

And

Wright Laboratory

August 1998

DAMAGE STUDIES ON INERTS AND EXPLOSIVES USING ROD-ON-ROD IMPACT AND SPLIT-HOPKINSON PRESSURE BAR TECHNIQUES

My V. Tran

Choctawhatchee High School

Abstract

Damage to inerts and explosives caused by impacts was studied in this investigation. The inert studied was sand (SiO_2, silicon dioxide), while the explosives studied were 1, 3, 5- trinitro-1, 3, 5- triazocyclohexane (RDX) and the plastic bonded explosive, PBXN-109. PBXN-109 is composed of 64% RDX, 20% aluminum, and 16% hydroxy terminated polybutadiene (HTPB), a rubbery binder. Analyses were conducted on previously tested samples and samples tested specifically for this study. The previously tested PBXN-109 samples were shot by rod-on-rod impact. Scanning Electron Microscope (SEM) images of these samples were used to map out the damage done to the sample and to determine their respective particle size distributions. New tests were conducted on wet sand and dry sand of one particle fit using Split-Hopkinson Pressure Bar (SHPB) Technique. The particle size distribution of these sand samples were determined using the Coulter LS 100Q Particle Size Analyzer. SEM images of these samples were also taken to be studied.

Posttest analysis of the PBXN-109 showed that the particle size distribution was altered by the rod-on-rod impact. None of the largest RDX particles remained after the impact, while the number of smaller particles (0-100) increased. The study of the damage paths resulted in no definitive conclusions. The damage appeared to be random in some parts, while in other parts there appeared to be definite patterns. More studies on rod-on-rod impacted PBXN-109 specimens must be conducted in order to make an absolute statement on the presence of or lack of damage patterns. The analysis of the SHPB tested sand samples showed that the wet sand was damaged much less than the dry samples even though they were tested at much higher stress levels. Exactly how much less is still not known. There was no data on samples with binders to which the water data could be compared to quantify the effects of the water.

DAMAGE STUDIES ON INERTS AND EXPLOSIVES USING ROD-ON-ROD IMPACT AND SPLIT-HOPKINSON PRESSURE BAR TECHNIQUES

My V. Tran

Introduction

As a hard target penetrator passes through several feet of reinforced concrete, the explosive inside the penetrating vessel undergoes a great deal of damage due to the intense amounts of stress and strain. This damage may result in increased sensitivity or may even cause the explosive to detonate prematurely. This type of problem is one in which this study hopes to help solve. The purpose of this study is to develop a basic understanding of the behavior of explosives during an impact/penetration event by investigating the damage to explosive crystals. It is hopeful that predicting and designing explosives that can survive an impact will be made possible by doing this.

The Penetrator Explosives Survivability Protocol is a series of tests that develop equation of state data for explosives and determine whether an explosive can survive an impact. One of the main goals of this investigation is to collect enough data about explosives' behavior so that only a series of final verification tests are needed with the bulk of the analysis performed with computer modeling to determine the impact survivability of large families of explosives. Other goals of this study include determining three things: 1) how energy is transferred from an inert matrix to imbedded explosive crystals, 2) how the inert matrix behaves during an impact, and 3) how much of an effect the inert matrix has on the amount of damage done to the explosive crystals. This data will be collected through the analysis of PBXN-109, a plastic bonded explosive, specimen previously tested by rod-on-rod impact and by conducting new tests using the Split-Hopkinson Pressure Bar (SHPB). The SHPB tests will be conducted on sand (SiO_2), sand and water, sand and binder, 1, 3, 5- trinitro-1, 3, 5- triazocyclohexane (RDX), RDX and water, and PBXN-109 samples. Scanning Electron Microscope (SEM) and particle size analyzer will be used on these samples for post-test analysis.

RDX was chosen for this study because it is an explosive that is widely used and is also used in many explosive formulations, one of which is PBXN-109. PBXN-109 is composed of sixty-four percent RDX, twenty percent aluminum, and sixteen percent HTPB, a rubbery binder. SiO_2 was chosen because it is readily available, is safe to use, and is also morpholgically similar to RDX (see Figure 1). Thus, the way that sand behaves during an impact should be similar to the way that some explosives react. Figure 1(a) is of 100x sand, while figure 1(b) is of RDX at 100x.

(a)

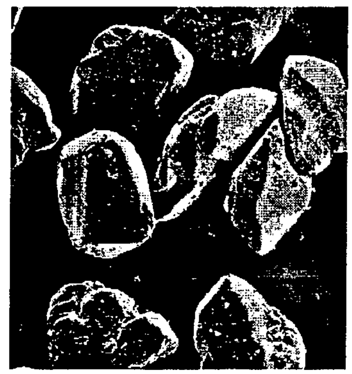

(b)

Figure 1

<u>Methodology</u>

Several PBXN-109 samples were previously tested by rod-on-rod impact. A rod-on-rod impact is where a stationary rod is struck by another rod of the same size shot at a very high velocity. The two damaged samples analyzed, CET-48 and CET-50, were shot at 85 m/s and 69 m/s, respectively. In order to study these specimens, Scanning Electron Microscope (SEM) images of the samples had to be taken. Before this could be done, however, the samples had to be cut at a certain distance from the impact point and wet sanded to provide a good surface to scan. The SEM images were then taken at one hundred times magnification (100x) and the individual images were taped together to form a collage of the sample. The collages of the two samples were visually analyzed and compared to SEM images of virgin RDX and undamaged PBXN-109. They were also used to determine the particle size distribution of the RDX particles in the sample and also to look for the presence of or lack of damage patterns.

Particle size distribution was determined by drawing a controlled number of random lines through SEM images of the same surface area. The particles that are intersected by these random lines are then manually measured (where the dimension is the largest) with a metric ruler. For this particular analysis, ten random lines were drawn on 10.5 in. x 6.5 in. portions of the SEM collages of CET-50 and the undamaged PBXN-109 samples.

To analyze for damage patterns, transparency films were placed over the SEM collages. The individual RDX particles were then mapped out by tracing the outline of the particles on these films. To make the analysis process easier, the damaged particles were distinguished from the undamaged ones by tracing them in different colors. The damaged particles were traced in red, while the undamaged particles were traced in blue. Also mapped out on these transparencies, by being colored in yellow, were the areas in the sample where the RDX had debonded from the polymer. These mappings were then visually analyzed for patterns.

The second major part of this study involved using the Split-Hopkinson Pressure Bar apparatus. The way that this test works is that a sample is placed in between two metal bars, the incident and transmitter bars, and a third metal bar, the striker, is fired and hits the incident bar (See Figure 2). This sends a stress wave through the bars and the sample, causing the sample to undergo a great deal strain.

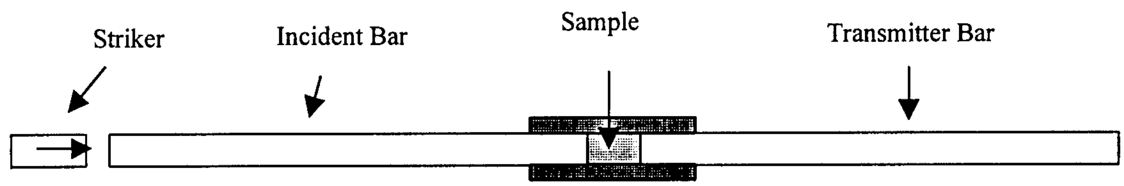

Figure 2

For the SHPB, it was intended that RDX and sand particles of only one particle fit (~200-300 micron) be used. This was planned to make quantifying crystal damage during post-test analysis a much easier process. In order to separate the sand particles into the ~200-300 micron range, a sieving apparatus had to be used. This device consists of a number of sieves, pans with wire mesh bottoms, stacked on top of one another, with the mesh size becoming progressively smaller going from top to bottom. The sample to be separated is placed into the top sieve; the stack of sieves is then vibrated. During this process, the particles are either retained on a given screen or pass through the mesh to be retained on a screen of a smaller mesh size. However, this was not the case with the samples sieved. The samples found to be between 210 and 297 microns were resieved in an attempt to verify the results from the initial sieving operation. It was discovered during this second sieving operation that the screens were becoming clogged with the sand particles and did not function as intended. Since the sieving operations were unsuccessful, sand that was guaranteed to be between 210 and 297 micron was purchased from Aldrich Chemical Company, Inc. and was used in the tests.

Some of this purchased sand was used to mix a PBXN-109 simulant. Also mixed was a sample of PBXN-109 consisting only of 210-297 micron RDX particles. Unfortunately, neither of the two mixtures could be used for testing due to bad solids packing. There were no small particles to fit in between the large particles; thus the samples were filled with many voids. As a result only shots on sand, sand and water, RDX, and RDX and water were carried out.

Before any shots could be performed, a holding device to contain the samples had to be designed and built. Since the samples to be tested were made up of smaller particles, a device had to hold these particles in place during the shots. This holding apparatus included a steel cylinder and two pistons, with both having O-rings. The sample would be placed in between the two pistons and all three of these would be centered in the steel cylinder (see Figure 3). The pistons are essentially extensions of the incident and transmitter bars. These pistons are needed to make loading easier and to hold the O-rings, which would prevent any water or crushed particles from spurting out of the sample cell.

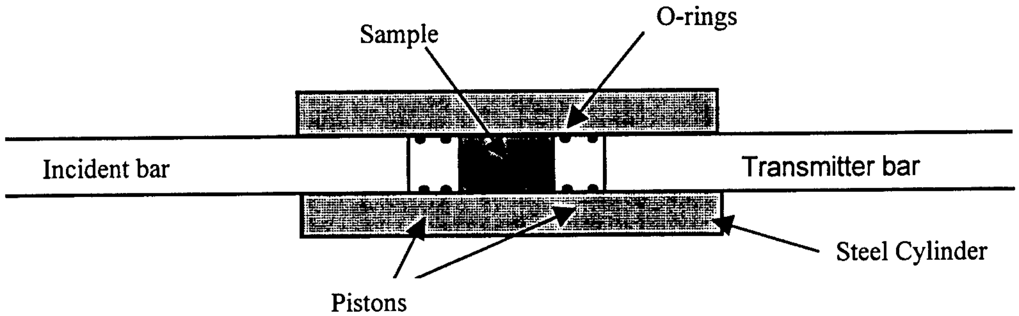

Figure 3

With the holding apparatus made, the tests could be conducted. However, due to a lack of time, only shots on the dry sand and wet sand could be taken. To take the shots, the sample had to be first loaded into the holding apparatus. The dry sand could be loaded just by placing a certain depth of sand in between the two pistons. Loading the wet samples, on the other hand, was a much more complicated process. Sand and water could not just be placed in between the two samples, for this would have left a large quantity of gas trapped in the sample. (The presence of gases has been found to alter the amount of damage to the particles.) Instead, the wet samples had to be loaded by a process called pluviation. The width of the sample cells was chosen to be 0.30 inch for all the shots. Thus, one of the pistons was placed in the steel cylinder 0.30 inch from one end. The cylinder was then submerged under water and placed next to a can of approximately the same height. This can was the stand upon which a plastic "density cup" of known internal volume was placed. Next, the sand was allowed to rain through the water and simultaneously into both the density cup and the holding apparatus. This was done by slowly pouring the sand into the water. After the cell was full, the sand was leveled off with a razor blade and the second piston was placed into the cylinder (with the sample now between the two pistons). Once the second piston was securely in place, the cylinder was taken out of the water and the pistons and sample centered in the cylinder. The sample was then ready to be placed into the SHPB to be tested. While waiting for the shot to be taken, the density cup was carefully taken out of the water. Its mass was then determined, and this along with its known volume was used to determine its density. The density of the sand in the density cup should be the same as that in the sample cell, since the two were loaded in the same way. Sand was pluviated to load all the wet shots.

There were a total of seven shots - three dries and four wets. The three dry shots were at drawback distances (of the striker) of 2, 3, and 4 inches. These distances equate to approximately 5000, 8000, and 11000 psi stress levels, respectively. The four wet shots were at 2 (~6000 psi), 4 (~16000 psi), and twice at a distance of 6 inches (~26000 psi and ~30000 psi). For posttest analysis, SEM images of these samples were taken and the particle size distribution of the samples was determined using the Coulter LS 100Q Particle Size Analyzer.

Results

Particle size distribution was determined for both undamaged and damaged PBXN-109 samples using the random lines method. The distribution for the damaged sample is very different from that of the undamaged. As seen in Figure 4, the damaged sample no longer had any of the 300+ micron particles. It also changed in that the percentage of particles ranging from 0 to 100 microns increased. Both the 0-50 range and the 51-100 range increased by approximately ten percent each. The graph shows that the larger particles were broken into the smaller particles. The lack of large particles is probably due to the fact that the original larger particles are more likely to come in contact with other large crystals. This means that the contact between crystals may be a reason why certain crystals fracture during an impact. This would in turn support the Crystal Lock-up Theory proposed by Dr. Joe Foster.

The study of SEM images of the damaged PBXN-109 samples showed that the damage to the sample was not uniform. Some areas seemed untouched, while every single crystal in another area was fractured. The mapping of the SEM images did indeed make damage analysis easier. However, no definite statement can yet be made. There were some damage paths discovered in the samples. These paths did not, however, continue throughout the sample. The damage seemed random in much of the sample.

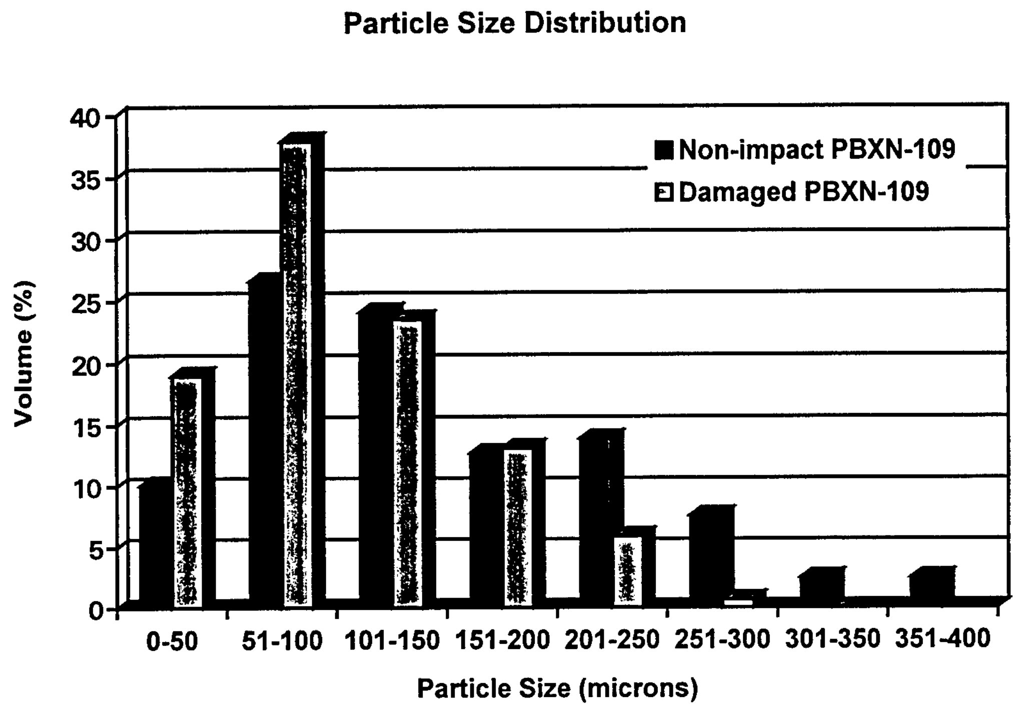

Figure 4

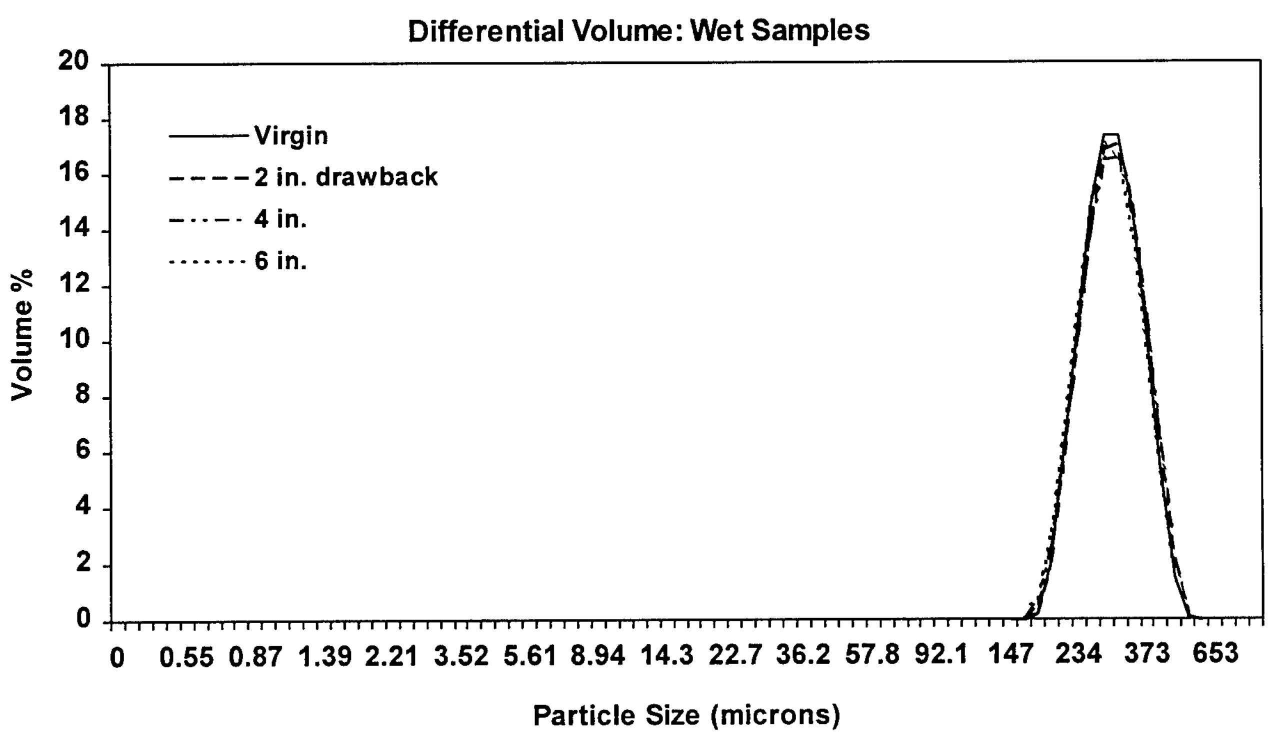

Figure 5

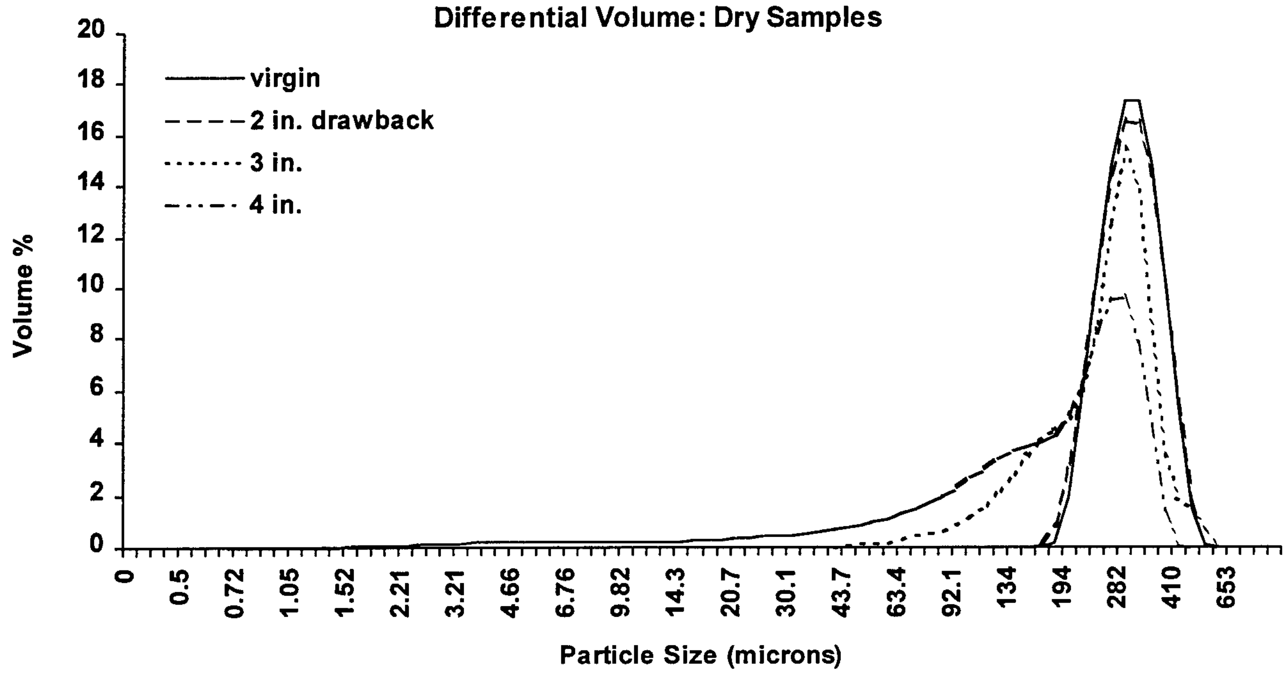

Figure 6

The data collected from the Split-Hopkinson Pressure Bar were as expected. The water significantly reduced the amount of damage. How much the damage was reduced by has not yet been quantified. None of the shots taken on the wet samples did much damage to the specimen. Not even at the highest stress level, approximately 30000 psi, was much damage done. The differential volume from all the samples seen in Figure 5 are fairly unchanged compared to the virgin sand data. By contrast, the dry shots underwent much more damage than the wet shots- at lower levels of stress. Even at a drawback distance of 2 in. (~ 5000 psi), the decrease in volume percent of 282 micron particles is noticeable (Figure 6). With every 3000 psi augmentation, the increase in damage is even more significant. The drawback distance of four inches was the highest level shot for the dry samples because even at that level the difference in the amount of damage was obvious. The dry sample was crushed into fines, while the wet sample (also shot at 4 in.) looked undamaged. This difference can also be seen by the SEM images in Figure 7. Figure 7(a) is of a wet sample shot at a drawback distance of 4 inches, while figure 7(b) is of a dry sample shot at the same distance. An increase to drawback of 6 inches would have been unnecessary. The sand would have been too fine to be analyzed effectively.

(a)

(b)

Figure 7

Conclusion

While not all of the goals originally set for this investigation were met, some interesting and useful information was gleaned from the experiments. The Split-Hopkinson Pressure Bar tests clearly showed that water, in this case acting as a binder for the sand, performed as a cushion during the impact event. It can be stated that the damage to the wet sand was insignificant, even at a drawback of 6 inches (30000 psi). The amount of damage to the dry sand, while not quantified into distinct volume percentages for each drawback distance, was shown to increase with increasing drawback distance. This finding suggests that a similar cushioning effect will be afforded to energetic particles imbedded in a rubbery matrix, e.g. the matrix (HTPB) found in PBXN_109 and many other military explosives. Similar test using PBXN-109 are not practical at this time, since there is no way to dissolve the HTPB away from the RDX component. Methods to accomplish this separation are being explored. If and when a separation method is found, experiments using RDX and binder will be accomplished. Plans to impact dry RDX and RDX/water are being defined at this time.

Damage was inflicted upon PBXN-109 during rod on rod experiments. The damage was found to be non-uniform in that there were no consistent damage patterns observed. This non-uniformity may have resulted from non-normal impact conditions. The RDX particle size analysis showed that a significant portion of the larger RDX particles was broken into smaller particles. The analysis suggested that the RDX particles in the impacted sample in the size range 0 to 150 microns increased from 60 to 81 volume percent and those in the 151 to 300 micron range decreased from 35 to 20 volume percent. There were no particles of RX counted that were of a particle size greater than 300 microns.

THE PROCESS OF TRAPPING CARBON AND BORON ATOMS IN AN ARGON MATRIX

Danielle D. Turner

Tehachapi High School
711 Anita Dr.
Tehachapi, CA 93561

Final Report for:
High School Apprenticeship Program
AFRL/Wright Laboratory

Sponsored by:
Air Force Office of Scientific Research
Bolling Air Force Base, DC

And

Wright Laboratory

August 1998

THE PROCESS OF TRAPPING CARBON AND BORON ATOMS IN AN ARGON MATRIX

Danielle D. Turner
Tehachapi High School

Abstract

Powder mixtures containing either carbon or boron carbide, were vaporized from a resistively heated tantalum cell at 2900K and co-condensed with argon onto a 10K barium fluoride window. The species trapped in the matrix were detected by Fourier Transform Infrared Spectroscopy (FTIR). The vibrational spectra of the carbon and boron species were then analyzed, which led to the identification of the trapped species. The sticking coefficient of argon that built up on the substrate window was found.

THE PROCESS OF TRAPPING CARBON AND BORON ATOMS IN AN ARGON MATRIX

Danielle D. Turner
Tehachapi High School

Introduction

The Air Force Research Laboratory/Propulsion Directorate has supported research and development of high energy density materials (HEDM) for the past decade. The main purpose of the HEDM program is to develop propellants that have higher densities and greater energy, which should "double or quadruple payloads" for the rockets and missiles of today [10]. The HEDM program seeks to develop revolutionary cryogenic propellant systems that can out perform the current state-of-the-art oxidizer/fuel system of liquid oxygen and liquid hydrogen. The target of this task is to produce and develop solid hydrogen doped with isolated energetic species. The improvements over using liquid hydrogen would be two things. First, an increased density over the liquid, and second, an added energy from these isolated species during combustion. Calculations of propellant systems using hydrogen and targeted energetic species have shown that they may improve the specific impulse (the thrust that can be obtained from an equivalent rocket which has a propellant weight flow rate unity [9]) by as much as 21%. Two of the best candidates of these target energetic species are carbon atoms and boron atoms. This is why they are the focus of this project.

Other efforts in the HEDM program have produced small samples of doped solid hydrogen with only a few tenths of a percent dopant concentration. This is far from the 2 to 5 percent of the dopant concentrations required. Part of the reason for this difficulty lies in the fact that solid hydrogen , or a hydrogen matrix, is a reactive medium. Rather than isolating the carbon or boron atom in the hydrogen matrix, it is more likely that they will react with the hydrogen to form hydro-carbon clusters or molecular species like CH or BH. Only a few exceptions, reactions and clustering detrimental to the energetic species are excluded.

However, this is not to say that the reaction products and clusters should not be ignored. With insight into reactions and clustering, suitable production methods can be designed. For this reason, argon was chosen as the matrix material rather than hydrogen in our experiment. Since argon is a non-reactive matrix host, it allows for all the attention to be focused on the interaction between the energetic species, itself, and not on the interaction between the species and their host. The issue of optimizing atomic concentrations of energetic species can be addressed and ideally, the same techniques developed from this work could be transferred to optimizing the atomic concentrations.

In this experiment (figure 2), carbon and boron species were produced by an effusive oven source. The cell was heated to 2900K producing a wide range of atomic and molecular species. These products were co-condensed with either an argon or an argon-hydrogen mixture onto a cold substrate. An FTIR spectrometer was used to determine the carbon and boron products that were released from the tantalum cell and trapped in the matrix. Interferometry was used to determine the thickness of the matrix.

Infrared spectroscopy was used in these experiments to detect the deposited species. The basic principle of IR spectroscopy is that the energies absorbed by these molecules are specific to the composition of atoms and bonds[7]. Therefore, characteristics of the molecules, like bond type and structure, can be determined from the IR spectra.

After the initial infrared spectrum was recorded, the matrix was annealed and the spectra were recorded again to see if any peaks grew, became smaller, or were formed. Hydrogen was used in some of the experiments because it is a good scavenger that helps to detect carbon atoms since carbon atoms cannot be found by infrared spectroscopy. This is because hydrogen bonds with carbon to form hydrogen-carbon bonds. To measure carbon atoms directly, a far ultraviolet light is needed to excite and detect them. Unfortunately, the ultraviolet system is not available due to lack of funding.

Experimental Procedure

A tantalum cell (figure 1), 1.00 in. long, 0.25 in. wide, with a 0.010 in. wall thickness, and 0.25 in. long solid caps on each end was filled with powder mixtures containing either carbon (Johnson Matthey, 99.9995% purity), or boron carbide (Alfa Aesar, 99+%). The cell containing carbon had a cylindrical graphite (carbon-12) liner (Poco Graphite, CZR-1) with a 0.020 in. wall thickness and a 0.030 in. diameter hole in the middle which was aligned with a similar hole in the tantalum cell. The cell is suspended between copper electrodes, which are water cooled, and then placed into a vacuum chamber, whose walls are also water cooled. A transformer was used to send a current through the electrodes to resistively heat the tantalum cell to a temperature of 2900K.

Approximately 5 Torr of argon or a 90% argon and 10% hydrogen mixture, which was flowing at a rate of 0.4 Torr per minute from a gas manifold that contained approximately 800 Torr, was deposited onto a barium fluoride substrate, which is suspended on a cold head maintained at 10K by a closed cycle helium cryostat. A reading by an interferometry apparatus was used to determine the thickness of the matrix. A helium/neon (He/Ne) laser was directed towards the matrix at 90° and reflected from the argon or the Ar/H_2 mixture that was building up on the substrate. A photodiode was used to detect the intensity of the reflected laser. A reference diode was used to detect the initial intensity of the laser just in case any accidental movements of the laser occurred. Then, the gate valve between the cryostat and the furnace was opened, allowing carbon and/or boron vapors to effuse through the hole in the cell, to co-condense with argon onto the barium fluoride substrate in the cryostat. Next, an FTIR spectrometer (Mattson Cygnus® 100 model IR - 10111) was used to determine the products of the matrix. The data was transmitted to a computer connected to the FTIR spectrometer. After the initial recording, this procedure was done a couple more times. The cryostat was warmed up for a brief amount of time around 32K, and was then cooled to 10K. Then another scan was taken to determine if there were any new products that developed on the substrate. This was done another time, but this time the temperature was increased to 32K for about a minute, and then cooled again. Infrared scans were taken again. If the cryostat were to be heated above 35K, then the whole matrix would evaporate.

The data was analyzed to determine the various carbon and/or boron species that developed during each scan. The position and area of every peak was measured. The position of the peak determines the type of specie that was developed.

Results and Discussion

The sticking coefficient of argon was calculated to find out how much of the argon that was let into the cryostat chamber stuck to the substrate. Typically, the sticking coefficient is defined as the number of molecules that stick to the surface divided by the number of molecules that collide with the surface [1]. For ease of calculations, we assume that all of the argon that is let into the cryostat has a chance of hitting the substrate. The calculations we used are as follows:

First, the volume of the flask on the gas chamber needed to be found with this equation derived from the ideal gas law:

$P_1V_1 = P_2V_2$ P= pressure, V= volume

P_1V_1 = pressure and volume of manifold with flask closed

P_2V_2 = pressure and volume of manifold with flask open

* The volume of the manifold was known.

* Solved for the volume of the flask; V_2

Then, the number of moles of argon that went into the chamber was found with this equation:

$\Delta PV = n_1RT$ $\Delta P = | P_1 - P_2 |$ P_1 = argon pressure in the gas cart at the beginning of the experiment. P_2= argon pressure in the gas cart at the end of the experiment; V = volume of manifold with flask open; R = gas constant (0.08206 Latm/Kmol); T = 298K; n_1 = number of moles of argon in the manifold.

Next, the thickness of the argon was found. It works by this: A red light (632nm) was aimed at the matrix at 90°. The light traveled through the substrate to the argon, and then came back out as a refracted beam. The incident beam either reflected off of the glass, or passed through and reflected off the argon matrix. The refracted beams interfered either constructively or destructively [1]. The intensity of this reflected light was detected by a photodiode and recorded with a computer and displayed as fringes (figures 3 and 4).

The equation used for the thickness of the argon buildup is:

$n(2d)\sin\theta = m\lambda$ n = index of refraction for solid argon (1.29); d = thickness of deposited argon; $\sin\theta = 1$ (laser hit substrate at 90°); λ= 632nm (He/Ne); m = number of maxima or fringes

* Solve for d.

* This found the total thickness of the argon matrix.

Then, the total volume of the deposited argon was found with this equation:

$V = d_{total}(\pi r^2)$ V = volume of the deposited argon;

d_{total} = the total thickness from the equation above; r = radius of the substrate

The next equation that was used was to determine the amount of argon, in moles, that was deposited on the substrate. The equation is:

$n_2 = (V\rho)/m$ n_2 = moles of deposited argon on the substrate;

V = volume of deposited argon; ρ = density of argon; m = molecular weight of argon

We assumed that the argon matrices were evenly distributed and homogenous.

Finally, the moles of deposited argon on the substrate were divided by the moles of argon from the manifold that were allowed into the cryostat chamber. The result was the sticking coefficient of argon. The same procedures were also used for hydrogen-argon matrices.

Here is an example of the various sticking coefficients that were found:

Table 1

Experiment #	Flow rate	Experimental Conditions	Sticking Coefficients (Unitless number)
Experiment 1	0.41 Torr/minute	Pure argon matrix	0.60
Experiment 2	0.44 Torr/minute	Pure argon matrix	0.42
Experiment 3	0.43 Torr/minute	90% argon, 10% hydrogen matrix	0.60
Experiment 4	0.40 Torr/minute	Pure argon matrix	0.60
Experiment 5	0.32 Torr/minute	Pure argon matrix	0.26
Experiment 6	0.40 Torr/minute	90% argon, 10% hydrogen matrix	0.53

Experiment 2 and experiment 5 may have had a low sticking coefficient for the following reasons: the fringes may have been a little difficult to read due to the spectra being noisy, or the infrared laser may have been misaligned. There is also a possibility that a slower flow rate may have had a negative effect on the sticking coefficient, as seen in experiment 8 on Table 1. Since only one experiment was done with that flow rate, more experiments are needed to verify this.

One experiment was tried with boron carbide, instead of carbon, in an argon matrix. Boron carbide was tried because boron is also a promising additive to make a higher Isp propellant. Unfortunately, the boron in the cell deteriorated the tantalum, causing the cell to break during the process of heating it up. A carbon liner was not used in this experiment because we were trying to get pure boron atoms. We didn't want the carbon liner to interfere with the results. However, a carbon liner may have prevented the boron from deteriorating the cell. This is a good experiment to try again in the future.

Throughout experiments 1-6, many species were observed by infrared spectroscopy. Some of the signals or peaks in the infrared spectra were identified as C_3 through C_{12}, and cyclic C_6 by comparison to other publishings on infrared spectra. There were also many other signals that were weaker or that remain unidentified (figures 5, 6 and 7). In an argon matrix, some of the clusters like C_3 will bond with other clusters and atoms to form larger clusters like C_6 or C_7. When hydrogen is mixed with argon, new peaks are formed that aren't seen in the pure argon spectra. These peaks are formed around these wavenumbers 3325, 3287, 3257, 3244, and 3239 cm^{-1} and are attributed to carbon-hydrogen bonds. In the hydrogen-argon spectra, the signal attributed to C_5 is smaller, indicating fewer C_5 molecules. This molecule is located around 2164 cm^{-1}. (figure 6) This is all normalized to the highest peak, C_9, which is around 1997 cm^{-1}. Similar intensities were noticed with C3, C6, and C9 in all of the matrices. Smaller peaks for C_4, C_7, C_8, C_{10}, and C_{11} were noticed when hydrogen was used showing that hydrogen takes away some of the atoms out of the matrix.

Conclusions

It has come to conclusion that hydrogen doesn't have any effect on the sticking coefficient of argon. Slower flow rates might have an effect on the sticking coefficient of argon, but more experiments need to be tried. Hydrogen combines with carbon to form new species detected by infrared spectroscopy. Boron carbide, without a carbon liner, destroys the tantalum cell when heated up. For future work, a carbon liner, when working with boron carbide, might aid the boron carbide from destroying the tantalum cell.

References

1. Atkins, P. W., Physical Chemistry, 2nd edition (W. H. Freeman and Company, NY, 1978) pp. 723, 1021.
2. Carrick, Patrick G., "Theoretical Performance of Atomic and Molecular HEDM Additives to Solid H_2," Proceedings of the High Energy Density Matter (HEDM) Contractors Conference, (Woods Hole, MA, June 1993).
3. Carrick, P. G., Personal Correspondence, 3 August 1998.
4. Freivogel, Patrick, Grutter, Michel, Forney, Daniel, Maier, John P., "Infrared Bands of Mass-selected Carbon Chains C_n (n=8-12) and C_n^- (n=5-10, 12) in Neon Matrices, Chemical Physics Vol. 216 (1997) 401-406.
5. Harper, Jessica, Personal Interview, July 1998.
6. Martin, Jan, M. L., "The Vibrational Spectra of Corannulene and Coronene. A Density Functional Study," Chemical Physics Letters, Vol. 262, (1996) 97-104.
7. Presilla-Màrquez, J.D., Larson, C.W., Carrick, P.G., "Fourier Transform Infrared Spectroscopy of the V_2 Vibration of BC_2 in Ar at 10 K," J. Chem. Phys., Vol. 105, No. 9, 1 September 1996.
8. Streitwieser, Andrew, Heathcock, Clayton H., Introduction to Organic Chemistry, 3rd edition (Macmillan Publishing Co., NY, 1985)
9. Sutton, George P., Rocket Propulsion Elements, 3rd edition (Wiley, NY, 1963).
10. Thompson, T. L., Proceedings of the High Energy Density Matter (HEDM) Contractors Conference, (Woods Hole, MA, June 1993).

Figure 1

Tantalum tube with end caps

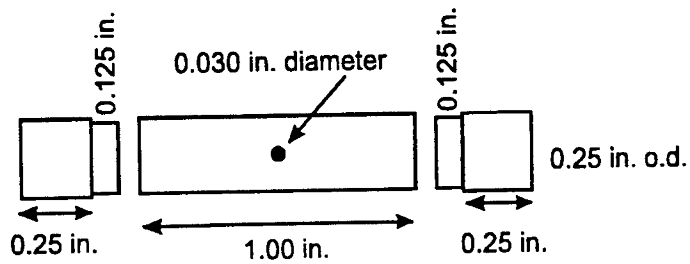

0.010 in. wall thickness of Ta tube; solid end caps

Graphite (Carbon-12) liner

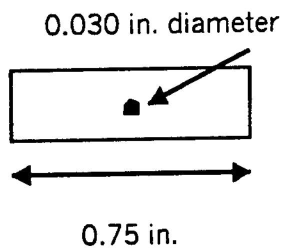

0.020 in. wall thickness of graphite liner

figures not drawn to scale

Figure 2

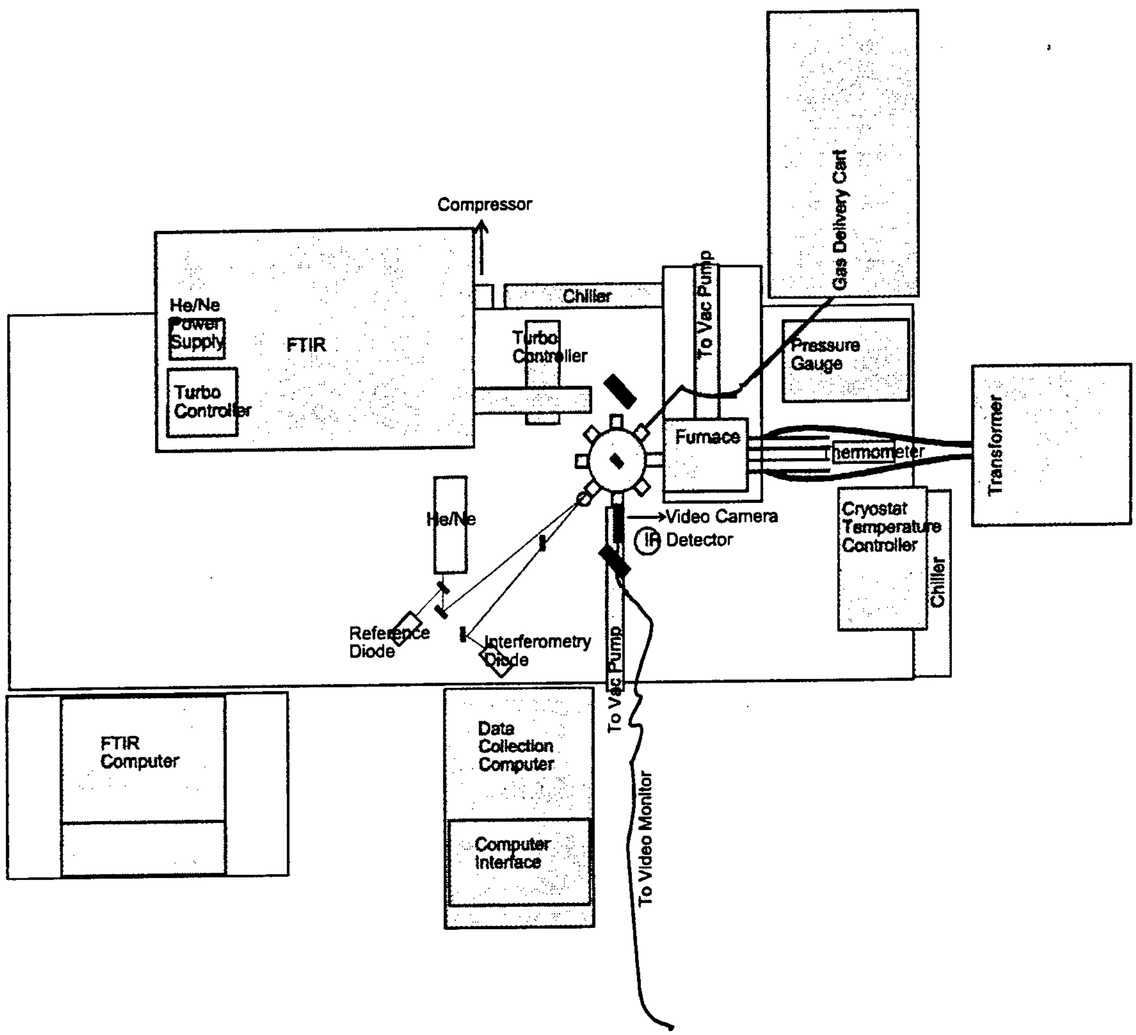

Not drawn to scale

Laboratory Setup

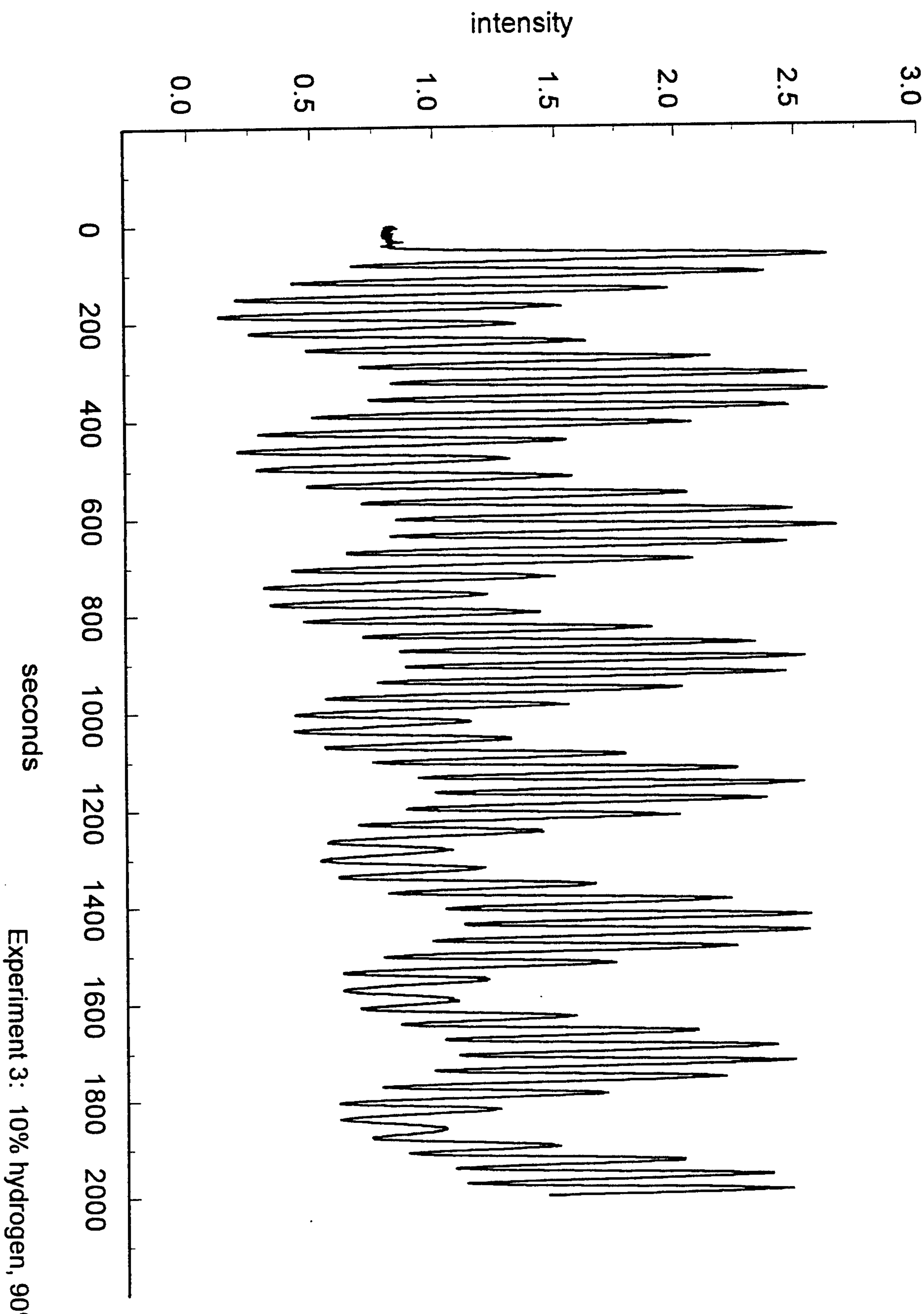

Figure 3

Experiment 3: 10% hydrogen, 90% argon

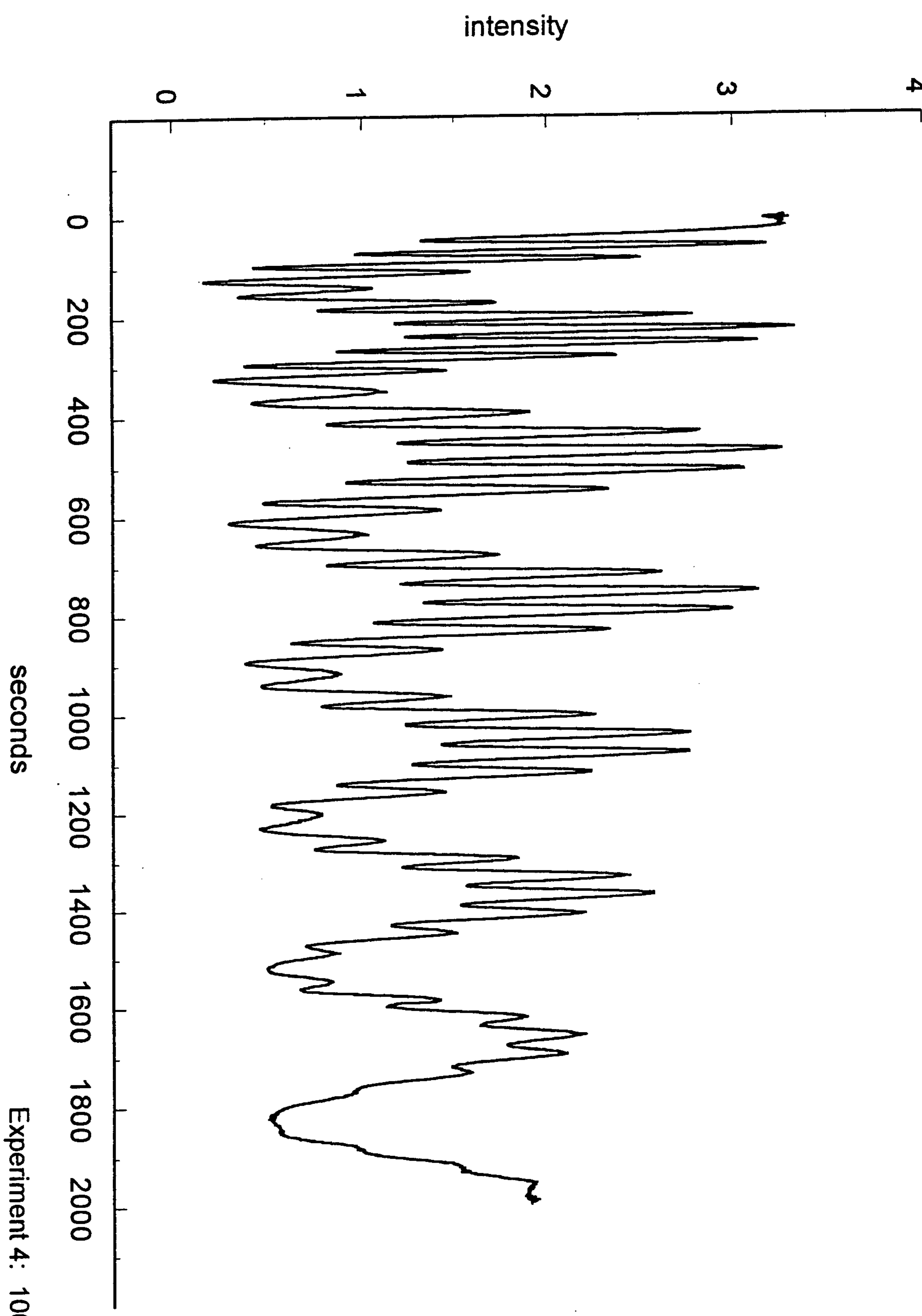

Figure 4

Experiment 4: 100% argon

Figure 5

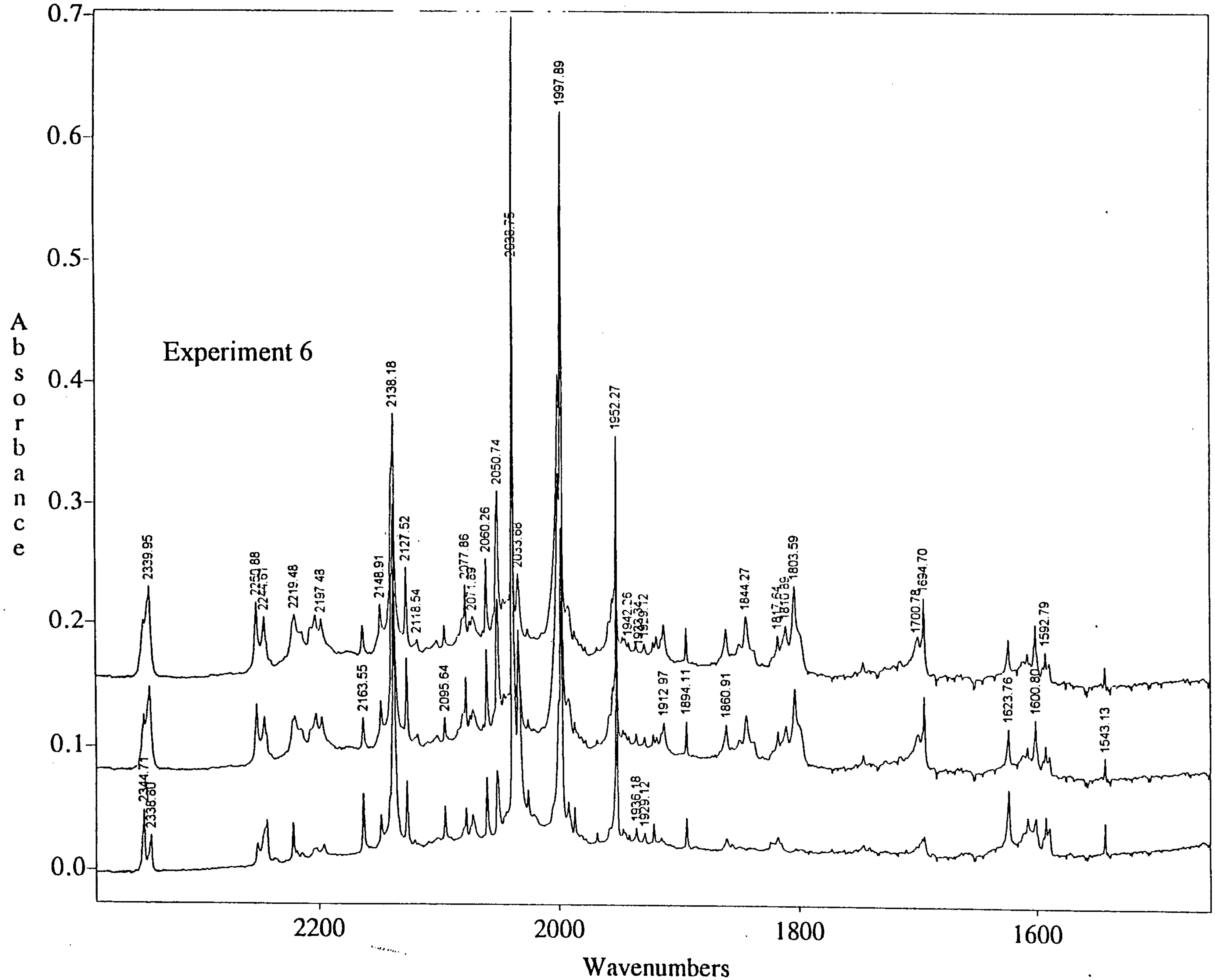
Experiment 6
Absorbance
Wavenumbers
0.0
0.1
0.2
0.3
0.4
0.5
0.6
0.7
2200
2000
1800
1600
2339.95
2344.71
2219.48
2197.43
2163.55
2148.91
2138.18
2127.52
2118.54
2095.64
2060.26
2050.74
1997.89
1952.27
1929.12
1936.18
1912.97
1894.11
1860.91
1844.27
1803.59
1700.78
1694.70
1623.76
1600.80
1592.79
1543.13

Figure 6

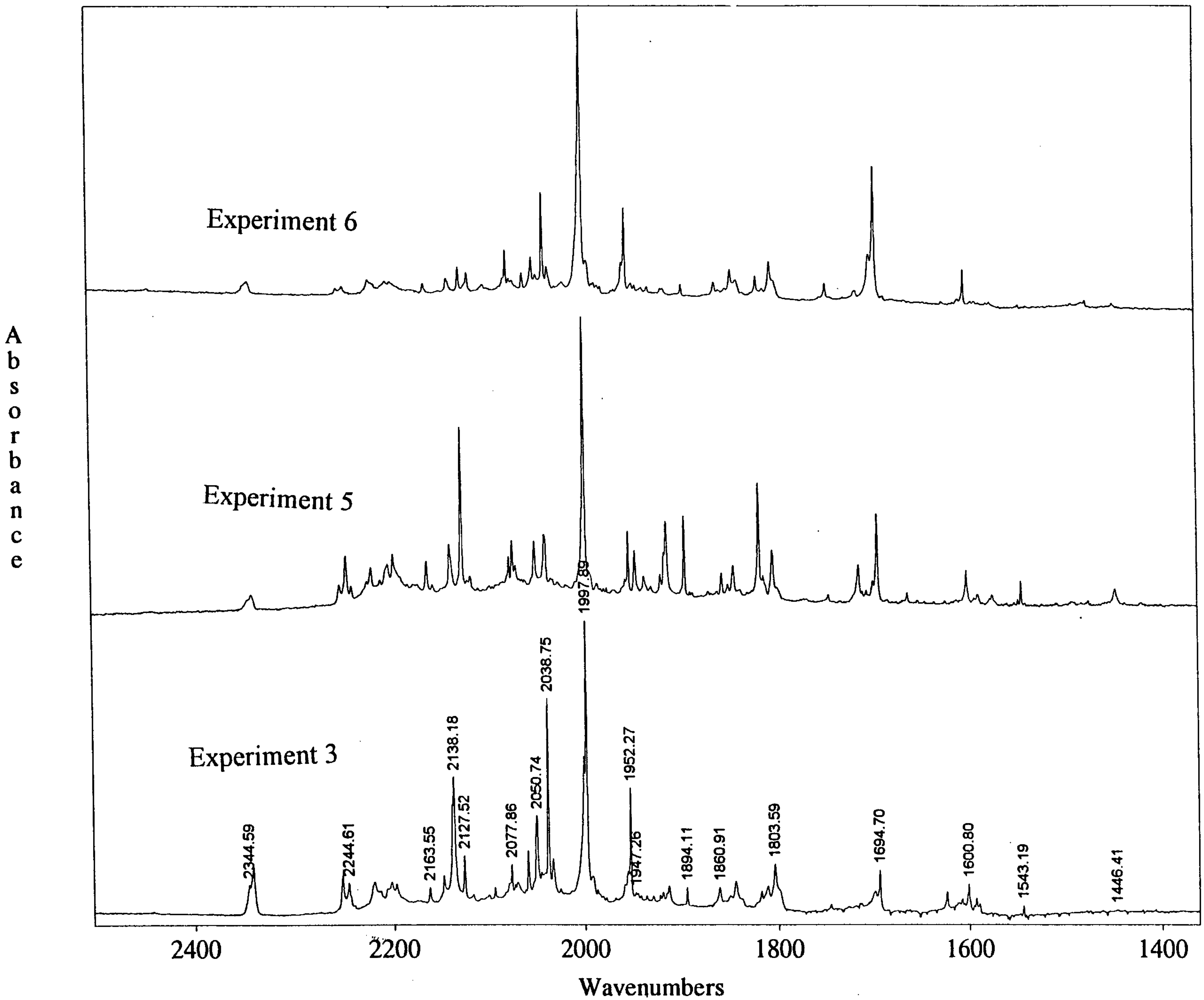
Absorbance
Experiment 6
Experiment 5
Experiment 3
2344.59
2244.61
2163.55
2138.18
2127.52
2077.86
2050.74
2038.75
1997.89
1952.27
1947.26
1894.11
1860.91
1803.59
1694.70
1600.80
1543.19
1446.41
2400
2200
2000
1800
1600
1400
Wavenumbers

Figure 7

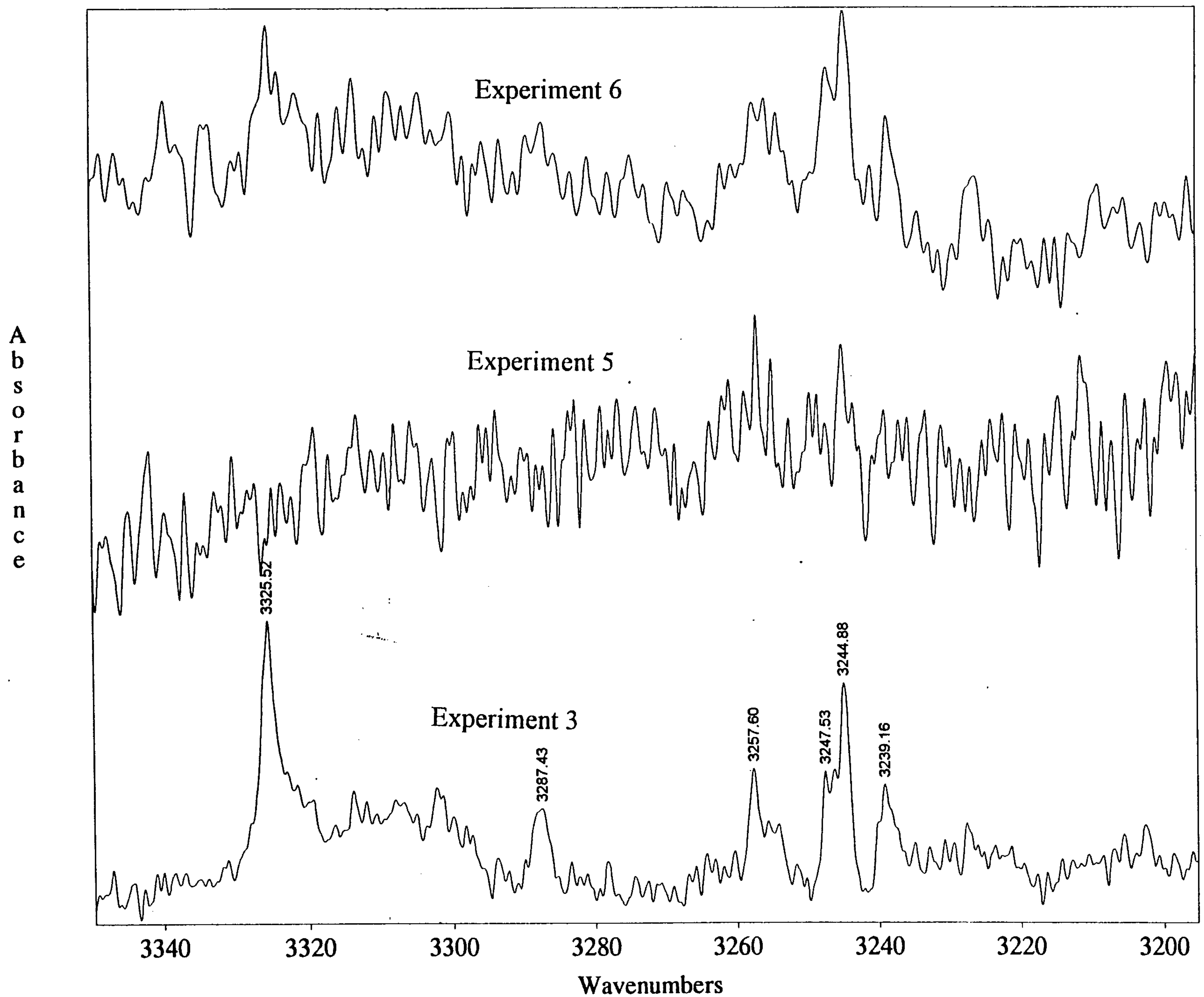
Experiment 6
Experiment 5
Experiment 3
3325.52
3287.43
3257.60
3247.53
3244.88
3239.16
Absorbance
3340
3320
3300
3280
3260
3240
3220
3200
Wavenumbers

Figure 8

Table 1
Measured vibrational frequencies (in cm^{-1}) for linear carbon molecules in the gas phase and rare gas matrices

Species	Mode	Ar-matrix	Ne-matrix	Gas phase
$C_3\ (X\ ^1\Sigma_g^+)$	$\nu_1\ (\sigma_g^+)$	1214.0 [19]	1226 [1]	1224.5 [20]
	$\nu_2\ (\pi_u)$	83 [3]	75 [3]	63.42 [21]
	$\nu_3\ (\sigma_u^+)$	2038.9 [19,22]	2036.4 [3]	2040.02 [23]
$C_4\ (X\ ^3\Sigma_g^-)$	$\nu_1\ (\sigma_g^+)$			2032(50) [8]
	$\nu_3\ (\sigma_u^+)$	1543.4 [24]	1547.2 [3]	1548.94 [25]
	$\nu_4\ (\pi_g)$			352(15) [26]
				339(55) [8]
	$\nu_5\ (\pi_u)$	172.4 [27]		160(4) [28]
$C_5\ (X\ ^1\Sigma_g^+)$	$\nu_2\ (\sigma_g^+)$			779(10) [9]
	$\nu_3\ (\sigma_u^+)$	2164.3 [29,30]	2166.4 [3]	2169.44 [31,32]
	$\nu_4\ (\sigma_u^+)$	1446.6 [30]	1444.3 [3]	
	$\nu_5\ (\pi_g)$			218(13) [33]
				216(10) [9]
	$\nu_6\ (\pi_u)$			535(10) [9]
	$\nu_7\ (\pi_u)$			118(3) [33]
				106(10) [9]
$C_6\ (X\ ^3\Sigma_g^-)$	$\nu_1\ (\sigma_g^+)$			2061(10) [10]
	$\nu_2\ (\sigma_g^+)$			1322(10) [10]
	$\nu_3\ (\sigma_g^+)$			489(10) [10]
	$\nu_4\ (\sigma_u^+)$	1952.5 [34]	1958.7 [3]	1959.86 [5]
	$\nu_5\ (\sigma_u^+)$	1197.3 [34]	1199.4 [3]	
$C_7\ (X\ ^1\Sigma_g^+)$	$\nu_3\ (\sigma_g^+)$			548(90) [8]
	$\nu_4\ (\sigma_u^+)$	2127.8 [2]	2134.6 [3]	2138.32 [35]
	$\nu_5\ (\sigma_u^+)$	1894.3 [2]	1897.5 [3]	1898.38 [35]
	$\nu_7\ (\pi_g)$			496(110) [8]
$C_8\ (X\ ^3\Sigma_g^-)$	$\nu_4\ (\sigma_g^+)$			≈ 565 [8]
	$\nu_5\ (\sigma_u^+)$	2063.9 [a]	2067.8 [b] [17]	
	$\nu_6\ (\sigma_u^+)$	1705.6 [a]	1707.4 [b] [36]	
$C_9\ (X\ ^1\Sigma_g^+)$	$\nu_3\ (\sigma_g^+)$			1258(50) [8]
	$\nu_4\ (\sigma_g^+)$			484(48) [8]
	$\nu_5\ (\sigma_u^+)$	2077.9 [a]	2081.1 [b] [36]	2079.67 [6]
	$\nu_6\ (\sigma_u^+)$	1998.0 [37,38]	2010.0 [3]	2014.28 [39]
	$\nu_7\ (\sigma_u^+)$	1601.0 [40]		
	$\nu_{15}\ (\pi_u)$			30(20) [39]
$C_{10}\ (X\ ^3\Sigma_g^-)$	(σ_u^+)		2074.5 [b]	
	(σ_u^+)		1915.4 [b]	
$C_{11}\ (X\ ^1\Sigma_g^+)$	$\nu_5\ (\sigma_g^+)$			≈ 440 [8]
	$\nu_7\ (\sigma_u^+)$		1938.6 [b]	
	$\nu_8\ (\sigma_u^+)$		1853.4 [b]	
$C_{12}\ (X\ ^3\Sigma_g^-)$	(σ_u^+)		2003.9 [b,c]	
$C_{13}\ (X\ ^1\Sigma_g^-)$	(σ_u^+)			1808.96 [7]

A STUDY OF THE INFLUENCE OF CERAMIC PARTICLES ON THE AGING BEHAVIOR OF ALUMINUM ALLOYS

Donald S. Weaver

Centerville High School
500 East Franklin Street
Centerville, OH 45458

Final Report for:
High School Apprentice Program
Wright Laboratory

Sponsored by:
Air Force Office of Scientific Research
Bolling Air Force Base, DC

and

Wright Laboratory

August 1998

A STUDY OF THE INFLUENCE OF PARTICLE REINFORCEMENT ON THE AGING BEHAVIOR OF ALUMINUM ALLOYS

Donald S. Weaver
Centerville High School

Abstract

The aging behavior exhibited by two similar aluminum alloys was studied. The first of the two alloys was the unreinforced Aluminum 7093 alloy. The second was the Discontinuously Reinforced Aluminum (DRA) sample, which is 15 vol.% SiCp/7093 DRA. Approximately 30 samples of each alloy were obtained and after being solutionized were heat treated at three different temperatures for multiple time spans. The samples were prepared and both Micro Hardness testing and Macro Hardness testing were done to investigate and document the differences between the matrix microstructures of the different stages in aging of both the unreinforced and DRA alloy. The original concept was that the aging curve for the DRA alloy would be much higher (stronger) in the beginning than the unreinforced alloy but then would reach a certain height ("peak age") and then would become increasingly lower (weaker) over time than the unreinforced alloy. Due to circumstances beyond our control we were unable to either prove or disprove this concept.

A STUDY OF THE INFLUENCE OF PARTICLE REINFORCEMENT ON THE AGING BEHAVIOR OF ALUMINUM ALLOYS

Donald S. Weaver

Introduction

In recent years, it has become apparent that reinforcing a normal metal alloy with a material such as SiC particles improves both the strength and stiffness of the alloy. However, adding this new material also changes the microstructure of the original alloy and thus many of its original properties. These changes are relatively unexplored in the 7xxx series alloys and are important in developing a fundamental understanding of the matrix response under loading or other such tests. One aspect our group was particularly interested in the change in strength (hardness) between the unreinforced Aluminum 7093 alloy and the DRA alloy with SiC particles.

Heat treating a metal has been used for many years to increase the strength of metals. Generally the aging curve follows the same path as shown in Figure 1. The material represented by the aging curve to the left is the reinforced alloy. It reaches its peak age sooner than the unreinforced alloy to the right. This comes into effect when trying to save time and energy while still trying to improve the strength of the alloy through heat treatment. The downside to the reinforced alloy is that although it does get stronger more quickly it also reaches peak age sooner and then becomes overaged and brittle whereas the unreinforced alloy does not have that tendency.

Figure1 Typical Aging Curves of Metals

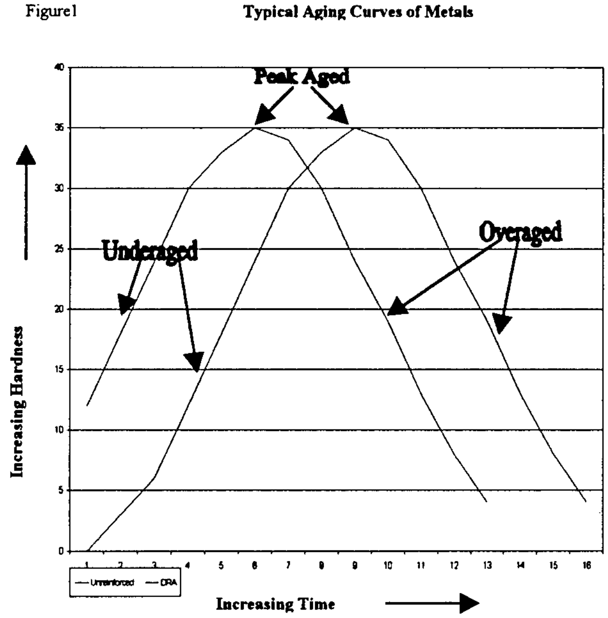

Research in the area of the 7xxx metals and alloys has not been extensively done and thus the point of this project was established: to measure and document the changes and differences between the aging behaviors of an unreinforced aluminum alloy and the same aluminum alloy reinforced with SiC particles.

Methodology

The whole process began by obtaining billets of the unreinforced and the DRA alloys and then extruding them to produce an even cylindrical specimen. From the metal rods fifteen pieces were cut off and subsequently cut in half to produce a total of thirty half-cylindrical samples of each alloy. After this the samples were taken to the Metalography Lab and the oxidation and other such material left over from the extrusion process was removed by hand from each of the sixty samples using 240 and 600 grit sandpaper on a grinding wheel. This was done to help eliminate causes of error in our later test results.

The next major step was the initial heat treatments. All sixty of the samples were solutionized and then water quenched before any heat treatments were performed. Solutionizing occurred at 490°C for 4 hours. This process causes all of the non-Al and non-Al with SiC particles and precipitates that were present in the alloy to come out. Water quenching the samples cooled them off rapidly to keep the precipitates from reforming in the alloy. After this was completed, the samples had to be stored in a freezer in order to keep the precipitates from reforming. The samples could not be left out of the freezer for very long because the alloy used in this experiment ages at room temperature, and that would introduce a great amount of error into the results.

Three sets of heat treatments were carried out. The first set was carried out at 100°C for each of the following times (all in seconds): 1500; 10,000; 20,000; 40,000; 55,000; 70,000; 86,400; 100,000; and 1,000,000 seconds. These times range from a little under half an hour to over 278 hours. Also, a sample of each alloy was kept as-solutionized (Zero time) for later reference. These times were chosen because they represent a wide span of the aging curve of the metal; there is a clearly underaged sample (No time), a close to peak aged sample (24 hours), and a clearly overaged sample (278 hours). The second set of heat treatments was carried out on nine different solutionized samples of each alloy for the same amounts of time, but at 120°C. The same is true for the third set, which followed the same times but took place at 140°C.

After the heat treatments were completed, the samples were frozen in the freezer in individually marked bags to keep them straight. The samples were then taken back to the Metalography Lab where they were mounted in a type of acrylic epoxy so as to expose them to heat and thus aging using the other traditional methods of mounting like hot-mounting. The acrylic epoxy sets in thirty minutes at room temperature so the error introduced to the results at this stage from exposure to heat was minimized as much as it could be. After the epoxy cured the samples were labeled and put back into their respective bags in the freezer.

The samples were then taken out of the freezer and mounted in an automatic polishing machine. They were sanded using 600-grit paper, and then a #8 Metlap was used with 15 through 3-Micron black diamond slurry. The samples were then either polished on the machine using microcloth and 1 Micron diamond slurry or by hand on an 8-inch wheel using many final polishing methods as recommended to us. After the samples had been final polished, it was decided that due to time constraints there was only time to look at six of the fifty-six samples using the SEM. The six samples to be looked were all from the 120 °C sample set: the two as-solutionized samples (no time), the two twenty four hour samples (peak aged), and the two 277 hour samples (overaged). The instructions we received to prep the samples for the SEM stated we had to clean the mounts, bake them out, and coat them in Carbon or Au-Pd to make them conductive. The only problem was that we could not bake the samples out to clean them off. Baking them for the time and at the temperature described would terribly skew the final results, so we investigated other methods of SEM preparation. We found out that our samples would be okay without baking them out if we put them through a special vacuum process that basically sucked the stuff out instead of heating it off. We knew this wouldn't be such a cause of alteration for the results so we decided to use this method.

We began the process by ultrasonically cleaning the mounts for 10 minutes in a beaker of 2-propanol (Isopropyl Alcohol). The dirty alcohol was replaced and the process was repeated. The samples were then placed into the vacuum machine and left to be cleaned for a while. After inspecting the samples to make sure they were clean enough, we discovered a residue on the sample. We cleaned the samples again using the alcohol and still no change. It was then that we realized that the material that was recommended for us to use was dissolving in the alcohol used to clean it. We found out that the material used dissolves slowly in the type of alcohol we used, but would have dissolved much faster if we had used a much stronger alcohol like acetone. The mounts we used were no longer any good for those samples so we tried to dissolve them out of the mounting material using acetone but that went very slow so I brought in my Dremel tool with a cutoff wheel and cut them out. We were told that the samples could be put into the SEM without being in a specific mount so we cleaned and repolished those samples by hand and were able to look at them using the SEM. Until the time that they were to be viewed, they needed to be kept in a dessicator that could be kept in a refrigerator. We ended up making our own dessicator out of a Mason jar and dessicator pellets. It was not necessary to keep the samples under vacuum.

After the samples were examined for microstructure differences using the SEM both the SEM samples and all of the 120 °C samples were tested for hardness. Micro Hardness testing, using the Vickers method, and Macro Hardness testing, using the Rockwell B method, was completed on all of the samples. The data was recorded and graphed and theories were made about the alloys.

Results

The results of our experiment were a great surprise to us. We (as well as our mentors) expected a more bell shaped curve, with the first samples of both being weaker and eventually getting stronger, only then to reach a peak age and begin to get more brittle and weak.

Our Macro Hardness Testing results showed quite the contrary, with the earliest times being the strongest and later times being weaker (see table below and graph on next page).

Sample #	Temp (C)	Time (sec)	Type	Test 1	Test 2	Test 3	Avg.
11	0	0	Al 7093 w/ SiC	79	77	75	77.000
21	120	1500	Al 7093 w/ SiC	74	73	73	73.333
22	120	10000	Al 7093 w/ SiC	65	52	57	58.000
23	120	20000	Al 7093 w/ SiC	60	62	52	58.000
24	120	40000	Al 7093 w/ SiC	58	57	57	57.333
25	120	55000	Al 7093 w/ SiC	49	39	50	46.000
26	120	70000	Al 7093 w/ SiC	46	45	47	46.000
27	120	86400	Al 7093 w/ SiC	42	44	43	43.000
28	120	100000	Al 7093 w/ SiC	49	47	47	47.667
29	120	1000000	Al 7093 w/ SiC	27	24	25	25.333
1	0	0	Al 7093	84	85	85	84.667
30	120	1500	Al 7093	73	73	76	74.000
31	120	10000	Al 7093	62	50	63	58.333
32	120	20000	Al 7093	43	45	37	41.667
33	120	40000	Al 7093	64	52	54	56.667
34	120	55000	Al 7093	59	58	53	56.667
35	120	70000	Al 7093	30	27	27	28.000
36	120	86400	Al 7093	24	25	26	25.000
37	120	100000	Al 7093	34	32	28	31.333
38	120	1000000	Al 7093	24	24	27	25.000

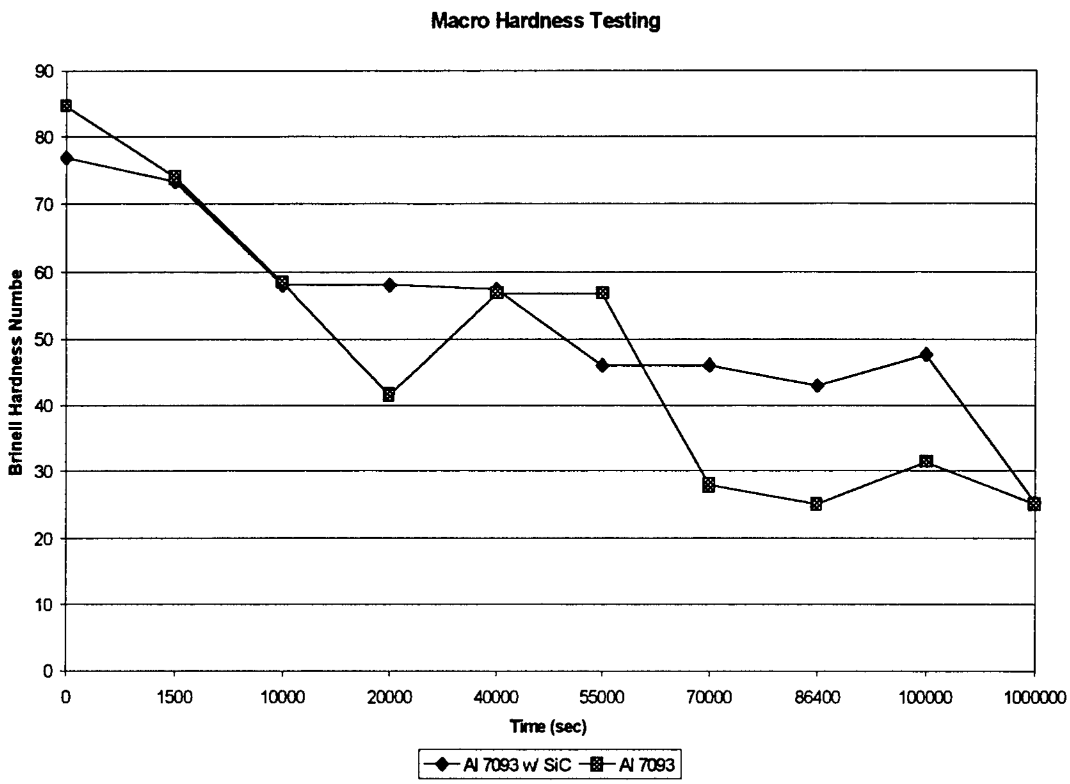

As the graph clearly shows, there is no gradual bell shape to the curve—it all goes one way.

Our Micro Hardness testing showed the same results. Instead of the curve we got a steady deterioration of strength (see table below and graph on next page).

Sample #	Temp (C)	Time (sec)	Type	S.D.	Avg.
11	0	0	Al 7093 w/ SiC	11.00	152.60
21	120	1500	Al 7093 w/ SiC	3.50	111.60
22	120	10000	Al 7093 w/ SiC	6.80	110.70
23	120	20000	Al 7093 w/ SiC	7.00	85.70
24	120	40000	Al 7093 w/ SiC	6.10	83.90
25	120	55000	Al 7093 w/ SiC	4.00	85.00
26	120	70000	Al 7093 w/ SiC	9.80	100.80
27	120	86400	Al 7093 w/ SiC	4.10	92.60
28	120	100000	Al 7093 w/ SiC	2.60	83.20
29	120	1000000	Al 7093 w/ SiC	4.70	77.90
1	0	0	Al 7093	11.00	126.80
30	120	1500	Al 7093	3.50	110.10
31	120	10000	Al 7093	6.80	105.20
32	120	20000	Al 7093	7.00	97.90
33	120	40000	Al 7093	6.10	79.40
34	120	55000	Al 7093	4.00	94.90
35	120	70000	Al 7093	9.80	98.00
36	120	86400	Al 7093	4.10	100.30
37	120	100000	Al 7093	2.60	93.60
38	120	1000000	Al 7093	4.70	64.60

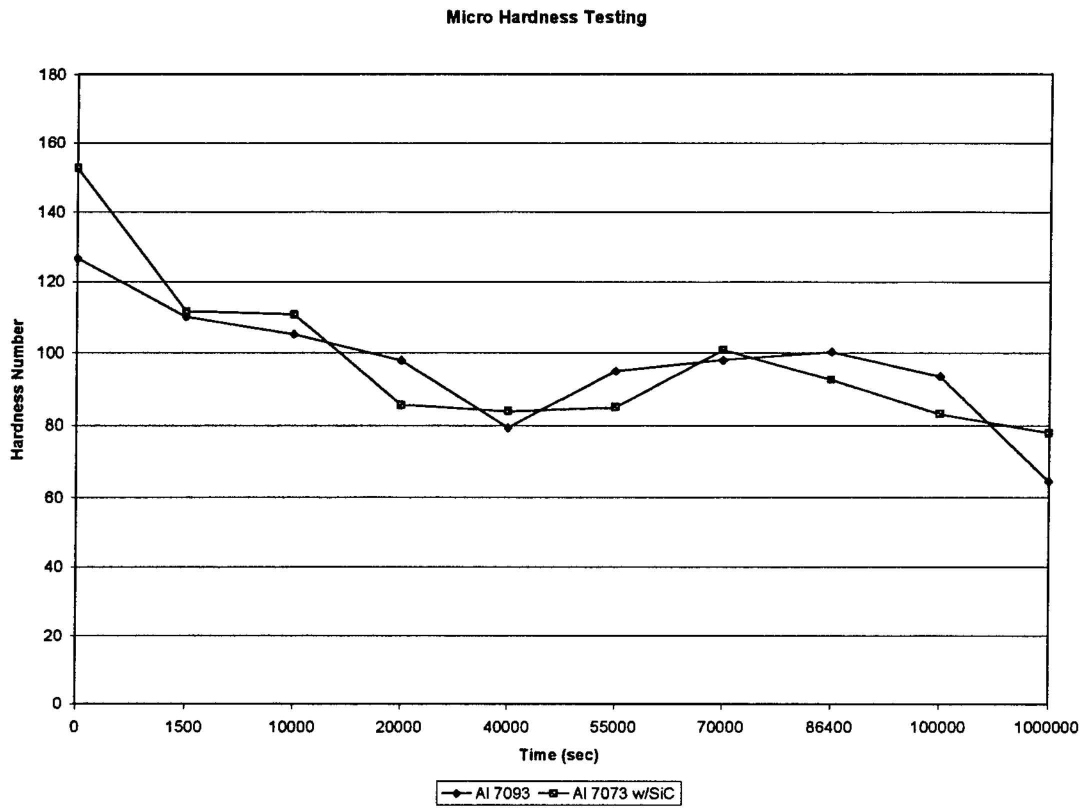

This graph shows the same result of the continued weakening of the alloys. This was not in the least what we were expecting.

Conclusions

Many conclusions can be drawn from our experiment but not very many are actually conclusive. It became apparent after some searching that the aluminum powder used in our experiments was donated to the lab and its contents were not entirely known. It was supposed to be at least 99% pure aluminum powder, and the only other significant element in the alloy would be the SiC particles that were added. However, while on the SEM we ran some EDS testing and found out that there was a very high amount of Sodium and Carbon particles besides those that were added to make the alloy.

So from this many theories arose. Perhaps the solutionizing treatment did not get rid of all of the foreign precipitates like it was supposed to. This would then mean that we were just further aging an already overaged sample. This would account for the steady downward path. In all hypothetical cases, that line could represent the tail end of the aging curve. The impure alloy could also mean that we were not simply testing an Aluminum alloy and an Aluminum alloy with SiC particles. There would be other elements in larger amounts that would drastically alter the microstructure thus changing the properties of the metals greatly. Which in turn means that the systems that are so dependent on each other that we were studying were being adversely affected by other variables.

There were many other possible sources for error in this experiment, such as the fact that all of the samples were heat sensitive and to be worked on they had to be taken out of the freezer. Also, when the samples were sanded and polished, it is possible that they formed a "work hardened layer" which would be harder than the actual heat-treated alloy. However, neither the Micro Hardness nor the Macro Hardness testing that we did would have been able to take a measurement past that layer and get a correct reading.

If they were to redo this experiment, I would like to think that they could learn from the problems we had and perhaps make the experiment more successful in the area that they were researching. I suppose that is what research is about—you try something and learn from it. This was a relatively unresearched area and I guess you could say that we did a lot of the groundwork for my research laboratory. Hopefully they will be able to continue researching the microstructures and aging behaviors of the Al 7093 alloy and the Al 7093 with SiC alloy. This research is the basis of new space-age alloys as strong as Titanium, as light as Aluminum, for use in not only the aerospace industry but in applications unforeseen to us.

We did learn a lot from the experience and being able to work with the tools and doing the processes of scientific research. It was a pleasure to be able to work with the fine people out at Wright Patterson Air Force Base, who were always willing to help. I would personally like to thank them for their help and understanding, and RDL for allowing me to have this opportunity to challenge myself and learn.

DEVELOPMENT OF ENVIRONMENTAL CHAMBER AND CONTROLS TO STUDY THE EFFECT OF ENVIRONMENT ON INTERFACE TRIBOLOGY

Ming Xia

Kettering Fairmont High School
3301 Shroyer Road
Kettering, OH

Final Report for:
High School Apprenticeship Program
Wright Laboratory

Sponsored by:
Air Force Office of Scientific Research
Bolling Air Force Base, DC

And

Wright Laboratory

August 1998

DEVELOPMENT OF ENVIRONMENTAL CHAMBER AND CONTROLS TO STUDY THE EFFECT OF ENVIRONMENT ON INTERFACE TRIBOLOGY

Ming Xia
Kettering Fairmont High School

Abstract

The development of the environmental chamber for a friction tester and how to control the humidity in the environmental chamber was studied. In order to measure friction between a ball and a disc in a given humidity condition, the dry nitrogen gas was used for lower the humidity in the chamber. The water vapor from a large flask was used to supply more humidity to the environmental chamber. Experimental result indicate that the flow rate of the gas has direct effect on the humidity in the chamber. After the humidity in the environmental chamber can be controlled very easily, then there are many materials in tribology can be tested in a given humidity in this chamber

DEVELOPMENT OF ENVIRONMENTAL CHAMBER AND CONTROLS TO STUDY THE EFFECT OF ENVIRONMENT ON INTERFACE TRIBOLOGY

Ming Xia

Introduction

In recent years, many scientists are studying the humidity and its effect on friction between two different materials. Because friction affect our lives in a profound way and we can see friction in our every day life, therefore the study of friction is very important and very useful. Here is some recent finding and result from their experiments. B. Bhushan concludes that the kinetic friction of a tape remains low in the 40-70% relative humidity range and the kinetic friction of a tape increases rapidly with increasing relative humidity above 70% {1}. F. P. Bowden and D. Tabor's experimental results indicated that the adhesion of glass surfaces rises rapidly at humidity above 80%{2}. The thickness of the water film increases rapidly at humidity greater than 90% and the high static frictional force is associated with a large adhesion between the surfaces{2}. B. Bhushan and Z. Zhao said that high relative humidity has no effect on static friction of the unlubricated surface and high relative humidity has effect on static friction of some lubricant surface{3}.

Discussion of Problem and Methodology

In order to measure friction between a ball and a disc in a given humidity condition, the dry nitrogen gas was used for lower the humidity in the chamber. The water vapor from a large flask was used to supply more humidity to the environmental chamber. The flow meter is used to measure the flow rate of the gas and a gas valve is used to turn on or turn off the gas from the nitrogen tank. The inlet and outlet valve is used to let the humid air into or out of the environmental chamber. A humidity sensor is connected to a IBM computer for data collecting. The data is displayed on computer in a graph format. A isolated strip heated is inserted into the chamber for additional control to the humidity. See complete diagram on next page complete detail of the environmental chamber setup.

Results and Conclusion

Base on the data collected from humidity sensor and the graphs displayed on the computer, the results indicated that the environmental chamber works perfectly to isolate itself from outside environment and the designs of the chamber is very good. From the relative humidity control graph, it showed that the flow rate of the gas has direct relationship with the relative humidity in the chamber. The more dry nitrogen gas flows into the chamber, the lower the relative humidity will be for the condition in the chamber. It has vs. verse effect for the water vapor gas in the environmental chamber.

Acknowledgments

Thanks are due to Dr. Steve Patton and Dr. Jeff Zabinski for their support and encouragement during the course of this research. This research was supported by the Nonmetallic Materials Division, The Materials Directorate of The Wright Laboratories, Wright Patterson Air Force Base, Ohio.

References

{1} Bhushan, B. (1996). "Tribology and Mechanics of Magnetic Storage Devices", Springer, NY.

{2} Bowden, F. P., and Tabor, D. (1950 and 1964). "Friction and Lubrication of Solids," Vol. I (1950) Vol. II (1964). Claredon Press, Oxford.

{3} Bhushan, B. and Zhao, Z. (1996). Friction/Stiction and Wear Studies of Magnetic Thin-Film Disk with Two Polar Perfluoropolyether Lubricants. IEEE Trans. Magn. 918-925.

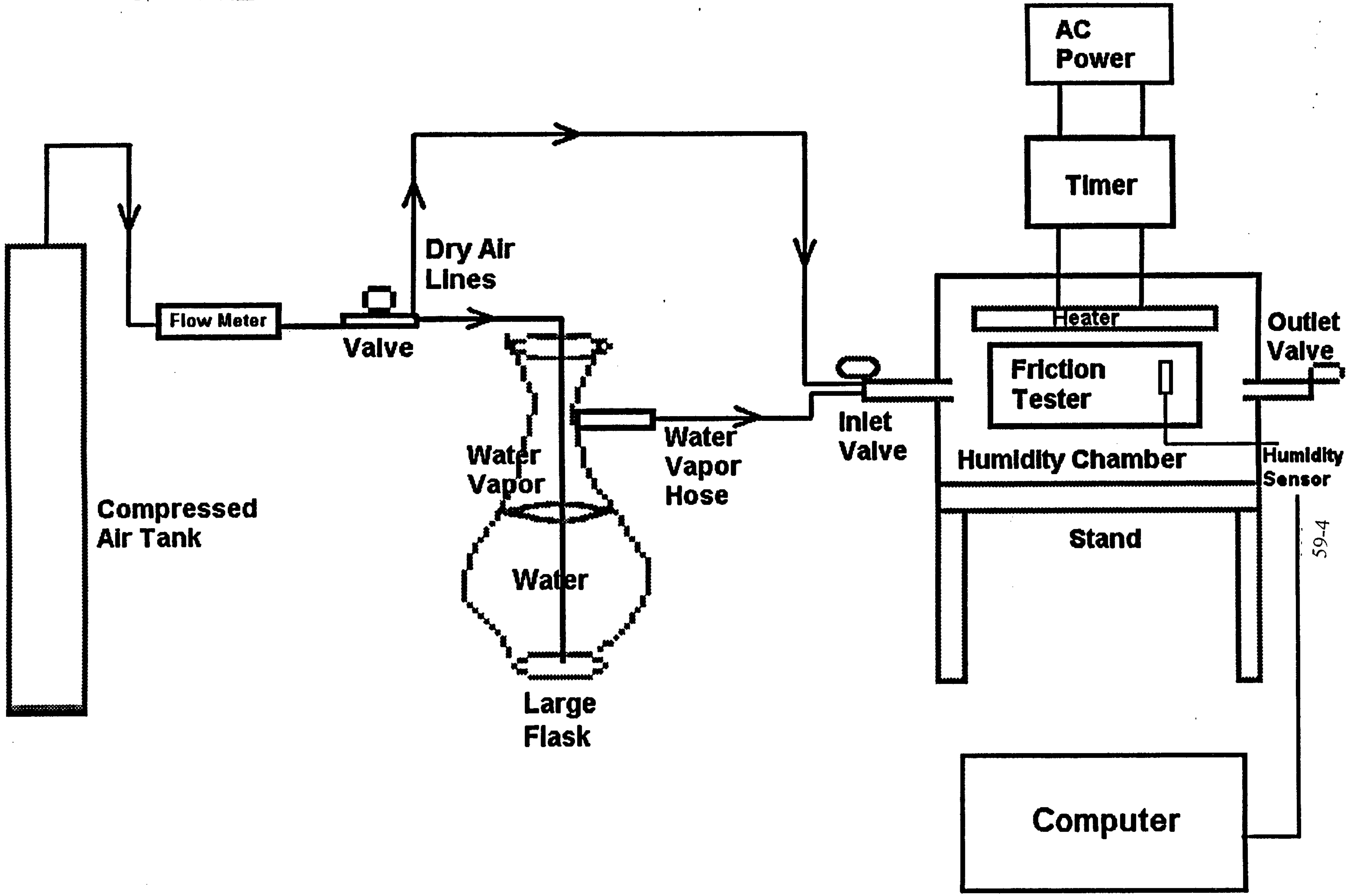
Compressed
Air Tank
Flow Meter
Valve
Dry Air
Lines
Water
Vapor
Water
Large
Flask
Water
Vapor
Hose
Inlet
Valve
AC
Power
Timer
Heater
Friction
Tester
Humidity Chamber
Stand
Outlet
Valve
Humidity
Sensor
Computer

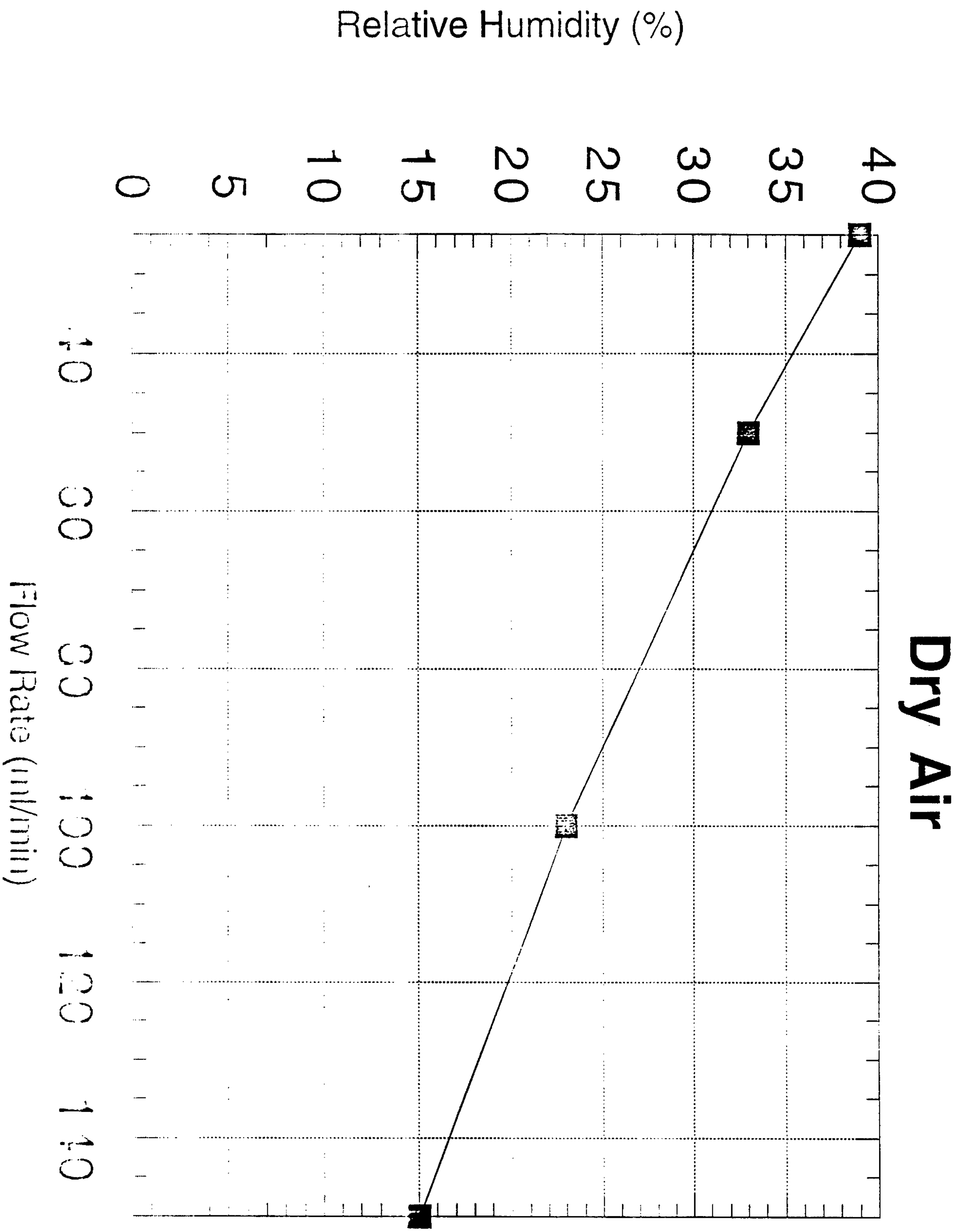
Dry Air
Relative Humidity (%)
40
35
30
25
20
15
10
5
0
Flow Rate (ml/min)

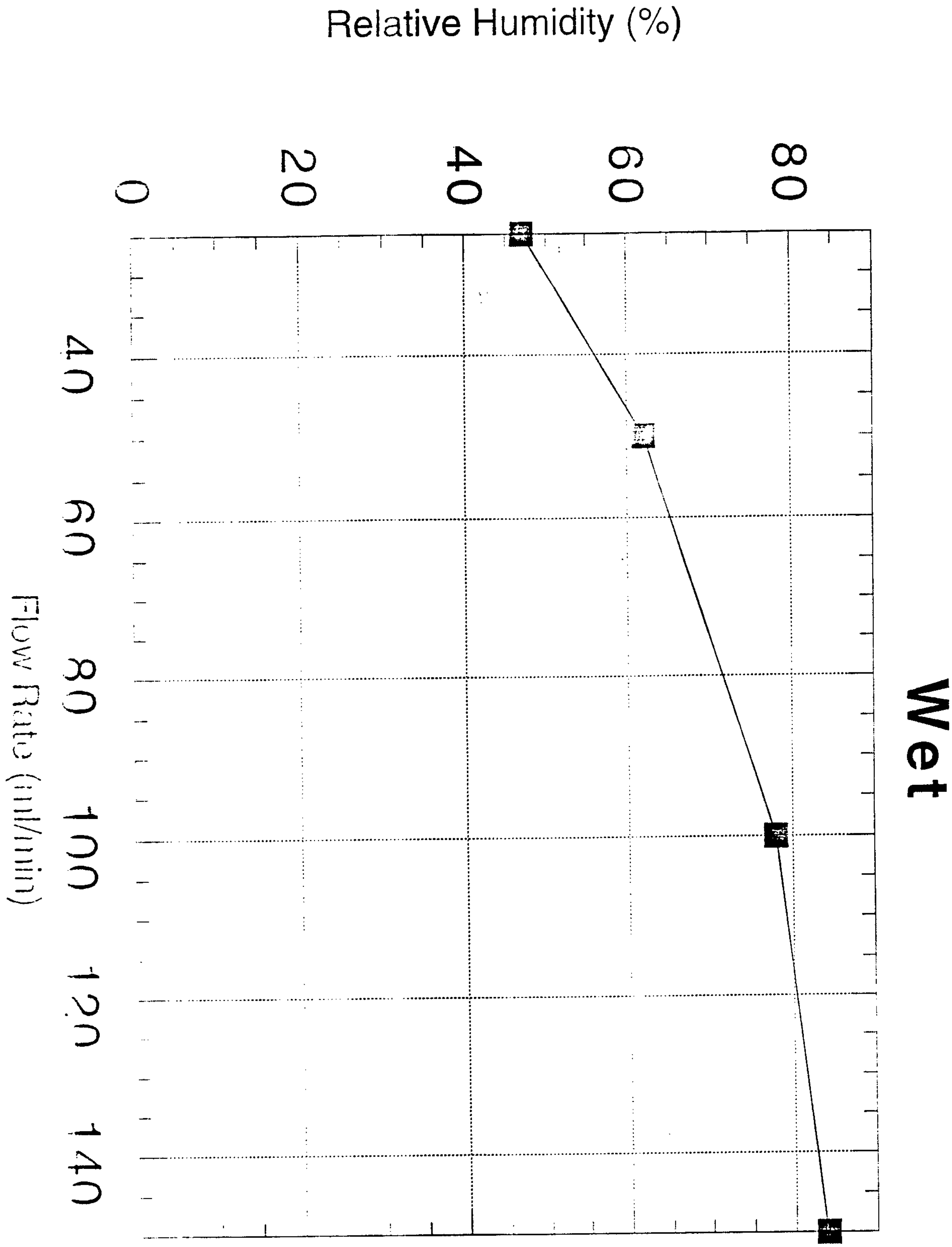
Wet
Relative Humidity (%)
0
20
40
60
80
40
60
80
100
120
140
Flow Rate (ml/min)